

# Fracture Characterization of Composite Bonded Joints under Fatigue Loading

Maria Victoria Castro Fernández

January 2013

**A dissertation submitted to the Faculty of Engineering of the University of Porto for the degree of  
Doctor of Philosophy in Leaders for Technical Industries of the MIT-Portugal Program**



## **Supervisor**

Marcelo Moura<sup>+</sup>

## **Co-Supervisors**

Lucas da Silva<sup>+</sup>

Antonio Torres Marques<sup>+</sup>

Thomas W. Eagar<sup>\*</sup>

<sup>+</sup>) Faculdade de Engenharia da Universidade do Porto, Portugal

<sup>\*</sup>) Massachusetts Institute of Technology, USA



# Preface

This has been developed through several years of research, trying to create a fatigue life assessment for bonded technology applied to composite structures. The results of it have been published in three articles and presented in some conferences.

## Articles

M.V. Fernández, M. F. S. F. de Moura, L. F. M. da Silva, A.T. Marques, “*Composite Bonded Joints under Mode I Fatigue Loading*”, International Journal of Adhesion and Adhesives, 31(5), 280-285, 2011.

M.V. Fernández, M. F. S. F. de Moura, L. F. M. da Silva, A.T. Marques, “*Characterization Of Composite Bonded Joints Under Pure Mode II Fatigue Loading*”, Composite Structure, 95, 222-226, 2013.

M.V. Fernández, M. F. S. F. de Moura, L. F. M. da Silva, A.T. Marques , “*Mixed-mode I+II fatigue/fracture characterization of composite bonded joints using the Single-Leg Bending test*”, Composites Part A: Applied Science and Manufacturing, 44, 63-69, 2013

## Conferences

M.V. Fernández, M. F. S. F. de Moura, L. F. M. da Silva, A.T. Marques, “Composite Bonded Joints under Mode I Fatigue Loading”, Advanced Computational Engineering and Experimenting ACE-X 2010, Paris, 8/9 July 2010.

M. V. Fernández, M. F. S. F. de Moura, L. F. M. da Silva, A. T. Marques, “*Estudo de Juntas Coladas de Material Compósito Sujeitas a Esforços de Fadiga em Modo I*”, Encontro Nacional de Materiais e Estruturas Compósitas (ENMEC2010), Porto, 6-8 September 2010.

M.V. Fernández, M. F. S. F. de Moura, L. F. M. da Silva, A.T. Marques, “Composite Bonded Joints under Mode II Fatigue Loading (ENF)”, ICCS 16, Porto, June 28/30, 2011.

M.V. Fernández, M. F. S. F. de Moura, L. F. M. da Silva, A.T. Marques, “Application of the Single-Leg Bending (SLB) in Composite Bonded Joints under Fatigue Loading”, AB 2011, Porto, July 7/8, 2011.



## Abstract

Composite materials are an excellent commitment between weight savings and material properties. For this reason, some industries have decided to use them as an opportunity to reduce maintenance and fuel costs. In general, there is a greater motivation in lowering the structural weight keeping the same performance. For example, several developments are being done nowadays, to increase the amount of composite materials used in the airframe construction. However, some difficulties arise in the assembly of the composite parts. The definition of suitable technologies to join the components is a challenge and bonding can be one of those technologies. In fact, with the recent developments of adhesives there is an increasing interest to use bonded joints as a joining methodology. In addition, many applications (aircrafts for example) undergo cyclic loading during operations, making fundamental the fatigue characterization of composite bonded joints. Therefore this thesis is focused mainly on fatigue behavior of composite bonded joints, while addressing several subjects related to it, such as manufacturing and certification. The main motivation is that a better understanding of this subject will increase the life in-service of the products manufactured with composite materials. For this research, two applications with an important potential increase of composite bonded joints were analyzed:

- wind blades, which are one of the largest structures built of composite and purely joined by bonding; these structures have very complex loading effects and fatigue must be accounted for, as their life in service is expected to be 20 years;
- airplanes, because they represent a highly regulated industry and are very keen on increasing the amount of composite material usage; the motivation lies behind the need of a more economical solution, with less stress concentrations and more fatigue resistance.

The overall understanding of this work was carried out by applying a system approach which was used to better organize the information. Also, the methodology was used to establish the boundaries and the relations between the different parts. Consequently, this thesis is divided in manufacturing processes (Assembly) and mechanical performance (Performance), and addresses the synergies between both domains. These two subjects were discussed in detail because:

- the manufacturing process affects markedly the joint's ability to sustain the load;
- composite materials are normally associated to high performance products which makes fundamental that the joints' performance are as "excellent" as the components to be assembled.

In the assembly, it was found that the surface treatment has a critical impact on the performance, and the utilization of peel ply in industrial application has to be done carefully. Only approved systems can be used (composite + peel ply + adhesive). In fact, a comparison between different failure modes was made to understand the impact of the surface treatment in the performance.

Still in the same section, the analysis of the costs and performance of an industrial process (in a Portuguese factory) was done. This was an opportunity to acquire the required knowledge to

understand the daily business limitations, and the economic reasons behind the use of this technology. Several models already developed were used for these purposes, i.e. cost modeling - to identify the relevant costs in these kinds of processes. In fact, it was found, that the adhesive (material) and the equipment play a key role in the expenses. The problem regarding these two factors is that they can also affect the performance, if the work is not done properly. For these reasons, a potential way to guarantee the success of the process, with good quality and low costs, is to have qualified and well-trained employees executing these tasks.

During the assessment of the performance, a fatigue analysis was performed considering pure modes (I and II) and mixed-mode (I + II) loading, to assess the life in service of the structure under these different failure modes. This is important because joints are usually designed to undergo these types of loading modes. A new method to calculate the energy release rate ( $G$ ) based on the crack equivalent concept, beam theory and specimen compliance was used, overcoming several limitations intrinsic to classical data reduction schemes. This method (Compliance Based Beam Method – CBBM) was used in Double Cantilever Beam (DCB) for mode I, End-Notched Flexure (ENF) for mode II and Single Leg Bending (SLB) for mixed-mode I+II tests. For Mode I, two different adherends' thicknesses were analyzed. One of the advantages of the proposed methodology is that it makes possible the development of an automated system to treat the data directly acquired from the tests. Effectively, the proposed CBBM avoids or diminishes the need of crack monitoring which is a laborious task, practically impossible to be done with the required accuracy in the ENF tests. This method also helped in defining the threshold. In fact, the threshold was defined as the first variation of the compliance in the fatigue tests and, from the results obtained for Mode I, it was proven that this definition fits the moment when the crack starts to propagate in a steady manner (linear crack growth – Paris law).

In summary the main outcomes of this work are:

- it can be concluded that the manufacturing process affects markedly the mechanical behavior of the joints;
- the proposed data reduction scheme (CBBM) proved its efficiency and enables to determine values for the Paris law constants under the different failure modes analyzed;
- the fatigue process is more severe in mode I (DCB); design of composite bonded joints under fatigue loading must take into account this aspect and solutions avoiding the presence of this loading mode must be envisaged;
- the effect of the adherends thickness in mode I loading tests also plays a key role on how the stresses are distributed along the test, thus influencing the failure mode.



## Resumo

Os materiais compósitos apresentam um excelente compromisso entre o seu peso e as suas propriedades mecânicas. Por esta razão, algumas indústrias encaram-nos como uma oportunidade para baixar os custos relacionados com a manutenção e consumo de combustível. Consequentemente, existe uma grande motivação para baixar o peso das estruturas tentando manter o mesmo comportamento mecânico. Por exemplo, na indústria aeronáutica vários desenvolvimentos estão a ser realizados para aumentar a quantidade de materiais compósitos utilizados na construção de aviões. Todavia, existe ainda uma dificuldade relacionada com a junção das diversas componentes em compósito, ou seja, é necessário definir uma tecnologia que permita usufruir das vantagens destes materiais na sua plenitude. As juntas coladas podem ser uma das tecnologias a responder a este desafio devido ao recente desenvolvimento que os adesivos têm sofrido. Neste contexto, tem vindo a aumentar o interesse na utilização da colagem como método de ligação entre os componentes de compósito. Adicionalmente, muitas das potenciais aplicações (aviões por exemplo) estão submetidos a solicitações cíclicas durante o seu período operacional, o que faz com que a caracterização da fadiga tenha uma relevância significativa. Por conseguinte, esta tese está focada principalmente no comportamento à fadiga de juntas coladas com substratos de material compósito, tendo em conta alguns aspectos relevantes, como é o caso da produção e da certificação. A principal motivação é o aumento da vida útil das estruturas projectadas em compósito envolvendo juntas coladas e submetidas a solicitações dinâmicas. Nesta pesquisa, duas aplicações com capacidade para aumentar o uso de juntas coladas em materiais compósitos foram analisadas:

- pás eólicas, porque são das maiores estruturas construídas em compósito e puramente unidas por colagem. Estas estruturas estão ainda submetidas a solicitações muito complexas e efeitos de fadiga, que devem ser contabilizados durante a sua vida em serviço que deverá ser de 20 anos.
- aviões, porque representam um sector altamente regulado e onde existe um forte interesse em aumentar a utilização de materiais compósitos. As principais motivações residem nos aspectos económicos e melhor comportamento mecânico devido à melhor distribuição de tensões e elevada resistência à fadiga deste tipo de ligações.

A engenharia de sistemas foi utilizada para melhor estruturar o projecto. Esta metodologia também foi utilizada para estabelecer os limites e as relações entre as diferentes partes. Assim sendo, esta tese está também dividida em processos de fabrico (ligação) e comportamento mecânico (desempenho), abordando as relações entre ambos os domínios. Estes dois assuntos são discutidos em detalhe porque:

- o processo de fabrico afecta marcadamente o desempenho da estrutura;
- os materiais compósitos estão normalmente associados a produtos de elevado desempenho, o que torna importante que o eficiência das juntas esteja de acordo com os componentes a serem montados.

No processo de ligação (assembly), verificou-se que o tratamento de superfície tem um impacto crítico sobre o desempenho, e que a utilização de “peel-ply” na aplicação industrial tem de ser feita com cuidado. Apenas sistemas aprovados podem ser usados (compósito +

“peel-ply” + adesivo). Uma comparação entre diferentes modos de rotura foi realizada para compreender o impacto do tratamento de superfície no desempenho das juntas.

Ainda no mesmo processo (assembly), realizou-se uma análise de custos e de desempenho de um processo industrial (numa fábrica Portuguesa). Esta foi uma oportunidade para adquirir o conhecimento necessário, de forma a entender as limitações do uso diário da tecnologia e as razões económicas. Vários modelos já desenvolvidos foram utilizados, como a análise de custos. Esta foi usada para definir os custos relevantes neste tipo de processos. De facto, verificou-se, que o adesivo e o equipamento desempenham um papel crucial no cálculo dos custos. Estes dois factores podem afectar o desempenho (mecânico e o processo produtivo), se o trabalho não for feito correctamente. Consequentemente, as tarefas devem ser executadas por funcionários experientes e bem treinados de modo a garantir o sucesso do processo com boa qualidade e baixo custo.

Na parte do desempenho mecânico, a análise à fadiga foi feita tendo em conta os modos puros de carga (I e II) e o modo misto I + II. O objectivo é avaliar como a vida em serviço da estrutura é influenciada pelos diferentes modos de rotura. Este aspecto é particularmente relevante porque as juntas são concebidas de forma a suportar este tipo de solicitações. Foi utilizado um novo método para calcular a taxa de libertação de energia ( $G$ ) baseado no conceito da fenda equivalente, na teoria de vigas e na flexibilidade do provete ( $C$ ), superando várias limitações inerentes aos métodos clássicos do cálculo do  $G$ . Este método (Compliance Beam Based Method - CBBM) foi utilizado nos ensaios Double Cantilever Beam (DCB), End Notched Flexure (ENF) e Single Leg Bending (SLB)) para os modos I, II e misto I+II, respectivamente. Para Modo I (DCB) duas espessuras diferentes foram ensaiadas. Uma das vantagens do método proposto (CBBM) é que torna possível o desenvolvimento de um sistema automatizado de aquisição dos dados, evitando a monitorização do comprimento de fenda (o que é praticamente impossível de executar com o rigor necessário nos ensaios ENF) ou, pelo menos diminui esta tarefa. O CBBM também permitiu a definição do limiar do início da degradação sob fadiga (threshold). Este limiar (threshold) foi definido a partir da variação inicial da flexibilidade que ocorre a partir de determinado instante do ensaio de fadiga. Para o Modo I provou-se que esta definição corresponde ao momento em que a fenda se começa a propagar de forma estável (com tendência linear – Lei de Paris).

Em resumo pode concluir-se que:

- o processo de fabrico afecta significativamente o comportamento mecânico das juntas coladas com substratos de material compósito;
- o método de cálculo proposto (CBBM) é eficiente e permite a determinação das constantes da lei de Paris tendo em conta os modos de rotura analisados;
- o processo de fadiga é mais severo em modo I (DCB); consequentemente, o projecto das juntas sob solitações em fadiga deve ter isto em conta e devem ser procuradas soluções para garantir a pouca presença de solicitações de modo I;
- o efeito da espessura do substrato em ensaios de modo I também desempenha um papel importante sobre a forma como as tensões se distribuem ao longo do ensaio, influenciando o modo de rotura.

## Résumé

Les matériaux composites présentent un excellent compromis entre leur poids et leurs propriétés mécaniques. Pour cette raison, certaines industries les envisagent comme une opportunité de réduire les coûts concernant l'entretien et la consommation de combustible. Par conséquent, il existe une grande motivation pour baisser le poids des structures tout en essayant de maintenir le même comportement mécanique. Par exemple, dans l'industrie aéronautique plusieurs développements sont en train d'être réalisés pour augmenter la quantité de matériaux composites utilisés dans la construction d'avions. Toutefois, il existe encore une difficulté en ce qui concerne la jonction des composants en composite, c'est-à-dire qu'il est nécessaire de définir une technologie qui permette de jouir des avantages de ces matériaux en plénitude. Les joints collés peuvent être une des technologies pour répondre à ce défi en vertu du récent développement que les adhésifs ont subi. Dans ce contexte, l'intérêt par l'utilisation du collage comme méthode de liaison des composants de composite a augmenté. En outre, maintes des potentielles applications (avions, par exemple) sont soumises à des sollicitations cycliques durant sa période opérationnelle, ce qui fait que la caractérisation de la fatigue ait une importance significative. Par conséquent, cette thèse est focalisée principalement sur le comportement vis-à-vis de la fatigue des joints collés avec des substrats de matériau composite, tenant compte de certains aspects importants comme la production et la certification. La principale motivation est l'augmentation de la vie utile des structures projetées en composite comprenant des joints collés et soumises à des sollicitations dynamiques. Dans cette recherche, deux applications avec la capacité d'augmenter l'utilisation de joints collés en matériaux composites furent analysées:

- pales éoliennes, parce que ce sont des plus grandes structures construites en composite et purement jointes par collage. Ces structures sont, en plus, soumises à des sollicitations très complexes et à des effets de fatigue, lesquels doivent être comptabilisés au cours de sa vie de service, qui devra être de 20 ans.
- avions, parce qu'ils représentent un secteur hautement réglementé et où il existe un fort intérêt à augmenter l'utilisation de matériaux composites. Les principales motivations résident dans les aspects économiques et dans un meilleur comportement mécanique dû à une meilleure distribution des tensions et à la haute résistance à la fatigue de ce type de liaisons.

L'ingénierie de systèmes fut utilisée pour mieux structurer le projet. Cette méthodologie fut aussi utilisée pour établir les limites et les relations entre les différentes parties. Ainsi, cette thèse est aussi divisée en procédé de fabrication (liaison) et comportement mécanique (performance) faisant une approche aux relations entre les deux domaines. Ces deux sujets sont discutés en détail car:

- Le procédé de fabrication affecte remarquablement la performance de la structure.
- Les matériaux composites sont généralement associés à des produits de haute performance ce qui rend important que la performance des joints soit en accord avec celle des composants à être montés.

Dans le procédé de montage (assembly) on a vérifié que le traitement de surface a un impact critique sur la performance et que l'utilisation de "peel-ply" dans l'application industrielle doit

être faite avec soin. Seuls des systèmes approuvés peuvent être utilisés (composite + “peel-ply” + adhésif). Une comparaison entre les différents modes de rupture a été réalisée pour comprendre l’impact du traitement de surface sur la performance des joints.

Encore dans le même procédé (assembly), on a fait une analyse des coûts et de la performance dans un processus industriel (dans une usine portugaise). Ce fut une opportunité pour acquérir les connaissances nécessaires, de façon à comprendre les limitations de l’utilisation journalière de la technologie et les raisons économiques. Plusieurs modèles déjà développés furent utilisés, tel que l’analyse des coûts. Celle-ci fut utilisée pour définir les coûts significatifs dans ce type de procédé. On a vérifié, en effet, que l’adhésif et l’équipement jouent un rôle clé dans le calcul des coûts. Ces deux facteurs peuvent affecter la performance (mécanique et processus productif) si l’on ne fait pas le travail correctement. Par conséquent, les tâches doivent être exécutées par des collaborateurs expérimentés et bien entraînés de façon à assurer le succès du processus avec une bonne qualité et un bas coût.

Dans la partie concernant la performance mécanique, l’analyse de la fatigue a été faite en tenant compte des modes pures de charge (I e II) et du mode mixte (I + II). L’objectif est d’évaluer comment la vie de service de la structure est influencée par les différents modes de rupture. Cet aspect est particulièrement important car les joints sont conçus de façon à supporter ce type de sollicitations. Une nouvelle méthode a été utilisée pour calculer le taux de libération d’énergie ( $G$ ) basée sur le concept de la fissure équivalente, la théorie des poutres et la flexibilité de l’éprouvette ( $C$ ), surmontant plusieurs limitations inhérentes aux méthodes classiques du calcul de  $G$ . Cette méthode (Compliance Based Beam Method - CBBM) a été utilisée dans les essais Double Cantilever Beam (DCB), End Notched Flexure (ENF) et Single Leg Bending (SLB) pour les modes I, II et mixte I+II, respectivement. Pour Mode I (DCB), deux épaisseurs différentes furent testées. Un des avantages de la méthode proposée (CBBM), c’est qu’elle rend possible le développement d’un système automatisé d’acquisition des données, en évitant le monitoring de la longueur de la fissure (ce qui est pratiquement impossible d’exécuter avec la rigueur nécessaire dans les essais ENF) ou du moins réduisant cette tâche. La CBBM a aussi permis la définition du seuil du début de la dégradation sous fatigue (threshold). Ce seuil (threshold) a été défini à partir de la variation initiale de la flexibilité qui a lieu à partir d’un moment déterminé de l’essai de fatigue. Pour Mode I, il a été prouvé que cette définition correspond au moment où la fissure commence à se propager de façon stable (avec tendance linéaire – Loi de Paris).

En somme, on peut conclure que:

- le procédé de fabrication affecte de façon significative le comportement mécanique des joints collés avec des substrats de matériau composite;
- la méthode de calcul proposée (CBBM) est efficace et permet de déterminer les constantes de la loi de Paris compte tenu des modes de rupture analysés;
- le processus de fatigue est plus grave en Mode I (DCB), en conséquence le projet des joints sous sollicitations en fatigue doit tenir compte de cet aspect et des solutions doivent être recherchées pour assurer la faible présence de sollicitations en Mode I;
- l’effet de l’épaisseur du substrat joue aussi un rôle important sur la façon dont les tensions se distribuent tout au long de l’essai, ayant une influence sur le mode de rupture.

## Acknowledgements

First of all, I would like to express my sincere gratitude to all the people I have met along this path. They have helped me in many different ways, making this demanding task possible. For this reason, I will like to thank all of them for their guidance, technical contribution, sharing experiences, interesting discussions, friendship and moral support.

In addition, I gratefully acknowledge my supervisor, Prof. Marcelo Moura from Faculty of Engineering of Porto University, for his continuous supervision and support. I really appreciated his accessibility and contributions to make this research experience stimulating and motivating. Also, I want to mention my co-supervisors, Prof. Antonio Torres Marques, Prof. Lucas Silva and Prof. Thomas Eager because they have helped me to improve this work.

I would specially like to thank my college Valentin Richter Trummer, for his continuous involvement in my work and support. In addition, I would like to acknowledge the effort and work done with Prof. Miguel Figueiredo, Rui Silva, José Almeida and Albino Dias in terms of the experimental work. Also, Albertina Pereira, Filipe Chaves, Dimitra Ramantani, Mariana Doina, Carla Canturri and Eduardo Marques for their conversations and time spent with me. I want to mention Carla Monteiro, for her hard work and efficiency helping me take care of the bureaucracy.

During the case study, I had opportunity to meet interesting people with different backgrounds. In particular to Ausenda Fernandes, João Novo, Nuno Tomas, Luis Lourenço, João Lobo, Vitor Pintor and all the shop-floor workers, whom made this work possible: I would like to express my sincere gratitude for their efforts, which made my ideas a reality. Also, I want to acknowledge the availability of RiaBlades and to thank them for opening the doors.

I want also to mention Airbus, specially Domenico Furfari and Marco Pacchione, because they gave the opportunity to make an internship at Airbus GE. This experience allowed me to bridge some of the investigated topics and their applications in real structures. They gave the opportunity see other environments and ways of working.

To my family and friends; I want to acknowledge them because they have been able to understand my efforts and choices in these four years. I specially would like to thank Miguel Campos, Maria Augusta Fernández and Segundo Castro for their patience and courage along the time.

Finally, I would like to mention my gratitude to MTI-Portugal Program and the Portuguese Foundation for Science and Technology for supporting the work presented here, through the individual grant SFRH/BD/42919/2008.

## Table of Contents

List of Abbreviations.....	XXV
I. <b>Introduction</b> .....	27
1 Motivation.....	27
2 Problem Statement .....	30
2.1 Aircraft Industry Background.....	31
2.2 Wind Energy Industry Background .....	32
2.3 Research Scope and Research Question .....	33
3 Product Life Cycle Management .....	34
3.1 Product Development.....	37
3.1.1 Concurrent Engineering.....	40
3.1.2 Systematic Product Development .....	42
3.1.3 Systems Approach .....	44
3.2 Technology Development Process.....	47
3.2.1 Technology Readiness Level (TRL) .....	48
4 Technology Analysis of Composite Bonded Joints .....	51
4.1 Definition of the Work.....	53
4.2 Identification of Alternative Technologies .....	55
4.2.1 Comparison Between Technologies .....	55
4.2.2 Comparison Between Structures.....	58
4.3 Thesis Development (Plan Outline) .....	59
II. <b>Assembly</b> .....	63
1 Maturity Level .....	64
1.1 Composite Manufacturing Technologies.....	64
1.2 Composite Bonded joints: Manufacturing Processes & Technologies .	66
1.2.1 Surface Pre-treatment.....	68
1.2.2 Peel-Ply .....	70
1.2.3 Grinding and Grit Blasting.....	72
1.3 Bonded joints in Industry.....	74
1.3.1 Bonded Joints in Civil Engineering Projects .....	74
1.3.2 Bonded Joints in the Transport Industry .....	75
1.3.3 Bonded Joints in the Wind Energy industry.....	78

2	Case Study - Wind Blade .....	82
2.1	Process Description .....	83
2.2	Process Performance .....	85
2.2.1	Efficiency.....	87
2.2.2	Ratio of the Process Velocity .....	93
2.2.3	Quality.....	94
2.2.4	Safety .....	98
2.3	Manufacturing Costs.....	98
2.3.1	Definition of the Questions to be Answered .....	99
2.3.2	Identification of the Relevant Cost .....	101
2.3.3	Diagram Process Operations and Material Flows.....	102
2.3.4	Relate Costs to What is Known.....	103
2.3.5	Understand Uncertain Characteristic .....	107
3	Risks.....	108
III.	<b>Performance</b> .....	111
1	Maturity level.....	111
1.1	Designing Bonded Joints.....	113
1.2	Failure Modes for Bonded Joints.....	115
2	Static Stress and Strain.....	117
2.1	Strength and Strain Analytical Approaches .....	117
2.2	Fracture Mechanics Approach.....	119
2.2.1	Mode I.....	123
2.2.2	Mode II.....	123
2.2.3	Mixed-Mode (Mode I + II).....	124
3	Fatigue.....	125
3.1	Fatigue Life.....	127
3.2	Fatigue of Bonded Joints .....	129
3.3	Defining Fatigue life .....	131
3.3.1	Safe-life .....	134
3.3.2	Damage Tolerant Philosophy.....	135
3.4	Fracture Mechanics for Bonded Joints .....	137
4	Experimental Work.....	141
4.1	Materials and Specimens.....	141
4.2	Specimen Preparation .....	142

5	Mode I .....	146
5.1	Manufacturing Process .....	146
5.2	Test Procedure.....	147
5.3	Model Validation .....	148
5.3.1	Compliance Calibration Model (CCM) .....	149
5.3.2	Beam on Elastic Foundation Model (BEFM) .....	149
5.3.3	Compliance Based-Beam Method .....	150
5.3.4	Paris Law .....	151
5.4	Fatigue Data Reduction Scheme.....	152
5.5	Static Fracture Characterization .....	152
5.6	Fatigue Results.....	154
5.6.1	Crack length .....	155
5.6.2	Maximum Energy Release Rate .....	157
5.6.3	Fatigue Assessment for Specimens $h_1$ .....	158
5.6.4	Fatigue Assessment $h_2$ .....	162
5.6.5	Effect of the Adherend Thickness ( $h_1$ and $h_2$ ) .....	167
5.7	Summary Results .....	168
6	Mode II .....	169
6.1	Test Procedure.....	169
6.2	Data Reduction Scheme.....	170
6.3	Static Results.....	171
6.4	Fatigue Results.....	172
6.4.1	Failure Characterization.....	172
6.4.2	Crack Growth .....	173
6.4.3	Fatigue Threshold .....	175
6.4.4	Fatigue Crack Growth Rate .....	176
6.5	Summary of the Results.....	179
7	Mixed Mode (I + II) .....	179
7.1	Test Procedure.....	180
7.2	Data Reduction Scheme.....	181
7.3	Static Results.....	182
7.4	Fatigue Results.....	183
7.4.1	Evaluation of the Mixity.....	183
7.4.2	Failure Characterization and Fracture Surfaces .....	184



7.4.3	Crack Propagation.....	185
7.4.4	Fatigue Threshold .....	186
7.4.5	Paris Law .....	187
7.4.6	Mixed-Mode Correlation for the Paris Law .....	190
7.5	Single lap joint Tests .....	191
7.5.1	Experimental Results .....	192
7.6	Summary of the Results.....	193
8	Perceived Value.....	194
IV.	<b>Concluding Remarks</b> .....	197
1	Case Study .....	197
2	Performance.....	198
3	Final Conclusions and Future Work.....	198
V.	<b>References</b> .....	203



## Table of Figures

<b>I. Introduction</b>	
Figure 1.1 - Boeing 787 airplane landing [4].	28
Figure 1.2 - Qantas A380 airplane flying over Sydney [5].	28
Figure 1.3 – Blade weight as a function of the size [6].	28
Figure 1.4 – Placement of Portugal and placement of the project in the wind blade industry.	29
Figure 2.1– The three pillars of sustainability.	30
Figure 2.2 – CO <sub>2</sub> evolution along with and without fuel efficiency improvements [10].	31
Figure 2.3 - Contribution of wind energy to European electricity consumption 2005-2030. [17]	33
Figure 2.4 – Required interaction to address properly the behavior of bonded joints.	34
Figure 3.1 – Product life cycle [22].	36
Figure 3.2 – Risk Matrix [25].	37
Figure 3.3 – a) traditional engineering; b) concurrent engineering [33].	41
Figure 3.4 – Relative scale of the costs when a changing of the design is necessary in the different PD phases [34].	41
Figure 3.5 – Comparison between traditional aircraft development and concurrent engineering development [35].	42
Figure 3.6 – Clark and Fujimoto PD information map [29].	44
Figure 3.7 – SIMILAR Process [39].	45
Figure 3.8 - Timeline for the emergence of the TRL scale [44].	49
Figure 3.9 – Overview of the TRL Level scale [44].	49
Figure 4.1 – SIMILAR process applied to bonded technology.	52
Figure 4.2 – The role of the main actors in the aircraft certification procedure [49].	53
Figure 4.3 – General Parameters that make possible to fulfill the requirements for an aircraft.	55
Figure 4.4– Selection of lay-up pattern for fiber-reinforced composite laminates. All fibers in 0°, +45°, 90°, or 45° direction. Note: lightly loaded minimum gage structures tend to encompass a greater range of fiber patterns than indicated, because of the unavailability of thinner plies [55]	56
Figure 4.5 – Parameters to be assessed for each activity in the assembly domain.	60
Figure 4.6 –Tasks developed for the Assembly.	61
Figure 4.7 – Parameters to be assessed for each activity in the performance domain.	61
Figure 4.8 – Performance Tasks	61
Figure 4.9 – Interfaces between the two domains (manufacturing and mechanical performance).	62
<b>II. Assembly</b>	
Figure II.1 – Process and sub-categories developed to define the Assembly capabilities of bonded joints.	63
Figure 1.1 – Fiber forms at different scales [61].	65
Figure 1.2 – a) Unidirectional thin-ply tape [62]; b) woven fabric[63]; both are composite carbon fibers.	65
Figure 1.3 – Co-cure process.	67
Figure 1.4 – Co-bonded process.	67
Figure 1.5 – Secondary bonding process.	68
Figure 1.6 – Classification of Surface treatments for Plastics [70].	69
Figure 1.7 – Relation between the $G_{IC}$ failure mode and wettability of the surface [73].	70
Figure 1.8 – Cross section of laminate with peel ply on top [68].	71
Figure 1.9 – Four possible fracture types in peel ply removal [68].	71
Figure 1.10 – Results obtained by Kim et al.; a) An evaluation of the surface roughness as a function of the Mesh n° of sandpaper, b) Joint strength as a function of the Mesh n° of sandpaper [66].	73
Figure 1.11 – Pedestrian bridge built for tests in Yverdon – Switzerland: a) detailed picture of the bonded CFRP plates, b) the bridge at the artificial cloud facilities [80].	74

Figure 1.12 – Adhesive bonding process to assembly composite pipelines: (a) Machining pipe ends and drying, (b) application of adhesive, (c) assembly, (d) tightening and cure (heated blanket) [69].	75
Figure 1.13 – Train with applied bonded joints [75].	76
Figure 1.14 - Commercial airplane models over time by percentage of composite [83].	77
Figure 1.15 – The A350 XWB features CFRP primary structures (materials per component) [84].	77
Figure 1.16 – Co-bonded structures used in the aircraft industry [82].	78
Figure 1.17 – Scaled design comparing a Boeing 747 with a Blade of 35m [86].	79
Figure 1.18 – Wind blade components [87].	80
Figure 1.19 – Sketch of a wind turbine blade and a cross section of a blade [87].	80
Figure 1.20 – Spar box concept – One piece blade [88].	81
Figure 1.21 - Possible loading modes for adhesive joints along a blade cross section [87].	82
Figure 2.1 - Five-step bonding process for a wind turbine blade. a: Adhesive is applied to the first shell in the fixed part of the mold, and to the second one, at the root end of the blade. b: The internal parts (spar or shear webs) are lifted into position. c: Adhesive is applied to the top of the spar or shear webs for the second shell bonding. d: The second shell is lifted over onto the spar or the shear webs. e: The mold is closed [88].	83
Figure 2.2 – Application of adhesive into the first main shell to put the spar box on top [88].	84
Figure 2.3 – a) Application of adhesive into the first shell to place the shear webs; b) view from inside the webs after they are in place.	84
Figure 2.4 – Exothermic reaction for Aristone resin (770E/T3) while curing with different hardeners (772H/T and 778H/T) (147g at 23°C) [91].	85
Figure 2.5 – Model of PDCA defined in ISO 9001 [94].	88
Figure 2.6 – SDCA for cost analyses.	89
Figure 2.7 – Average of the mount of total adhesive consumed (Until blade 170).	90
Figure 2.8 - Average of the amount of total adhesive consumed (from blade 185).	91
Figure 2.9 – Efficiency Ratio of adhesive consumption per blade manufactured.	92
Figure 2.10 – Normal function regarding three different time periods.	92
Figure 2.11 – Sketch of the complete process and times.	93
Figure 2.12 – The common defects regarding composite bonded joints [67].	94
Figure 2.13 – Amount of defects in % to compare which place has the higher incident number.	96
Figure 2.14 - % of defects considering the type of defect focus on the most common defects.	96
Figure 2.15 – Most common defects in blades: a) run-out in the web, and b) lack of adhesive in the web.	97
Figure 2.16 – Comparing the sample left with the main shell + web flange.	97
Figure 2.17 – Bond line + flange thickness measured at the joint after being cured.	98
Figure 2.18– Sketch cataloguing each process step associated.	103
Figure 2.19 – Adhesive consumed per blade from 100 to 175.	104
Figure 2.20 – Normal distribution regarding the 2 changes in the process	105
Figure 2.21 – Adhesive bonding used for the webs at the end of the project.	106
Figure 2.22 – Adhesive bonding used for closing the blade the end of the case study.	107

### III. Performance

Figure III.1 – Process to design a joint or a structure	111
Figure 1.1 –Double lap joint configuration [55].	112
Figure 1.2 –Single lap joint configuration proposed in EN2243 - 1 [103].	112
Figure 1.3 – Single lap joint analyzed [104].	113
Figure 1.4 – Types of adhesive bonded joints [55].	115
Figure 1.5 – Typical failure mode for bonded joints [55].	116
Figure 1.6 – Difference between cohesive and adhesive failure modes [55].	116
Figure 2.1 – Representation of the bending moment factor of Goland & Reissner; a) undeformed joint and b) deformed joint [111].	117
Figure 2.2 – Stress distribution along the bondline a) shear stress for Volkersen and Goland and Reissner methods; b) peel stresses in the bondline for SLJ [111].	118

Figure 2.3 – Adhesive Shear-strain curves and mathematical models [106].	119
Figure 2.4 – Typical load $P$ versus displacement ( $\delta$ ) plot for a Mode I (Double Cantilever Beam specimen) using CFRP adherends and epoxy-paste adhesive [115].	120
Figure 2.5 - Modified Beam Theory [116].	122
Figure 2.6 – Crack propagation modes: Mode I crack opening, Mode II forward shear and Mode III out-of-plane shear [126].	122
Figure 2.7 – DCB specimen for Mode I testing with a) piano hinges and b) loading blocks [116].	123
Figure 2.8 – Methods to test for the fracture characterization in Mode II [129].	124
Figure 3.1 – Fatigue lives of several application [59].	126
Figure 3.2 - Typical cyclic loading parameters [69].	126
Figure 3.3 – Example of a Peak ( $P$ ) and Trough ( $T$ ) counting for a constant amplitude loading.	127
Figure 3.4 – Wind Blade full scale testing [141].	128
Figure 3.5 – Fatigue test of a PC-9 Aircraft [142].	128
Figure 3.6 – Variables that influence fatigue life of adhesive joints [59].	129
Figure 3.7 – Fatigue failure modes: adhesive debonding and adherend failure.	130
Figure 3.8 – Fatigue failure by delamination.	130
Figure 3.9 – B-47 aircraft [164].	133
Figure 3.10 – Applicable regulations for the Aircraft Certification taking into account the fatigue requirements [166].	134
Figure 3.11– S-N curves for aluminium and low carbon steel.	135
Figure 3.12– Typical $da/dN$ plot as a function of the stress intensity factor ( $K$ ).	136
Figure 3.13 – Havilland Comet jets [173].	137
Figure 3.14 – Specimen used in Mostovoy and Ripling work, to assess the behavior of bonded joints under fatigue and Liquid Water Stress Corrosion Cracking [179].	139
Figure 4.1 – Specimens tested.	142
Figure 4.2 – SLJ configuration tested.	142
Figure 4.3 – Cut plies to be laminated.	143
Figure 4.4 – Compaction during the hand lay-up using the scraper [190].	143
Figure 4.5 – Curing cycle applied to the laminate: pressure and temperature applied.	144
Figure 4.6 – Cured plate.	144
Figure 4.7 – Pressure application with grips a) and detail of the vertical grips (b) [190].	145
Figure 4.8 – ENF Specimen prior finishing.	145
Figure 4.9 – SLJ manufactured following EN2243-1.	146
Figure 5.1 – Geometry of a DCB specimen with load blocks [116].	147
Figure 5.2 - Experimental setup of DCB tests under fatigue cyclic loading.	148
Figure 5.3 - Experimental variation of the compliance ( $C$ ) as a function of the crack length ( $a$ ).	149
Figure 5.4 - Schematic representation of the crack equivalent concept and FPZ [189].	151
Figure 5.5 – $P$ - $\delta$ curve for the $h_1$ specimens tested statically.	153
Figure 5.6 - $P$ - $\delta$ curve for the $h_2$ specimens tested statically.	153
Figure 5.7 – R Curves for $G_{Ic}$ obtained with DCB specimens.	154
Figure 5.8 – Fracture surfaces of a bonded joint with cohesive failure for $h_1$ .	155
Figure 5.9 – Fracture surfaces of a bonded joint with cohesive failure for $h_2$ .	155
Figure 5.10 – Plot of $a$ vs. $N$ to compare the equivalent crack length ( $a_e$ ) and the crack length measured ( $a$ ) for $h_1$ specimen 3.	156
Figure 5.11 – Plot of $a$ vs. $N$ to compare the equivalent crack length ( $a_e$ ) and the crack length measured ( $a$ ) for $h_2$ .	157
Figure 5.12 – Plot of $G_{I_{max}}$ versus $a$ considering the three methods for $h_1$ .	157
Figure 5.13 – Plot of $G_{I_{max}}$ versus $a$ considering the two methods ( $h_2$ ).	158
Figure 5.14 – Identification of the $G_{th}$ in specimen 3 using the CBBM.	159
Figure 5.15 – Fatigue crack growth rate as a function of energy ratio $G_{I_{max}}/G_{Ic}$ considering the BEFM and the CBBM, $h_1$ Specimens.	161

Figure 5.16 – Paris curves for all the specimens tested for $h_1$ , these points were used to determine the Paris law constants. ....	162
Figure 5.17 - Complete propagation rate for Specimen 5 with the CBBM method to determine $G_{th}$ . ....	163
Figure 5.18 - Fatigue crack growth rate as a function of energy ratio $G_{lmax}/G_c$ considering the BEFM and the CBBM for Specimen- $h_2$ . ....	166
Figure 5.19 - Fatigue crack growth rate as a function of energy ratio $G_{lmax}/G_c$ considering the BEFM and the CBBM Specimen 6- $h_2$ . ....	166
Figure 5.20 – Paris plots for the two thicknesses tested $h_1$ and $h_2$ specimens. ....	168
Figure 6.1 - Schematic representation of the ENF test. ....	169
Figure 6.2 - Setup used for the 3-point bending test. ....	170
Figure 6.3 - $P$ - $\delta$ curve for the <i>ENF</i> specimens tested statically. ....	172
Figure 6.4 – R Curves for $G_{II}$ obtained with ENF specimens considering the methods described in Section III.5.2 [120]. ....	172
Figure 6.5 - Fracture surfaces of a bonded joint with a cohesive failure. ....	173
Figure 6.6 - Variation of the compliance ( $C$ ) and the equivalent crack length ( $a_e$ ) as a function of the number of cycles (Specimen 4). ....	174
Figure 6.7 – Complete propagation rate curve for specimen 1 with the CBBM to determine $G_{th}$ . ....	175
Figure 6.8 – Comparison between the average Paris law with the one obtained for each specimen. ....	178
Figure 6.9– Average Paris law adjusted to the results off all specimens. ....	178
Figure 7.1 – Schematic representation of the SLB test and geometry of the specimens (width B). ....	180
Figure 7.2 – Experimental setup of SLB tests under fatigue cyclic loading. ....	181
Figure 7.3 - $P$ - $\delta$ curve for the <i>SLB</i> specimens tested statically. ....	182
Figure 7.4 - R Curves for $G_{Tc}$ obtained with SLB specimens. ....	183
Figure 7.5 - Specimen 1 R Curves for $G_I$ , $G_{II}$ and $G_T$ . ....	183
Figure 7.6– Plot of mix ratio as a function of $G_T/G_{Tc}$ along the test for the specimen 4 and 5 tested with 50% of the static load. ....	184
Figure 7.7– Typical evolution of $G$ along the SLB test for specimen 3. ....	184
Figure 7.8– Fracture surfaces of the specimens tested with 70% of the load; a) delamination, b) cohesive failure in the adhesive. ....	185
Figure 7.9 – Fracture surfaces of the specimens tested with 50% of $P_{max}$ . ....	185
Figure 7.10 – Plot of compliance as a function of the number of cycles (for 70% of $P_{max}$ ). ....	186
Figure 7.11– Typical compliance ( $C$ ) versus number of cycles ( $N$ ) for 50% of $P_{max}$ . ....	186
Figure 7.12 – Complete propagation rate for Specimen 1 for 50% of $P_{max}$ . ....	187
Figure 7.13 – Stable crack growth (linear region) of the six specimens tested at 50% of $P_{max}$ and the respective average law. ....	188
Figure 7.14 – Paris law and verification of the general law for each specimen at 50% of $P_{max}$ . ....	190
Figure 7.15 – Paris-law $m$ parameter as a function of the mixity. ....	190
Figure 7.16 – Crack propagation curves for all the samples tested with the equivalent geometry ( $h=2.7$ mm). ....	191
Figure 7.17 – Schematic representation of the SLJ tested. ....	191
Figure 7.18 – Setup used SLJ test. ....	192
Figure 7.19 – Single lap joint tested (specimen 3): at 1000N and at 2000 N. ....	192
Figure 7.20 – Crack propagation as a number of cycles and the variation of the compliance. ....	193
Figure 7.21 – Typical failure surface a SLJ tested. ....	193

#### IV. Concluding Remarks

Figure 3.1 – Supported single lap joint configuration (dimensions in mm) [193]. ....	201
--	-----

## Table of Tables

<b>I. Introduction</b>	
Table 3.1 – Improvement options in the different fields related to product development [19].	38
Table 4.1 – Comparison between different joining mechanisms [59].	58
Table 4.2 – Comparison between wind blades and aircrafts.	59
Table 4.3 – Activities defined in each domain to fulfill this work.	60
<b>II. Assembly</b>	
Table 1.1 – Key points regarding different composite manufacturing technologies [7], [60], [64], [65].	66
Table 2.1 – Average and Standard deviation of the material consumed along the case study in different stages.	92
Table 2.2 – Normal cumulative probability of having the consumptions inside the BOM values.	92
Table 2.3 – The dimensions of quality design [26].	95
Table 2.4 – All costs related to the bonding process.	101
Table 2.5 – Definition of each relevant cost.	102
Table 2.6 – % of the Costs as a function of the total cost of the process.	102
Table 2.7 – Average and Standard deviation induced by the changes in the process.	105
Table 2.8 – Difference between the total amount of material and the one used for bonding.	107
<b>III. Performance</b>	
Table 2.1 - Test methods to measure the adhesive fracture toughness under mixed-mode conditions and different mixity angles. [131], [135]	125
Table 4.1– CFRP elastic orthotropic properties for a unidirectional ply aligned in the $0^\circ$ direction [192]	141
Table 5.1 – $P_{max}$ for the specimens tested statically.	153
Table 5.2 - $G_{Ic}$ obtained for DCB specimens tested statically.	154
Table 5.3 – Number of specimens failing per type of failure.	155
Table 5.4– Energy fatigue threshold of DCB tests ( $h_1$ ).	159
Table 5.5 – Paris law constants for $h_1$ specimens.	162
Table 5.6 – Energy fatigue threshold of DCB tests ( $h_2$ ).	163
Table 5.7 – Actual initiation for crack growth ( $h_2$ ).	164
Table 5.8 - Paris law constants for $h_1$ specimens.	167
Table 6.1 – Comparison of the crack length at the beginning and at the end of the test for $h_1$ specimens.	175
Table 6.2 – Energy fatigue threshold of ENF specimens.	176
Table 6.3– Paris law constants of the validated specimens.	176
Table 7.1 – Data obtained from the SLB specimens tested statically.	183
Table 7.2– Energy fatigue threshold for SLB Specimens (50% of $P_{max}$ ).	187
Table 7.3 – Paris law constants of the validated specimens tested at 50% of $P_{max}$ .	188





## List of Abbreviations

### Technical Abbreviations

<i>CFRP</i> – Carbon Fiber Reinforced Polymers	<i>GFRP</i> – Glass Fiber Reinforced Polymers
<i>CoV</i> – Coefficient of Variation	<i>K</i> – Fracture Toughness
<i>DCB</i> – Double Cantilever Beam	<i>LL</i> – Lower Limit = BOM – 10%
<i>DT</i> – Damage Tolerance	<i>RTM</i> – Resin Transfer Molding
<i>ENF</i> – End-Notched Flexure	<i>SLB</i> – Single Leg Bending
<i>FCG</i> – Fatigue Crack Growth	<i>SLJ</i> – Single Lap Joint
<i>FPZ</i> – Fracture Process Zone	<i>T<sub>g</sub></i> – Glass Transition Temperature
<i>FRP</i> – Fiber Reinforced Polymers	<i>UP</i> – Upper Limit = BOM + 10%
<i>G</i> – Energy release rate	<i>VARTM</i> – Vacuum Assisted Resin Transfer Molding
<i>G<sub>c</sub></i> – Critical Energy release rate	

### Acronyms

<i>PLM</i> – Product Lifecycle Management
<i>INCOS</i> - International Council on Systems Engineering
<i>PD</i> – Product Development
<i>AC</i> - Advisory Circulatory
<i>EASA</i> – European Aviation Safety Authority (EUROPE)
<i>FAA</i> – Federal Aviation Administration (USA)
<i>JAA</i> – Joint Aviation Authorities (WW)
<i>ANAC</i> – Agencia Nacional de Aviacao Civil (Brasil)
<i>Formerly ATA</i> - Air Transportation Association of America <b>Now is A4A</b> – Airlines for America
<i>CE</i> – Concurrent Engineering
<i>ESA</i> – European Space Agency
<i>DoD</i> – U. S. Department of Defense
<i>TRL</i> – Technology Readiness Level
<i>CAD</i> – Computer Aided Design
<i>EDM</i> – Engineering Data Management



## **I. Introduction**

### **1 Motivation**

As the world is evolving to a fuel crisis and considering the impact of the CO<sub>2</sub> and other contaminant released to the air, a lot is being done to diminish the fuel consumption. Recently, cars, airplanes, trains are being made from composite materials in a regular basis because of the weight savings which means less fuel consumption per km. One of the best examples how this evolution is happening, is the aircraft industry. Two of the biggest civil aircraft manufacturers (Airbus and Boeing) have been investing in research because of these advantages. The results are presented in the Boeing 787 aircraft (Figure 1.1) where 50% of its weight depends upon composite materials and the largest commercial Airbus A380 (Figure 1.2) has 25% of composite materials [1]. Additionally, the upcoming Airbus A350 aircraft (also with 50% of its structural weight in composite) exemplifies a distinct design approach adopted in pursuing weight and performance benefits of composites [2]. One of the biggest successes has been Eurofighter Typhoon (Military Aircraft), where 70% of the airframe surface area is made of Carbon Fiber Composites (CFCs) and 12% of Glass Reinforced Plastics (GFR). The lightweight materials made the airframe and engine 10 to 20% smaller and 30% lighter [3].

Another very important application of composite materials concerns the renewable energies, as is the case of wind energy (on-shore and off-shore), which also depends on the relation between weight savings and performance (Figure 1.3). Lighter structures have better performance, i.e. a lighter wind blade is able to produce more energy with the same wind load (for blades of the same size). As a result, the industry of wind blades represents a high investment with affordable return. The technological trend is to develop bigger and lighter blades to improve their production capacity. In general, these scenarios lead the society to the next step in weight savings which could be an entire aircraft fuselage of composite materials or a new blade with a larger expected life or more power with the same size.



Figure 1.1 - Boeing 787 airplane landing [4].



Figure 1.2 - Qantas A380 airplane flying over Sydney [5].

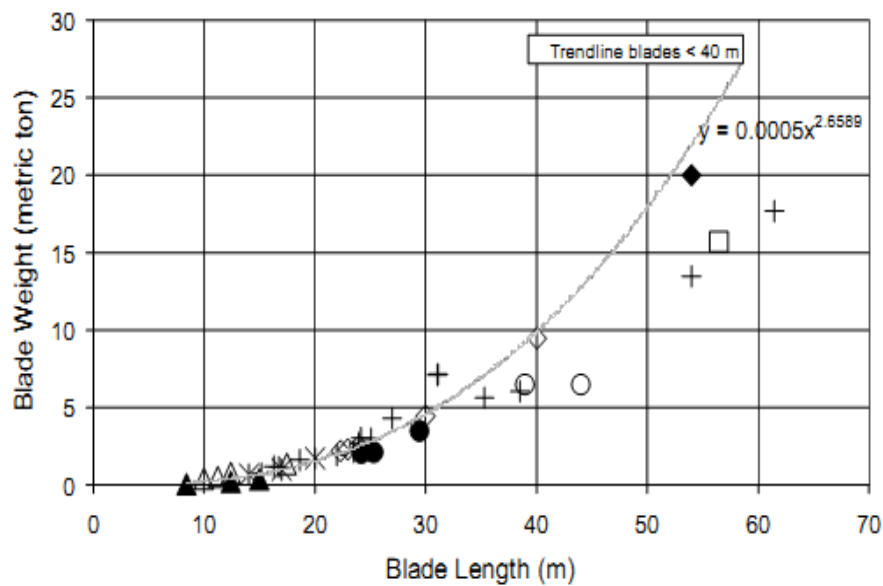


Figure 1.3 – Blade weight as a function of the size [6].

All these applications and others coming from high performance products plus the necessity of weight saving are using composites as next generation solutions. *“However, even with these significant reductions, almost all composite structures require some type of post-processing and/or assembly operations. Since both of these operations add to the total cost of the final*

product in many instances, it is advantageous to minimize these operations if possible. In addition, many of the post-processing and assembly operations, such as trimming, drilling, and fastening, are more expensive for composites than metals. Trimming requires greater care because dull tools or incorrect feeds can cause heat damage or delaminations. Drilling is complicated by the abrasive nature of carbon fibers that can result in accelerated tool wear and splintering of the surface plies. During assembly, composites will tend to delaminate if excessive force is used to pull out gaps often encountered during assembly [7]". Therefore the application, in any possible scenarios, of bonded joints has to be reliable and consistent with the performance of the adherends, because it will represent general savings without knock-down of the properties and less post-processing limitations.

Just to give the overall industrial scenario Portugal's position in the market is also presented in Figure 1.4. It shows how Portugal is related to the whole product cycle life. Indeed, Portugal is a manufacturer country that invests in "industrialized" development, where technology research in a long term basis can present a chance to get more profit on composite materials as a recently shallow explored subject that will open new markets and possibilities. This constitutes an opportunity to be taken. In fact, the amount of composite materials used in general has increased in the last years because of a deep knowledge in more complex strategies and products. Investing in the development of composite manufacturing and assembly processes can launch research in Portugal to this new paradigm. For example, a project has been launched by Salvador Caetano enterprise, to work with Airbus Military [8]. The main focus is composite parts, namely its manufacturing and assembling.

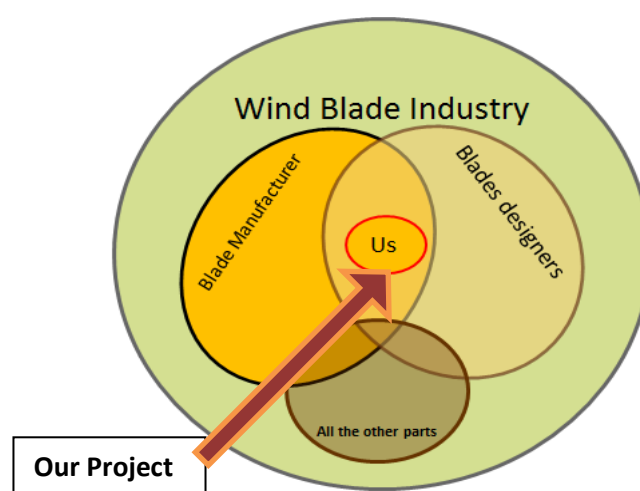


Figure 1.4 – Placement of Portugal and placement of the project in the wind blade industry.

Joining all these pieces together, manufacturing and improving composite applications plus the industrial capabilities and excellence is an innovation opportunity for Portugal and the research community.

Considering this preamble, one motivation of this work is to give an overview about industrial manufacturing processes, costs and mechanical performance. Also, understanding how a composite bonded joint, subjected to fatigue loading, behaves is important to complete the picture and to decide how these structures can be designed. Several aspects have to be addressed to comprehend the different parts that are involved in the design. For this reason, this project focuses in technology management, manufacturing management, performance and their relations and dependencies.

## 2 Problem Statement

Sustainable development is, nowadays, a crucial issue to be taken into account in any industrial activity. In order to achieve this goal the equilibrium between the different subdomains involved in any action must be guaranteed. Jonathon Porritt [9], define sustainability as *"The economy is, in the first instance, a subsystem of human society... which is itself, in the second instance, a subsystem of the totality of life on Earth (the biosphere). And no subsystem can expand beyond the capacity of the total system of which it is a part."* Indeed, the dimensions of sustainability normally are: environmental, social and economic and these "three pillars" are known to be interdependent and can be mutually reinforcing (Figure 2.1). These three pillars and the adoption of new materials in the new future challenges can create new opportunities with promising developments. This is normally demonstrated with evaluated milestones that have been reached along the time.

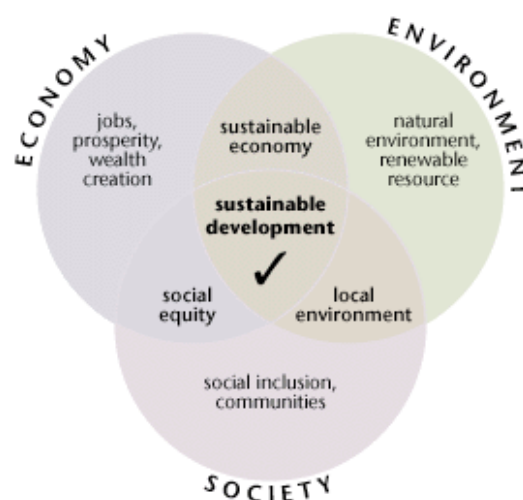


Figure 2.1– The three pillars of sustainability.

## 2.1 Aircraft Industry Background

The International Airline Transport Association (IATA) has a fuel efficiency program where the association defines a reduction of more or less 25% in fuel until 2020 (1.5% per year from 2009 to 2020). IATA carries 93% of the world's international air flights states. In their technological research they found that *“New aircraft are 70% more fuel efficient than 40 years ago and 20% better than 10 years ago”*. B787 (Figure 1.1) and A380 (Figure 1.2) are aiming to a consumption of 3 liters per passenger per 100 km. These important gains are better than the ones obtained for a compact car [10], where *“more airframe structure components made of lightweight composite material”* can be responsible for a total impact in reduction between 8% and 20% [11]. Finally, in this tentative to reduce carbon emissions, they have stated that the “normal” renewal of fleet (27% of the total fleet) can represent 21% reduction of the emissions compared to a scenario without fleet renewal (Figure 2.2). From the economical point of view, airlines will likely spend \$1.5 trillion on new aircrafts; while the overall airline capital expenditure for achieving carbon-neutral growth for 2020 is expected to be around \$1.6 trillion [12]. From the sustainability point of view and considering that labor and fuel represent the largest cost component in airlines operations, this is not only an opportunity to “save” the environment but also to help the economy.

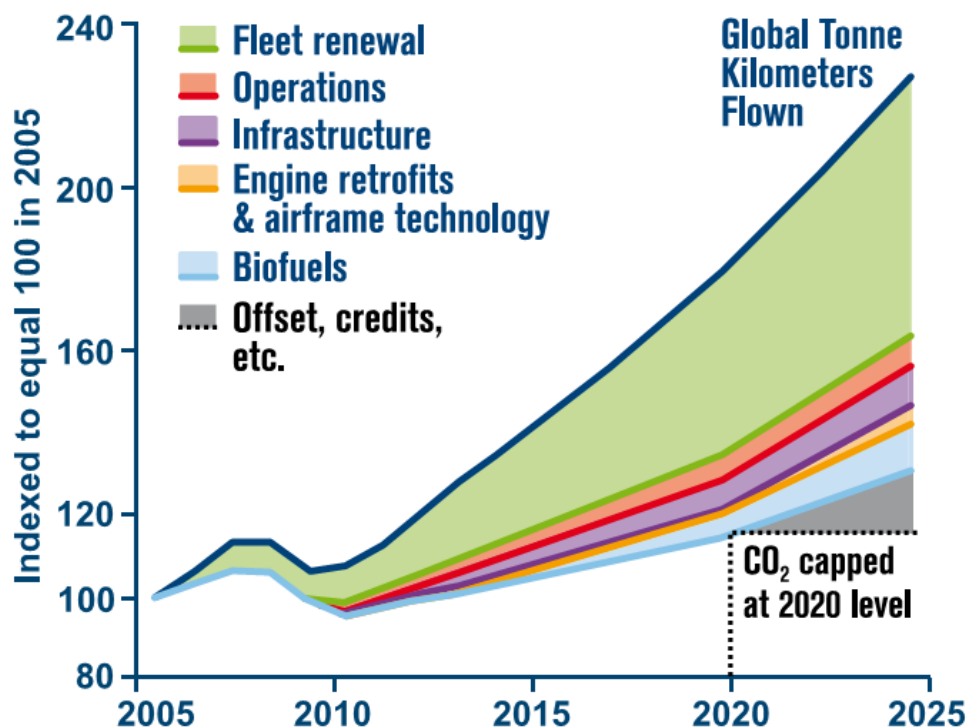


Figure 2.2 – CO<sub>2</sub> evolution along with and without fuel efficiency improvements [10].

Lufthansa is a good example as they are aligning economic and environmental sustainability. They set a new record in 2011, 4.18 liters of fuel per passenger in 100 kilometers [13]. *“In the air, developments such as more efficient engines, aerodynamic wings, nanotechnology in aircraft paint and new composite materials help ensure that the aircraft of Lufthansa Cargo consume as little kerosene as possible. In addition they refer as an example, the impact of reducing weight in cabin accessories. “One kilogram less weight on all Lufthansa German Airlines aircraft reduces kerosene consumption by 30 tons per year. Examples of recent weight reductions: due to the use of composite materials, the newly introduced light containers weight 14 kilograms less than their predecessor model. Some 30000 new service carts will be deployed at Lufthansa over the next three years. The new model is one-third lighter than the previous trolley, reducing jet fuel consumption by about 9000 tons per year [13].”*

## 2.2 Wind Energy Industry Background

On the other hand, the energy developed from renewal sources is also important to keep the comfort of the society with an acceptable price and with a low carbon foot print. The Global Energy Wind Council (GWEC) has defined that at the end of 2011 the installed power was 238 GW, representing cumulative market growth of more than 20% [14]. For example, this year (2012): *“the European Union has passed the milestone of 100 GW of installed wind power capacity, according to the European Wind Energy Association (EWEA)”*[15] which is equivalent to 62 coal power plants. In fact, it is forecasted that the contribution of wind energy will grow to 22.6% in 2030 with 300 GW installed (Figure 2.3). Whatever the economical conditionals are, wind energy has the potential to be the cheapest power source in Europe, but like any emerging technology, it faces significant barriers. Portugal has two of the ten biggest onshore wind farms in Minho with an installed capacity of 240 Megawatts and around 120 turbines installed [16]. In fact, *“the wind power industry has grown in leaps and bounds. In recent decades, to fuel its development, the wind industry has borrowed materials, systems and products from other sectors: defense, for sensors; aerospace and shipbuilding, for blades; and the mining industry, for gear technology”* [17]. This technological paradigm is shifting; the option of borrowing is coming to an end. *“The industry needs to develop new technologies to meet requirement of ever increasing scale.” “A strong wind energy sector does not only mean reduced CO<sub>2</sub>, cleaner air, and secure biodiversity. Sustainable economic growth, reduced energy import dependence, high quality jobs, technology development, global competitiveness, and European industrial and research leadership – wind is in the rare position of being able to satisfy all these requirements”* [17].



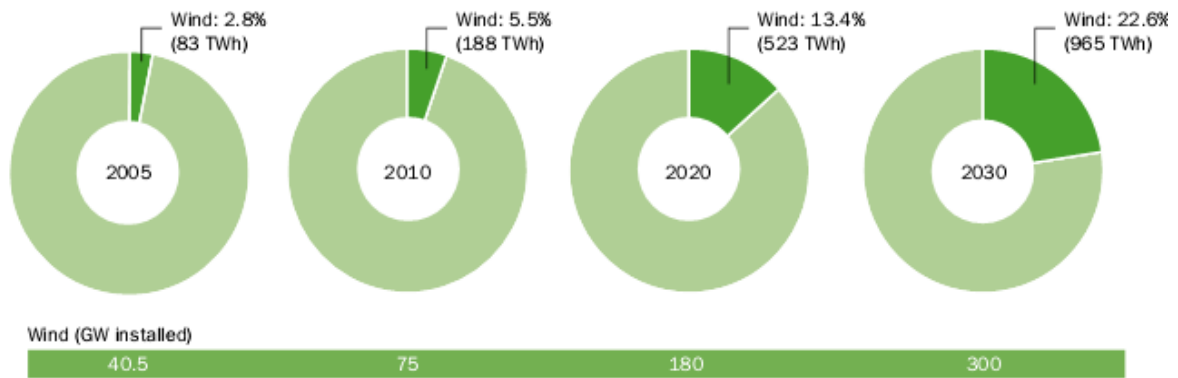


Figure 2.3 - Contribution of wind energy to European electricity consumption 2005-2030. [17]

## 2.3 Research Scope and Research Question

There are two main queries to be discussed: what is the situation of composite assembly methodologies in the development of “environmental friendly” structures and how can the bonding technology be improved? Lightweight materials are means to achieve these improvements; this is a research and a marketing opportunity. In fact, the European wind industry employs 192000 people [18]. By consequence being part of the manufacturing process or development of any of these industries can imply:

- more research opportunities (there are several developments in this area);
- and better industrial opportunities (because this is a growing market).

However, the opportunity in this case comes from the limitations, as is the case of assembly processes, which is one of the critical aspects of composites. Reliable and efficient designed bonded joints can be an answer and a tool to achieve the goals defined for the future. In fact, if the bonded technology is improved, it can be a way to achieve even more weight reduction, which implies more efficient behavior for lightweight structures. In other words, the intention of this thesis is assist the answer of:

- **How can bonded joints perform better in a structure, during their life in-service?**

So, what is a structure and how to address it? A structure is something built by aggregating different elements and defining complex relations between them. But it can also be seen as a product, as something that is built with a purpose and that it is going to be sold in the market. The quality of the bonding technology will have an impact in the structure, i.e., an airplane or a blade, with direct consequences to the customers and their lives.

Taking this into account and the research question, the main scope of this thesis is to address bonding technologies for composite structures, where there is a strong relation between management (production) and performance of the product itself. Figure 2.4 shows the relations drawn between performance, design and manufacturing process; finally, showing two questions open that motivate this work. In fact, a case study was made to learn about process-property dependencies and process improvement. In addition, static and fatigue fracture characterization were performed in order to better understand the behavior of composite bonded joints under different loading modes and its influence on the life in service. The final outcome will be an overview of the performance mainly focusing in the fatigue behavior and on its impact concerning the applicability of composite bonded joints in the industry. All these points create a set of relations that can be included in a management system. In general, the proposed relations drawn in this thesis are made to create a reliable basis for future work in any horizontal or vertical project involving bonded technology and to help defining the Product Life Cycle of a structure.

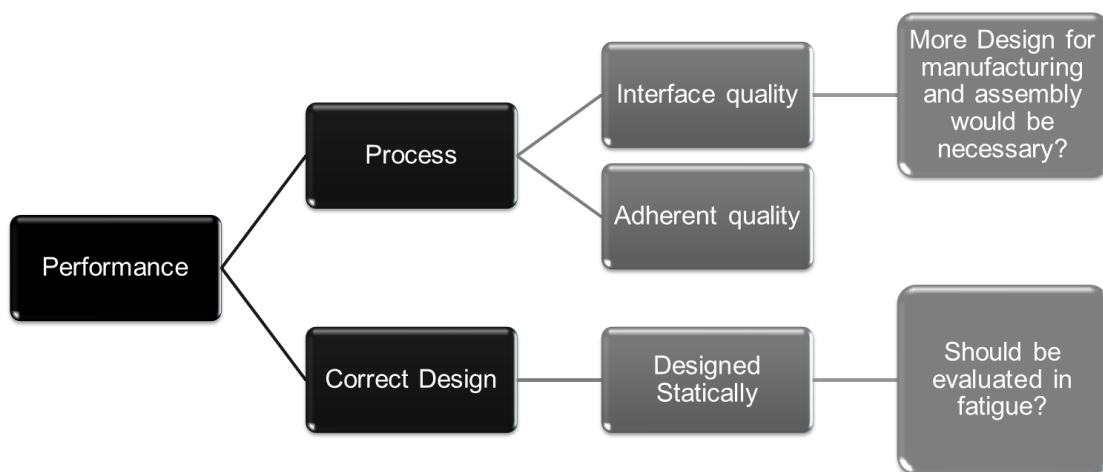


Figure 2.4 – Required interaction to address properly the behavior of bonded joints.

### 3 Product Life Cycle Management

Products can be broadly categorized as market-pull products or technology-push products. With a market-pull product, the marketing center of the company first determines that sales could be increased if a new product is designed to appeal to a particular segment of its customers. A technology-push begins with a technical breakthrough, as it opens the way for a new product. A good example of technical breakthrough is the aircraft industry, where developments have been done by prior guaranteeing a mature technology. In fact, the technology used for civil aircraft is not “*scientific developments state of the art*”, but more, reliable and mature state of the art. While military aircraft have different requirements and

certification processes, allowing a different development. To address also the wind energy industry, it is coming to a period where this industry will define its own technological improvement and it will follow its own technical breakthrough. In many cases, the technology itself may not point to a particular product, but instead, to new capabilities and benefits that could be clustered in a variety of ways to create a number of different products [19], [20]. In fact, bonded joints have enough maturity to be applied in some products like cars, tools, wind mills. Others, i.e., aircraft industry, have several limitations to use this technology.

In terms of development, a product can be **complex, if it is a sum of assemblies and sub-assemblies leading to the final structure of the product** (example: airplanes, cars, blades, etc.). For these products the way to manage development is important because:

- knowledge of the behavior becomes a key tool to understand the actual capabilities of the designed structures in real life services;
- it reduces the risk with well and broad lessons learnt data base;
- it helps identifying links between problems in services and design or manufacturing limitations.

Product Lifecycle Management (PLM) appeared as a solution in the late 1980s, when engineers understood the increase in the amount of information they had to deal with, like CAD (Computer Aided Design) systems [21] and with the improvement of the information technologies [22]. Sääksvouri and Immonen [23] stated that *“PLM does not refer to any individual computer software or method. It is a wide functional totality; a concept and set of systematic methods that attempts to control the product information.”* In other words, it is a systematic way of managing information by controlling all the tasks of product development and the information produced. In general, the idea is to guide the information along the process on how to handle it and then to storage. According to the definition by Kenneth McIntosh [24]: *“Engineering data management – EDM (currently the appropriate acronym would be PLM) is a systematic way to design, manage, direct, and control all the information needed to document the product through its entire lifespan: development, planning, design, production, and use”*.

The product life cycle (Figure 3.1) starts with the definition of a Concept (Phase 0: Concept Development) and finishes when a product reaches the end of its service life (Disposal/Recycling) (Figure 3.1). In fact, Thimm et al. [22] also considered marketing requirements where the expectations of the customer analyzed in detail. In the first stage materials, material properties and their technologies are taken into account to see how they

match with the requirements. After, the developments, the process goes through the prototyping, it can be considered as the interface between the development and the production. The next stage (Phase 1 - Manufacturing) is the product manufacture. This is related to the maturity of the process and the profit, i.e., as the learning curve increases the profit increases as well. In the distribution stage, the delivery stage is taken into account, and it is where the service life begins (Phase 2 – Life in service). Finally, the product is used and it has to be maintained until a certain moment in its life service where it has to be taken out of service. At this point, it can be recycled as raw material or part, remanufactured to be something else, the same part (but corrected) or disposed in a landfill.

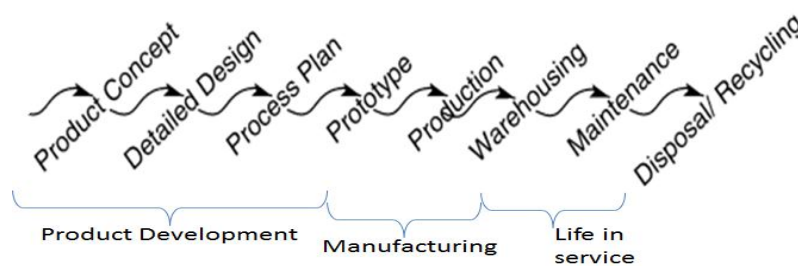


Figure 3.1 – Product life cycle [22].

Whatever the product is, the main goal of PLM is to reduce the risk when making the development of a product or selecting a technology to be used in it. In fact, technology selection is normally addressed in the concept phase and the detailed design. Therefore, all the technologies, the material properties and the behavior of the product are forecasted in the Product Development (PD) process mainly during the detailed design. Normally, the selection process is based on previous experience knowledge and on potential benefits. In fact, it is a commitment between risks and benefits, done during PD, that shows its results when the product is in service. It has to be proven proper while the prototype is tested and it has to be reliable during its life in service.

Concerning the application of bonded joints, the idea of using bonded technology shall be defined during the PD. A technology can be proposed in the concept phase, when the rough design is being done. During the detailed design a proof of concept and a proof of performance can demonstrate the expected outcome. This is particularly important because the knowledge database for bonded technology is limited. In general, it is considered that the larger knowledge of a technology diminishes the risks because there are less unknowns. Depending on the industry, some can take a higher risk but in general they all take moderate risk (Figure 3.2) as a baseline for decisions.

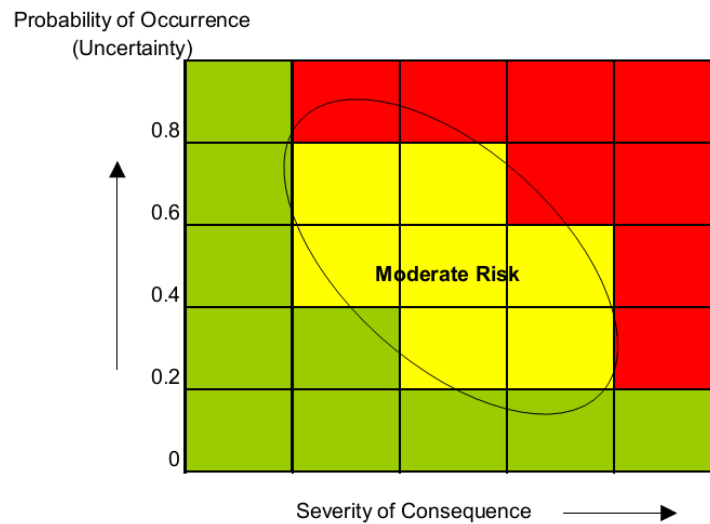


Figure 3.2 – Risk Matrix [25].

### 3.1 Product Development

Product Development (PD) is, in fact, one of the most important tasks in the entire life of a product. It is a sequence of tasks employed by an enterprise to conceive, design and commercialize a product. Many of these steps are intellectual and organizational rather than physical [19]. In other words one of the current challenges for companies is the need to design new products and get them into the market at the proper time, not only with good performance but also with higher perceived value than its competitors [26]. In fact, Takeuchi and Nonaka [27] in 1986 already addressed that companies need to be flexible and quick in developing new products to excel relative to other companies. PD should be predefined and well-managed to ensure a consistent success of all projects/processes. Table 3.1 has the main improvement options in different subjects [19]. Hence, within the globally scaled scenario, product management is composed of complex, overlapped processes [28] where success is mandatory.

Along history, PD process has evolved to real complex scenarios where multidisciplinary teams have to work together. Initially, it was a Non-system approach where there was no concern for interaction, upgrades, changes or customer needs. In other words, different domains (design, manufacturing and marketing) were not taken into account and linked together, taking only manufacturing into account. PD evolved then to a Systems approach where the knowledge of several domains, like manufacturing, design and marketing, contributes various concepts to PD in different fields (Table 3.1): *Systems Engineering*, *Systems Architecture* and *Systems Analysis*. For the case of PD, *Systems Engineering* deals mainly with the requirements, the concept generation and evaluation (how the system performs). It deals with the benefit-risk trade

process (trade-off analysis). *Systems Architecture* defines the top-level systems perspective and interactions with “environment”. In other words it defines the boundary conditions and the scope of the system. Finally, *System Analysis* is the actual analysis of the prototype in the scenario defined by the boundary conditions (*System Architecture*) with the input of the requirements and the general concept (*System Engineering*). It involves market analysis, cost analysis, risk analysis, etc. and shall perform in the sense to foresee the outcome of the product when released into the market (e.g. Clark and Fujimoto Model [29] or Generic PD [19]).

**Table 3.1 – Improvement options in the different fields related to product development [19].**

<b>Fields</b>	<b>Improvement</b>
<b>Quality assurance</b>	It specifies the phases a development project will pass through and the check points (objectives to be match) along the way. When these phases and checkpoints are chosen wisely, following the development process is one way of assuring the quality of the resulting product.
<b>Coordination</b>	A clearly articulated development process acts as a master plan which defines the roles of each of the player on the development team. This plan informs the members of the team when their contributions will be needed and with whom they will need to exchange information and materials.
<b>Planning</b>	A development process contains natural milestones corresponding to the completion of each phase. The timing of these milestones anchors the schedule of the overall development project.
<b>Management</b>	A development process is a benchmark for assessing the performance of an ongoing development effort. By comparing the actual events to the established process, a manager can identify possible problem areas.
<b>Improvement</b>	The careful documentation of an organization’s development process often helps to identify opportunities for improvement.

Brown and Eisenhardt [30] defined three streams of research: PD as a **Rational Plan, Communication Web and Disciplined Problem Solving**. The **rational plan** defines “that successful PD is the result of (a) careful planning of a superior product for an attractive market and (b) the execution of that plan by a competent and well-coordinated cross-functional team that operates with (c) the blessing of senior management”. It mainly focuses on the financial part of a product, when this happens normally the performance measurement are profits, revenue and market share. These studies are often exploratory and their perspective is broad. **Communication web** has evolved from the pioneering work of Allen at MIT (1971, 1977) who stated that communication is the center, and that the better the links between the members and key outsiders are, the more successful the development process will be. “These studies emphasize depth, not breadth as in the rational plan, by looking inside the “black box” of the

*development team*" [30]. The third is **Disciplined Problem Solving** that evolved from the Japanese practices in the 1980's. The formula for success, in these models, relies in a balanced activity between relatively autonomous problem solving teams and the discipline of a *heavyweight* leader and strong top management. This last category clearly assumes a system approach, where the result is a fast, productive development process and a high-quality product concept [30]. In this context, the design function includes engineering design (mechanical, electrical, software, etc.) and industrial design like aesthetics, ergonomics and user interfaces. From the manufacturing point of view, the design function is primarily responsible for designing and operating the production system in order to manufacture the product, while marketing and environment (like country policies or regulations) define boundary conditions and interactions between customers' expectations and needs, and product opportunities and limitations [19].

In general, PD can be considered the nexus of competition for many firms as well as the central organizational process for adaptation and renewal. It is critical to the viability of the firm, yet it is challenging to understand [30]. Stark [31] has established that the best way to gain these advantages is by (1) improving internal and external efficiency, reducing all the non-relevant costs and (2) fostering innovation of product, process and organization [28]. According to these needs, enterprises are refocusing on their core competences, while the product is becoming again, after the 1990s new economy experiences, the enterprise value creator and the whole production process is reassuming its role.

These systems approach and technology development theories have been the baseline for this thesis. They have been used to define the main requirements, needs, tools, results and the final evaluation of several different subjects as a whole. In fact, some of the requirements came from the aircraft industry while the actual application is from wind blades (manufacturing process). The aircraft industry presents a long history of controlling and defining requirements for a complete scope of behaviors and this makes a baseline for the analysis of the requirements. In terms of manufacturing wind blades present a recent history and represent a successful application which can be considered a good baseline for bonding application.

It is important to remember that problems and limitations in a joining technology are particularly important because it is considered as a "*weak link*" where several materials can be in contact, making a standard analysis more complex. As a consequence, understanding how the product development process is done and when the decision is taken can give the missing

inputs to standardize the application of bonded technology in high performance structures. In fact, concurrent engineering and systematic product development can give the first input. On the other hand, industries like wind blades or aircrafts have invested in research based on the outcome of this development process, driving their motivation and efforts towards a specific direction. For that reason concurrent engineering and engineering systems have been used to improve the structures along the life cycle of the product.

### 3.1.1 Concurrent Engineering

Concurrent Engineering (CE) was developed in the 80's in Japan, by Honda, as a joining technique to use the methodologies already available at that time. The main goal is to provide methods and tools that allow the development of products with high perceived value, in all the stages of the product's life in a short period of time [32]–[34]. Although this is not a new concept, it has received a boost from newly developed information technologies like the Internet and tools derived from Artificial Intelligence.

CE is based in *“Developing functional products appealing to the public, in a short period of time, with the minimum cost, with the objective of improving the life quality of the end user”* [34]. In addition, the aircraft industry has seen this as an opportunity to reduce the lead time of aircraft development. CE nowadays is based in computerized systems and, as the majority of those systems, its main purpose is to treat the complex information available and present it in a simple way taking into account synergies [33]. The definition that better suits this idea is: *“Way of working based in information systems and founded with the idea of converging or concurring the information regarding the complete cycle of the product that is being developed”* [34].

Considering the evolution of PD along the time, the difference between generic PD (Figure 3.3a)) and CE (Figure 3.3b)) is time oriented, where one function should be prepared before the predecessor ends. Figure 3.3 shows the different timeline for both approaches. The advantage of CE is mainly related with delays and costs incurred when a late change in the design has to be done (Figure 3.4).



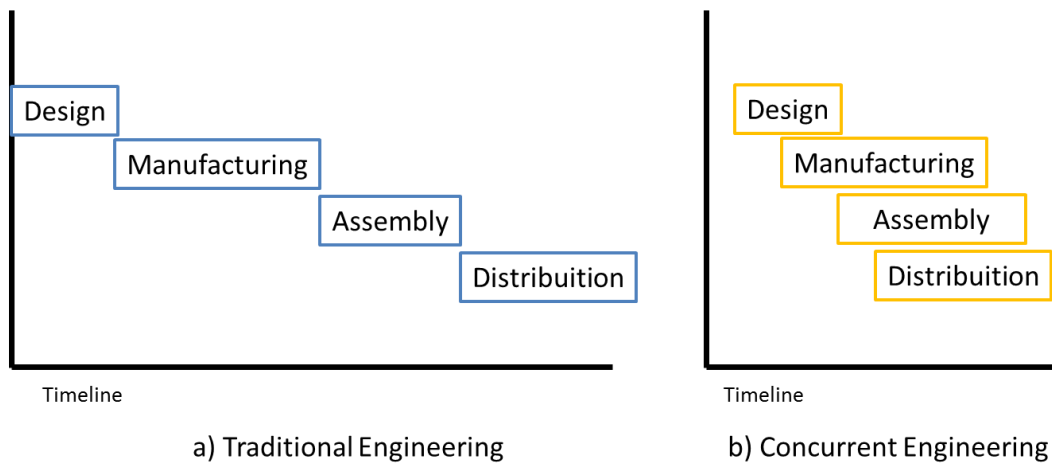


Figure 3.3 – a) traditional engineering; b) concurrent engineering [33].

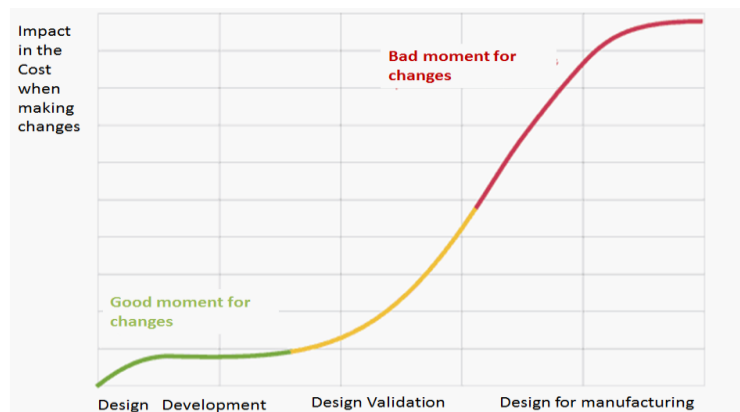


Figure 3.4 – Relative scale of the costs when a changing of the design is necessary in the different PD phases [34].

It is important to remember that the assembly and distribution are determined at the beginning of the development, taking into account the time needed to ramp-up all these stages and the necessary quality. In the concrete case of aircraft industry, time span for the assembly ramp-up allows the overlap with distribution because the first aircraft is delivered several months before the second.

As already mentioned, CE has been implemented in the aircraft industry as an opportunity “to overlap the work with much reduced overall timescale and better integration by use of multidisciplinary teams” [35]. Figure 3.5 shows the relations to aircraft development, where the time is shortened by shifting the manufacturing process inside the detailed design. This also helps to identify the problems regarding the manufacturing ramp-up sooner and to have the aircraft for the first flight faster. In this case, the development of maintenance techniques starts prior any aircraft is in-service, due to regulations. This information is taken from airlines’ experience and fatigue full-scale tests (which starts some time before the 1<sup>st</sup> delivery) [36].

With them, the inspection periods and some suitable standard repairs are defined. Actually, the aircraft can only be certified if the first inspection periods are decided and the conceptual repairs are frozen.

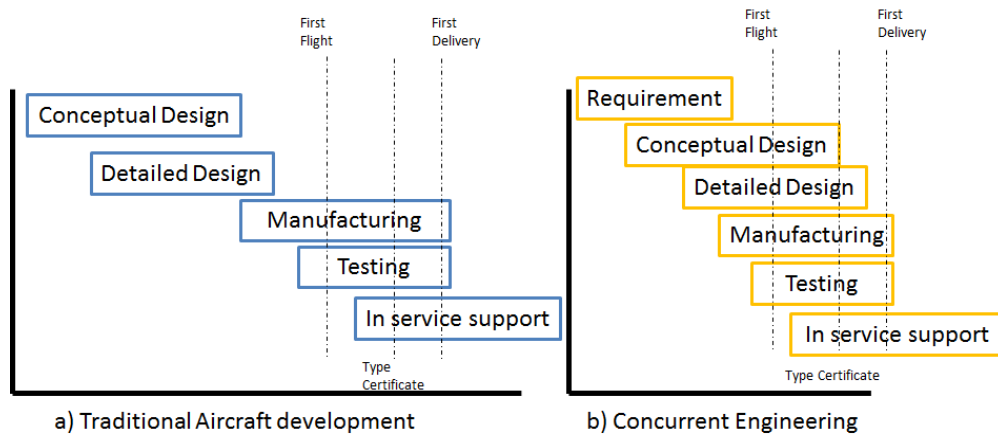


Figure 3.5 – Comparison between traditional aircraft development and concurrent engineering development [35].

CE is only achievable when, inside product development is not only considered the product but the life cycle of it. This method involves all the people and resources in the life cycle of a product. It is the responsibility of the team and all the important decisions should take into account the information available from suppliers and subcontractors [34].

For bonding technology, if this methodology is applied in the research prior to development, several issues can arise before the technology is put in service. For this work, CE was used as baseline to understand how the research shall be done and what can have an impact in the in-service performance of composite bonded joints. In addition, this methodology was used because there are several interactions between the different domains that have to be analyzed. Therefore, to complete the work, a systematic product development approach was analyzed, to find tools and methods to better understand how to relate the development process with the life in service of any high performance structure.

### 3.1.2 Systematic Product Development

One of methodologies for organized and prioritized PD was developed by Clark and Fujimoto [29]. This methodology was developed based in the automotive industry and considering complex product assembly [29]. They defined the PD process mainly from the technical point of view. Following their perspective the PD process can be viewed as the transformation of the data about market opportunities in technical information for the manufacturing process. Figure 3.6 presents the proposal of a generic sequence of detailed activities for a product

development. Their main four stages are concept generation, product planning, product engineering and process engineering [30], [37], [38]:

1. Concept Generation: it is focused on the objectives of the customer. In fact, it tries to define, simulate and analyze the customer's interest and preferences. It focuses as well in the technical facilities and the economic sustainability and it is this interpretation of the market that is materialized in the concept.
2. Product Planning: it is defined as a detailed project, where the concept defined is transformed in technology, costs, layout, specifications, etc.
3. Product Design: the main focus is to install the technical plan (engineering needs) defined in the previous stages. It is normally composed by: project, manufacturing and testing.
4. Process Design: this is the way to transfer the details of the product to the way how it is going to be built (process). All the information about the project is transformed in tools, software, and training for the shop-floor workers. For a proper integration, a general consistency standard has to be defined which includes organizational structure, qualification of the working teams and the involvement of the suppliers during the development process.

This development process has been mainly focused in quality, speed and productivity. In fact, Clark and Fujimoto introduced product integrity in their model. It (product integrity) can be internal which *"refers to consistency between the function and structure of a product – e.g. the parts fit together"* or external, when *"it is a measure on how well a product's function, structure, fit the customer's objective"* [29]. In fact, this is a standard practice in aircraft building. Anyway, it shall be a baseline for several structures where complex customer needs, general requirements and technological limitations are joined.

Clark and Fujimoto's methodology represents one systematic approach for PD. The different dimensions taken into account were the first steps to what is understood as PD nowadays, where not only manufacturing is studied when a new product is developed.

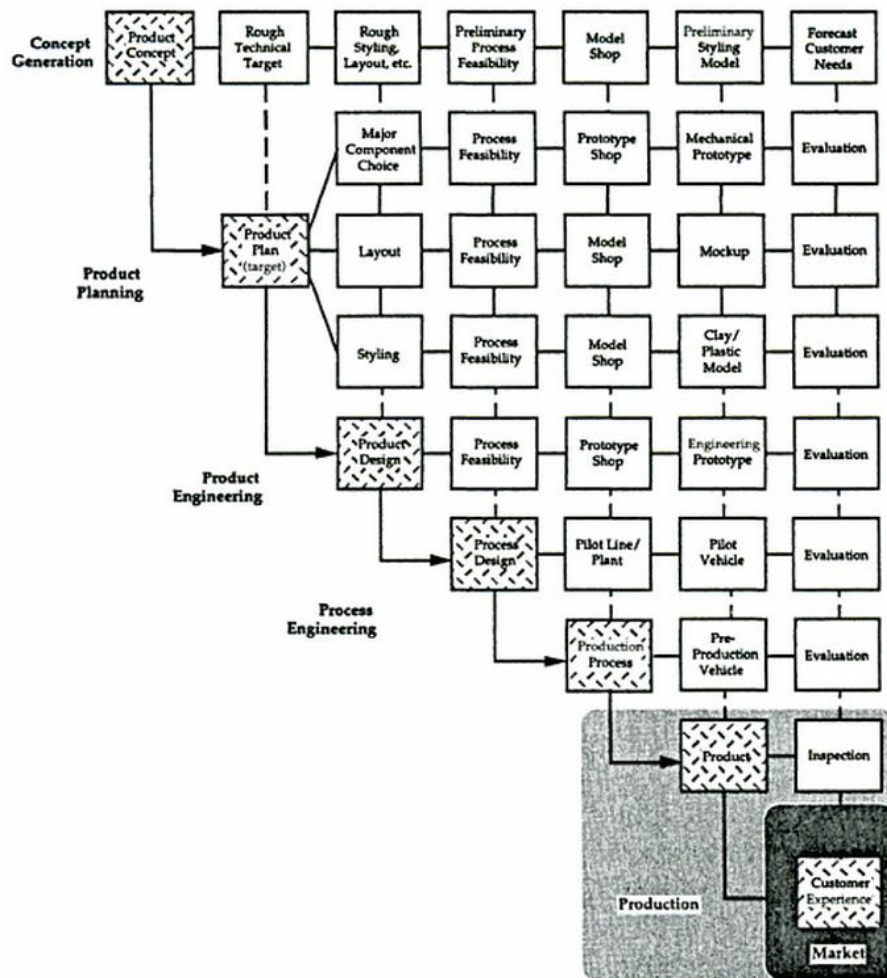


Figure 3.6 – Clark and Fujimoto PD information map [29].

### 3.1.3 Systems Approach

Going into detail in the systematic PD, different perspectives shall be included, i.e. customer need, manufacturing, performance, etc., systems engineering appeared as a grand unified theory with the purpose of making things work better. It is the generic approach used for the **Disciplined Problem Solving, and the basis for nowadays Product Development (PD)**. It is considered as an interdisciplinary process that ensures the customer's needs are satisfied throughout a system's entire life cycle [39]. Basically it can be used to all the Life Cycle or only during some phases, because it can define ways to separate and link different subjects. According to Senge [40] *systems thinking is a discipline for seeing wholes. It is a framework for seeing interrelationships rather than things, for seeing patterns of change rather than static "snapshots"*. The International Council on Systems Engineering (INCOSE) defines **Systems Engineering as an interdisciplinary approach and means to enable the realization of successful systems. It focuses on defining customer needs and required functionality early in the development cycle, document requirements, then proceeding with design synthesis and system**

validation while considering the complete problem. Systems Engineering integrates all the disciplines and specialty groups into a team effort forming a structured development process that proceeds from concept to production to operation. Systems Engineering considers both the business and the technical needs of all customers with the goal of providing a quality product that meets the user needs [41]

In fact, systems theory is a valid option for multidisciplinary research in technology development. The ideas behind the CE and PD can be used to analyze and better understand a technology. In this work, this has been applied by using one approach to the bonded technology (SIMILAR Process).

### 3.1.3.1 SIMILAR Process

Bahill and Gissing [39] developed a re-evaluation methodology for engineering systems using a systematic approach, and this process is known as SIMILAR (Figure 3.7). Actually, it has been defined in INCOSE (International Council on Systems Engineering) by consensus as a widely accepted approach [41]. In fact, the first two steps, **State the Problem** and **Investigate Alternatives**, are part of *Systems Engineering*, where constraints and options are defined as a function of the requirement. The third and fourth, **Model the System** and **Launch the System**, are *Systems Architecture* where the environment, where the system will work, is clarified. The last step, **Assess Performance**, is *Systems Analysis* where the intention is to verify if the assumptions and the scenarios modeled in the steps before give the expected results. From the PD perspective, this system can run as a loop until a final prototype is obtained or the product is placed in service. The end depends on the preliminary definition of the expected outcome at the beginning of the product development. The SIMILAR process generic description is presented in the points below.

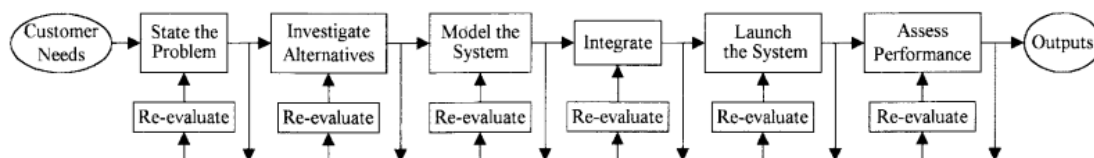


Figure 3.7 – SIMILAR Process [39]

1. *State the problem.* Stating the problem is the most important systems engineering task. It entails identifying customers, understanding customer needs, establishing the

need for change, discovering requirements and defining system functions [20], [21]. In fact, the term *customer* and *stakeholder* include anyone who has a right to impose requirements on the system [42]. In an engineering environment the problem starts with a top-level function that the system must perform. This includes all the requirements the system must have. It has to be stated in terms of **what** has to be done and not how [39]. Inputs come from end users, operators, regulatory agencies, marketing, manufacturing, etc. Nowadays the problem statement starts with a reason for change followed by vision and mission statements for the company, but in subsequent interactions goals are defined [39].

2. *Investigate alternatives.* Alternatives are investigated and evaluated based on performance, cost and risk figures of merit [42]. From the engineering point of view, this is multi-criteria assessment, where decision aiding techniques should be used to reveal the preferred alternatives, and should probably be redone whenever more data is available. For design of complex systems, alternative designs reduce project risk. Investigating bizarre alternatives helps to clarify the problem statement [39]. In fact, some of these alternatives can be potentially valid scenarios to be modeled (even if they will not be used in the final solution). They can be used when the screening process has already started, as a change in the criteria available, to achieve the optimum route to the goal. In this work, the alternative is understood as different available technologies and how they are placed in two different scenarios. This means, different technologies applied to different products and/or different materials.
3. *Model the system.* Running models clarifies requirements, reveals bottlenecks and fragmented activities, reduces cost and exposes duplication of efforts. In an engineering environment, models will be developed for most alternative designs. The model for the preferred alternative will be expanded and used to help manage the system throughout its entire lifecycle. Many types of system models are used, such as physical analogs, analytic equations, state machines, block diagrams, flow diagrams, object-oriented models, mental models, and computer simulations. Running these models clarifies requirements, reveals bottlenecks and fragmented activities, reduces cost, and exposes duplication of efforts. In the business environment, models and simulations are run to analyze the process and find the *as is* and, through analysis, determine the *to be* [39].
4. *Integrate.* Integration means designing interfaces and bringing system elements together so they work as a whole. In fact, in this point all the subsystems have to be put together. This requires extensive communication and coordination [42]. Creating

the bridge between the different functions makes possible for the different subsystems to work as a whole. In fact, interfaces between them must be designed, as well as their natural boundaries. In general the defined interfaces should minimize the amount of information to be exchanged between the subsystems to prevent errors and mistakes. The most difficult problem in the business environment is assuring that all activities are totally integrated under a common direction or business plan that supports the vision/mission and goals [39].

5. *Launch the system.* Launching the system means running the system and producing outputs - making the system do what it was intended to do [42]. Considering Engineers, they produce design for a product and the process is embedded in the system that makes it possible.
6. *Assess performance.* Performance is assessed using evaluation criteria, technical performance measurements and figures of merit (FOM). FOM (sometimes called measures of effectiveness) are used to quantify requirements. Technical performance measures are used to mitigate risk during design and manufacturing. Metrics are used to help manage a company's processes [39]. In fact, **measurement is the key**: if you cannot measure it, you cannot control it. If you cannot control it, you cannot improve it [42].
7. *Re-evaluation.* Re-evaluation should be a continual and iterative process with many parallel loops. Even if all the loops are not used, feedback of the next step processes has to be analyzed to address how to improve or re-design if needed in the future [41].

### 3.2 Technology Development Process

The crucial objective of a lifecycle is to achieve a system that is “successfully” used in the “real world” and the decisions made in the development of this system must be made with that goal. Hence, the first point is to understand [43]:

- what success would be for the different stakeholders
- and what real world and “environment” will be the system exposed to.

In other words, the development of new product capabilities typically depends upon the prior success of advanced technology research and development (R&D) efforts [44]. Effectively, evaluating and managing science, technology risk and the maturation of critical new technologies is mandatory to the success of advanced technology systems development projects.

Systems that depend upon the application of new technologies inevitably face three major challenges during development: performance, schedule and budget. Research and Technology (R&T) programs typically advocate based on the argument that these investments will substantially reduce the uncertainty of all three dimensions [45]. There are a range of challenges, both organizational and methodological facing the technology assessment community. For example, achieving the right level of technology maturity across multiple subsystems is an ongoing challenge to development success of all advanced technology systems, establishing the right metrics for these technologies is essential. In fact this has to include a variety of figures of merit (FOM), like cost and performance, assuring the consistency of the assessment is critical to guarantee the success [44].

The ideal approach to technology readiness would involve the following characteristics: *Clarity* (the process would involve clear decision criteria for determining risks and maturity), *Transparency* (the process should be formal and consensus based but no over bureaucratic) and *Crispness* (the decision made during the development should be made by or with the ownership of senior management). They must be crisp, timely and keyed to annual R&D and system program budget planning requirements [45].

Actually from the development of CE systems also the development of technology has been understood differently. Several CE rules are being applied to the development and success of a technology. This has defined the maturity level in several ways. Several disciplines are taken into account. It can be design, manufacturing, performance, maintainability, value and risk. This could also be applicable for bonding technology. Depending on the industry different maturity levels can be presented, mainly because they come with the main requirements of the structures.

### 3.2.1 Technology Readiness Level (TRL)

The main purpose of this development process is to assess the maturity of evolving technologies prior to incorporate that technology into a system or subsystem. When a technology is first invented or conceptualized, it is not suitable for immediate application. Instead, new technologies are usually subjected to experimentation, refinement, and increasingly realistic testing. Once the technology is sufficiently tested, it can be incorporated into a system/subsystem.

Technology Readiness Level was introduced by NASA, in the mid 70's, as an independent discipline, with defined figures of merit (FOM) to allow a more effective assessment of, and



communication of regarding the maturity of new technologies [44]. It evolved through time (Figure 3.8) and Mankins [46] in 1995 wrote down the definitions and examples of the process.

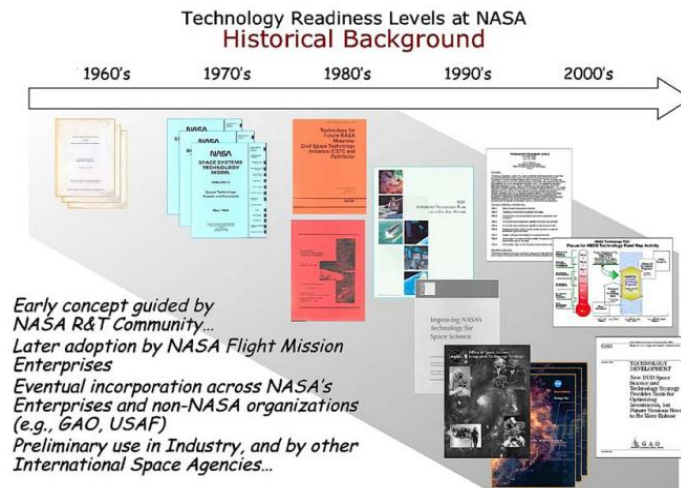


Figure 3.8 - Timeline for the emergence of the TRL scale [44].

The definition given by NASA of each step is presented below (Figure 3.9) [44], [46]:

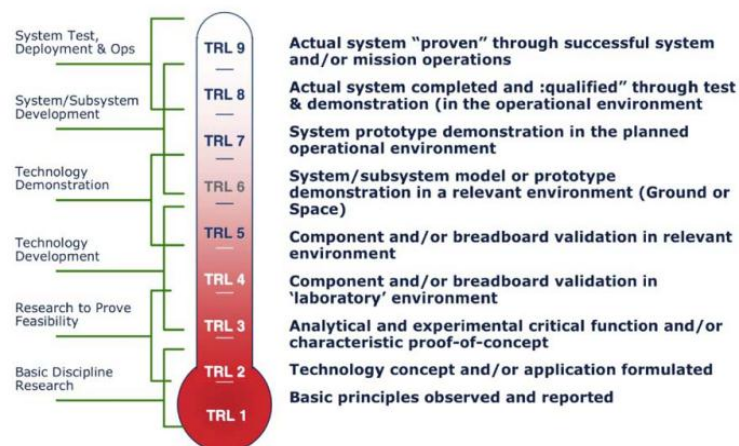


Figure 3.9 – Overview of the TRL Level scale [44].

**TRL 1** Basic principles observed and reported: Transition from scientific research to applied research essential characteristics and behaviors of systems and architectures. Descriptive tools are mathematical formulations or algorithms.

**TRL 2** Technology concept and/or application formulated: Applied research. Theory and scientific principles are focused on specific application area to define the concept.

*Characteristics of the application are described. Analytical tools are developed for simulation or analysis of the application.*

**TRL 3** *Analytical and experimental critical function and/or characteristic proof-of-concept: Proof of concept validation. Active Research and Development (R&D) is initiated with analytical and laboratory studies. Demonstration of technical feasibility using breadboard or brassboard implementations that are exercised with representative data.*

**TRL 4** *Component/subsystem validation in laboratory environment: Standalone prototyping implementation and test. Integration of technology elements. Experiments with full-scale problems or data sets.*

**TRL 5** *System/subsystem/component validation in relevant environment: Thorough testing of prototyping in representative environment. Basic technology elements integrated with reasonably realistic supporting elements. Prototyping implementations conform to target environment and interfaces.*

**TRL 6** *System/subsystem model or prototyping demonstration in a relevant end-to-end environment (ground or space): Prototyping implementations on full-scale realistic problems. Partially integrated with existing systems. Limited documentation available. Engineering feasibility fully demonstrated in actual system application.*

**TRL 7** *System prototyping demonstration in an operational environment (ground or space): System prototyping demonstration in operational environment. System is at or near scale of the operational system, with most functions available for demonstration and test. Well integrated with collateral and ancillary systems. Limited documentation available.*

**TRL 8** *Actual system completed and "mission qualified" through test and demonstration in an operational environment (ground or space): End of system development. Fully integrated with operational hardware and software systems. Most user documentation, training documentation, and maintenance documentation completed. All functionality tested in simulated and operational scenarios. Verification and Validation (V&V) completed.*

**TRL 9** *Actual system "mission proven" through successful mission operations (ground or space): Fully integrated with operational hardware/software systems. Actual system has been thoroughly demonstrated and tested in its operational environment. All documentation completed. Successful operational experience. Sustaining engineering support in place.*

The dimensions referred are actually addressed in each level. For example an idea has to be evaluated in the first TRL by defining the working principles and the main advantages. In TRL3 the manufacturing process has to be proven by the *proof-of-concept* and the performance has to be verified the *concept validation*. Passing TRL3 represents focusing on the requirement for an application and the relation to it by prototyping. Finally TRL7 and the rest represent the preparation to enter in service, by copying the operational environment.

The fact that is impossible to reach a certain maturity level without an application makes this methodology *product oriented*. It is mainly applied in aircraft and space industry but it can also represent a good assessment method for the bonding technology in general. In addition, it can be a driver to future research because one of the products presented here are airplanes.

In this work, the TRL methodology was seen as a tool to understand what industries are looking for. This means what they will invest in terms of research and how can they assess the outcome of the composite bonded technology in the overall product. In general, it can represent a baseline for the assessment of bonding technology in any product (airplanes and/or wind blades).

## 4 Technology Analysis of Composite Bonded Joints

Assessing the applicability of composite bonded joints in structures one of the firsts issues presented here. Considering aircraft regulation, it has been stated that multidisciplinary teams should be used to guarantee the success of the project [47], [48]. In fact, Advisory Circulatory (AC) 20-107B [47] of the Federal Aviation Agency (FAA), regarding composite materials in aeronautics, states in point 6.c (page 4) “*Structural bonding: ...Many technical issues for bonding require **cross-functional teams for successful operations***”. This makes important to considerer a systematic approach to improve the applicability of bonded joints in a long-term basis considering different domains.

The SIMILAR approach was used to better suit the analysis of the data. The tasks defined in section 3.1.3 are detailed here for bonded technology. Figure 4.1 shows the development of the thesis assumed as a system. The re-evaluate stage (R) is not included in Figure 4.1, because the re-evaluation was intrinsic to each stage. The first steps represent the definition of the thesis structure, while the others are shown during the development of the thesis. Making an analogy to systems theory and product development, the thesis structure represents the problem definition or the concept phase while thesis development is already the system

running or the design phase. Finally, all the work done is evaluated at the output (this can be equivalent to a “prototype”).

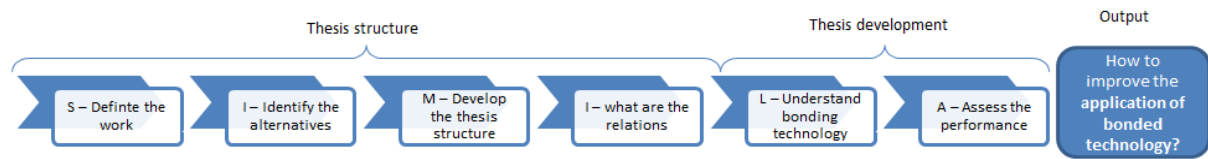


Figure 4.1 – SIMILAR process applied to bonded technology.

- The first step is to **define the work (State the problem)**; it is used to show the applicable products and their requirements. It addresses the scope of this work defining where the assumptions are applicable and what is intended to find out.
- Afterwards is the **identification of alternative technologies (Investigate alternatives)** in general joining technologies, which are equivalent to bonding.
- **Thesis development (Model the system)** is how the thesis was done and how information is presented in it.
- **What are the relations** represents the **integration**; it defines the links of a dimension (design, manufacturing, etc) with the others.
- **Understand bonding technology** is the system running (**Launch the system**), which in this case is presented along of the thesis;
- and **assess the performance** is the outcome of a case study and several experimental tests. The experimental tests were made to characterize fracture of bonded joints under fatigue loading.

These two final steps are interrelated, mixing the required information needed to understand bonding technology with the actual assessment of the results. In fact, there is no possible separation because the information presented in one section depends also on the other.

Identification of other technologies (section 4.2) was made as a baseline for comparison. It was used to set a picture in terms of needs, benefits, disadvantages and maturity in assembly and performance domains. In fact, in the PD process, it is normally done by choosing the appropriate technology for the product. As an alternative, the “readiness level of a technology” can be used to assess what should be obtained (in terms of performance or reliability), adapting the technology to the product. This tends to be a clear assessment between development, risk and the technology used. It is also important to take into account that some technologies can only be used when they are considered mature for the application, and thus, may need an investment to mature it, if they are chosen to be used in the product.

#### 4.1 Definition of the Work

The objective of this work is to increase the application of bonded joints in composite structures subjected to fatigue loading. Specifically, two industries are presented here: windmill and aircraft industry. The main reasons, to take these products into account are:

- both are complex structures subjected to fatigue loading effects;
- the structures are designed accounting for weight savings;
- amount of composite material used;
- the commercial interest which reflects on dedicated research;
- complexity not only as product but also in the requirements and behaviors, being a clear constrain related with strict regulations;
- and how the assessment is done not only to fulfill the expected requirements but also to improve the technology.
- Also wind blades present a full bonded structure and aircraft are performance and reliability oriented.

Considering the constraints of the application of bonded technology in structures, regulations play a key role in the success of a project. For example, in the aircraft industry those requirements have to be defined and checked by the authorities, to decide what is the expected performance and outcome for a certain type of aircraft. Figure 4.2 presents a sketch of the relations between aircraft developers and the regulation authorities.

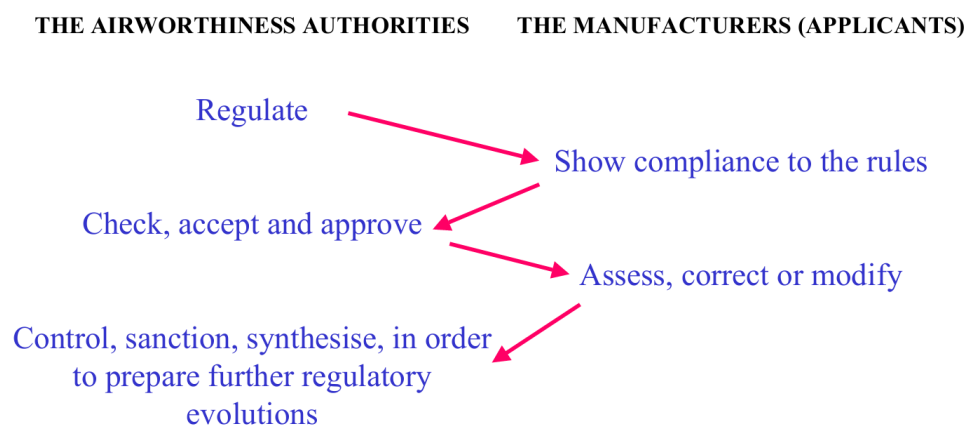


Figure 4.2 – The role of the main actors in the aircraft certification procedure [49].

There are two major types of documents for aircraft manufacturing, those are divided in regulations and guidelines:

*ATA Chapters:* This specification defines a widely-used numbering scheme for aircraft parts and the organization of printed aircraft maintenance information. ATA Spec 100 contains format and content guidelines for technical manuals written by aviation manufacturers and suppliers and is used by airlines and other segments of the industry in the maintenance of their respective products. This document provides the industry-wide standard for aircraft systems numbering, often referred to as ATA system or chapter numbers [50], [51].

*Regulations:* Each country has its own regulatory agency and its laws. In Europe, it is EASA (European Aviation Safety Authority) where the applicable regulation is defined by the Acceptable Means of Compliance (AMC) [52]. In USA, it is FAA (Federal Aviation Agency) where the regulation is presented by the FARs (Federal Aviation Regulations), in the Code of Federal Regulations (CFR) [53]. There is still the JAR (Joint Aviation Requirements) which defined a unified regulation with the one developed in the USA. These were developed by the JAA (Joint Aviation Authorities) that was superseded in 2009 by the EASA, leaving only the open training organization [54]. In general, they present the regulation divided by codes and are applicable by type certification, i.e., by type of aircraft.

The guidelines are normally presented as AC (Advisory Circular). They have several recommendations and issues raised by the authorities. These documents are guidelines to achieve certification.

The recommendations and rules for composite materials are focused in the performance of the product and the quality of the process. The performance shall guarantee the life in-service through all expected conditions and in the case of damage. Figure 4.3 shows a tree diagram with the main actions/parameters used to fulfill the requirement for an aircraft. They are mainly related with reliability, to guarantee that calculations and approximations are in agreement with the expected outcome. It is proved with the first flight test of an aircraft type. Also the in-service requirements are addressed, like predicted maintenance periods that can be adjusted, as airlines' experience increases.

The requirements from the clients are price/cost and quality oriented. The price is transformed in costs for the manufacturing company and can be addressed as the costs of developing a new aircraft or manufacturing it. The rest of the costs depend on several criteria, being the main: fuel consumption, maintenance/inspections and repairs. For example, any structure has to be able to sustain limit load without failing, for a limited period of time. The assumptions made along the development must prove their validity by testing procedures.

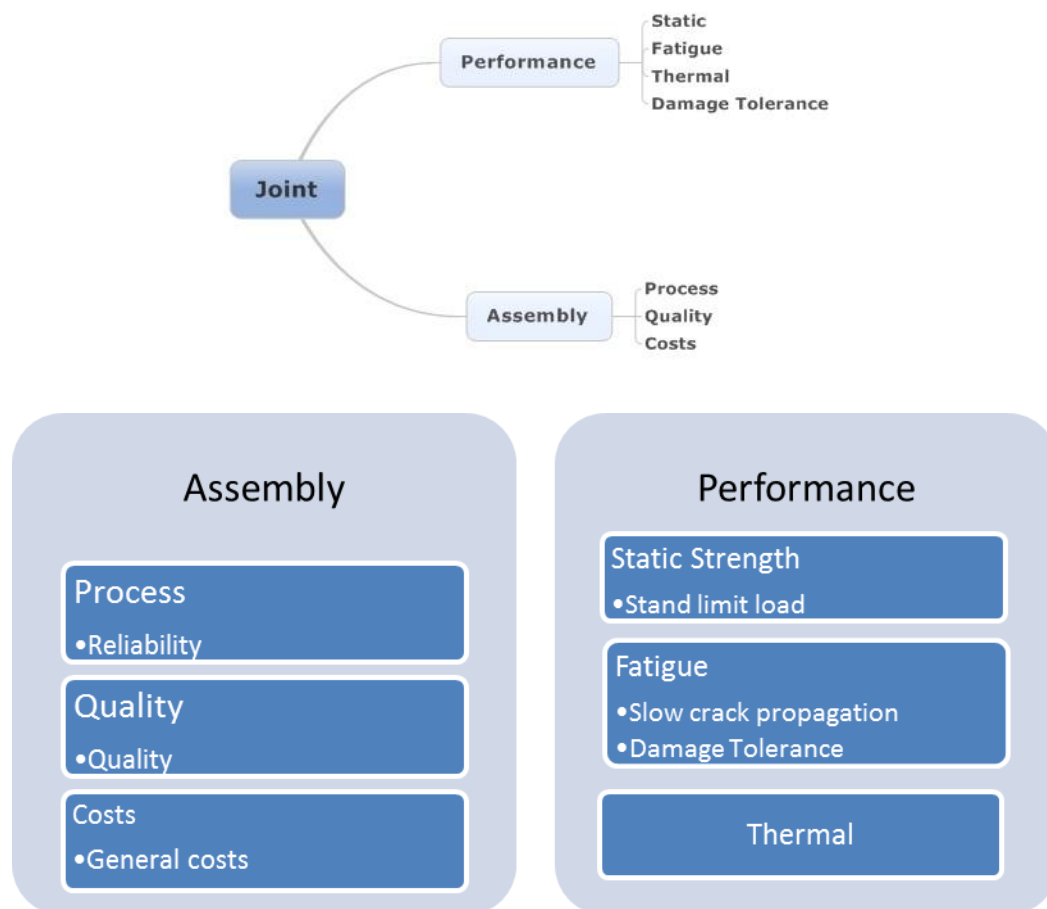


Figure 4.3 – General Parameters that make possible to fulfill the requirements for an aircraft.

## 4.2 Identification of Alternative Technologies

Considering that the proposed system is to assess the bonding technology as a joining procedure in building structures. The alternatives to this technology are normally bolted and bonded + bolted (State of the Art to ensemble aircrafts). This is not really to assess the best performance, but to understand what technology fits better the needs and expectations of the customer. The main idea is to compare these possibilities (bonded and bolted) in the two domains and summarize the relations between the advantages, limitations and applications. In fact, the intention here is to make a fair summary on why and how the bonding technology can be applicable also in the aircraft building, if it fulfills the requirements. This was not assessed for the wind blades because bonding is already being used and there are no comparable alternatives.

### 4.2.1 Comparison Between Technologies

The major points of comparison between bonding and bolting technologies are the materials being joined and the reliability. Bolted joints represent a mature technology with a full hand of

NDT (Non-Destructive Testing) and general knowledge. Metals are less prompt to bearing failure and have fewer problems with the corrosion of the bolts. The bolts are normally from aluminum and sealants are used to close any “open space” between plates.

On the other hand, for bolted composite components, the parts (to be assembled) are already cured, which means if they do not match, it has to be machined or shimmed (it can damage the fibers) which is also a problem due to thickness tolerances (variation of the thickness). This variation of the laminate thickness usually occurs due to an inevitable uneven curing cycle and thermal residual stresses that are associated to exothermic reaction of the resin. Anyway, if the parts do not match, the components have to be repaired or rebuild (this is also applicable to secondary bonding<sup>1</sup>). In addition, bearing failure is also a problem. In fact, Hart-Smith [55] has developed a diagram with a parametric study of composite bolted joints taking into account different parameters. Figure 4.4 shows the assessment of the lay-up, considering the load transfer into the laminate. To prevent the bearing, a quasi-isotropic lay-up (0, 90,  $\pm 45$ ) should be used. Concerning the corrosion problems, special Titanium bolts have to be used to prevent it. Actually, the bolts are corroded by a galvanic pair, so isolating the bolts from the composite can also help.

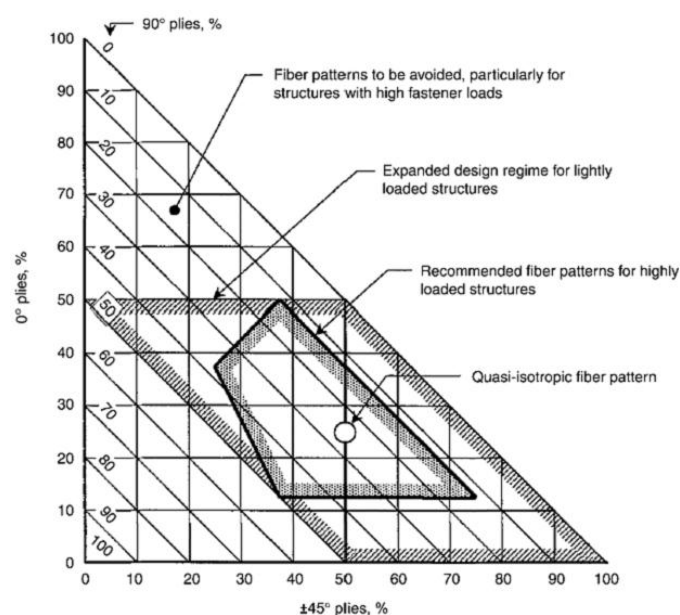


Figure 4.4– Selection of lay-up pattern for fiber-reinforced composite laminates. All fibers in 0°, +45°, 90°, or 45° direction. Note: lightly loaded minimum gage structures tend to encompass a greater range of fiber patterns than indicated, because of the unavailability of thinner plies [55]

<sup>1</sup> The definitions of the bonding process are presented in section II.1.2 - Composite Bonded joints: Manufacturing Processes & Technologies



For composite materials, the main advantage of bolting/riveting versus bonding is reliability, because:

- the defects are easily detected in bolted/riveted joints during visual inspection; additionally, the bolts are pre-selected (only the ones without defects are used);
- the technology is well known in almost any material;
- the failure normally occurs in steps; the stepped failure starts when one bolt/rivet fails and the others fail in sequence;
- the manufacturing process does not affect completely the performance, e.g., a hole done in the wrong place or a bolt/rivet incorrectly placed does not affect completely the availability to withstand the load.

In fact, this last point is the main reason why bolting technology is nowadays being used in the aeronautical industry. All the points mentioned above make this technology a low risk application. Theories like multi-site damage [56] have been developed to enlarge the security margin of these joints under fatigue loading. They are largely used in the aeronautical industry [57], [58]. In this theory, several small cracks may coalesce to form a large crack, which may then progress fast leading to ultimate failure when the joint is not able to stand the required residual strength (limit load).

Considering the manufacturing process (assembly), bolted joints are mainly characterized by drilling, which is difficult, expensive and has significant recurring costs. Table 4.1 shows a summary of the comparison between the technologies. In fact, co-bonded presents much more advantages: the fresh laminate can be carefully laid-up, in a proper mold, to match the cured surface without inducing extra stresses because it is joined while curing (this means no extra curing cycles). The time used for assembly is the same used to cure the second part, which makes the process quicker. In addition, there is no need for drilling a hole, which makes the utilization of other non-quasi isotropic lay-ups possible. For these reasons, co-bonded technology has more potential to make the process less expensive. On the other hand, secondary bonding depends on the electricity costs, because there is a need for a third curing cycle. Indeed, for riveting the costs are affected by the usage of expensive rivets or bolts (titanium), special tooling to drill the holes and long hours of work. Titanium bolts are used to avoid corrosion problems. Special tooling has to be used to avoid damage in the fibers and delamination [7]. For bolting/rivet, the process can be automated which transforms the drilling in operation time and it makes possible not to account the labor.

Finally, the limitations that have prevented, up till now, the larger utilization of bonded technologies in the aircraft industry are related to insufficient bonding due to surface problems, like incompatible peel-ply or contamination. The CS (Certification Specification) 25.601 defines *“the aeroplane may not have design features or details that experience has shown to be hazardous or unreliable. The suitability of each questionable design detail and part must be established by tests. In fact structured product and process development is imperative to successful product design and complete fulfillment of all the requirements”*. The technology has to be mature enough, guaranteeing its application in the aircraft industry and to prevent these problems from occurring. This is actually what research is looking for, a reliable technology to increase the amount of bonded joints.

**Table 4.1 – Comparison between different joining mechanisms [59].**

Parameter	Secondary Bonded	Co-bonded <sup>2</sup>	Bolted/rivet
Surface preparation	Extensive	Extensive	Easy/not mandatory
Joining of dissimilar materials	Good	Good	Limited
Added weight to structure	Low	Low	High
Fatigue resistance	High	High	Poor
Corrosion resistance	High	High	Poor
Inspection by NDT	Very limited (due to kissing bonds)	Very limited (due to kissing bonds)	Adequate
Ease of disassembly	Difficult	Not possible	Easy <sup>3</sup>
Resistance to degradation by environment	Poor	Poor	Poor
Time to assemble	Slow	Quick	Slow

#### 4.2.2 Comparison Between Structures

Any technology is applicable to different products (in this case structures), with different conditions but using the same principles, most of the times. For this reason, in some structures a technology can be successful and used everywhere, and in others it can be a complete “disaster”. In this scenario, the alternatives considered shall not only address the equivalent technologies but also the potential applications. By consequence, blades and aircrafts shall be analyzed; to understand what kind of structure and in-service conditions are behind this potential application. This is important because applying a suitable technology in a product does not mean it will be successful in another product. In general, structures depend on

<sup>2</sup> The definitions of the bonding process are presented in section II.1.2 - Composite Bonded joints: Manufacturing Processes & Technologies

<sup>3</sup> When using bolts, they can be disassembled but in the case of rivets, it is not simple. Larger holes have to be done to remove them and this is limited by the tolerances, which means that it cannot be always done.

successful application of the technology that best suits their demands in-service and in-service conditions depend on the type application. Table 4.2 shows a comparison between wind blades and aircrafts.

**Table 4.2 – Comparison between wind blades and aircrafts.**

Point to be addressed	Aircrafts	Wind Blades
Size and Design	Aircrafts are designed as a junction of several smaller parts. They are much smaller than a blade. The main structures are designed in terms of fail-safe and damage tolerance.	These are designed in term of complex bonding processes. Several materials are inside each part, e.g. the shells have foam, balsa, GFRP and resin. The main structure is defined to be flexible enough to move with the wind but without touching the other blades or the tower.
Components	The components joined with different technologies. It is normally divided in sub-assemblies and assemblies due to the complexity. Their structures are categorized taking into account the airworthiness.	All the subcomponents in the blade are bonded. It is fully composite materials where several lay-ups are used, taking full advantage of the orthotropic properties. It can be equivalent to the wing of an aircraft.
Maintenance	Aircrafts are designed to be inspected and maintained, fatigue and damage tolerance analyses are mandatory.	These structures are designed to avoid crack propagation. Inspection and maintenance costs are high, they are also limited due to weather conditions – e.g. moisture or a windy environment does not allow to perform a repair or inspection.
Safety and Risk	In this industry the risks have to be avoided and anything that can jeopardize the safety is not allowed.	For wind blades, safety and risks are necessary but not mandatory. Several risks can be taken without jeopardizing the performance.
Environmental Conditions	They are designed to be used in a wide range more or less from - 50°C to + 40°C. In general, they are not allow to fly in unstable weather conditions	Wind blades are theoretically designed to support extreme windy conditions plus rain and -20°C to 40°C.
Similarities	Both products suffer from the severe working conditions, thermal effects/fatigue, corrosion, impact. Both use building blocks approaches for design, and the structures are designed for fatigue. Also, they are validated with full scale tests – static and dynamic.	

### 4.3 Thesis Development (Plan Outline)

As shown in Table 4.3, the thesis is divided into two main parts. One is related with the performance and it is considered the functional part of the system. This means the expected properties and behavior of the structure. The other is the physical, i.e., the actual product and how it is built - in this case the assembly process (manufacturing of bonded joints).

To analyze the applicability of this technology, these two categories have to be analyzed in detail (Table 4.3) because there are some dependencies from the manufacturing process and the performance that affect the outcome of the overall process. The criteria chosen for both domains have different scenarios and this establishes different boundary conditions, inputs, outputs and requirements. In fact, the maturity level represents the literature review and the information gathered through this research in terms of what is applied and available in the industry. The performance represents the capability of reaching the expected properties (i.e., reliability for manufacturing and static strength for mechanical performance). Finally the risks and perceived value present the summary of the results obtained in this work.

The manufacturing process addresses the maturity level of technologies available through a literature review and the industrial environment standard processes, as well as how these processes are. In fact, the maturity level is not matched with the TRL scale, but it gives the background needed to review the following sections regarding this subject. Figure 4.5 presents in detail the points addressed along the section. In fact, a case study was carried out to understand, in a real industrial environment, the process performance and the costs. To complete this, a final risk assessment is presented to define how important is the manufacturing process in the overall performance of a joint. The sequence of subjects is shown in Figure 4.6, where the bibliographic review is presented in the maturity, while the case study is the scenario for the process performance and cost analysis.

Table 4.3 – Activities defined in each domain to fulfill this work.

<b>Manufacturing Process (Assembly)</b> (Figure 4.5)	<b>Design (Performance)</b> (Figure 4.7)
<ul style="list-style-type: none"> <li>• Maturity level</li> <li>• Performance</li> <li>• Costs</li> <li>• Risks</li> </ul>	<ul style="list-style-type: none"> <li>• Maturity level</li> <li>• Static performance</li> <li>• Fatigue performance</li> <li>• Perceived value</li> </ul>

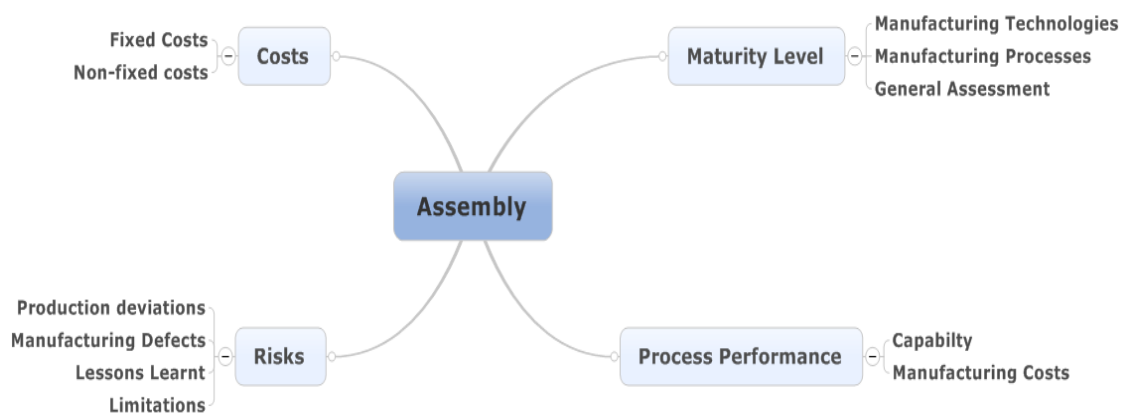


Figure 4.5 – Parameters to be assessed for each activity in the assembly domain.

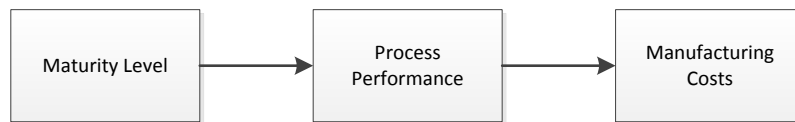


Figure 4.6 –Tasks developed for the Assembly.

The other domain is the performance, where a similar analysis is made. The methods to assess the static strength and the fatigue analysis are presented through a bibliographic review. Figure 4.7 presents the subjects addressed there. The maturity level is embedded in the different methodologies for the static and fatigue assessment. Figure 4.8 presents the sequence of subjects to be addressed in detail in the thesis.

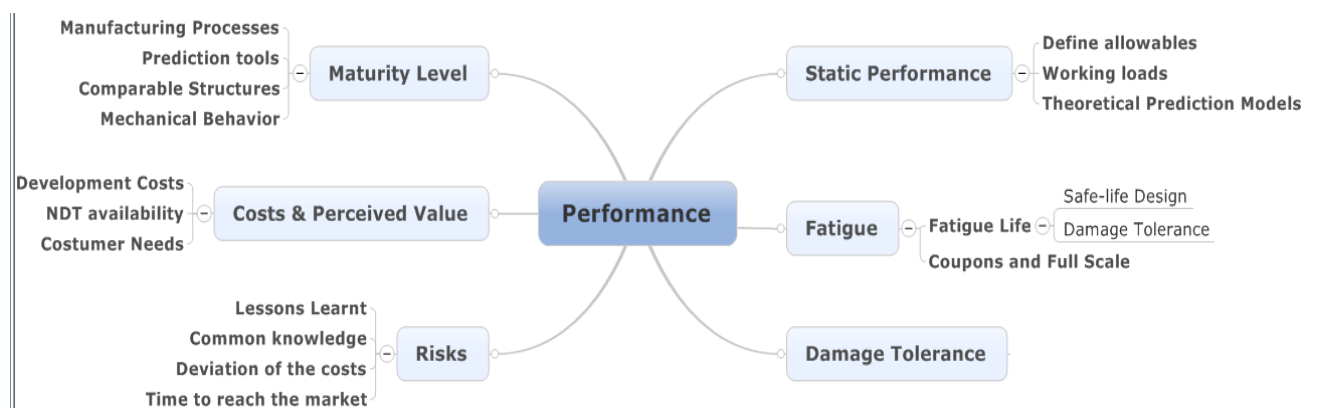


Figure 4.7 – Parameters to be assessed for each activity in the performance domain.

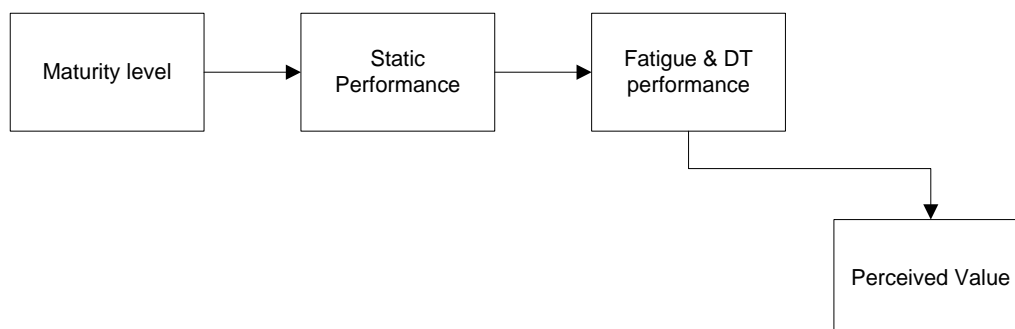


Figure 4.8 – Performance Tasks .

The interfaces of these domains (Performance and Assembly) are defined in two tasks. One is the *Maturity Level*, where there is a clear exchange of information, i.e., the models developed to study the behavior of the joints can only be reliable if the joints are properly manufactured. The other link is the *Process Performance*, which relates the process capability with the mechanical performance of the structure, i.e., the *design allowables* (design values) can be

determined with more or less confidence, depending on the capability of the manufacturing process. In fact, complex interactions have to take place between these activities to guarantee the best possible outcome.

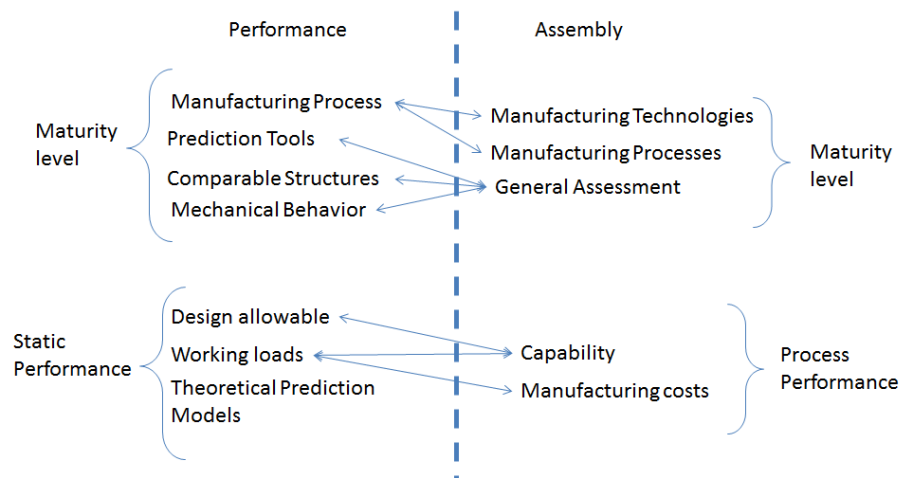


Figure 4.9 – Interfaces between the two domains (manufacturing and mechanical performance).

This work presents an innovation in terms of:

- how bonded joints are applied in two specific industries (wind blades and aircraft);
- the problem of applicability and compatibility of this joining technology;
- and finally, the bonded joints are studied in terms of fatigue:
  - by applying a fracture mechanics methodology to assess the fatigue life on composite bonded joints;
  - testing different loading modes (I, II and I + II) and comparing them in terms of the Paris-Law;
  - and the definition of the fatigue threshold in terms of compliance's variation during these tests.

All these aspects are studied in detail in the following sections.

## II. Assembly

From the manufacturing point of view, this category is called Assembly and not manufacturing because the main purpose of this work is related with the capability of joining composite parts or elements to create a structure. Aström [7] has stated for composite materials that *“when fabricating components and structures from traditional construction materials, manufacturing is usually a matter of machining, molding... With fiber-reinforced composites, the situation is different, in general that both the material and the component are manufactured simultaneously”*. In other words, the material is created as part of the manufacturing process, when the fibers (FRP – Fiber Reinforced Polymers) are laid up and the curing cycle begins (Composite Part). This creates a dependency that is not normally considered - to understand the mechanical behavior it is important to understand the process as well. Figure II.1 shows a summary of the work done in this thesis regarding this subject, the main flow goes from the maturity level towards the risks, and “sub-processes” are presented in each main section to have a better understanding of the tasks addressed here.

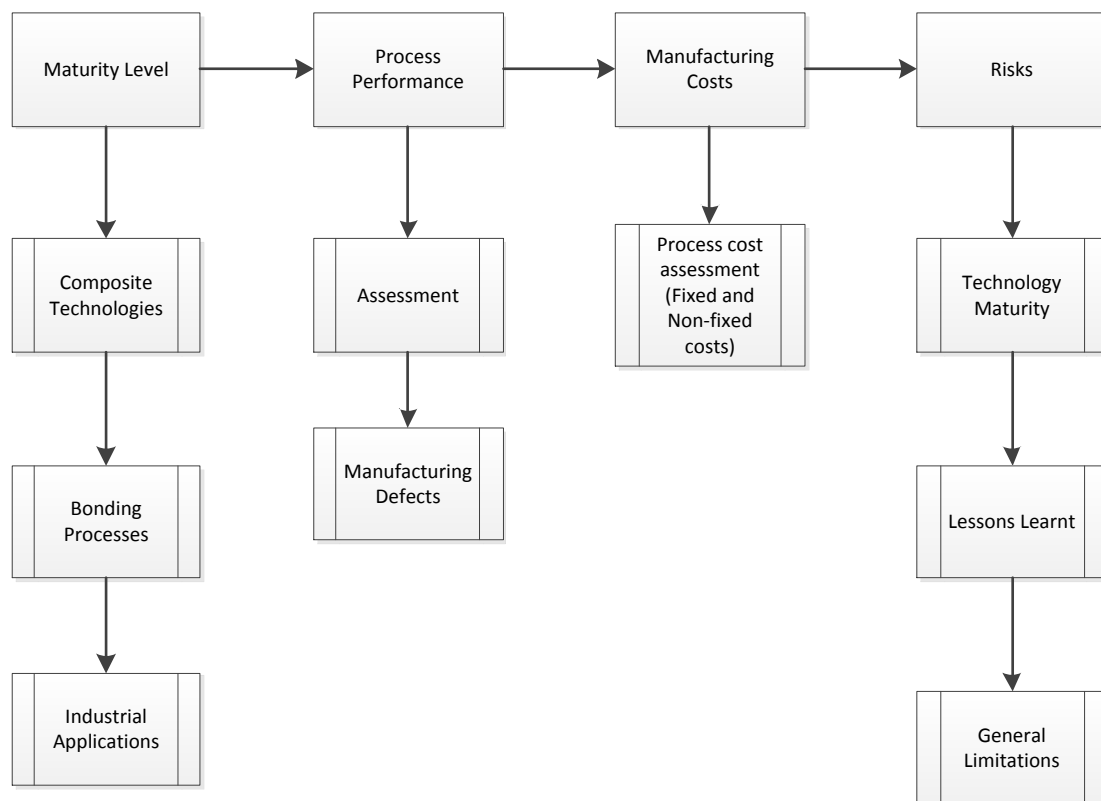


Figure II.1 – Process and sub-categories developed to define the Assembly capabilities of bonded joints.

The maturity level represents what is already available, from manufacturing processes to actual applications. The process performance, manufacturing costs and risks were done using the data obtained from a **case study for wind blade manufacturing**. The case study was done by analyzing the technology applied to the wind industry. It aimed to understand the manufacturing process itself and the most common defects. In addition and taking the opportunity of the information available the cost analysis was done using *Cost Model*. Finally the risks represent a summary to understand better the impact of the different parameters process in the structure.

## 1 Maturity Level

### 1.1 Composite Manufacturing Technologies

Composite materials create a product from many different manufacturing processes, but the process-property dependency defines what suits it better [7]. The principle behind composite manufacturing is the mixing of the reinforcement (fibers) with the matrix and solidifying it by using heat and pressure into the desired net shape. There are two main categories: open molding and closed molding [60], [61]. Open molding is the method used longest in industry [7]. It is called like this when the gel coat and the laminate are exposed during the whole process. Closed molding is when the composite is processed inside a mold (two sided mold set, or with a vacuum bag). In fact, there are a variety of processes associated with these categories. This variety makes possible for manufacturers to produce cost efficient products. This is advantageous because this expertise allows the manufacturer to provide the best solution for the customer, but the fact is that choosing a technology depends upon a number of factors including cost, materials, size, volume and performance. Theoretically, independently of the technology chosen, the principles for manufacturing of composites products are the same: aligning the fibers, then making single filaments, tows and fabrics (mats, weaves, braids, knits). Afterwards the “Bed” consisting of many layers of fabrics (lay-up) has to be made and the interstices between filaments have to be filled with liquid matrix and wetting the fibers and the last step is curing the resin. Depending on the moment the resin is applied, the process can be classified as wet or dry [61]. The wet processes (i.e. open mold) use liquid resin that is applied on top of the dry fibers after the lay-up, while in dry processes there is no need to use resin, because the fibers are already impregnated (before the lay-up).

The fibers or reinforcements are normally made by joining together different filaments (Figure 1.1a). Those filaments then form tows (Figure 1.1b) and different tows make fabrics (Figure



1.1c), like tape or woven. Actually tape (Figure 1.2a) is referred when resin is used to combine the tows. When it is not used and tows are together by woven the fibers (Figure 1.1c – woven fabric) or stitching, it is called fabric (Figure 1.2b).

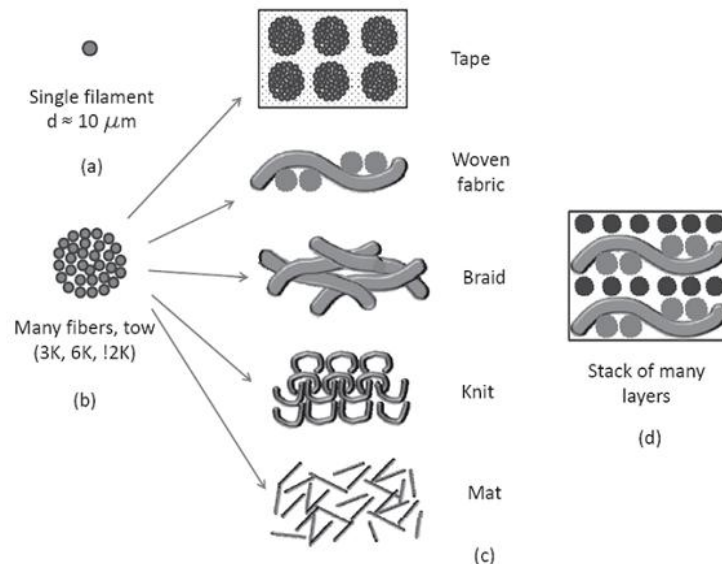


Figure 1.1 – Fiber forms at different scales [61].

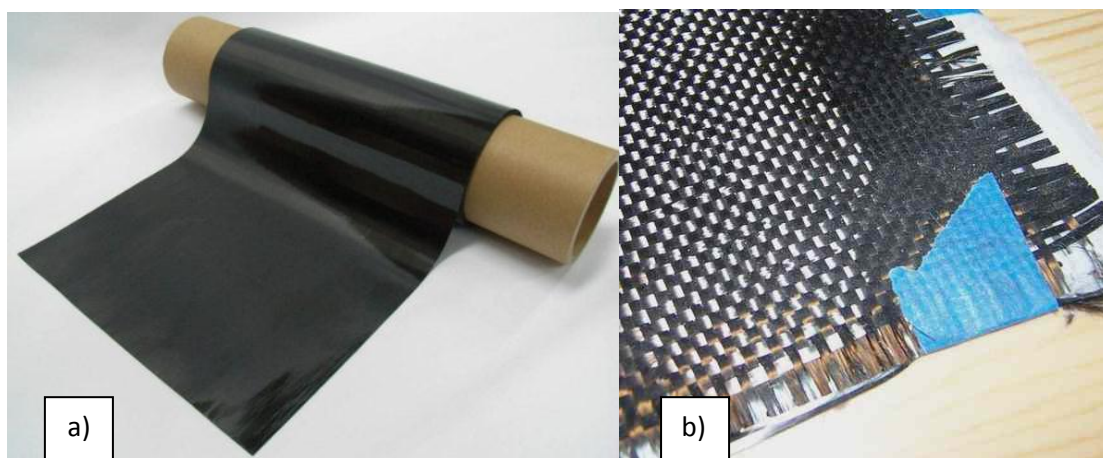


Figure 1.2 – a) Unidirectional thin-ply tape [62]; b) woven fabric[63]; both are composite carbon fibers.

In general, the rule of thumb is that for good quality, the whole process should be broken down into small steps and each step done at a different time. For low cost manufacturing, many steps may be combined so the process can be done at one time or a lesser number of times. The selection of the process depends on weighing these two parameters carefully : quality and cost [61].

The process can be organized in: open mold, close molding, autoclave. Table 1.1 present a short description and a comparison between some processes. It includes capabilities (parts per

year), cost, type of material used and some description for the most common processes. There are several other relevant processes like filament winding, compression molding, pultrusion; these technologies can be studied in detail in [60], [61], [64], [65].

**Table 1.1 – Key points regarding different composite manufacturing technologies [7], [60], [64], [65].**

	<b><i>Open mold</i></b>	<b><i>Closed molding</i></b>	<b><i>Autoclave</i></b>
<b><i>Cost</i></b>	Cheap	Tooling is expensive	Toolings and materials are expensive
<b><i>Type of material</i></b>	<i>Woven fabric</i>	<i>Woven fabric</i> <i>Some special cases pre-preg.</i>	<i>Pre-preg</i>
<b><i>Description</i></b>	Fibers are placed by hand and on top of them resin is placed and it has to be cured.	The fibers are placed also by hand on the mold. The resin is placed with aid of a tool. Pressure and/or temperature is applied to compact and cure the piece	The lay-up is made in controlled temperature. Afterwards pressure is applied to compact properly. Then high temperature is applied to cure.
<b><i>Examples</i></b>	Wet lay-up Spray-up	Resin Transfer Molding (RTM). Compress molding. Vacuum Assisted Resin Transfer Molding (VARTM).	Vacuum bag molding
<b><i>Advantages</i></b>	Short curing cycle. Normally there is no need to apply temperature.	The quality of the pieces produced is better. The costs are less than for autoclave technologies.	High quality parts

## 1.2 Composite Bonded joints: Manufacturing Processes & Technologies

Similar to composite manufacturing, bonding them has a high level of process-property dependency. Any process used for bonding manufacturing has three main factors to be taken into account: pressure, temperature and surface pre-treatment. Pressure is to hold the parts to be bonded together (adherends) while the adhesive is curing. Temperature depends on the type of adhesive, but it has to be enough to become solid, sometimes reaching the glass transition temperature ( $T_g^4$ ). Finally, the surface pre-treatment guarantees the properties of the joint. Some options have been studied to improve the behavior of the joints with the existing pre-treatment. Composite bonded joints when analyzed by the manufacturing process can be divided in three: co-cured, co-bonded or secondary bonding, independently from the technology used to manufacture the composite part.

<sup>4</sup>  $T_g$  is the transition of amorphous polymers from a rubber state to a hard state, depending upon the material it can be ductile or brittle. Normally the  $T_g$  is associated to mechanical properties of the adhesive.

**Co-cured (Figure 1.3):** The composite adherends are cured together at the same time (independently from the manufacturing process), guaranteeing a chemical bond and it can be made with or without adhesive, because the resin is used to bond the parts together. The main advantage of the process is that there is no possibility of contamination in the surface. This type of process is preferred over other bonded technologies because there is a reduced number of parts and the structural performance and reliability of the method is expected to be better than those of secondary bonding [66]. In general, there is no probability of contamination, which makes this option less risky than the others. The limitation of this technology is the need for tooling/autoclave, which limits the size of the parts that can be produced.



Figure 1.3 – Co-cure process.

**Co-bonded (Figure 1.4):** It is a joining technology feasible with or without adhesive, which can be considered as a step between co-cured and secondary bonding. In this process, one of the adherends is already cured and the other is un-cured. In this case, the risk of a non-effective bond is diminished because one side has covalent links between the resin and the adhesive. When compared with co-curing, the main disadvantages are the amount of parameters that should be controlled like the surface condition and the bondline thickness [66] and the necessity of two curing cycles.

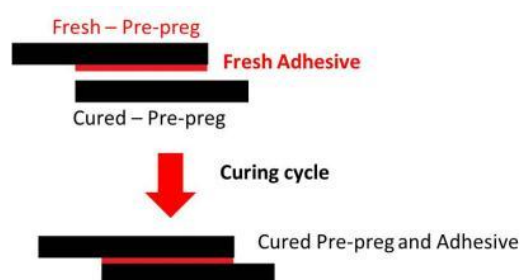


Figure 1.4 – Co-bonded process.

**Secondary bonding (Figure 1.5):** this process always uses adhesive for joining. The adhesive is inserted between the adherends when they are both already cured. This process is more flexible and does not need to be made in an autoclave or in a closed mold. It makes easier to assemble complex and/or large composite parts, without requiring any extra mold or tooling. When compared with co-bonded structures, the main disadvantage is the need for an extra curing cycle [66].

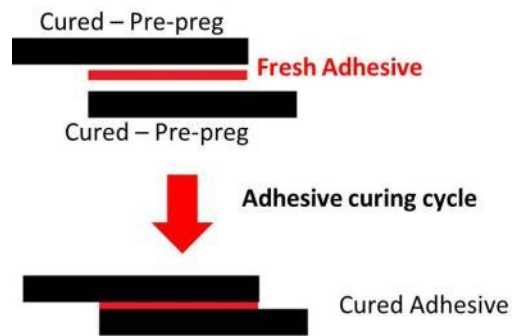


Figure 1.5 – Secondary bonding process.

In the co-bonded joints and secondary bonded joints, the cured parts need a surface pre-treatment to guarantee adhesive bonding. The main issue regarding the secondary bonding process and the co-bonded is the effect of the bonding surface in the mechanical properties of the structure. A detailed description of the surface preparation methods and its effect is presented in the next section.

### 1.2.1 Surface Pre-treatment

*“It is well established that to form an effective bond, intimate molecular contact between adhesive and adherend is required. The correct surface pre-treatment will optimize this degree of contact, which may be brought about by chemical modification of the adherend surface”* [67].

Nowadays, surface preparation and bonding techniques are well known for metal-to-metal bonding; however, for composite-to-composite or composite-to-metal bonding there are gaps that need to be filled [68]. One gap is ways to improve the performance by surface activation, like plasma treatment. In fact, it is already being used but there are some unknowns that have to be discovered. The second one and probably most important is a lack of a well-established Non-Destructive test (NDT) to guarantee the quality of the surface. There are some developments regarding laser beam as controller, but there is no record about its application in the industry. It was developed in a U.S. project called Composite Affordability Initiative (CAI), where Boeing led the quality assurance effort [48]. The lack of NDT (to determine kissing bonds) plus the high process-property dependency define the importance of the surface pre-treatment. The process relies on the establishment of intermolecular forces between a substrate and the polymeric adhesive itself [69]. The mechanical performance of any joint design is irrelevant if the adhesion between the parts is poor. Actually, the integrity of the bond is clearly defined by the pre-treatment of the substrate, because it confers the required surface properties by removing contamination from the environment or the processes and in some cases it creates a chemically active surface. Figure 1.6 shows a classification of the

surface treatments for plastic materials. It is divided in three groups: Physical, Chemical and Mechanical. The first two imply a chemical activation of the surface by a physical (Plasma) or a chemical treatment (etching). The mechanical treatment is only related with the roughness of the surface, and this is the main procedure applied for FRP in industry.

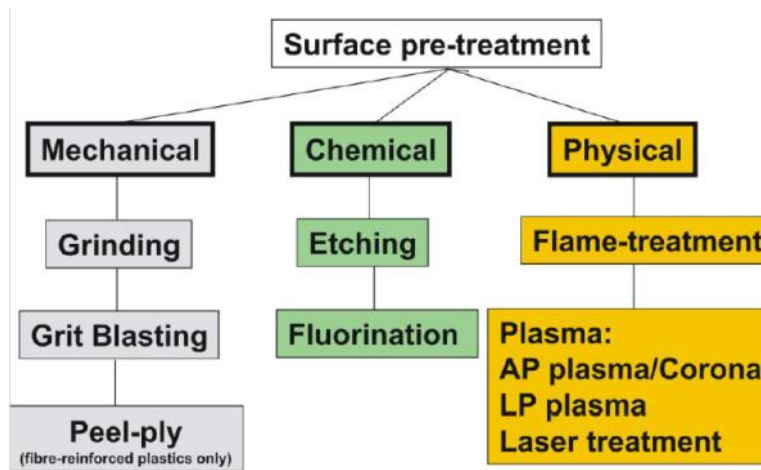


Figure 1.6 – Classification of Surface treatments for Plastics [70].

Real et. al [71], Chin & Wightman [72], Dillingham & Oakley [73] have analyzed the effect of the surface preparation on the strength of the joint. Dillingham & Oakley [73] in their study assessed the quality of the surface, evaluating the wettability of the surface with the energy release rate ( $G$ )<sup>5</sup> and the failure mode. In fact, the drop tests were used to assess the compatibility of the surface with the adhesive – the bigger the drop more compatible is the surface and the adhesive. Figure 1.7 shows this relation where the adhesive failure corresponds to the smaller drops (less wettability) and lower  $G$ , and cohesive failure (adhesive in both sides) corresponds to the higher values. This example clearly shows the mentioned dependency. For joints with low value of  $G_i$  the failure is adhesive (adhesive only in one side) which means the surface was not properly prepared. In fact comparing the failure modes (Figure 1.7), cohesive failure (this means adhesives in both sides) has doubled the value of  $G_i$ .

In general, the need to assess the surface properties of an adherend is most likely related with two fundamental questions: on the one hand, there is a need to know the condition of the surface as delivered (from internal or external sources). On the other, there is a requirement to determine the chemical and the physical changes that have been brought by a specific pre-treatment applied as part of the adhesive bonding system. In the latter category, the need may be related to a quality assurance requirement. This is more likely to be encountered during the development of a new or improved pre-treatment process because most of assessment can

<sup>5</sup> Please check Section III.2.2 for a complete explanation of the Energy release rate ( $G$ ) and Mode I.

only be done by relying in destructive testing. In all cases, the performance of the adhesive joint is directly related to the successful application of such a pre-treatment, and an important part of the development of a new pre-treatment procedure or the quality assurance of an established process is the assessment of the surface characteristics, both in terms of topography and chemistry [69]. Considering the importance of the proper preparation of the surface, the role of the techniques to achieve good bond strength in composite have to be understood [68].

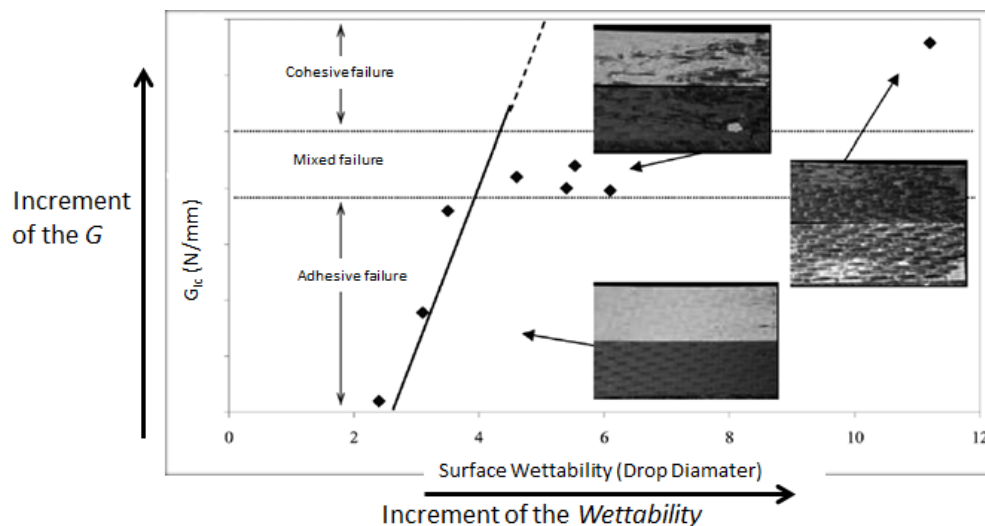


Figure 1.7 – Relation between the  $G_{IC}$ <sup>6</sup>, failure mode and wettability of the surface [73].

Peel-ply removal, sanding and grit blasting are three most common methods used in the industry to prepare composite for adhesive bonding. In fact, these methods are all mechanical which means the surface is “enlarged” at micro-scale and it creates a mechanical interlocking for the adhesive. In other words, the effect of surface roughness and material removal has an impact on the quality.

### 1.2.2 Peel-Ply

The peel ply is a fabric added as the last layer in the lay-up of the fresh composite part to be bonded. Basically it covers the external surfaces prior to bonding. When it is being cured, the epoxy in the part becomes viscous and flows making the peel ply part of the cured laminate (Figure 1.8). Then peel-ply will only be removed from the surface immediately before bonding to guarantee a clean surface [74], [75]. In general peel plies can generate active surfaces for a limited period of time (in this research was found out between 4 and 12 hours). In any case, the morphology of the surface and the quality is dependent on the nature of the fabric and type of weave used.

<sup>6</sup>  $G_{IC}$  is the critical energy for a crack propagation in Mode I loading (peel).



Flinn and Phariss established in a work for the FAA [68], how the peel-ply separates from the laminate. They presented a sketch shown in *Figure 1.9* to explain better. Where 1 (blue arrow) shows the fracture of the epoxy resin between the peel ply and the underlying carbon fibers or 2 (pink arrow) interfacial between the peel-ply fabric fibers and the epoxy matrix. In severe cases of poor surface preparation the peel ply fibers may fracture and leave material on the composite surface (3 – green arrow) or there may be interlaminar failure in the composite (4 – light blue arrow), if the adhesion between the peel ply and the resin is too strong.

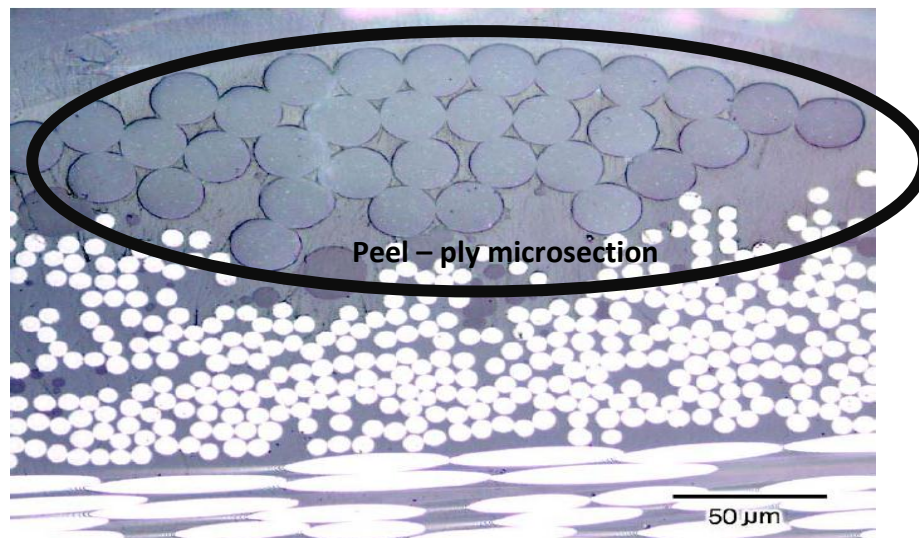


Figure 1.8 – Cross section of laminate with peel ply on top [68].

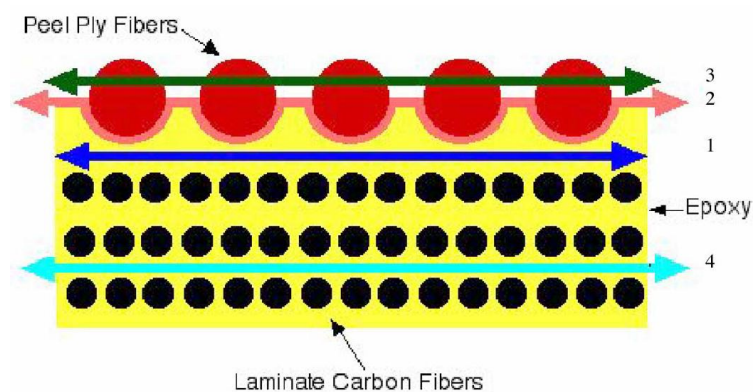


Figure 1.9 – Four possible fracture types in peel ply removal [68].

Unfortunately not all the peel plies are suitable for all matrix resins. Hart-Smith et al. [76] in 1996 stated that “the variety of peel plies is a testimony to the fact that there is no universal peel ply suitable for all laminating resins and all adhesive...”. Flinn and Phariss in their work for the FAA [68] demonstrated that a significant difference in bond quality occurs when the peel plied is changed. They tested polyester and polyamide peel plies, with the same adhesive and the same substrate. The result for the polyamide peel plies bonded with an epoxy adhesive

(MB1515-3) had adhesive failure with an average  $G_{Ic} < 0.165$  N/mm and with the polyester peel ply is 0.812 N/mm. It was found in the bond surface small fibers fragments of the polyamide peel-ply and the adhesive does not have a composition that is compatible with epoxy surfaces containing amides [68]. Other evidences regarding the effect of the peel ply are mentioned in [67], [74], [76]. In general, the authors have established that, if there are no guarantees of compatibility, the specimens have to be grinded. Wegman [74] reports that *“a study made by Pocius and Wenz [77], also evaluated peel ply materials and reported that abrasion techniques were better than the peel ply”*. In this case the reduction of the properties was caused by fluorocarbon residuals transference from a “release” polyamide peel ply. Hart-Smith et al. [76] in their work found that the applicability of “release” polyamide peel ply can deteriorate the properties of the bond line. Klapprott in 2004 [78] investigated the key factors affecting peel ply surface preparation. In this work, he established that *“the reliability and durability of the ultimate adhesive bond is strongly influenced by peel ply weave details and its encapsulation level during cured and also on the toughness of the impregnating resin system”*. He optimized the toughness of the resin with the peel ply toughness to have a surface without peel ply fibers on top.

As a final remark, Hart Smith et al. [76] stated that *“All composite surfaces to be bonded or painted will be grit blasted, regardless from what surface protection was applied... the absence of service problems in bonded, co-bonded and co-cured composite structures can be assured only by effective durability testing which can be completed in the short term, both at the start of a program, to select the materials, and as a quality-control test during production. What is still missing from the composite world is a test equivalent to the wedge-crack test for metal bonded structures”* [76]. Industries, in general, have found a way to deal with this, mainly by testing. In fact, it is well-established, that Mode I tests (peel loading) can help to assess the behavior of the system (peel ply + resin + adhesive) because this loading mode is considered the weakest mechanical behavior of bonded joints.

### 1.2.3 Grinding and Grit Blasting

Mechanical abrasion will remove the surface “coating” and change the topography of the adherend surface. When applying mechanical abrasive pre-treatments to FRP like glass fibers or carbon fibers, a number of points must be addressed. Excessive grinding or sandblasting can damage the fibers, leading to a weakening of surface plies and decreasing  $G_{Ic}$  for the adhesive joint [73]. In general, to control this process, normally the resulting dust is assessed. It must be white or just slightly grey. If the dust color changes to dark grey or black, this means the fibers



have been damaged and in extreme cases this can result in loss of the required materials properties [70].

Grinding is mainly a manual process, and can be done with different mesh roughness. Kim et al. [66] studied different bonding methods in single lap joint (SLJ) specimens being one of the parameter was the surface roughness. They found that finer surfaces can give more reliable results and better performance (Figure 1.10). The roughness of the specimens grinded, with sandpaper 220 mesh varies almost a 100% (from roughness of 0.94 at the lower limit to an upper limit of 2.05) and this has a direct impact on the strength where the lower value is 18.9 MPa and the maximum is 28.1 [66]. On the other hand, specimens polished with 320 and 400 sandpaper present almost the same values and a lower scatter. In fact, the probable cause for these different results could be related with the abrasive “power” of the sandpaper. As the samples were polished manually, some of the surfaces polished with 220 could have damaged fibers prior to bonding.

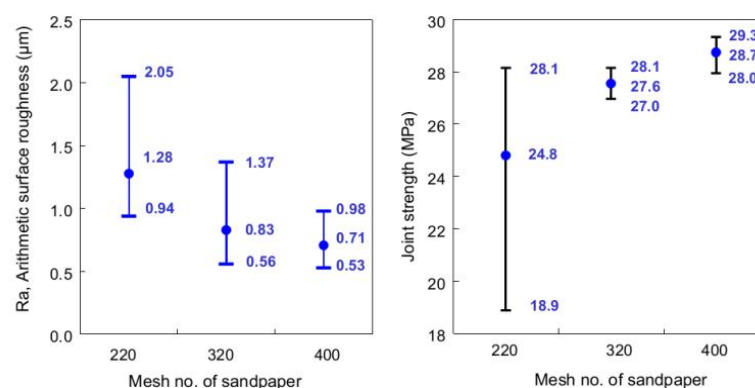


Figure 1.10 – Results obtained by Kim et al.; a) An evaluation of the surface roughness as a function of the Mesh n° of sandpaper, b) Joint strength as a function of the Mesh n° of sandpaper [66].

Grit blasting has been successfully employed for many decades as an integral part of many metal surface pre-treatment processes. It is also called abrasive blasting, because the process consists on the impact of abrasive particles on a component to clean or modify its surface properties [79]. In the case of composite materials, it removes contaminants such as mold release agents and roughens the surface. This provides a better wettability in the surface and it can allow the formation of covalent links with thermosetting adhesive, and/or mechanical interlocking between the adhesive and substrate. The knock down factor is related to the damage that may be induced below the surface of the laminate by the blasting process and has been postulated as a source of weakening of the laminate [73].

### 1.3 Bonded joints in Industry

As already mentioned at the beginning of this work, composite bonded joints are getting more common as the amount of composite materials used in structures is increasing. Three examples of adhesively bonded composite structures will be described briefly. The first is related to civil engineering, because it includes one of the largest industrial composite assembly operations, like pipelines. The second is the general application of bonded technology in transportation, like trains or ships but mainly in the aircraft industry. The last one is the application of bonded joint wind energy.

#### 1.3.1 Bonded Joints in Civil Engineering Projects

Civil Engineering projects have been using methodologies to assemble large composite structures, for a lot years. One of the most recent examples is light weight bridges (reinforced concrete, FRP or other composite materials) for emergency or pedestrian purposes, glass structures (*eyecatcher*) or long components like the pipelines assemblies for fluid liquid.

- A successful pedestrian bridge was built by Swissfiber and Sika (Figure 1.11) using the advantage of pre-tension FRP plates and the fact that bonding technology is suitable to join different materials. In this case, bonding technology was applied to bond of CFRP plates to concrete, GFRP, metals and wood (Figure 1.11a). The joints were made with a very high mechanical strength adhesive that has also good chemical resistance against aggressive media [80]. Considering this type of application, special attention has to be given to the environmental effect because humidity and extreme temperatures can affect the long term properties of the adhesive.

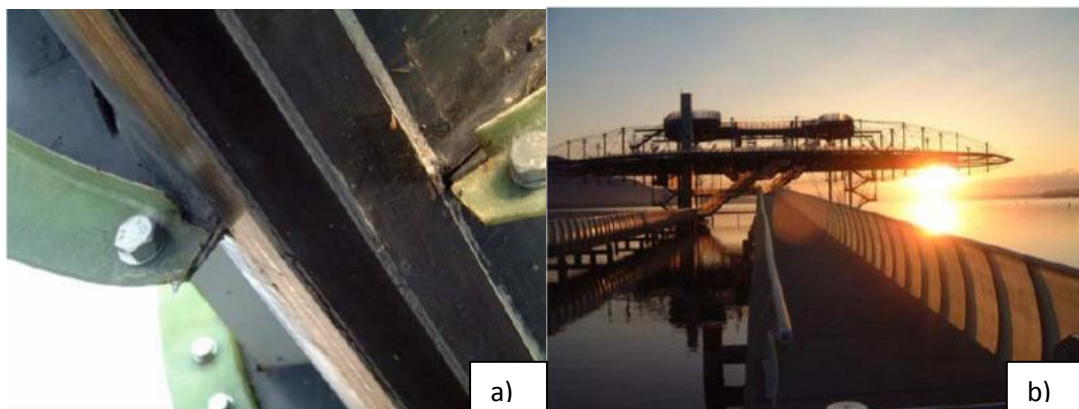
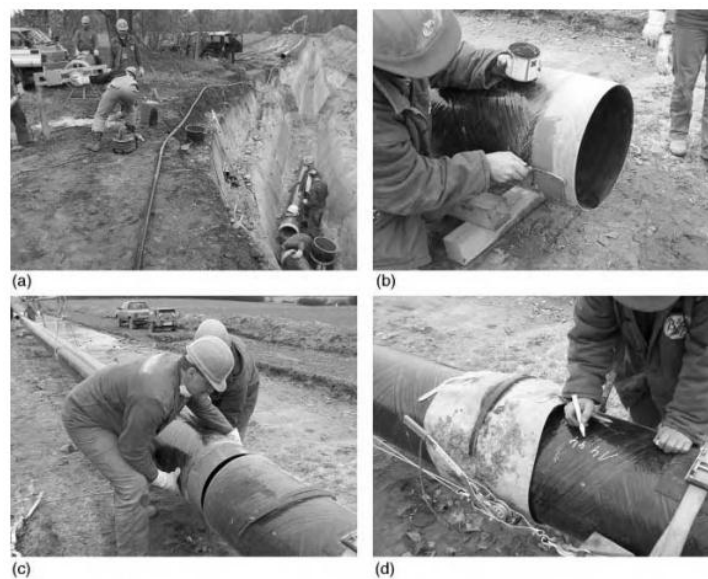


Figure 1.11 – Pedestrian bridge built for tests in Yverdon – Switzerland: a) detailed picture of the bonded CFRP plates, b) the bridge at the artificial cloud facilities [80].

- The other case is the assembly of 12-meter length filament wound tubes into pipelines which extend tens of kilometers. It involves hundreds of adhesive joints which must be

performed often under difficult environmental conditions. Fluid transport, firewater and cooling systems are produced in this way. The main requirement is water-tightness, and considerable work has been done to define economical efficient designs. Pipe suppliers have developed bonding procedures, and train and certify adhesive bonders. Figure 1.12 shows an example of the bonding operations employed to produce a bonded cone and taper connection. Adhesive is applied and heating blankets are placed around the joint to cure the adhesive. The success of these operations shows that adhesive bonding has developed into a viable industrial assemble method for composites [69].



**Figure 1.12 – Adhesive bonding process to assembly composite pipelines: (a) Machining pipe ends and drying, (b) application of adhesive, (c) assembly, (d) tightening and cure (heated blanket) [69].**

### 1.3.2 Bonded Joints in the Transport Industry

The modern light-weight design adopted in the transportation construction over recent years has revolutionized it. This has been possible due to the intelligent application of modern bonding technology in cars, ships, trains and also airplanes. This has allowed the bonding of hitherto unrealizable combinations of materials, i.e., bonding glass with steel, aluminum with magnesium and bonding of fiber-reinforced composite materials with metal. Figure 1.13 shows a strengthening steel framework construction using elastically-bonded prefabricated GRP lightweight structures and bonded window elements. Also, adhesives can offer additional functions, e.g. damping, electrical insulation and corrosion protection. These extremely flexible bonding techniques have also resulted in a significant increase in vehicle rigidity. Today, adhesive bonds are able to meet the highest requirements and can be excellently combined with mechanical joining techniques such as clinching, riveting, screwing and also spot welding [75].



Figure 1.13 – Train with applied bonded joints [75].

Considering the aeronautical industry, for example Boeing 787 and Airbus A350 have more or less 50% of their structural weight in composites (Figure 1.14). In fact, this is more than double when compared with the already in service A380 (since 2008) and this presents different and complex challenges. In fact, reliability in terms of performance plays a key role in this kind of industry, thus justifying the investment of governments and companies in the last 15 years to improve it [48]. Airbus (Figure 1.15) design solution for assembly is co-bonded structures with fail safe rivets while Boeing wing-box presented as design solution a co-bonded structure (Figure 1.16). *“The wing box of the 787 Dreamliner is a cantilevered beam that carries the wing to the fuselage and supports leading- and trailing-edge devices, control surfaces, engines and landing gear. It represents a portion of the wing section that begins at about the center of the airplane and stops at approximately one-half of the span of the wing 15.2m. The structure measures 5.5m at its widest point and weighs 24947 kg, including a great deal of test-only hardware and instrumentation”* [81]. Mitsubishi regional jet has co-bonded structures between the stiffener and the skin in the Horizontal Tail Plane (HTP) and in the Vertical Tail Plane (VTP) with the derivable schedule at the beginning of 2015 (Figure 1.16) [82]. These are all parts that are important for the stability of the plane but they can be damaged without jeopardizing the complete aircraft.

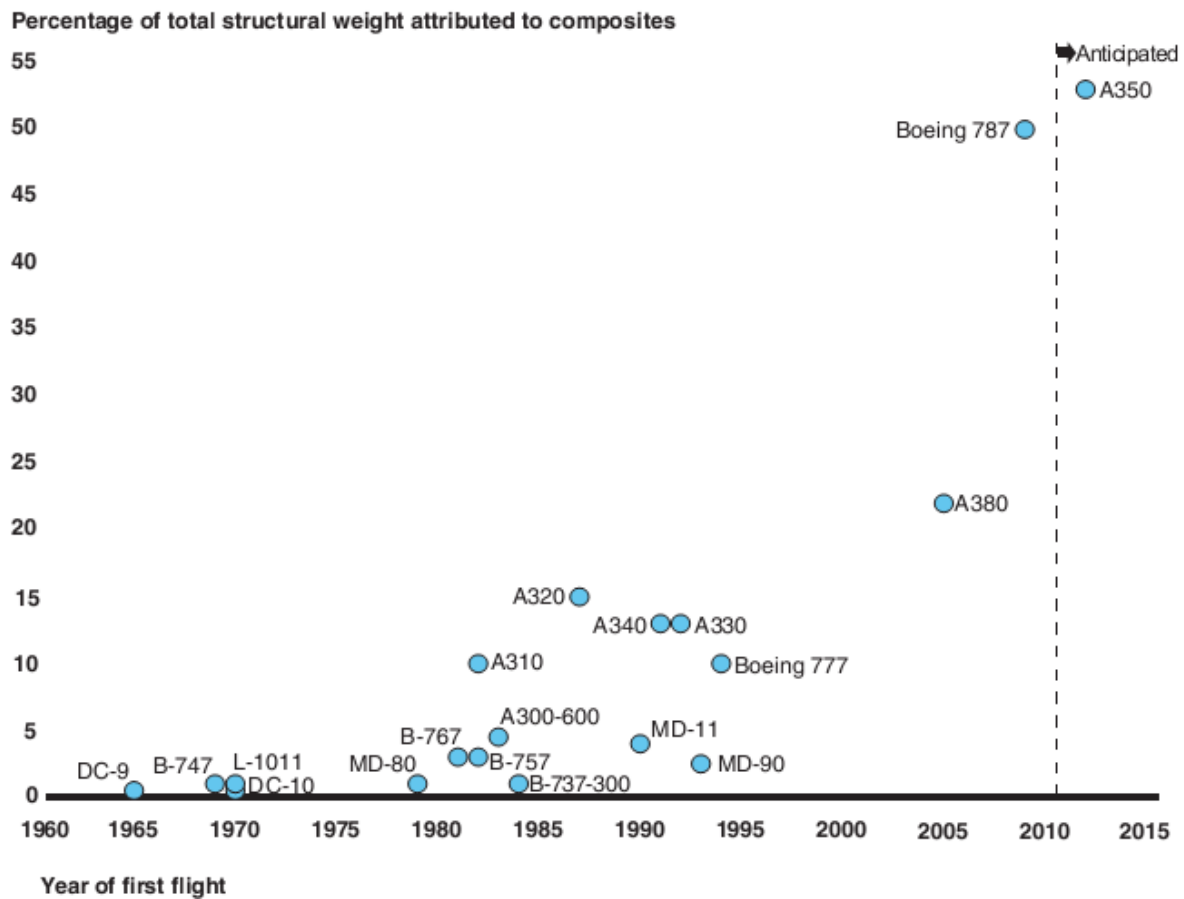


Figure 1.14 - Commercial airplane models over time by percentage of composite [83].



Figure 1.15 – The A350 XWB features CFRP primary structures (materials per component) [84].

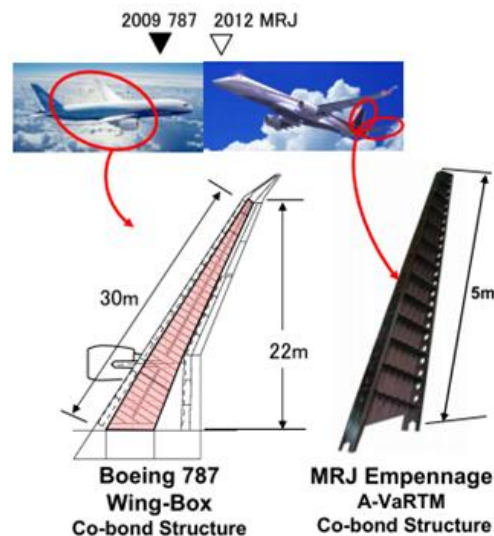


Figure 1.16 – Co-bonded structures used in the aircraft industry [82].

However, in general, the application of bonded joints is limited to secondary structures (as the proposals presented before). This means to structures that does not affect the airworthiness of the aircraft. For primary structures (structures that allow the airplane to fly) the AC 107B for composite materials [47] defines: “For any bonded joint, Federal Aviation Regulation (FAR) 23.573 [85] (a)(5) states in part: “the failure of which would result in catastrophic loss of the airplane, the limit load capacity must be substantiated by one of the following methods—**(i)** The maximum disbands of each bonded joint consistent with the capability to withstand the loads in paragraph (a)(3) of this section must be determined by analysis, tests, or both. Disbands of each bonded joint greater than this must be prevented by design features; or **(ii)** Proof testing must be conducted on each production article that will apply the critical limit design load to each critical bonded joint; or **(iii)** Repeatable and reliable non-destructive inspection techniques must be established that ensure the strength of each joint.” Point **(i)** in this AC addresses the usage of mechanical arrestors or interlockers, like fail safe rivets. Point **(ii)** defines that each joint shall be tested prior to the entry in service of the aircraft. Point **(iii)** defines a reliable NDT method which at this point is still in development (at least for kissing bonds<sup>7</sup>). At this point these limitations make difficult the application of “just bonded joints” in this industry.

### 1.3.3 Bonded Joints in the Wind Energy industry

The wind industry uses bonding technology in a big scale (Figure 1.17). These are the biggest products joined only by bonding. The blades can go up to 65m onshore and they can be even

<sup>7</sup> Kissing bonds: They represent bonded surfaces that for any reason hold only a residual strength of the standard value, normally known as Zero-volume disband. In other words, the interface is bonded but bond strength is not assured.

bigger for offshore. The demand for larger wind turbines with very high reliability is one of the main driving forces for current research and development in blade design. The current design of the blade is based on a beam concept with an aerodynamic shell. The structure is designed for a fatigue life of more than 20 years (over  $10^9$  cycles).

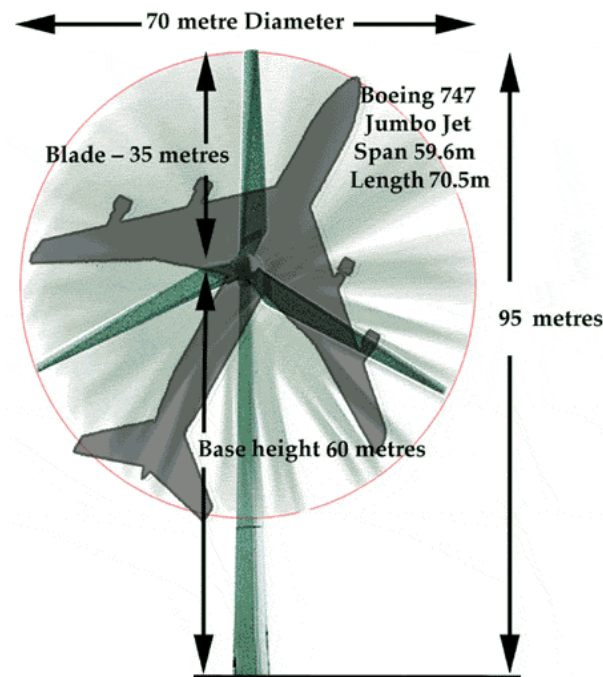


Figure 1.17 – Scaled design comparing a Boeing 747 with a Blade of 35m [86].

The blades are normally produced by VARTM. However, they can also be manufactured with prepreg. It enables higher resin properties, higher level of automation, and more consistent process, thus enabling reduction in blade weight [86]. Independently from the technology, blades are normally manufactured by component and finally they are assembled together. Figure 1.18 shows the cross section of the blade, the components and the joints numbered. Basically, the leading edge (1) is a link between the upper (pressure side) and lower shell (suction side). Joints 2 and 3 are the link between the shear webs and the both main shells and finally the trailing edge is the back part joint (4) of the two mains shells. Another kind of configuration can be used when a spar-box is used instead of the shear webs.



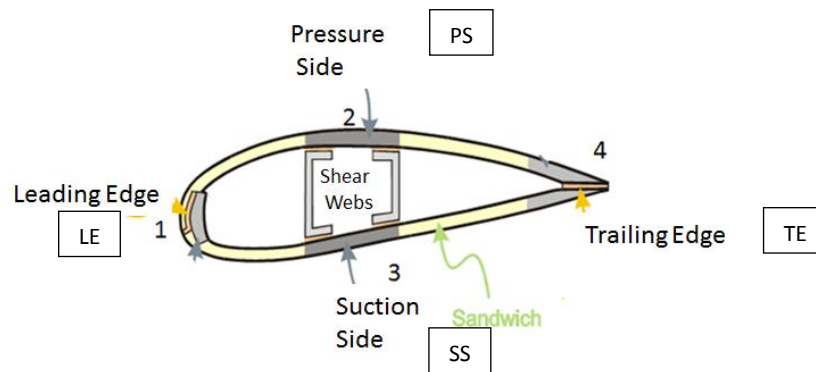


Figure 1.18 – Wind blade components [87]

From the structural point of view, the blade is made by an aerodynamic shell with a beam in the middle of it (Figure 1.19). The load carrying laminates are normally called Girders and mainly manufactured with unidirectional laminates. In fact, they are supported by webs that prevent the structural buckling of the blade. The aerodynamical shell is usually made as a sandwich construction consisting of thin glass-fiber skins enclosing light weight core material like balsa wood or plastic foam (Polyvinyl chloride). The supporting webs are placed on top of the Girders which then makes the beam design. There are other ways to build wind blades like the spar box concept (Figure 1.20), where the beam is manufactured completely and then assembly with the main shells. Comparing this structure to the aircraft primary structures, bonding webs (Figure 1.19) or spar-box (Figure 1.20) represents it. Any failure in this part will provoke the premature failure of the blade. In other words, those joints should not fracture and proper design criteria are needed for that purpose.

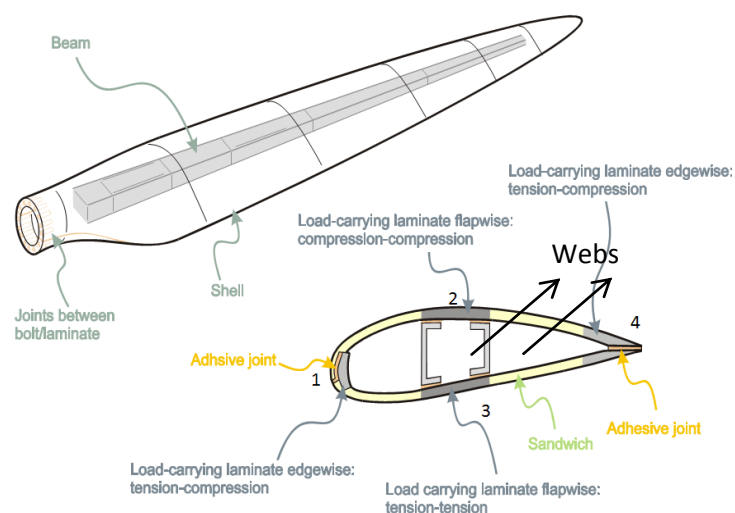


Figure 1.19 – Sketch of a wind turbine blade and a cross section of a blade [87].



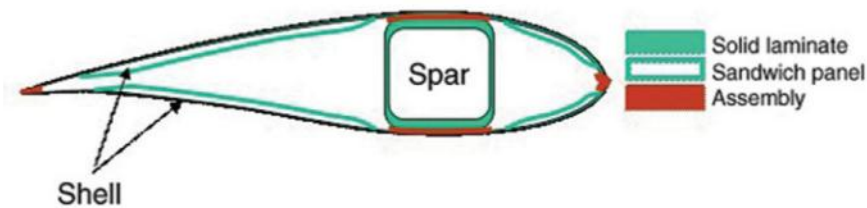


Figure 1.20 – Spar box concept – One piece blade [88].

The fact is that modern wind turbine blades are complicated aerodynamic and engineering structures. As with aircraft wings, aerodynamic forces created by the movement of air passing along the surfaces of the blade create a lift and allow energy to be extracted from the wind. However, a wind turbine blade has a far more complex geometry and is subjected to complex structural loads [89]. All these parameters have to be accounted not only for the structure itself but also for the individual parts (Upper Shell – Pressure side, Lower Shell – Suction Side, Beam – Webs, and the bonded joints). The adhesive and joints should be robust and relative easy to use in practical engineering design. Yet, they should be based on rigorous analysis of the stress state in wind turbine blades and should account for the possible failure mode that may develop [87]. To guarantee this, parameters like low mass, fatigue resistance and stiffness are important for the design criteria. Low mass is important to guarantee the performance, but it also means less maintenance in situ, which could also be related to the fatigue resistance. The stiffness must be evaluated adequately to prevent any contact with the tower during severe wind gusts [89] or between blades. Figure 1.21 shows a simplified way of analyzing the adhesive joints in the blades. Details that are expected to play a minor role like curvatures and thickness variations are disregarded. As shown in Figure 1.21, the simplified joint configurations (“elementary cases”) are loaded with axial forces and bending moments. This is a simplification, since the joints in a real structure are likely to be subjected to three-dimensional stress state. However, to make the design feasible this simplifications have to be taken into account [87].

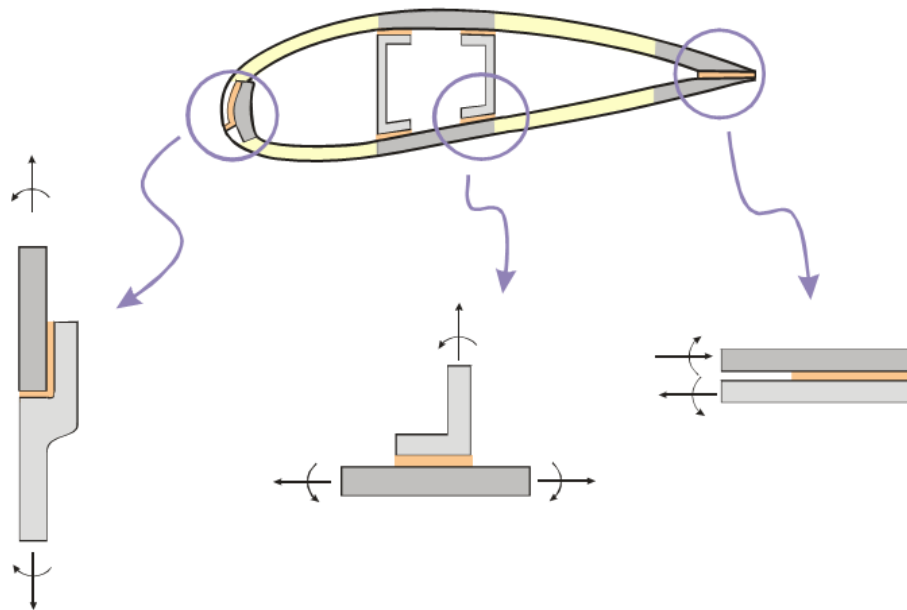


Figure 1.21 - Possible loading modes for adhesive joints along a blade cross section [87].

## 2 Case Study - Wind Blade

Wind blades can be viewed as a typical structure where bonded joints can be successfully applied. The reasons are:

- they are presented in several sizes, from small blades to almost 80 m wind blades;
- their expected life overcomes 20 years in service under different environmental conditions;
- the complexity of the stresses present in the joints, not only from the design but also those coming from the manufacturing process;
- and finally the fact that the integrity of the structure depends on the joints.

Indeed, they present a lot of opportunities:

- to understand the dependencies between the process and the mechanical behavior;
- to gather a complete picture of a product, a technology and the expected properties along the time;
- to define the needs and limitations of the aeronautical industry considering the similarities between the two products (at least the blades with the wings);
- to address the costs to validate the technology - this means to validate the actual costs with the ones predicted and to define the conditions needed to have a better process

performance. In addition, it can be used to compare different technologies in a risk/cost scenario.

## 2.1 Process Description

The most common concepts used in manufacturing wind blades consider all the subcomponents of the blades infused (VARTM) in separate molds and subsequently assembled by adhesive joining (Figure 1.18) [89]. The subcomponents manufactured are the upper and the lower shell in the embedded girder and the shear webs. The webs are not identical, because they account for the geometric differences between the leading and the trailing edge.

The process after the infusion of the parts is apparently very simple but it is the “heart” of the structure. A generic process to bond the blade is presented in Figure 2.1. The adhesive is applied to the shell that is in the fixed part of the mold, then the adhesive is poured (Figure 2.3-a)) from the root to the tip (Figure 2.1.a – black arrow). Afterwards the webs are placed on top and the excess of adhesive is cleaned (Figure 2.1.b). This stage ends here with the curing of the adhesive, normally following the manufacturers’ instruction and guaranteeing the defined  $T_g$ . Normally it takes around two hours, but it still depends on many conditions.

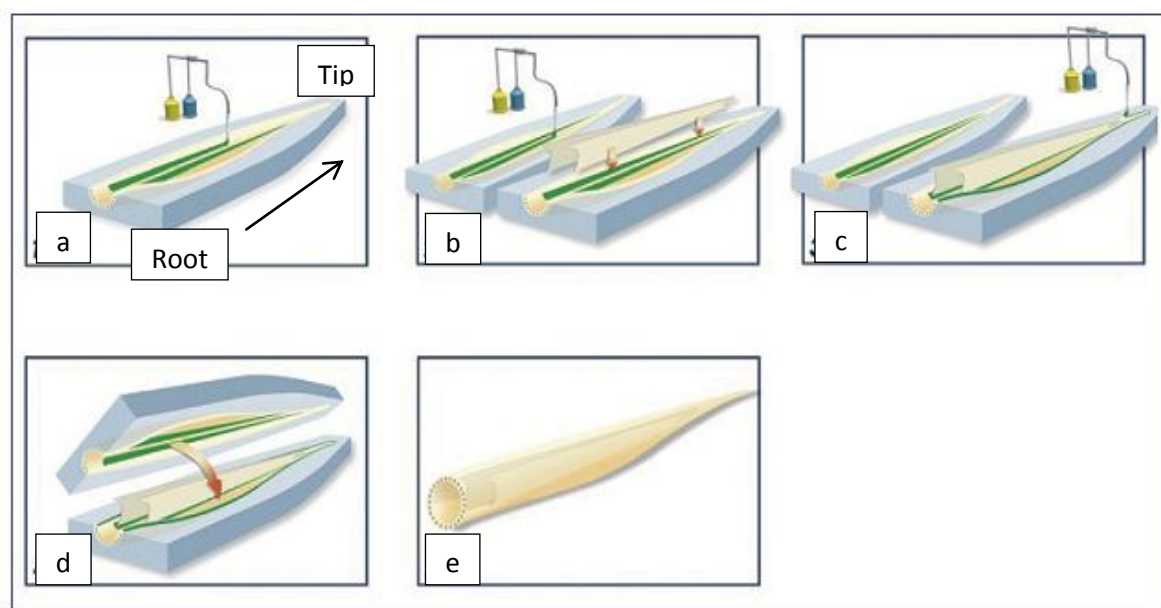


**Figure 2.1 - Five-step bonding process for a wind turbine blade.** a: Adhesive is applied to the first shell in the fixed part of the mold, and to the second one, at the root end of the blade. b: The internal parts (spar or shear webs) are lifted into position. c: Adhesive is applied to the top of the spar or shear webs for the second shell bonding. d: The second shell is lifted over onto the spar or the shear webs. e: The mold is closed [88].

The second part begins with the preparation of the blade to be closed (Figure 2.1.c-e). There is a need, before closing the mold prior bonding, to check if the pieces match perfectly together. Then, the adhesive is first placed in the Leading Edge (LE) main shell (Figure 1.18) again in the

fixed part (Figure 2.1.c). Subsequently it can be placed on top of the webs (or spar) or on the moving shell (lifting part of the mold) (Figure 2.1.d) where the webs will be bonded and afterwards in the Trailing Edge (TE) main shell (Figure 1.18). The mold is then closed (Figure 2.1.e) and the excessive amount of adhesive is removed from the places that are reachable. The final curing cycle lasts at least 5 hours.

If the blade is manufactured with a spar, then a large amount of adhesive is placed normally with the width of the spar (Figure 2.2). If shear webs are applied then two rows of adhesive are placed (Figure 2.3a). The height of adhesive placed on the main shell is around 15 mm but it can vary depending on the tool used, the important thing is to guarantee the squeeze out after placing the webs (Figure 2.3b). In fact, the lack of squeeze out is considered as a defect.



Figure 2.2 – Application of adhesive into the first main shell to put the spar box on top [88].

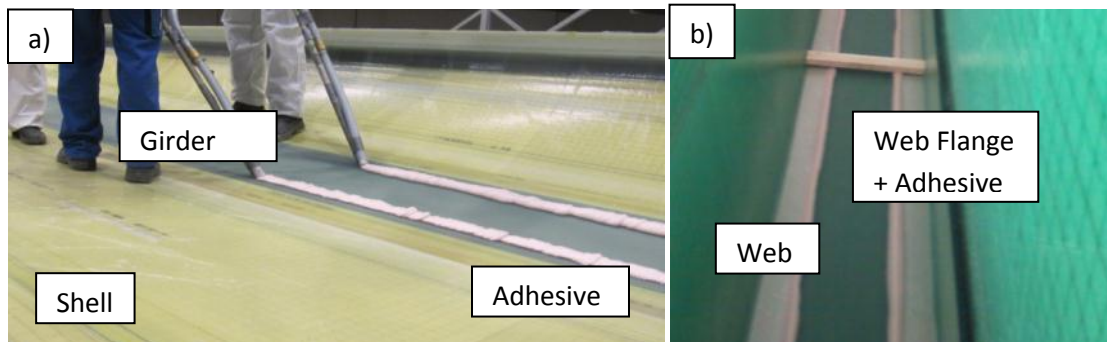


Figure 2.3 – a) Application of adhesive into the first shell to place the shear webs; b) view from inside the webs after they are in place.

Some of the process parameters which affect the performance are temperature, time (pot life), equipment and tools, the shop-floor workers and the adhesive.

- Temperature is related with the sensitivity wind blades'<sup>8</sup> adhesives have to it. On one hand the adhesive need temperature to cure (around 80°C). On the other, the mold has to cool

<sup>8</sup> The adhesives normally used in wind blade industry are high bond strength two-component epoxies. Their specific working time, substrate compatibility and weatherability make them to work on the limit. For these reason, their

down enough after curing the infused part to properly place the adhesive. If the mold is still warm, there is a risk the adhesive will cure before placing the webs on top of the main shell. A cooler temperature in the environment can help to quicker cool down the mold or to avoid quick heat up of the adhesive.

- The time is related with the amount of time available to pour the adhesive and to clean. Trained workers normally perform these tasks quicker and better. The amount of time required is around 50 minutes for the first application of the adhesive (webs - Figure 2.1.a) and 1 hour 30 minutes for the second (when the blade is being closed - Figure 2.1.c), but the time before the adhesive starts to cure depends on its type and temperature. Figure 2.4 shows an example of two adhesives used for the wind blade industry. The blue line represents a quicker hardener for the webs, while the red line is the adhesive used for closing the blade. When comparing these times (the exothermic reaction and the working time available), it is easy to understand there is no much margin for problems or “mistakes”.
- The equipment, the tools and the workers have a direct impact on the speed and the quality of the joints. Well trained workers with good equipment and tools can guarantee a better finishing, e.g. defects like lack of squeeze out will not happen and the surface will be cleaner.

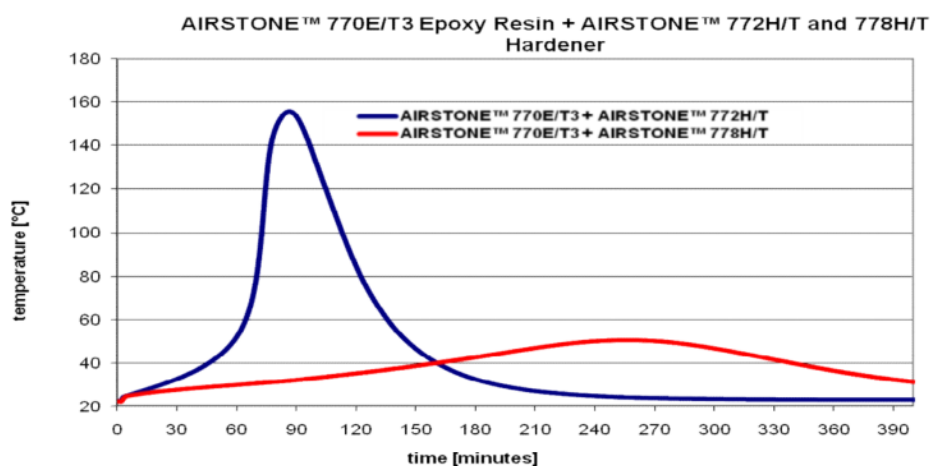


Figure 2.4 – Exothermic reaction for Airstone resin (770E/T3) while curing with different hardeners (772H/T and 778H/T) (147g at 23°C) [91].

## 2.2 Process Performance

Quantitative performance measurements tell something important about products, services, and the processes that produce them. Actually, companies have been measuring costs, quality,

---

composition is changing, to include acrylates and polyurethanes, this challenge the use of epoxies in this market [90].

quantity, cycle time, efficiency, productivity, etc [26] as long as ways to measure them are already available. Independently of the index to be evaluated, these are tools to understand, manage, and improve what organizations do. Performance measures give the opportunity to know how well the company is doing, if it is meeting the goals, if the costumers are satisfied, if the processes are statistically in control and where improvements are necessary [92]. There is much variation in the way performance metrics are calculated in practice, but it is vital to understand how a metric coming from a particular company or industry is calculated prior to making any decision [26]. More often, multidimensional units of measure are used. These are performance measures expressed as ratios of two or more fundamental units. These may be units like km per liter (a performance measure of fuel economy), number of accidents per million hours worked (a performance measure of the companies safety program). Performance measures expressed this way almost always convey more information than the single-dimensional or single-unit performance measures. Ideally, performance measures should be expressed in units of measure that are the most meaningful to those who must use or make decisions based on those measures [92]. The list below presents some examples of indexes that can be used to asses a manufacturing process.

1. *Efficiency* is the ratio of the actual output of a process relative to some standard value [26]. For example, it can be defined as how the product is done with the minimum possible material.
2. *Ratio of the process velocity* is also known as throughput ratio. It is the total throughput time to the value added time. Value added time is the time in which useful work is actually being done in the unit.
3. *Quality* can be a process characteristic indicating the degree to which the process output (manufactured products) conforms to requirements (Do the products match the specification?). It can be measured as the number of defects in a time scale number of defects per part manufactured.
4. *Safety* measures the overall health of the organization and the working environment of its employees.

Performance metrics are not only for the organization to improve the process and the costs but also for the designers to learn the limitations and capabilities for the technologies in a

determined product. This point becomes even more important when specialized work<sup>9</sup> is inherent to the organization and cross functional teams are not able to work together.

### 2.2.1 Efficiency

In general, efficiency means the quality or degree of being efficient [93]. One of the most pragmatic ways is to define it as a comparison between the production and the costs (for manufacturing) (Equation (2.1)). Other set of considerations or parameters can be addressed in this part, but in this work efficiency is understood as the **ratio between the amount of adhesive used in each blade and the Bill of Materials (BOM) established value**<sup>10</sup>. This ratio can assess the actual deviation and the possibility to improve the costs. Any efficiency assessment can only be done in a controlled system independently from how it is performing.

$$Efficiency = \frac{Adhesive\_consumed}{Adhesive\_ (BOM)} \quad (2.1)$$

In general, values closer to 1 in this parameter are the expected outcome. Higher values represent that more than expected was used. Lower values represent the best results possible and even margin for improvement. To get these values in a proper way with a good reliability, a variation of a tool called Plan-Do-Check-Act (PDCA) [26], [37], [94], normally used in Continuous improvement. PDCA is a process based quality tool that focuses in the performance of a task by controlling. The PDCA model shown in Figure 2.5 covers all the requirements considered in ISO 9001 [94], but does not show processes at a detailed level. The problem is that PDCA can only be applicable when it is stabilized and under control which was not the case of the results presented in this case study. When that is not possible a modification of the cycle called SDCA (Standardize-Do-Check-Act) is also available in the Kaizen Methodology [95].

<sup>9</sup> The method of job specialization involves breaking down a task to its lowest level and designing jobs around each part. This creates specialization, expertise, and improved quality.

Read more: [What Is Job Specialization & Job Evaluation? | eHow.com http://www.ehow.com/about\\_6721655\\_job-specialization-job-evaluation.html#ixzz27narg0pf](http://www.ehow.com/about_6721655_job-specialization-job-evaluation.html#ixzz27narg0pf)

<sup>10</sup> This is a “theoretical” value that a blade uses of adhesive. It normally comes from experience.

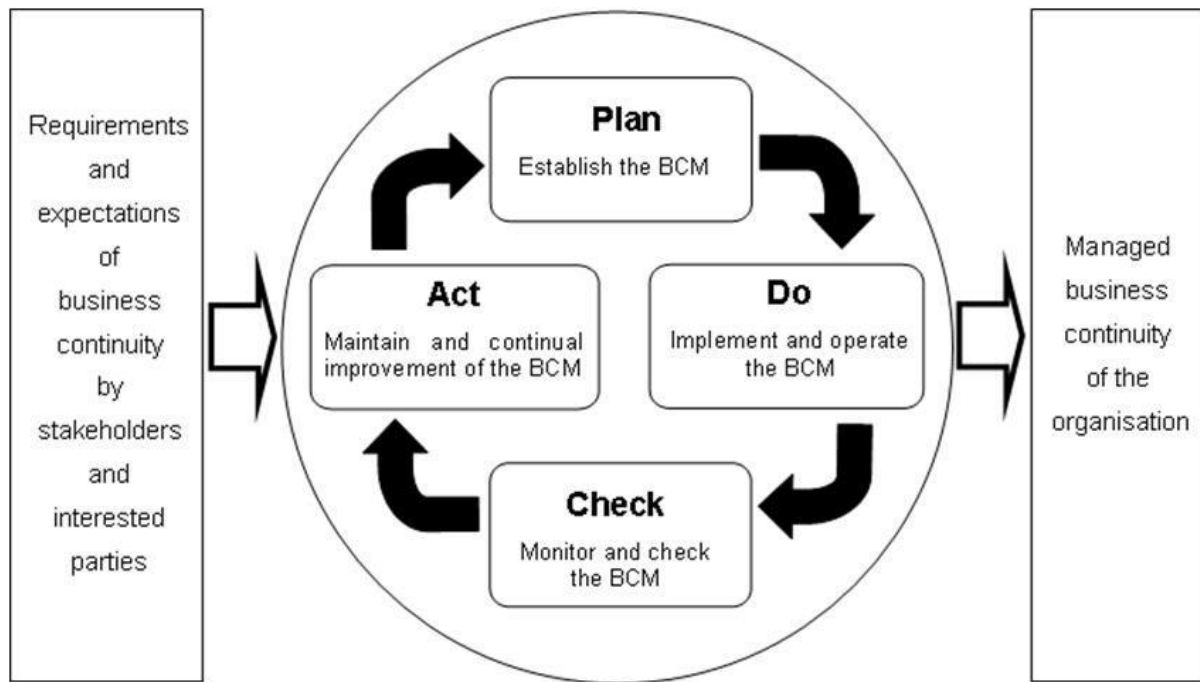


Figure 2.5 – Model of PDCA defined in ISO 9001 [94].

#### 2.2.1.1 Standardize – Do – Check – Act (SDCA)

Understanding how the process is affected when it is running in a “steady pace” is vital for the success of any project and to understand how reliable is the information obtained. In other words, to understand how the production changes along time, the process has to be in control and well balanced, therefore SDCA (Standardize, Do, Check & Act) was used. This tool is valid as any other tool, where controlling and improving is done. Figure 2.6 present the overall method used to run this exercise. Basically, the principle behind SDCA (which is a particular case of Plan, Do, Check & Act<sup>11</sup>) is to make the objectives and the actions plan (tasks) to achieve them. The results obtained are compared with the goal to be achieved and at the end the action is made official if it fits the goals [95].

<sup>11</sup> SDCA was used because PDCA can only be done when the process is already standardized. In fact, PDCA is to improve a process while SDCA is to standardize it.



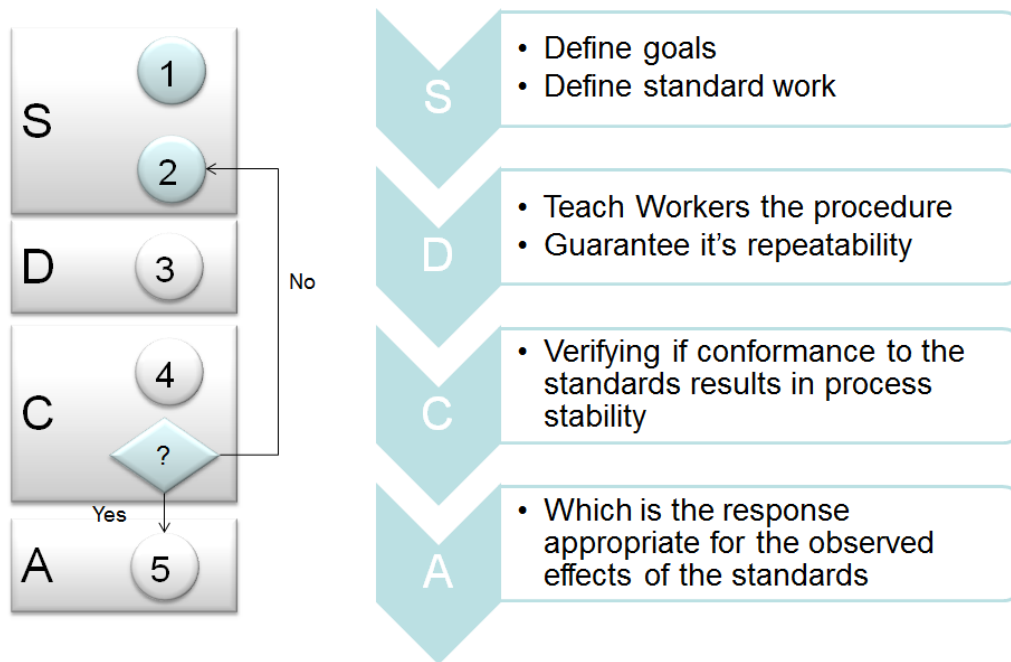


Figure 2.6 – SDCA for cost analyses.

### 2.2.1.2 Standardize

This phase begins with the identification of an issue or a need. Then, an analysis has to be performed to understand what are the specific causes for the problem, e.g. why it is not done in the same way all the time. Finally a set of goals to be achieved have to be clearly stated and actions to solve the problem defined. *In this case, the first two goals were:*

1. ***diminish the deviation of the material consumed and lower it;***
2. ***and improve the quality of the product.***

To achieve the first goal a clear and easy Standard Work<sup>12</sup> was missing. Defining clear ways of working and steps is one of the best paths to lower the effect of human behavior in any process. The second was more complex. As no clear reason or problem was found on the analysis made for quality improvement is presented in 2.2.3 Quality.

### 2.2.1.3 Do

The **Do** was running the produced Standard work with the shop-floor workers guaranteeing its repeatability. This means checking best practices and trying to avoid errors already embedded in the process.

### 2.2.1.4 Check - Results

There are four main stages where clear lines to check the process behavior were drawn, more or less each “batch” is divided in 30 blades. In fact, this process was made from the blade 50

<sup>12</sup> Standard Work – Quality tool, document to define the way of working.

(moment when the case study started) until the blade number 175<sup>13</sup>. It can be considered that the SDCA cycle run 4 times and the assessed variable was the amount of adhesive used in for each blade. The tolerance given for the variable is 10%, making these points the lower limit (LL) and the upper limit (UL) and 1 represents the theoretical amount of adhesive used (BOM value) in each blade.

Initially, it was necessary to learn about the process (Figure 2.7 - 1) and how it was being done. Then the 1<sup>st</sup> step was to define what the steps were and the tasks performed (Figure 2.7 - 2). The final step of SDCA was point 3 (Figure 2.7), where the process was already stabilized and under control. The problem was that as any manufacturing process changes occurred, so stages 4<sup>rd</sup> and 5<sup>th</sup> are the evidence of those changes. The changes in the process<sup>14</sup> made difficult to quantify the improvement, but the objective was reached. Figure 2.7 and Figure 2.8 show the evolution consumption of adhesive along the time of this study.

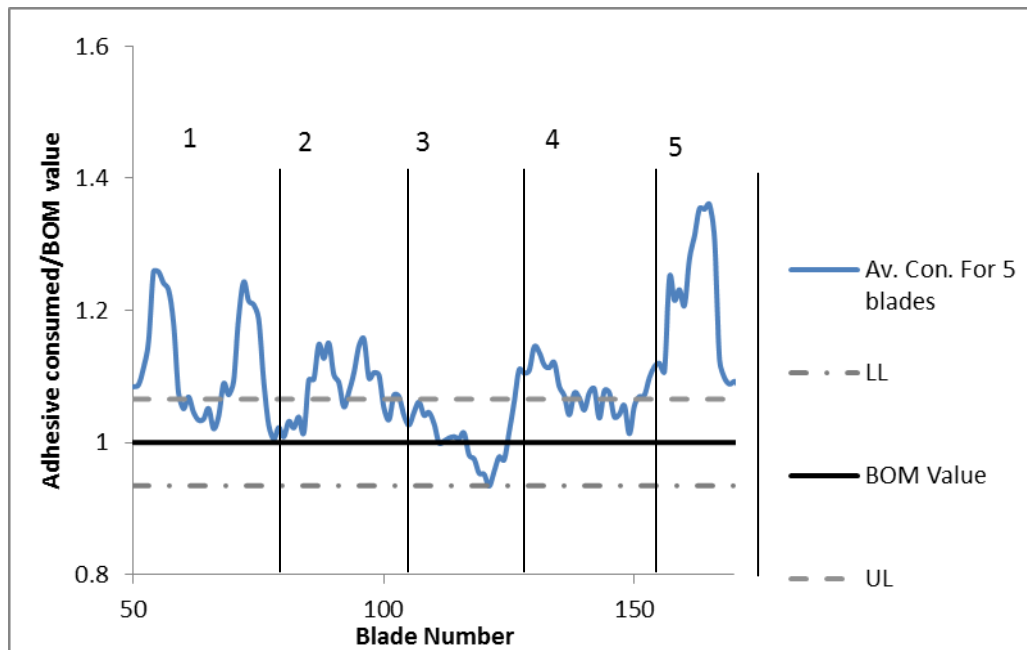


Figure 2.7 – Average of the mount of total adhesive consumed (Until blade 170).

At the end of the project, after all the changes were standardized and stabilized, the achieved results presented values smaller than the actual BOM (Figure 2.8) which implies that it is possible to improve the performance even more than what was obtained until now.

<sup>13</sup> These are the blades' numbers used during manufacturing.

<sup>14</sup> The changes are detailed in the section 2.3.

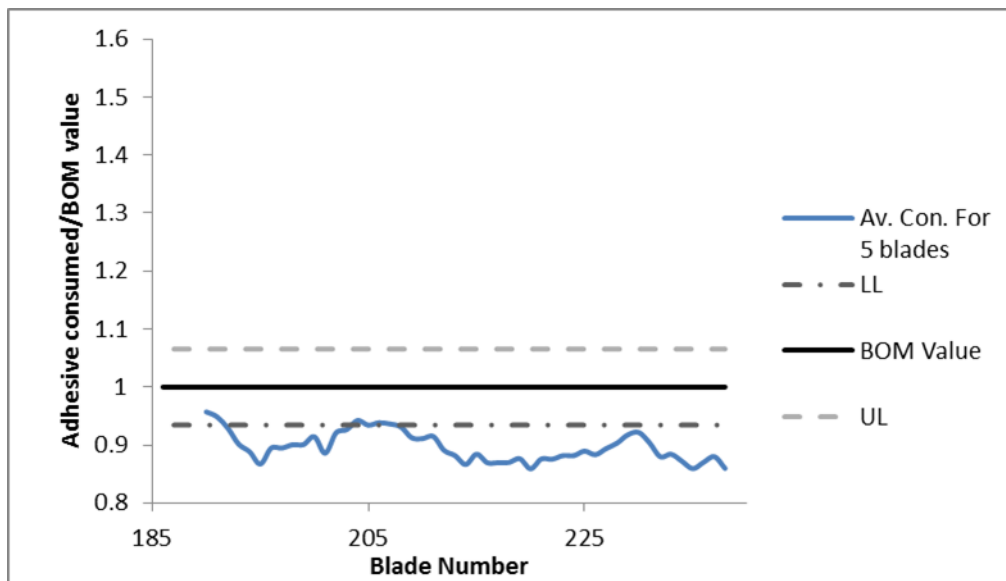


Figure 2.8 - Average of the amount of total adhesive consumed (from blade 185).

#### 2.2.1.5 Results

The SDCA cycle was running until blade 125, but to give a complete overview of the evolution of the process, all the results are presented here. The average value of adhesive consumed, between blade 1 and blade 175, was 1.09 and the standard deviation 0.15. This poor value shows how difficult this process can be, and this efficiency can affect not only the manufacturers of the blades but also the performance of the blade. It actually shows that something was wrong.

Focusing only on the blades where the SDCA was run, Figure 2.9 shows the amount of adhesive used in each blade as a function of the BOM value. The improved performance was actually visible comparing the results from 1 to the 3 stages (Figure 2.9, Table 2.1 and Table 2.2). Transforming the results in a Normal Distribution Function (Figure 2.10), the average value is clearly shifting to 1 and the standard deviation (Std. Dev.) goes from 0.16 to 0.08 (Table 2.1). Table 2.1 shows this variation for the 3 stages. The final assessment of the statistical quality control was to address the cumulative probability of having a value in between the BOM limits.

Table 2.2 shows the probabilities of having the adhesive consumed inside the expected limits. While at the beginning of the work, the values around the UL (BOM upper limit) were around 30%, at the end the probability of having a consumption value below the LL (BOM lower limit) is almost 40%, and almost 70% if the blades were bonded with the expected amount of adhesive.

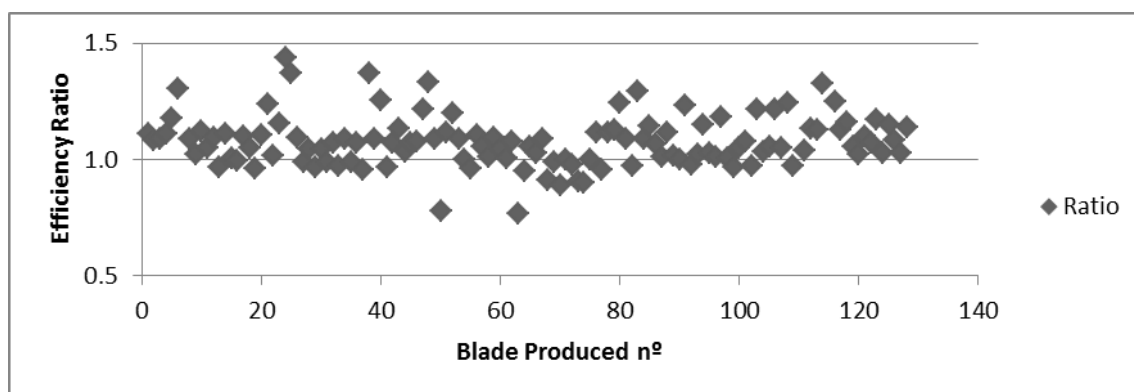


Figure 2.9 – Efficiency Ratio of adhesive consumption per blade manufactured.

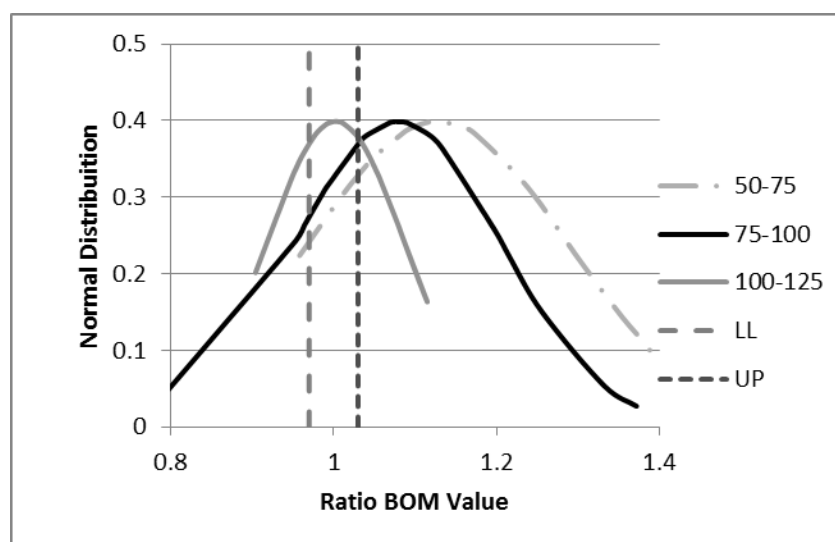


Figure 2.10 – Normal function regarding three different time periods.

Table 2.1 – Average and Standard deviation of the material consumed along the case study in different stages.

Stage	<i>Blade nº</i>	<i>Av.</i>	<i>Std. Dev.</i>
<b>1</b>	50-75	1.13	0.16
<b>2</b>	75-100	1.08	0.12
<b>3</b>	100-125	1.00	0.08

Table 2.2 – Normal cumulative probability of having the consumptions inside the BOM values.

Cumulative Probability			
<i>Stage</i>	<i>Blade</i>	<i>LL</i>	<i>UP</i>
<b>1</b>	50-75	0.143	0.307
<b>2</b>	75-100	0.191	0.355
<b>3</b>	100-125	0.384	0.674

### 2.2.2 Ratio of the Process Velocity

Considering process velocity in terms of manufacturing, it is understood as a controlled speed for a specific task to manufacture a product. This process can run at two different paces. The 1<sup>st</sup> stream is when the webs are bonded in the main shell (Figure 2.1 from a to c) and the 2<sup>nd</sup> is when the blade is closed (Figure 2.1 - d and e). This means the 1<sup>st</sup> part ends when the adhesive of the webs is bonded, being that moment the beginning of the 2<sup>nd</sup> part. Independently from the stream, there are two main factors that directly influence the velocity: the time needed to cool down the mold and the time needed to heat it up. This will become a bigger limitation with an increase in the blade size. Figure 2.11 shows a sketch with the complete process, being the limit of the 1<sup>st</sup> part the end of the black circle.

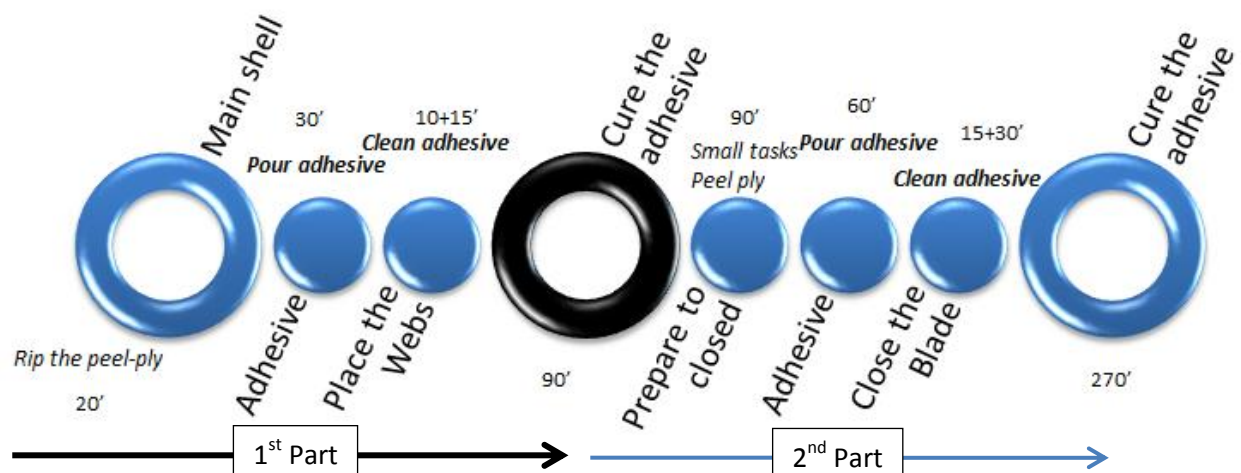


Figure 2.11 – Sketch of the complete process and times<sup>15</sup>.

Ratio of the process velocity is then given by the following Equation (2.2), where the cycle time is the time needed to finish one blade and the working time is the time where the process is creating extra value on the blade.

There are three clear moments: when the adhesive is placed and when the adhesive is clean, plus the “extra” time needed to fulfill the task. The process itself takes around 165’ but from this only 45’: 30’ to pour the adhesive and 15 to clean it - represent added value. The extra 10’ considered inside the clean adhesive phase is related to the time needed to actually move the webs from where they are standing to the mold and placed them properly. Considering bonding the webs the velocity corresponds to 30% of the cycle time but the *operation time*<sup>16</sup> represents almost 50% of the cycle time (90’) which cuts the margin from improvement. This means that on 30% of the cycle time value is generated. Two options can be used to reduce

<sup>15</sup> The times needed to cool down are not taken into account here, because it varies with the season.

<sup>16</sup> Operation time is the sum of the setup time and run time for a batch of parts that are run on a machine [26].

the cycle time, one is to overlap tasks and the other is to improve the operation time, by having more efficient heating and cooling systems for the mold.

$$\text{Ratio\_of\_Velocity} = \frac{\text{Working\_time}}{\text{Cycle\_time}} \quad (2.2)$$

The second part of the process (when the blade is going to close) has an even larger setup time, but in this case it is not taken into account, because the workers and the resources can perform other tasks while the blade is in the final curing. In fact, it can be affirmed that this final task does not have any impact on the velocity of its predecessor, but the opposite is not truth. Any delay in bonding the webs implies automatically a delay in finishing its manufacturing of it. The second part is a process that takes more or less 195 minutes, without curing (Figure 2.11 – for the 2<sup>nd</sup> part the complete cycle is 270 minutes). From these 270 minutes only 90 minutes are useful, the rest is normally a group of minor tasks and the rip off the peel ply which means that the velocity is 50% of the cycle time. Consequently, there is also a margin to improve the operation time of the mold and the general tasks.

### 2.2.3 Quality

The quality specifications of a product or service derive from decisions and requirement made relative to the expected performance of the design. The dimensions of quality are listed in Table 2.3. In general, the lack of any of these dimensions is understood as defects. The typical defects are: disbonds, kissing bonding, poor cure, cracking within the adhesive and delamination in the adherend (Figure 2.12).

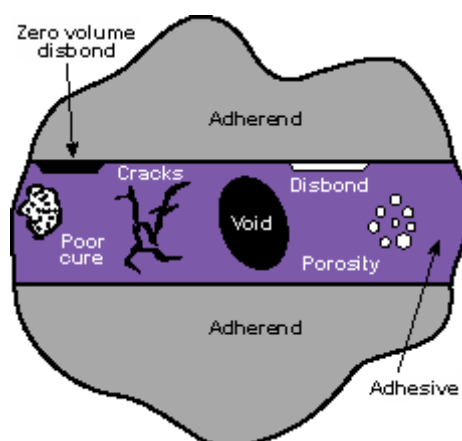


Figure 2.12 – The common defects regarding composite bonded joints [67].

Table 2.3 – The dimensions of quality design [26].

<b><i>Dimensions</i></b>	<b><i>Definition</i></b>	<b><i>Impact on Bonded joints</i></b>
<i>Performance</i>	Primary product or service characteristics: the fulfillment of a claim, promise, or request.	Normally associated to the mechanical properties of the product and the mechanical behavior of it.
<i>Features</i>	Secondary characteristics added.	No holes, possibility of a smooth surface, directly after finishing the manufacturing.
<i>Reliability</i>	Consistency of performance over time, probability of failing, useful life.	E.g. Process-property dependency can change the life in service of a product.
<i>Serviceability</i>	Ease of repair.	Depending on the product, if secondary bonding is an option, it can be re-bonded. If not application of bolts, replacement or patches are the options.
<i>Aesthetics</i>	Sensory characteristics (sound, feel, look, etc.).	N/A
<i>Perceived quality</i>	Past performance and reputation.	Normally, this is a limitation because the lack of control and the excess of adhesive inside a blade can harm the blade or at least the root.

The quality analysis was applied in the context of blade manufacturing. The total number of defects during the time of the study was 132 in 61 blades produced which means a ratio of 2.15 defects per blade (Equation (2.3)).

$$Quality = \frac{Bonding\_defects}{Parts\_produced} = \frac{132}{61} = 2.15 \quad (2.3)$$

The defects can be categorized from the place where they were found or as the type of defect. Considering the place, they were mainly found in the shear webs (Figure 2.13). The trailing edge (TE) is the most affected in both sides the suction side (SS) and the pressure side (PS), while in the leading edge (LE) the web has fewer defects.

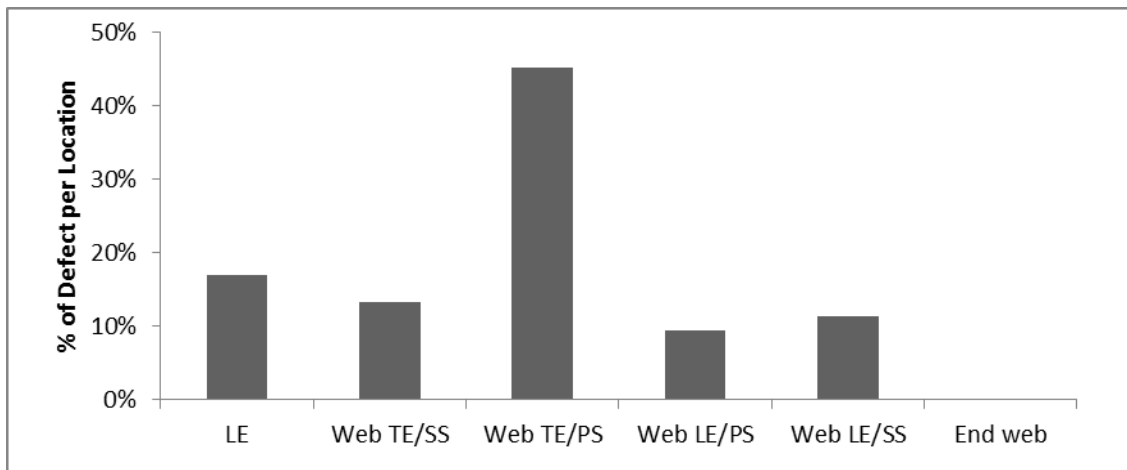


Figure 2.13 – Amount of defects in % to compare which place has the higher incident number.

Figure 2.14 shows the defects per type. The type of defect can be lack of adhesive, excess of it (means out of specification), air bubbles, weak bonds, lack of adhesive in the run-out (without chamfer). The most important (the ones in more number of incidents) are **run-out** (Figure 2.15a)), which defines without a chamfer and **lack of adhesive** (Figure 2.15b)), which is actually standing for values below the minimum specification (1 mm).

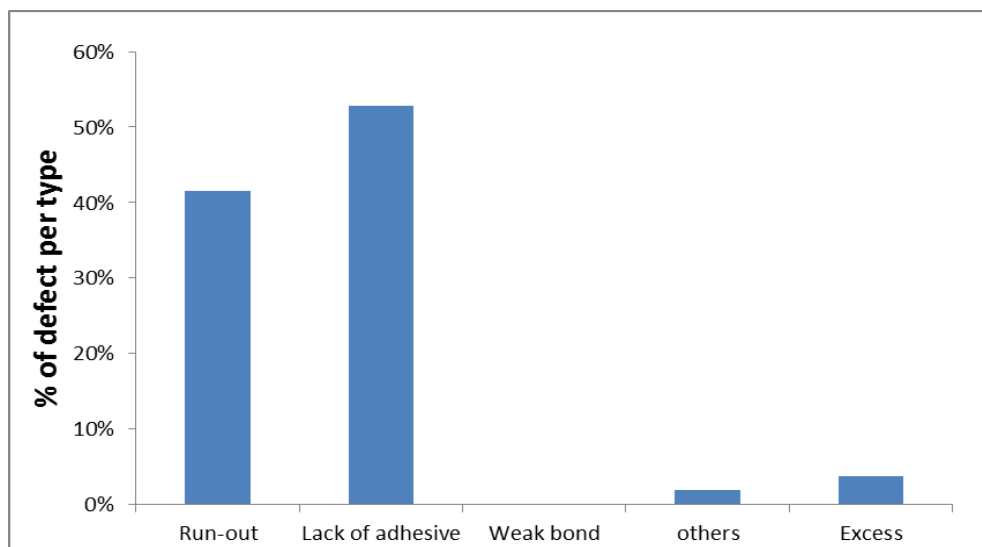


Figure 2.14 - % of defects considering the type of defect focus on the most common defects.



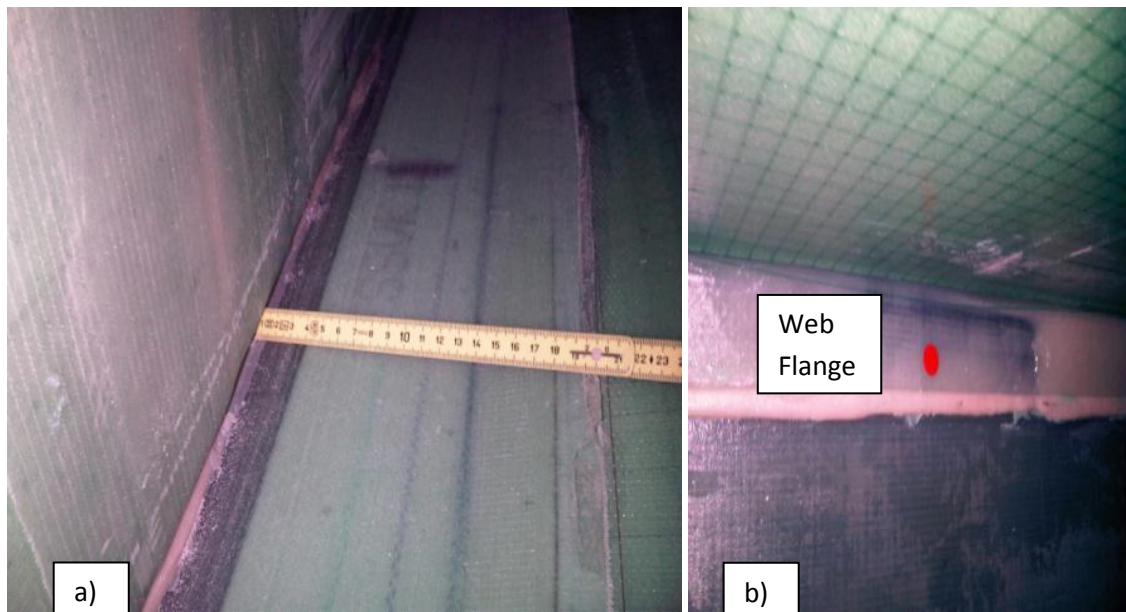


Figure 2.15 – Most common defects in blades: a) run-out in the web, and b) lack of adhesive in the web.

The defect **lack of adhesive** is related to how the specification is measured if the values are so small and the surfaces have curvatures. A campaign was made to assess the actual bond line thickness by comparing bonded samples with thicknesses smaller than 1 mm with the “real joint” (Figure 2.16). The bond line thickness and the web flange thickness (Figure 2.17) was measured by drilling a small hole in the run-out. The flange is around 4.5 mm (this was defined in a previous measurement) which subtracted from the 6.52 mm measured with the caliper gives a value of  $\approx 2$  mm.

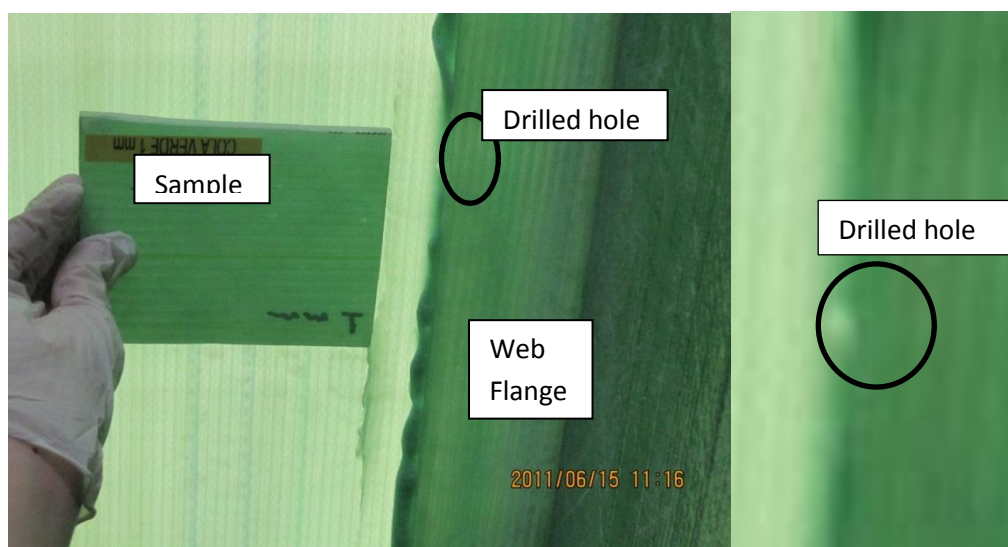


Figure 2.16 – Comparing the sample left with the main shell + web flange.

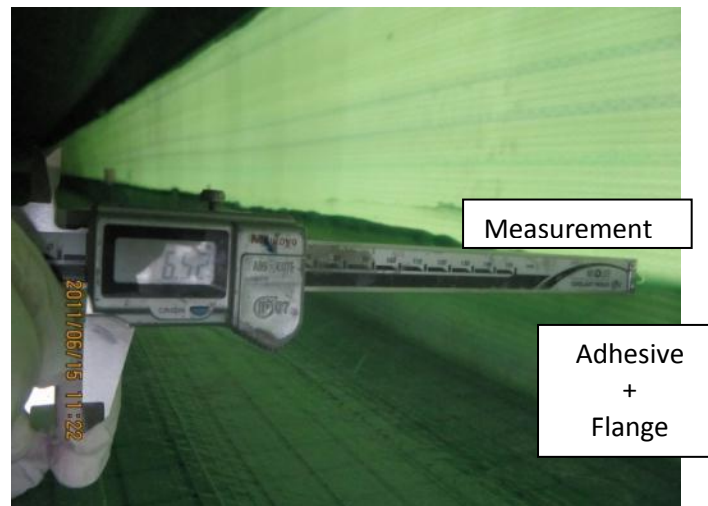


Figure 2.17 – Bond line + flange thickness measured at the joint after being cured.

#### 2.2.4 Safety

There is no index for the safety assessment in this particular case. But it has to be taken into account because adhesive materials, resins and composite fibers are extremely aggressive for the environment and the health. Companies like Gurit [96] and Dow have clearly defined the best practices for general health and safety regarding their products. This index can be defined taking into account the rules of the companies and the actual behavior of the workers or the problems with resins, adhesives or other chemicals in a period of time which can jeopardize the health of the workers.

### 2.3 Manufacturing Costs

Cost can be seen in a design-to-cost or design-for-cost context. Design-for-cost is the conscious use of engineering process technology to reduce life cycle cost while design to cost provides a design satisfying the functional requirements for a given cost target. Accurate cost data is a critical factor for successfully implementing cost estimation system [97] (in fact, the potential costs savings is the main drive for the aeronautical industry to invest in this technology). Costs, research and manufacturing are normally evaluated on the potential benefits, so project proposals are often evaluated on the basis of “usual costs” such as capital costs, raw materials and utilities [98] and this is also applicable to research. Production cost is a vital metric for engineering and management analysis when affordability is the key issue facing design engineers and manufacturers of composite components [99]. It can be seen as a clear value, where the relation between part, materials and values is derived or as “soft” where features of the process have to be analyzed. The combination of both costs can then be difficult to be understood. In fact “*cost analysis*” can be seen almost chimerical [100]. Process-Based Cost Model (PBCM) appears then as an engineering tool to guide and learn more about a process

and a technology or a set of technologies depending on the case. PBCM involves gathering information about technical context and costs, to obtain well weighted scenarios that can help further decisions. In other words, it must be able to address implications of change in product design and/or product operation (including production volume). The process map describes operation costs and then a decision about alternative technologies can be taken before operations are in place [99], [100].

Kirchain et al. defined four critical steps in the PBCM [101], and a fifth step regarding the uncertainties to try to capture the complexity of this process.

1. Define the question: *What costs are going to be modeled?*
2. Identify relevant costs elements: *What cost should be considered?*
3. Diagram process operations and material flows: *What resources will be modeled?*
4. Relate costs to what is known: *How detailed relationships can be build?*
5. Identify uncertainties<sup>17</sup> inherent to the process.

The metric used can be a rate, a Cost per unit (to compare technologies) or a Cost per period of time.

### 2.3.1 Definition of the Questions to be Answered

According to Field et al. *the notion of “context” lies at the heart of effective use of engineering cost estimates* [100]. In fact, engineers typically emphasize the dynamics of cash-flows and the evaluation of their net present value in order to select among alternatives. But what is to be defined in the appropriate scope can be understood as answering a question. The questions considered can make vary significantly the results. *A classic example of this difficulty can be developed from a consideration of the following question: how will cost change if a material substitution is under-taken? While the simplest evaluation would focus upon the price differential between the current and new material, in general there is far more to it* [100]. The questions presented below are needed to give the context and to understand what costs are relevant in this work.

- *Cost of What?* Carefully understand processing boundaries  
Bonding process, waste and the Bill of Materials (BOM) cost for the manufactured blade
- *Cost to Whom?* Perspective determines pertinent costs

---

<sup>17</sup> **Uncertainty** is the indefiniteness or variance of an event. It captures the phenomenon of observations, favourable or unfavourable, falling to the left and right of a mean or median value

The manufacturer to improve the revenues by lowering the costs without affecting the quality of the product (Design for costs)

- *Cost Varying How?* What technical changes are being considered?

Only by controlling and standardizing a process can the variation be understood. The process was standardized first and the impact of the changes was assessed. It has strong dependencies to the material and this varies with the equipment and the shop-floor workers.

- *Cost Compared to What?*

In this particular case study was to address the cost of bonding a blade, considering the 2 stages mentioned above (section 2.2.2 - Ratio of the Process Velocity), when compared to the overall cost. Also, it is an opportunity to understand how the process is really related to the functional costs of it. In other words, *this exercise was run to compare it with the BOM value of a blade, to understand the impact of this part of the manufacturing cycle in the overall production.*

In any modeled scenario there are some remarks that have to be taken into account:

- The bonding process can be considered as one big process from the moment the shear webs are bonded until the blade is finally closed and “ready”.
- Exclusive fixed costs are mainly related to the equipment: two-component metering and mixing equipment is normally “expensive”. Their actual value cannot be considered as part of the problem (*because it was not available*) but it gets easily dissolved in a year’s production (depending also on the time of equipment). The problem is that they need regular maintenance because of the chemical corrosion.
- Finally the size of the blade has a direct impact in the amount of the material used, in the amount of waste, the wear of the machine and this has a direct implication in the costs.
- Manufacturing costs have always a direct implication in the manufacturer’s profit. But when the blade goes to service concerns, like reliability, safety and product performance (in general) are also important. A failure in the manufacturing is not an option, because companies can lose a market share. Therefore, the “improper” cut of costs in the manufacturing process can imply an extra cost in the maintenance of the product, which can then be a problem for the manufacturer. Independently of the case study, this issue has to be taken into account because high performance products are sold with the guarantee of excellent performance.

- To account for the variation, a standardization process was run because no process out of control can be analyzed. Analyzing this kind of process can mislead analyzers to understand the process and the causes of variation.

### 2.3.2 Identification of the Relevant Cost

To identify what are the relevant costs, it is important to understand clearly the context and the aim. Considering that process was mainly controlled by the material expended in each blade, this gave the opportunity to learn about what are the relevant costs. The costs are listed out in Table 2.4. From this list, to identify the relevant one *“it is left to the modeler to determine which set will be considered [99]”*. This is because the context defined previously is the 1<sup>st</sup> input to be considered. In other words, the costs are relevant if they are related or can help to reach the objectives.

Table 2.4 – All costs related to the bonding process.

<b>Theoretical costs</b>	
Material	Mold
Energy	Equipment
Labor	Mold Maintenance
Equipment maintenance	Insurance
Waste	Tooling
BOM cost of the blade	Cleaning products
Consumables (Globes, mask, tyveks, etc.)	Etc.

The costs chosen in this work are related with the impact they actually have on the overall cost. In this case, costs taken into account are only recurrent. Fixed costs were not addressed because the facilities and the rest of the equipment (molds) are used in all the stages of the manufacturing process.

Table 2.5 clearly defines and gives measurement criteria for each one of the parameters defined as relevant. Material and waste have an impact 88% (Table 2.6) on the overall cost of the process. In addition, the other costs are dependent of these two parameters as well that is why they have been marked in bold in Table 2.6. In addition, energy is also considered because it is an important value even if it was not defined in this work. Electricity costs have an impact in the overall cost of the product. The fact is that the costs for heating a 45m mold (any press or autoclave – in general) for several hours have an impact in the bill which means that even if

the value was not considered here it is also a source that can be taken into account if available. Table 2.6 shows the ratio of the costs compared to the overall costs of the process and the blade BOM, therefore bonding the blade corresponds to 13% of the total cost to manufacture it.

Table 2.5 – Definition of each relevant cost.

Relevant costs	Definition
<b>Material</b>	Average consumption of adhesive per blade – BOM's adhesive costs (Cost per kilo).
<b>Energy</b>	kW/h consumption per time of curing adhesive
<b>Labor</b>	Team per time used during the process
<b>Equipment maintenance</b>	Costs involved in the maintenance per usage
<b>Waste</b>	Euro/kg, regarding policies for hazardous materials
<b>BOM cost of the blade</b>	Total BOM's cost of a blade complete by produced

Table 2.6 – % of the Costs as a function of the total cost of the process<sup>18</sup>.

Parameter	% of the cost
<b>Material:</b>	<b>56%</b>
Energy:	0%
Labor:	10%
Equipment:	2%
<b>Waste:</b>	<b>32%</b>
<b>Total cost of the process</b>	<b>100%</b>
<b>Impact on the cost of the blade</b>	<b>13%</b>

### 2.3.3 Diagram Process Operations and Material Flows

After identifying the relevant costs, they shall be associated to physical task; Figure 2.18 shows the sketch of the correlation between the costs defined in the previous section and the process.

<sup>18</sup> Total Cost of the Process = Material + Energy + Labor + Equipment + Waste

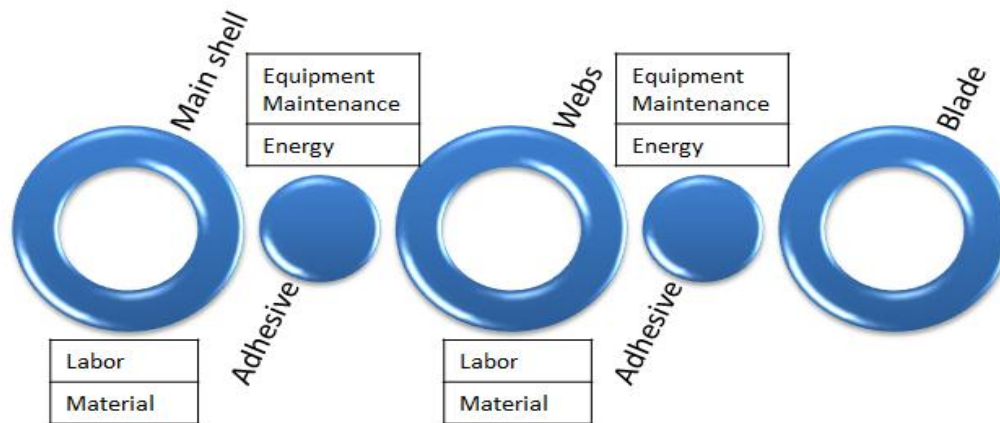


Figure 2.18– Sketch cataloguing each process step associated.

In this section **Adhesive** (Figure 2.18) is considered as the moment when the applied adhesive has to cure, that is why the equipment maintenance and the energy are included here. Normally, after usage, all the possible materials have to be clean to avoid degradation of it and the mold has to be turned-on to cure the adhesive. The main shell, the webs and the blade are the association between the process and the changes in the product. The **Main shell** (MS) is when the adhesive is applied for the 1<sup>st</sup> time. The **Webs** is the moment when the adhesive is applied to close the blade. Finally, the **Blade** is the finished good ready to leave the manufacturing cycle. In these stages the most important factors are the labor and the material, because:

- they represent at least 50% of the cost
- and they are a cause for variation or increase the risks.

#### 2.3.4 Relate Costs to What is Known

Concerning blade manufacturing, the costs are mainly concentrated in four main aspects:

- the amount of material consumed depends on the equipment;
- the material's waste can have extra costs to be send to garbage;
- the excess of adhesive can jeopardize the life in service of the product and increase the amount of material wasted (and going to garbage);
- labor, which is a highly manual task; "good" workers have "better" performance and consequently the costs are lowered.

##### 2.3.4.1 Variability

The data values for any process or product always vary, i.e., there are no identical products. The differences among products may be large, or they may be immeasurably small, but they are always present. The variation, if the data values are measured, can be visualized and

statistically analyzed by means of a distribution that best fits the observations. This distribution can be characterized by: location (average value), spread (span of values from smallest to largest) or shape (the pattern of variation –whether it is symmetrical, skewed, etc.) [102]. In general variation is accepted as a problem, if it is reduced quality is improved. Methods like “six sigma” clearly address the variation and propose ways to control the variation and to improve it [27], [102]. But in this case, an analysis was made of two parameters that changed (material and the equipment), to create a database that can be used later for reference, regarding the real impact of changing the material and the equipment in the process.

In fact stages 4 and 5 in the SDCA addressed those changes (2.2.1 Efficiency). Stage 3 represents the process (Figure 2.19) when it was stabilized and was working “properly” and stages 4 and 5 represent the change in the equipment and material respectively. Comparing the results shown in Figure 2.20 and Table 2.7, the effect of both parameters creates at least an increment in the average consumption, the distribution curves are then shifted to the right (which is not good). The problem is that when changing the material the deviation also increases (Figure 2.19 – 5 and Table 2.7) creating then more chances for “mistakes”. Table 2.7 shows that at stage 5 the value of the standard deviation (Std. Dev.) is 0.22 which is more or less 20% of the average value.

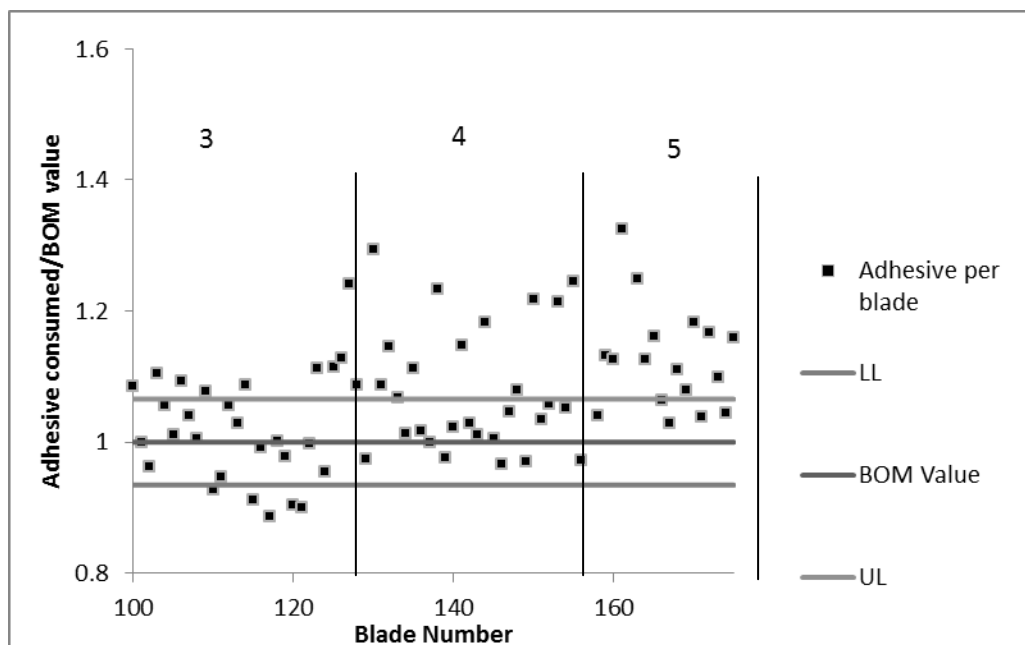


Figure 2.19 – Adhesive consumed per blade from 100 to 175.



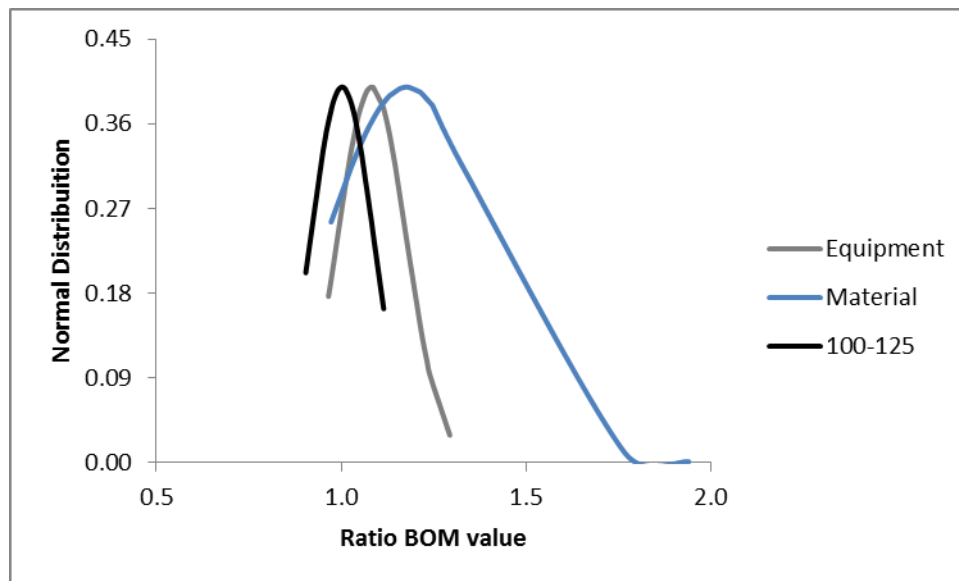


Figure 2.20 – Normal distribution regarding the 2 changes in the process

Table 2.7 – Average and Standard deviation induced by the changes in the process.

Stage	Blade	Av.	Std. Dev.	Comments
3	100-125	0.97	0.17	Stable process
4	125-150	1.08	0.09	Change of equipment
5	150-175	1.18	0.22	Change of material
6	186-241	0.90	0.05	Final controlling stage

Why the material has a bigger impact on the changes? Some hypotheses have been drawn:

- Because the changes provoked by the equipment were not stabilized when the materials were changed;
- the material affects the equipment and the way of working, increases the uncertainties and the risks and this is reflected in the consumption;
- the high variation is just inherent to the process and cannot be controlled.

In fact, could be an effect of all three hypotheses. The process has an inherent variation that needs to be under control all the time. The material even if it has more or less the same characteristics of the predecessor, definitely has other limitations and needs different ways of working, so it affects workers and equipment (which implies automatically that more parameters are affected). It can conclude that if the process was stabilized after changing the equipment and before changing the material the standard deviation can be lowered instead of increasing (Table 2.7 – Std. Dev.).

About the equipment, what is the real impact in the process?

- Changing equipment affects the way how the adhesive is applied but not really the way of working, which makes the effect of this change much smaller;
- the problem comes then, as long term effect, while workers can learn to work properly with an adhesive; some parts of the equipment can be very sensitive to it.
- Figure 2.21 shows the behavior of the equipment used for web bonding by comparing the *total amount of material used*<sup>19</sup> with the actual amount used to bond. Figure 2.22 is the same, when the blade is being closed. Here the differences deserve a reflection, how can these changes be prevented- the 0.05 standard deviation (5.5% of the average value), it comes mainly from the problems in the equipment. Therefore keeping a well maintained equipment can be a solution. Anyway, this small difference is dissolved in the total amount used (Table 2.8).

Other point to be considered is that long term effect seems to be deterministic in the good performance of the process. Figure 2.22 clearly shows that there are moments where the deviation between the material used in the blade and the material consumed is around 10%. The bigger problem can be if this is not detected on time, because it can create a cascade effect and the final outcome can be the initial status of the process (Figure 2.9). It is not expected to have always the same value of adhesive used for bonding, but a reasonable limit is 5 or 10% of the BOM value.

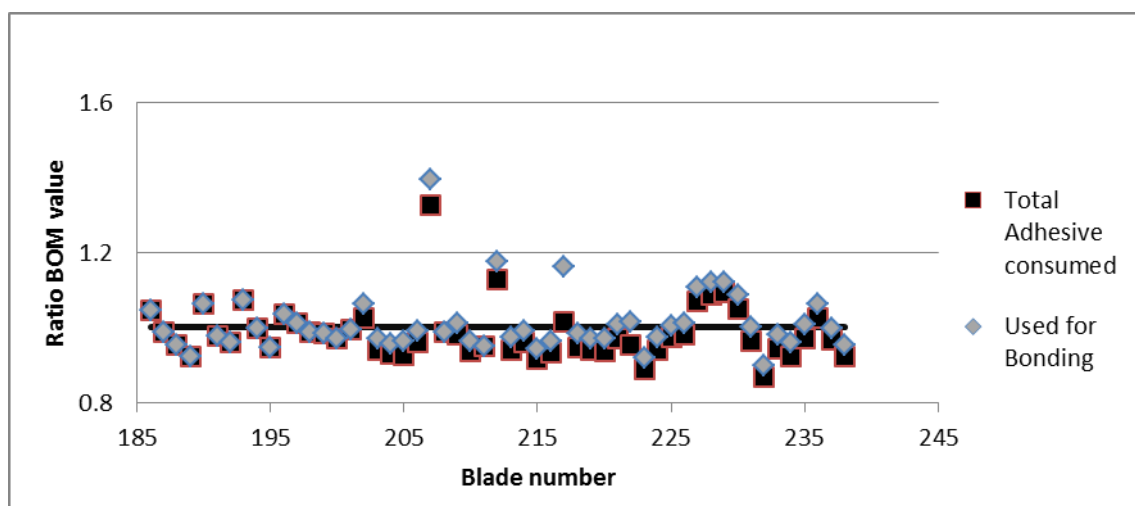


Figure 2.21 – Adhesive bonding used for the webs at the end of the project.

<sup>19</sup> *Total amount of material used* considers also failures of the equipment, pre-run, cleaning and tests during the bonding process.

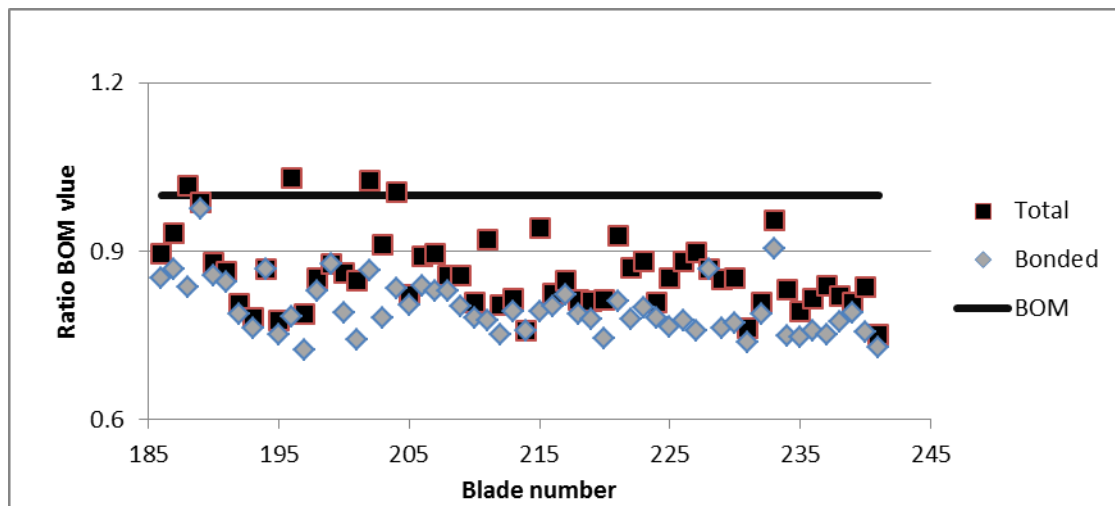


Figure 2.22 – Adhesive bonding used for closing the blade the end of the case study.

Table 2.8 – Difference between the total amount of material and the one used for bonding.

Blade bonding	Total (BOM ratio)	Bonded (BOM ratio)
Av.	0.86	0.80
Std. Dev.	0.07	0.05
CoV <sup>20</sup>	8.1%	6.3%

### 2.3.5 Understand Uncertain Characteristic

Cost modeling is a data driven process. The amount, quality, reliability among others define what analyzes can be performed and determine the usefulness of them. But the scenarios chosen are not always complete. Consequently, in order to better support this work some sense of uncertainty and risk has to be present at the same time [25]. The work performed captures uncertainty between dependent and independent variables, but the limited amount of work and the potential errors while registering make this study just an open door, to look for more information and details if necessary.

One factor is human unpredictability. *“Over and above the total effect of all relevant factors, there is a basic and unpredictable element or randomness in human responses that can be adequately characterized only by the inclusion of uncertainty in the analysis [25].”* In this case, one can be the reaction of a worker when the machine is not working property which can cause a severe variation, in the consumption. Another, can be the setup of the equipment, if it

<sup>20</sup> Coefficient of Variation is the Standard Deviation divided by the average value.

is done improperly it provokes a malfunction in the machine. This unpredictability can be decreased by training, which can accelerate the learning curve and improve the results by preventing “*expensive errors*”.

Anyway, how to generate a risk-adjusted cost estimate? It is important to understand the phenomena mentioned previously, but take into account the technical risk of each decision made. Different material can have a different reaction prior to curing. One can start to curse before the other for the same range of temperatures. Adhesive cured within an open blade can represent a problem not only in the repairing time but also in the quality of the blade. This can finally have an impact in service of the blade.

### 3 Risks<sup>21</sup>

This section is a summary and an assessment of the potential consequences when related to “mistakes” and uncertainties. It will help to understand which can be considered as a relevant cost and which are the actual benefits of the technology.

After controlling process and costs, the adhesive, by its own, can clearly be related to a set of criteria but not all are deterministic for the success of any project. Concerning the process, composite structural bonding:

1. needs to be controlled, and needs constant follow up;
2. if the materials are changed, the compatibility of the parts used in the equipment have to be checked (chemical corrosion).
3. Preventive maintenance (e.g. proper cleaning) will keep the process more steady with less deviation, and this is translated in less waste;
4. the equipment and tools can play a key role (as mentioned above) - the equipment plays a major role in the performance of the process (not only in terms of cost but in general quality) and the tools can be used to tune the process (improving the amount of adhesive applied in the part to be assembled);
5. finally, the shop-floor workers can be distributed in other tasks while the adhesive is curing. For example, a blade spends more or less 5 hours for curing the adhesive. In a 3 shifts company (24h work), it represents 20% of a day working hours.

On top of the costs, there is the impact of the decisions made in the actual properties of the material that have a direct impact in the structure behavior. Bonding processes are complex

---

<sup>21</sup> Risk is an uncertainty which, if it occurs, will have an adverse effect upon project objectives.

with a hand full of dependencies from the material to the shop-floor way of working. What is clear is that the uncertainties (addressed in the section above) can be directly related to the performance, this means there is an increment in the risk associated here. For that reason special attention should be given to these final remarks to guarantee a joint able to carry the load:

1. any changes in the material should be prepared with time, foreseen compatibility problems between resin, peel ply and adhesive;
2. temperature can create stress concentrations (peak point, due to the exothermic reaction and changes in the curing cycle);
3. The Tg is a good way to guarantee the “expected properties” but only destructive tests can check if the surface is free of kissing bonding, therefore testing sample are needed for products where safety is a main asset;
4. even if everything is properly done and controlled, contamination can happen. This cannot be forgotten at any moment during manufacturing (work carefully);
5. the impact of the defects in general performance can be minimized if more suited prediction models and surface preparation are carried out.



### III. Performance

Any structure to be manufactured has to be designed first, in order to guarantee the expected performance and in service behavior. For this reason, this section is called Performance – it addresses how the joints that will be manufactured have to be designed and what fundamental aspects should be taken into account. In general, the performance of any dynamic structure has to be seen in terms of static strength but also in relation to fatigue behavior. This is particularly important because failure by fatigue can occur abruptly at loading well below the static strength and cause several losses. Figure III.1 presents a typical sequence of how the assessment of a part to be designed or developed should be done. It is also the base structure for the next chapters of this thesis.

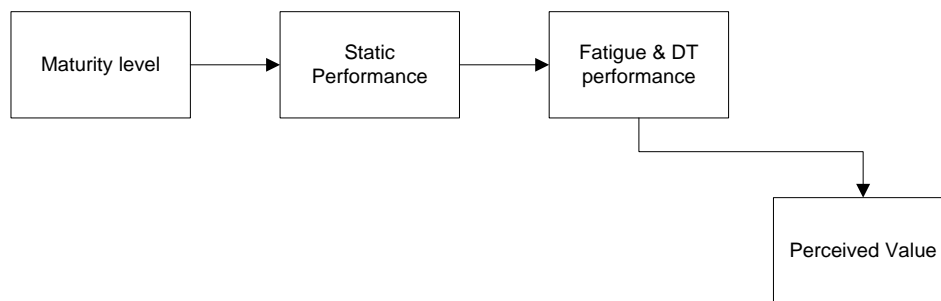


Figure III.1 – Process to design a joint or a structure <sup>22</sup>.

#### 1 Maturity level

As mentioned before, composite materials and bonded joints are significantly different from metals. Their properties are defined in the manufacturing process which means that the joint is created with the part. A bonded joint can be viewed as being a result of three different aspects:

**Bonded joint** = Raw materials (composite + adhesive) + manufacturing process + design of the joint.

If any of these three items is modified, the final quality is affected and that could affect the mechanical strength. That is why, in composite structure analysis, any “little” modification can have strong consequences.

A structural adhesive joint is the one that is able to transfer load between different components. In the aeronautical industry the joints are normally classified as High-Load Transfer (HTL) or Low-Load Transfer (LLT). The difference between them is how stresses pass from the component to the joint. A good example is the Double Lap Shear joint (DLJ) (Figure 1.1) for HLT and the Single-Lap Joint (SLJ)

---

<sup>22</sup>DT – Damage Tolerance

for LLT (Figure 1.2). The DLJ promotes a shear deformation and minimizes the free deformation by the no eccentricity of the load. The unsupported SLJ on the contrary has a secondary bending effect that comes from the load eccentricity and provokes an extra stress at the run-out.

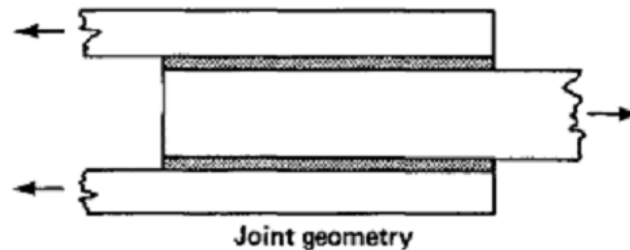


Figure 1.1 –Double lap joint configuration [55]

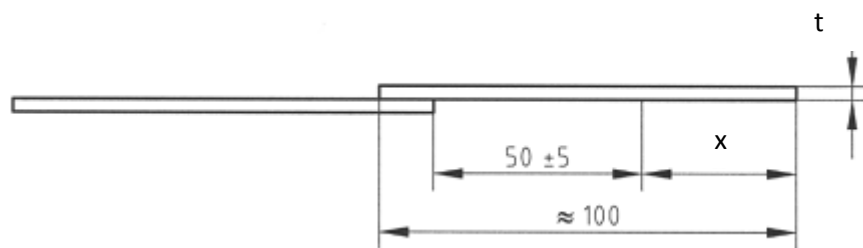


Figure 1.2 –Single lap joint configuration<sup>23</sup> proposed in EN2243 - 1 [103].

In general the stresses induced in the adhesive can be shear ( $\tau$ ) or peel ( $\sigma$ ). *Peel stresses result in extension or compression of the material, known as direct strain ( $\epsilon$ ) whilst shear stresses cause a sliding deformation, known as shear strain ( $\gamma$ )* [69]. Peel stresses in tension lead to Mode I loading, while shear stresses are responsible for Mode II loading. Figure 1.3 shows a single lap joint and the corresponding stresses induced by tensional loading  $N$ . It becomes obvious that these joints behave under mixed-mode I+II loading.

<sup>23</sup> Where  $t$  is the thickness and  $x$  is the length needed for the clamping system.



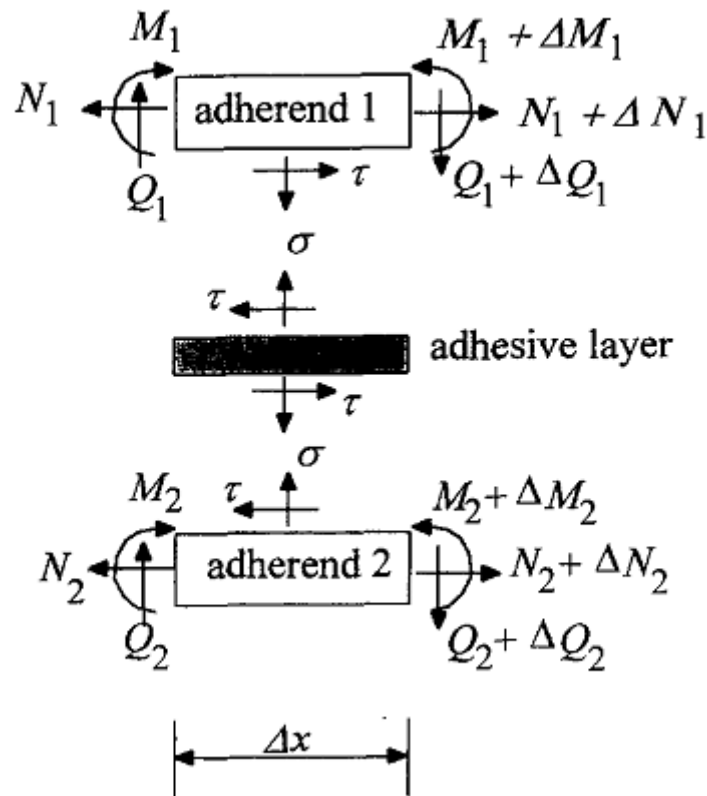


Figure 1.3 – Single lap joint analyzed [104].

These stresses and strain are linked to the adherend stiffness; less stiff adherends allow bigger deformations which can be a source of stress (particularly in the SLJ due to the peel stress at the end of the overlap). Other stresses can be inherent to the part – residual stress (e.g. coming from the manufacturing process) – or provoked in service (deformation, thermal, corrosion, impact). Independently from where the stresses come from, they have an impact on the ability of the material or parts to sustain loads. In this work, we are only concerned with the stresses coming from mechanical loads. They can be understood in terms of forces or moments that can arise from a wide range of external sources [69].

Designing a structure may be divided into several steps. It begins with defining the loads that the complete structure has to withstand. Then a prediction is made to define the critical regions. In general, joints are considered as weak points and extremely sensitive to fatigue [76] due to the complexity of the stresses and the generalized design assumptions.

## 1.1 Designing Bonded Joints

The design of a joint is based on the prediction of the loads and stresses which are expected in the structure. In fact, the loading system is normally defined by a function, taking into account the global structure. Normally, a Global Finite Element Model (GFEM), using a rough geometry of the major

components, is used to obtain the loads inside the components. Afterwards, the integration of the parts shall be done with the defined loads and considering, also, the behavior of the parts (eccentricity of the load path, materials mismatching, stress concentrations, etc.). Anyway, the joint solutions depend on the engineering skills to define the best available materials and design techniques [55]. In other words, there is a close relation between the materials to be joined, the nature of the stresses to be transmitted and the method of joining adopted [105]. For bonding, what has been proven is that the joints are strong in shear but the strength in peel is much lower. This is particularly important for metallic bonded joints. But in the case of composite materials the peel strength of the adherend can be lower than that of the joint itself. In fact, Hart-Smith [106] in 1973 already stated that *“the peel strength in the composite is far less than the typical strength of a structural adhesive”*. So for composite bonded joints, a good design practice - that is to arrange the joint to transfer the applied load in shear - must avoid any premature failure of the structure.

In general, the details of the design vary with the load intensity which is directly related with the thickness of the adherends. Thicker members (adherends) allow less deformation of the joint and this is then translated in high load transfer. As a result, thinner members can be joined effectively by simple large overlaps (Figure 1.4 – Left), while thicker members require the more complex stepped-lap joints [55] (Figure 1.4 – Right).

From all the geometries, the most common design due to its simplicity is the lap-shear joint. To predict the stress and define the validity of the system (adherends + adhesive) two approaches can be followed. One is related to the strength of materials theory based on stress or strain analysis. The second method is a fracture mechanics approach where the presence of a defect is considered and a progressive damage analysis is used to predict joints strength. Indeed, this last methodology has opened a door for several developments in this field and finite element analysis. The crucial issue is the ability to understand how peel and shear stresses develop and coexist in a I + II mixed-mode loading.

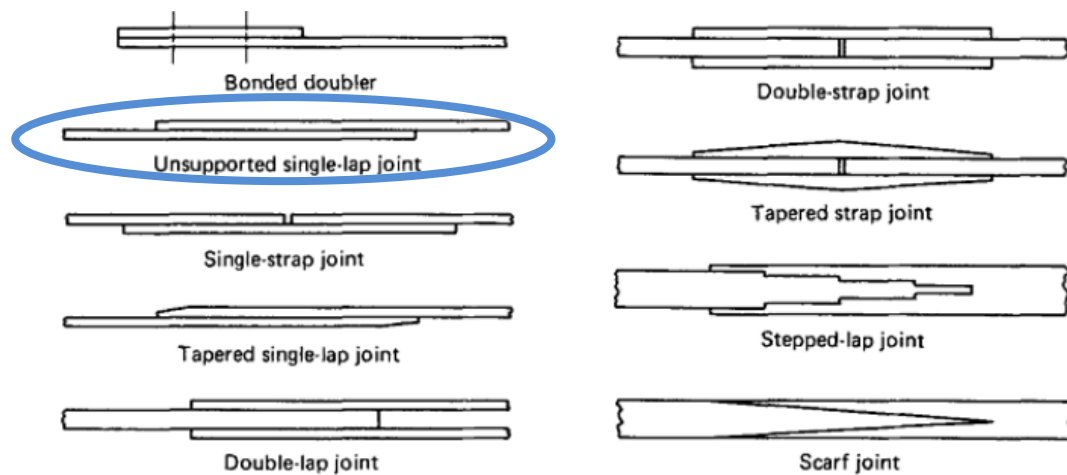


Figure 1.4 – Types of adhesive bonded joints [55].

Independently of the design model used, experimental validation is a key feature of the joints conception.

## 1.2 Failure Modes for Bonded Joints

Independently from the design methodology, the importance of validating the failure mode has been proven [68], [76], [78]. A lot of discussion about this importance as a way to guarantee the correct design and manufacturing process is ongoing. Effectively, composite materials and bonded joints present different failure modes which can affect the static strength and the fatigue life.

Considering the performance of the joint in a structure, three distinct and characteristic failure modes have been established in the literature [106]:

1. **Adherend failure:** failure of the adherend in the vicinity of the joint due to the in-plane stresses resulting from the combination of direct load stresses and bending induced by the eccentricity of the load path (Figure 1.5 - a).
2. **Cohesive Failure of the Adhesive:** failure in the adhesive, i.e., when there is adhesive in both parts of the joint (Figure 1.5 - b). It mainly happens when shear stresses are predominant. The lay-up of a standard composite part contains also  $90^\circ$  and  $45^\circ$  layers which affect the stiffness of the adherend and promote a failure on it, when they are too close to the bond line (neutral axis). Nevertheless, it is still important to characterize it and to understand the actual behavior of the joint for design.
3. **Surface ply delamination:** it is an effect of the peeling stresses; when the stresses allowed during deformation exceed the interlaminar strength of the composite a delamination failure can occur. For SLJ this normally happens due to the eccentricity of the load and the effect of the lay-up. It normally occurs within an interface between layers of the laminate at

the end(s) of the joint (Figure 1.5 - c). As already mentioned, if there is a  $90^\circ$  or  $45^\circ$  ply close the bondline, those will be more prompt to fail than  $0^\circ$ .

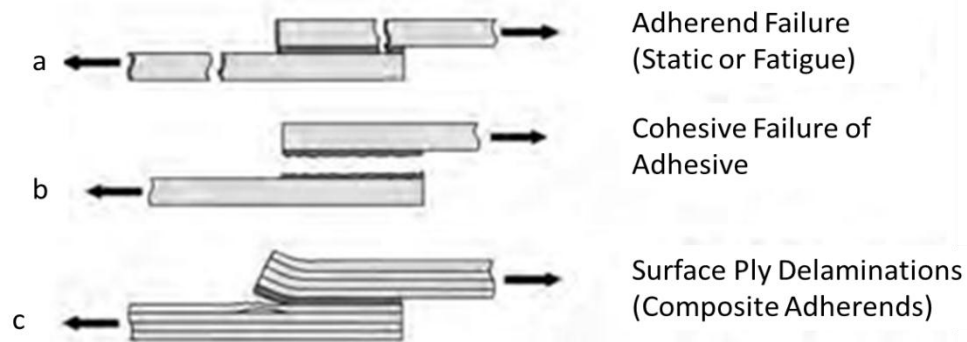


Figure 1.5 – Typical failure mode for bonded joints [55].

Hart-Smith has established that adherend failure is the strongest, but it implies that the weakest link is outside the joint. In this work only cohesive failure and surface ply delamination are considered joint failure. The delamination is only addressed as part of the results while the cohesive failure is studied in detail. The reason lies in the validation of the failure mode. From the certification point of view, it is established that the cohesive failure is the desirable, because it means that the joint is fully working.

Finally, to remember what was presented in Section II.1.2 (Composite Bonded joints: Manufacturing Processes & Technologies), there is another type of failure known as adhesive failure (Figure 1.6). This type of failure only happens when there is a problem on the surfaces. From the regulation point of view or any prediction model, adhesive failure is not valid. It indicates a lack of adhesion between the adherend and the adhesive material [47]. The load is not being transferred to the adhesive [55].

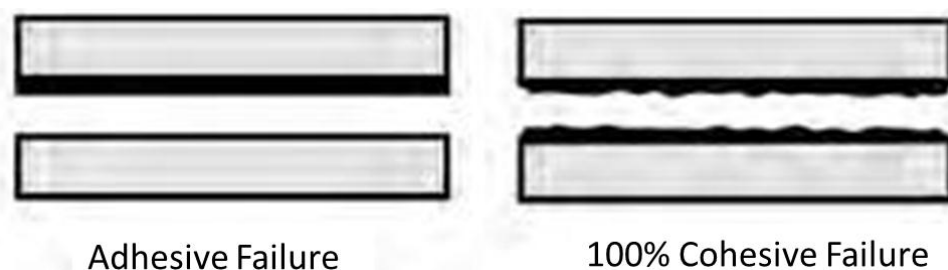


Figure 1.6 – Difference between cohesive and adhesive failure modes [55].

## 2 Static Stress and Strain

### 2.1 Strength and Strain Analytical Approaches

From the strength of materials point of view, there has been a lot for work along the years to evaluate the stress distribution along the bondline. The problem is that most of these approaches depend on the geometry of the specimen. The first approaches for SLJ were made by Volkersen and Goland & Reissner [107]. Actually, subsequent developments on various types of adhesive joints have been performed as is the case of Hart-Smith [55], [106], Tong and Thomsen [108].

**Volkersen's** model (1938) [109] was the first successful attempt of analyzing adhesive bonded joints. This is a 1D bar model, where the adherends deform only in the longitudinal direction and uniformly through the thickness [110]. The adhesive layer is modeled as continuously distributed shear springs [108] and its deformation is given by the differential extension of the bars. The biggest limitation of this model is that it neglects the peel stress because the adherend deforms only in tension and it only considers the elastic domain [105], [107].

The **Goland & Reissner** model proposed in 1944 was originally suggested for single lap joints. It took into account the rotation on the overlap due to the eccentricity of the load path. It raises a non-linear problem, since the joint displacements are no longer proportional to the applied load [105]. The eccentricity of the load was solved by defining a bending moment factor,  $k$ , which relates the bending moment on the adherend at the overlap end,  $M_0$ , to the in-plane loading, by the relationship:

$$M_0 = kP \frac{t}{2} \quad (2.1)$$

As the load increases, the overlap rotates bringing the line of action of the load closer to the center-line of the adherends, as shown in Figure 2.1.

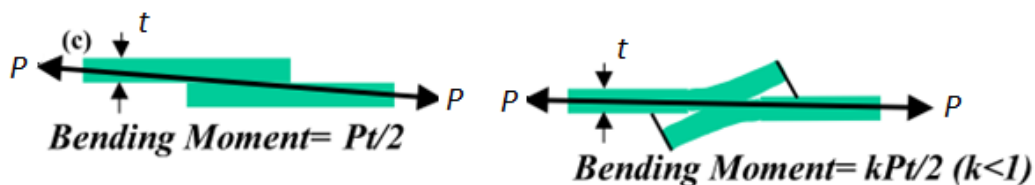


Figure 2.1 – Representation of the bending moment factor of Goland & Reissner; a) undeformed joint and b) deformed joint [111].

When comparing the stress distribution between these two methods (Figure 2.2), Goland & Reissner model is able to define the stress distribution, taking into account the stress concentrations at the

end of the overlap (Figure 2.2a); and the peel effect due to the rotation of the joint (Figure 2.2b), while Volkersen do not address any peel stress. Considering the Volkersen model, this solution is more representative of a double lap joint (DLJ) than a SLJ since the effect of the secondary bending moment in the adherends is much smaller for the DLJ configuration [107], thus making it possible to neglect the peel stresses.

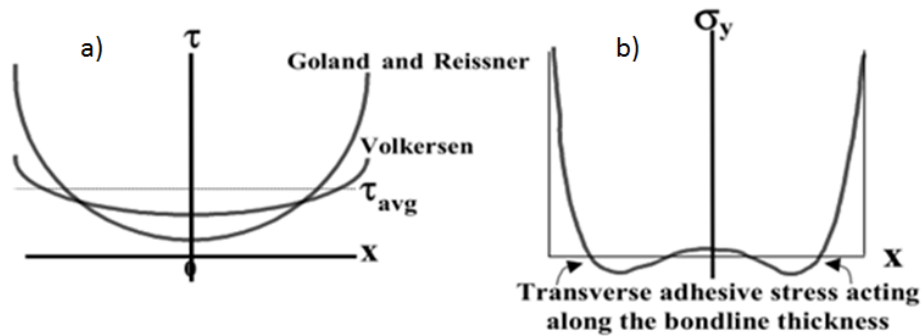


Figure 2.2 – Stress distribution along the bondline a) shear stress for Volkersen and Goland and Reissner methods; b) peel stresses in the bondline for SLJ [111].

**Hart-Smith** took into account the effect of large deflections, but considered the individual deformation of the upper and lower adherends in the overlap, thus neglecting the adhesive layer. The main improvement is an alternative expression for Goland and Reissner bending factor taking into account the stiffness of the adherends [107] and, in a second part, the inclusion of the plasticity effect of the adhesive. This method is divided in three parts. The 1<sup>st</sup> consists on the evaluation of shear stresses considering an elastic analysis; the 2<sup>nd</sup> also concerns the determination of the shear stress with an elasto-plastic approximation [106], [112], [113], where the plastic behavior is only placed at small zones of the overlap edges. This is a bi-linear closed form solution as shown in Figure 2.3. The final part (3<sup>rd</sup>) is the calculation of the peel stresses considering an elastic behavior, and is based on Goland and Reissner work [110]. In 1974 Hart-Smith made an assessment on design and behavior of composite bonded joints [112]. In this report, he summarizes the application of the elastic-plastic analysis taking into account the basic governing parameters. In fact, most of the findings are related to the behavior of thicker sections: *“For somewhat thicker sections, the adherend strength increases more rapidly than the bond shear strength, indicating that lap-joint inefficiency may be limited. For still thicker sections, particularly with filamentary composite, peel stress failure dominate and stress concentration techniques are needed to make lap joints effective”*. The inefficiency of the SLJ arises from the eccentricity of the load path.

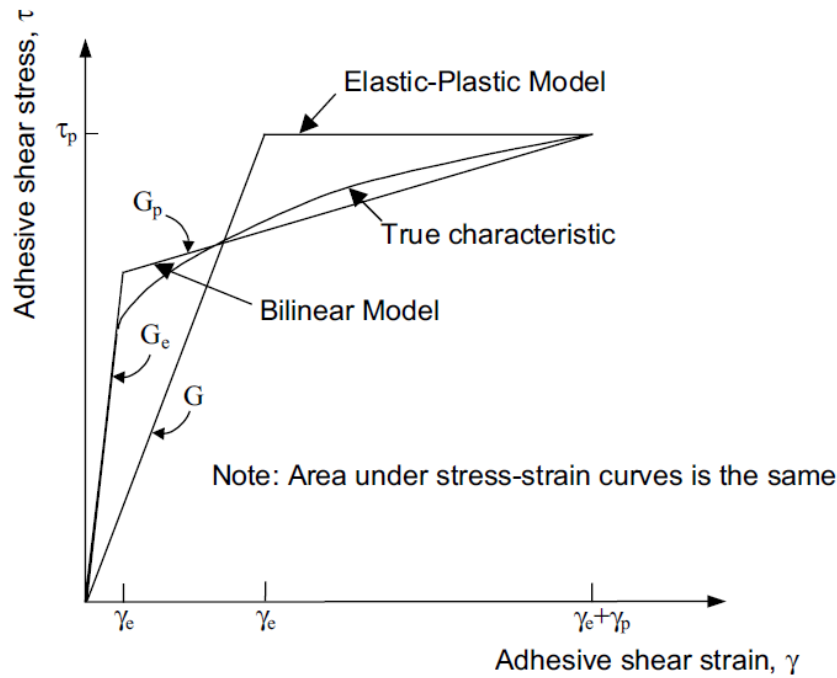


Figure 2.3 – Adhesive Shear-strain curves and mathematical models [106].

In fact, with the increment in complexity of the solutions, computational programs are mandatory. Hence, one of the biggest efforts has been to solve the behavior of realistic bonded joints by using the finite element method and fracture mechanics approaches [107].

There have been a lot of developments in the last couple of years for Unified theories. This means promoting more general approaches that try to take into account the maximum amount of parameters (different materials, different adherend thickness, adhesive thickness, geometries, etc.). Some of these models are presented in [108], [114]. The problem is that the complexity of these solutions, most of the times, create a need for computational solvers.

## 2.2 Fracture Mechanics Approach

Fracture mechanics allows the study of structures that contain a flaw or a crack. Griffith's work assumes that *the energy of a crack tip must remain finite, suggesting that an energy-based criterion on a critical stress state at which a continuum material would yield or fail is measurable. The fracture mechanics theory recognizes that a material's resistance to crack propagation is related to the energy required to separate adjoining material* [69]. In other words the growth of a crack in a plate, where direct stresses are applied, will occur when the energy absorbed by the plate (because of the deformation) reaches the limit value to form a new fracture surfaces. The energy supplied is known as the Energy Release Rate ( $G$ ). When  $G$  reaches the initial value characteristic of the material ( $G_c$ ), crack propagation takes place. In addition, some parametric studies like the one proposed by Hart-

Smith [106] can represent a good baseline for comparison. Dillard concluded that “*fracture mechanics offers a powerful tool to characterize failure of both monolithic materials and bonded systems. Based on the concept that all real material systems contain (or may develop) flaws that can significantly alter the resulting stress state, fracture mechanics has proven uniquely appropriate for characterizing the structural integrity of a wide array of materials and structures. Fracture mechanics has been applied to adhesive joints with success for characterizing the critical and subcritical debonding*” [69].

Blackman et al. in 1991 [115] made a review of the  $G$  calculation methods for DCB in mode I available at that time. They define that “*if the specimen behaves in a linear elastic manner upon loading, there are four linear-elastic fracture mechanics (LEFM) methods for analyzing the data contained in the load displacement plots (Figure 2.4)*”.

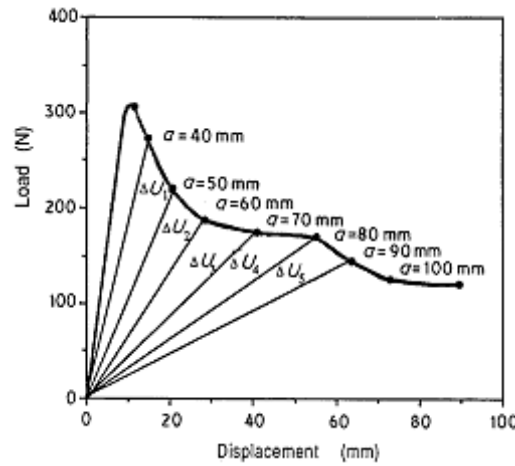


Figure 2.4 – Typical load  $P$  versus displacement ( $\delta$ ) plot for a Mode I (Double Cantilever Beam specimen) using CFRP adherends and epoxy-paste adhesive [115].

The first method group is the “*Area*” Method where the values of  $G$  are calculated from the area below the  $P$ - $\delta$  curve. The  $G$  may be defined by Equation (2.2).

$$G_a = \frac{\Delta U}{B\Delta a} \quad (2.2)$$

where  $B$  is the width of the specimen and  $\Delta U$  is the area under the  $P$  -  $\delta$  trace and  $\Delta a$  is the increment of the crack length from  $a_1$  to  $a_2$ . This method is not recommended by the ASTM [116] because “*it will not yield an initiation value of  $G_{IC}$  or a delamination resistance curve*”. In fact, this method only gives the value of the total area below the  $P$  -  $\delta$  curve.

The second is the *Compliance Based Method* where Irwin-Kies defined that the adhesive fracture energy is a function of the compliance ( $C$ ) variation. Equation (2.3) gives the relation defined by Irwin- Kies [115], [117], [118].



$$G = \frac{P^2}{B} \frac{dC}{da} \quad (2.3)$$

where  $P$  is the load and  $C$  is given by Equation (2.4), where  $\delta$  is the applied displacement corresponding to the load  $P$ .

$$C = \frac{\delta}{P} \quad (2.4)$$

The application of this method requires the plot of  $C$  versus crack length  $a$  [115].

The third is an extension of the compliance based method. It is the application of a simple beam theory to define  $C$ . This method depends on the type of load and geometry of the specimen because  $C$  is defined as a function of the second moment of area. In this case  $C$  is given by Equation (2.5):  $E_s$  is the flexural modulus of the adherend (in this case CFRP substrate arms),  $a$  is the crack length and  $I$  the second moment of area of the specimen arm section, i.e.,  $I = B(h/2)^3/12$ , where  $h$  is the specimen's height.

$$C = \frac{\delta}{P} = \frac{2a^3}{3E_s I} \quad (2.5)$$

The fourth method is an extension of the third, to correct for deviations regarding the behavior of each tested system. In general, they are *Compliance Calibration Based Methods* like the Modified Beam Theory (*MBT*). This method allows the determination of an effective Young Modulus ( $E_{if}$ ) that depends on the characteristic of the specimens being tested. In this case  $G$  can be given, for direct loads (Mode I) by Equation (2.6) where  $\Delta$  is a crack length correction to account in Double Cantilever Beam (DCB) tests for crack tip root rotation (Figure 2.5). The  $E_{if}$  can be determined with Equation (2.7) considering the initial part of the load-displacement curves.

$$G = \frac{3P\delta}{2B(a + |\Delta|)} \quad (2.6)$$

$$E_{if} = \frac{64(a + |\Delta|)^3 P}{\delta B h^3} \quad (2.7)$$

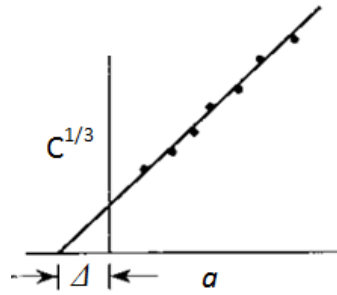


Figure 2.5 - Modified Beam Theory [116]

Finally, in the recent developments regarding the Effective crack length ( $a_e$ ) [119]–[121], the crack length is given as a function of the current compliance ( $C$ ) and the Young's Modulus ( $E_f$ ). One example is the Compliance Based Beam Method (CBBM) which will be analyzed in detail in Section III.5.3 - Model Validation.

Whatever calculation method is used, the understanding of how the loading is applied and what kinds of deformations are taking place, it is important to define the right relation. Consequently, to have a better understanding, Westergaard [122], [123] defined three different loading modes: *mode I*, *mode II* and *mode III*, as shown in Figure 2.6. Indeed, the first one is considered as an opening process while the other two are shear events. Mode I is done by applying traction, this means that the load acts perpendicular to the crack plane. Mode II is characterized by a shear loading perpendicular to the crack front and mode III by shear loading parallel to the crack front [117], [124]–[126]. The fracture criterion to be used must include the contribution of each mode when multi-axial stress fields are taken into account.

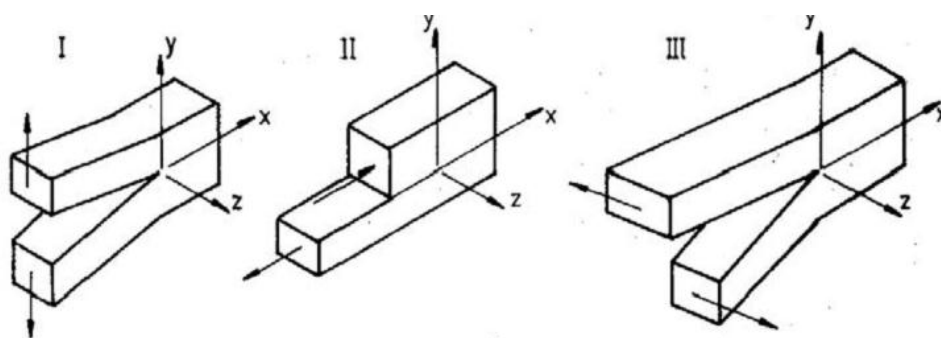


Figure 2.6 – Crack propagation modes: Mode I crack opening, Mode II forward shear and Mode III out-of-plane shear [126].

Nowadays, there are suitable and well established methods mainly based on fracture mechanics techniques like the Virtual Crack Closure Technique (VCCT) and cohesive elements implemented in the FEM package Abaqus [127].

### 2.2.1 Mode I

The Double Cantilever Beam (Figure 2.7) is the most common method used for the characterization of Mode I failure. This method is already normalized in ASTM 5528 [116] or ISO 15024 [128] standards. It is based on a specimen with a pre-crack loaded in Mode I. During the test, the applied displacement and load are registered as well as the evolution of the crack length [116], [121], [128] 128].

Figure 2.7 shows the specimen used for this test. The specimen can be fixed to the testing machine with the help of piano hinges or loading blocks. Afterwards, a controlled displacement speed is applied guaranteeing that there is stable crack propagation. All the values along the test are registered (displacement, load and crack length). With these parameters different methods can be used to calculate the  $G_{Ic}$ .

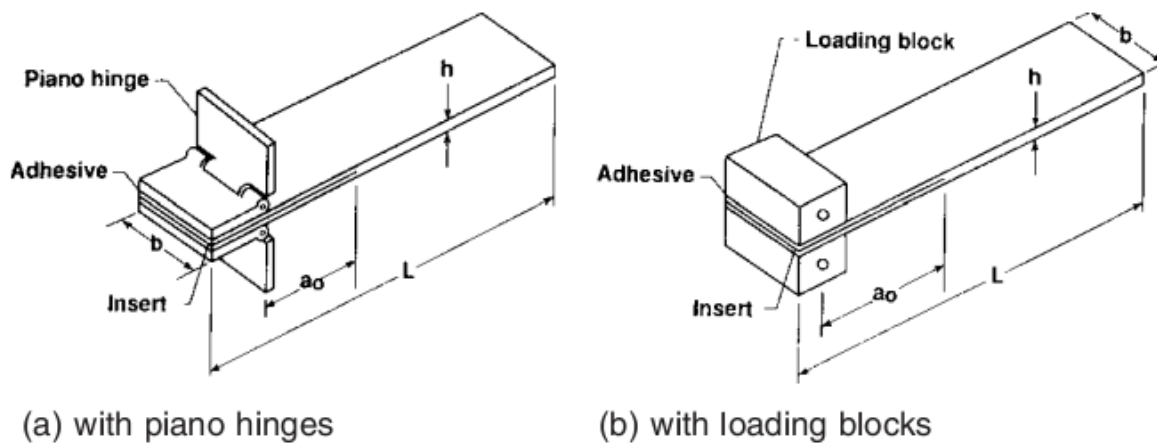


Figure 2.7 – DCB specimen for Mode I testing with a) piano hinges and b) loading blocks [116].

### 2.2.2 Mode II

For Mode II there is no clear Standard but the industries have been defining different of ways testing the joints depending on the product being tested. For composite materials the ELS (End-Load Split), ENF (End-Notched Flexure) and the 4 ENF (Four-Point End-Notched Flexure) tests are very common [129].

The ELS is sensitive to the clamping system and presents some difficulties in determining the  $G_{IIc}$  since large displacement can develop, for example, in the case of ductile adhesives. The 4ENF requires special testing equipment and presents difficulties because some friction is generated at the pre-crack. The ENF is probably the most common way of testing in Mode II because it is simple. The biggest limitations are difficulties to read the crack length during its growth and, under certain circumstances, the unstable crack propagation.

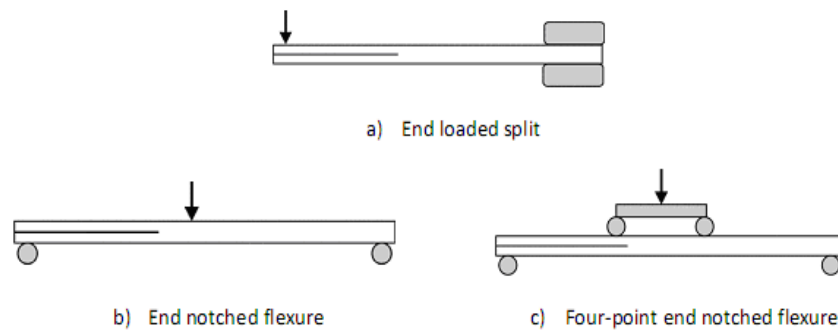


Figure 2.8 – Methods to test for the fracture characterization in Mode II [129].

### 2.2.3 Mixed-Mode (Mode I + II)

Despite the advances in recent years and the exponential growth in which these applications occur, a complete knowledge of adhesive joints behavior under mixed-mode I+II loading is still missing. This is a fundamental issue since adhesive joints are often loaded under mixed-mode conditions. In fact, many practical adhesives applications involve the use of single lap joints, which leads to a combination of in-plane tension and shear (Modes I and II, respectively) [130]. Therefore, fracture characterization under mixed-mode I+II loading associated to fracture mechanics based design approach, detailed modeling and quite likely structural element testing are essential tasks in order to understand how structures behave in real scenarios. There are several types of tests used for fracture characterization under mixed-mode I+II loading (Table 1). The Mixed Mode Bending (MMB) test provides a large range of variability of mode mixity but requires a complex setup. The Asymmetric Double Cantilever Beam (ADCB) allows some mode mixity variation but in the region of the fracture envelop close to pure mode I. On the other hand, tests like Crack Lap Shear (CLS), Fixed Rate Mixed Mode (FRMM) [131] and Single Leg Bending (SLB) promote intermediate mixed mode values. Recently, the methods proposed by Dillard et al. [132] and Spelt et al. [133] have been using special setups for bonded joints fracture characterization that allow large variations of mode-mixity [134].

**Table 2.1 - Test methods to measure the adhesive fracture toughness under mixed-mode conditions and different mixity angles. [131], [135]**

Type of test	Schematic Representation	Degree of Mixity, $\phi$ (°)
Asymmetric Double Cantilever Beam (ADCB)		$\approx 0 - 34^\circ$
Single Leg Bending (SLB)		$\approx 41^\circ$
Crack Lap Shear (CLS)		$\approx 49^\circ$
Asymmetric Tapered Double Cantilever Beam (ATDCB)		$\approx 20^\circ$
Mixed Mode Bending (MMB)		$\phi \approx f(c)$
Fixed Rate Mixed Mode (FRMM)		$\approx 41^\circ$

### 3 Fatigue

The engineering importance of fatigue lies in the frequently observed occurrence of failure under repetitive loading, at far smaller loads than those required to cause quasi-static failure. In fact, fatigue in engineering structures is a loss of properties over time due to oscillation of stresses [69]. This loss has been responsible for approximately 80% of the failures in service [122], which means economic losses, injuries or even worse. In some cases, the failure may occur suddenly after years of service due to fatigue problems. When it fails, many similar parts may be in service and a counter action is needed which can represent an expensive remedy [69].

The determination of the fatigue life and resistance of any structure is an important aspect in the design of economical and reliable structures. Effectively, it is important to know how long a structure could be in use under specific conditions. In fact, when the subject is fatigue it is impossible to separate the expected loads (mechanical, thermal, etc.) in the prediction tools from the life in service because the load varies with time and type of use. A way to create this relation is the definition of the cycles that simulate the working conditions. Figure 3.1 presents the theoretical number of cycles for different products and the impact of the allowable stresses in the life span.

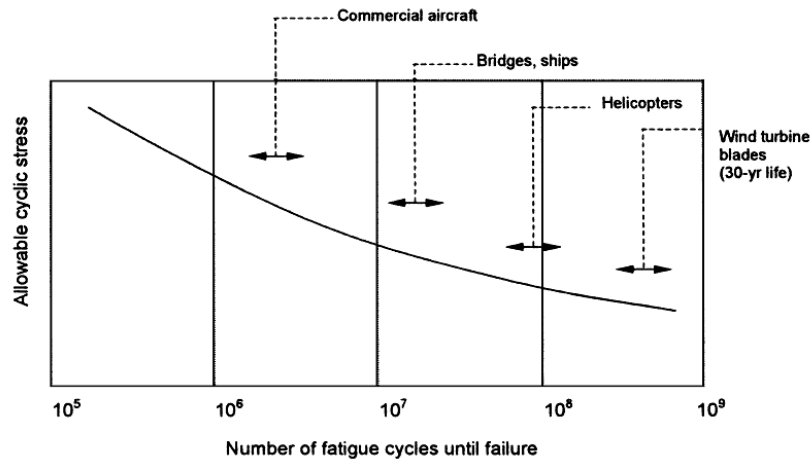


Figure 3.1 – Fatigue lives of several application [59].

Fatigue is seen as a load that varies within a cycle, the detailed way to characterize this variation is known as load spectrum. A cycle is defined as the time between adjacent peaks (Figure 3.2) while frequency is the number of cycles per time unit [136]. It is useful to characterize the load spectrum in terms of peaks and trough (Figure 3.3 –  $P$  and  $T$ ) to describe how the load varies. Complex loading scenarios can be built with varying loads between cycles to account for the “real life in service”. In general, these load spectrums are defined by previous experience. In addition, the static loads that are applied define the limit values for the peaks and the troughs.

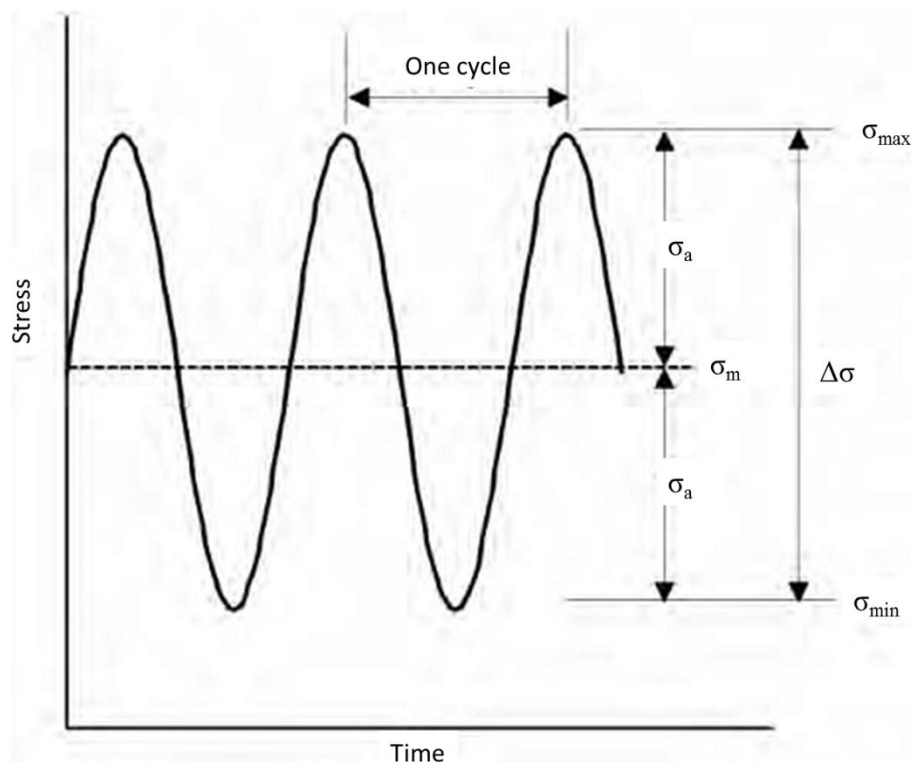


Figure 3.2 - Typical cyclic loading parameters [69].

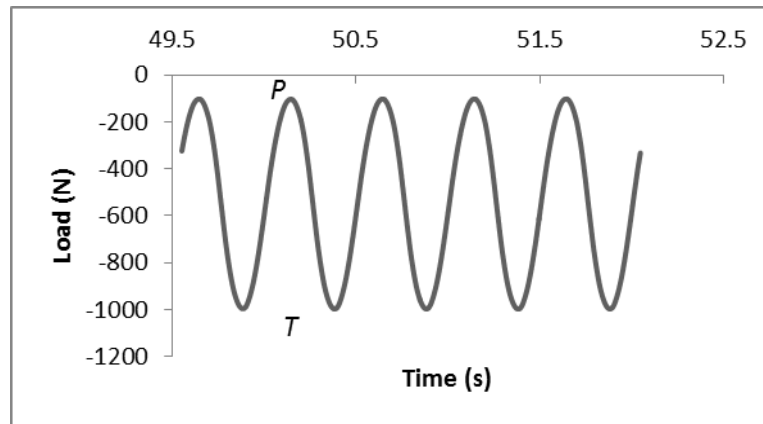


Figure 3.3 – Example of a Peak (*P*) and Trough (*T*) counting for a constant amplitude loading.

The key parameters used to describe fatigue spectra are defined by [69]: Maximum stress ( $\sigma_{\max}$ ) or Maximum load ( $P_{\max}$ ), Stress ratio or load ratio ( $R = P_{\min}/P_{\max}$ ) and frequency ( $f = 1/\text{cycle}$ ) in Hz.

General analyses of the fatigue behavior can be considered a complicated process because a set of variables that can directly affect the behavior must be taken into account, especially for adhesively bonded joints. Some of the factors are: air bubbles in the adhesive, absence of homogeneity, environmental conditions, geometry, different sources of stress concentrations, etc. [137].

### 3.1 Fatigue Life

The fatigue process is divided in three stages: initiation - nucleation of a macroscopic crack, propagation (subsequent evolution) and finally catastrophic failure [138]. The initiation of the damage generally occurs at the ends of the overlaps and at defects, like inclusions or gaps, due to stress concentrations in these zones. It starts with micro-plasticity, then there is micro-cracks nucleation and merge between them leading to development of a macroscopic crack. Localized creep can also take part if the tests are made in tension (end of the 1<sup>st</sup> stage) [69], [139]. The initiation is not easy to be characterized because of the high stress concentrations in a bonded joint. This makes it difficult to clearly observe a well-marked initiation phase [69]. Quaresimin and Ricotta [138] have already studied this. In fact they have defined that the initial part of the fatigue life in composite joints is from 20% to 70% of the service life depending on the overlap length and stress levels. The end of this stage is defined as the threshold, because the propagation rate increases.

The next phase is the propagation (stage 2) of the crack up to a critical length (crack growth). It is normally characterized by a stable propagation and when it reaches a critical length ( $a_c$ ) there is a quick and catastrophic failure (stage 3) [140]. In general, the mechanism mentioned before will influence the propagation as well [69]: the size of the fracture process zone will remain more or less constant but the micro-plasticity will affect a larger area, as the damage already initiated in the previous phase will affect the crack growth.

By definition, the study of fatigue of bonded joints can be considered in terms of the mechanisms of fatigue damage, taking into account changes in the physical behavior and in the chemical structure of the adhesive, or its mechanical response (ability of sustain load) [69]. To evaluate these effects in a structure in a long term basis, the standard options are:

- making tests with short duration and extrapolating the results [137];
- creating prediction models which are able to simulate service conditions;
- creating a full scale test (e.g. wind blade - Figure 3.4) to proof the behavior of the structure.

The first method requires extrapolation of the results, causing reliability issues and should be used carefully. The second one always requires an experimental validation but with the new tools available, like more powerful simulation programs and computers, it is being used more often. Normally only experienced engineers can approve with full confidence such models which imply that they should also be used carefully. Full scale testing (Figure 3.4 and Figure 3.5), for movable structures is the best way to proof that the assumptions, the models and the tools used are fitting the expected results. Anyway, due to their high cost and due to definition of the correct boundary conditions, care should also be taken in this case.



Figure 3.4 – Wind Blade full scale testing [141].

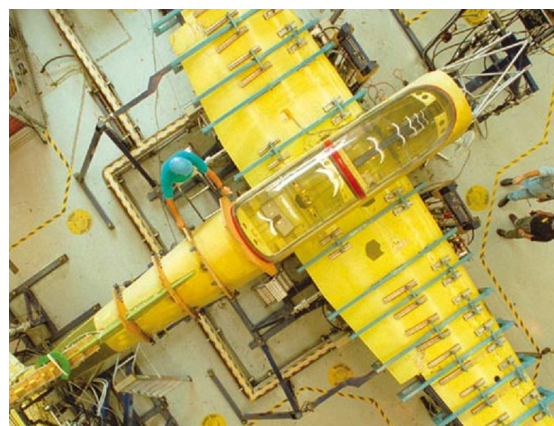


Figure 3.5 – Fatigue test of a PC-9 Aircraft [142].



### 3.2 Fatigue of Bonded Joints

“The mechanisms that cause fatigue of polymeric materials are fundamentally different to the ones in metals, where the source of the crack nucleation is located at the grain level. For composite materials, the major source for stress concentrations and subsequent growth of defects are initial damage (cavities, cracks, poor curing, etc.) that originate during manufacturing, or damage sustained during service” [59]. On the other hand, adhesives are affected by the deformation and breaking of crosslinks along the process [69]. Stress and deformation affect all the materials subjected to load: fibers, resin and adhesive. This means that the materials joined and the adhesive chosen will affect the final outcome. Goeij et al. [59] has made a summary of the parameters affecting the behavior and a table comparing the parameters on static and dynamic composite adhesive joint failure is presented in Figure 3.6.

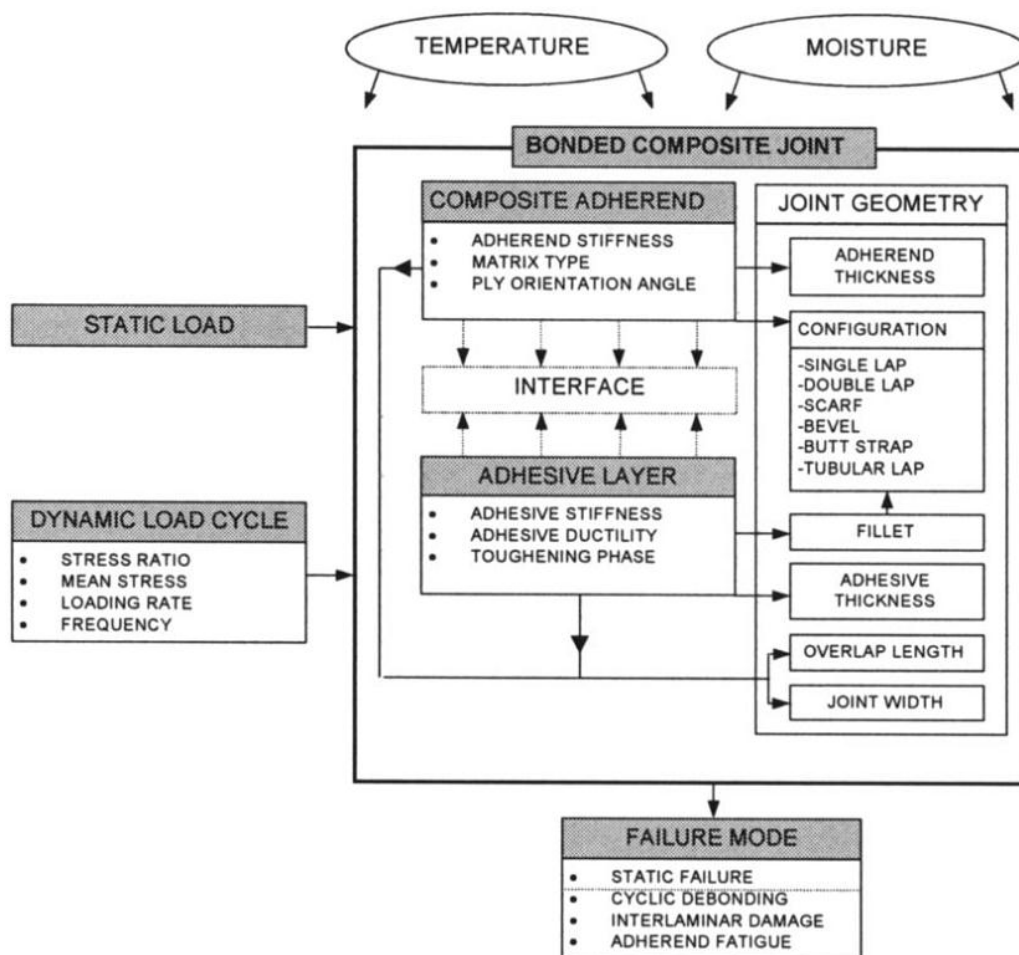


Figure 3.6 – Variables that influence fatigue life of adhesive joints [59].

Johnson and Mall [143], [144] established that the failure modes applicable to composite joints are: cyclic debonding of the adhesive (Figure 3.7), adherend fatigue (Figure 3.7) or delamination (interlaminar damage) (Figure 3.8), or a combination of these. It can be considered as the same type

of static failure. The interface ply orientation has a direct effect on the failure type and this affects the propagation rate. For specimens with  $0^\circ$  plies, the fatigue life is larger than for the other lay-up ( $90$  or  $\pm 45$ ) [143], [145]–[147]. One of the limitations for prediction of the behavior of composite bonded joints is the overall effect of interface, because it changes completely the propagation rate. In fact, this behavior is completely different when compared with the effect of the interface in metal bonded joints.

In addition, Hadavinia et al. [148], [149] addressed also that “wet” environmental tests (55% of relative humidity) affected the fatigue life. *“This is reflected in the change in the locus of failure from being cohesive through the adhesive layer in the ‘dry’ environment to... the interface”*. Also there is an effect on the threshold: for a dry environment the  $G_{th}$  value represents 20% of the  $G_c$  but for a wet environment the value is only 4%. This is also in agreement with the results presented in [59], because there is tendency to fail towards the interface.

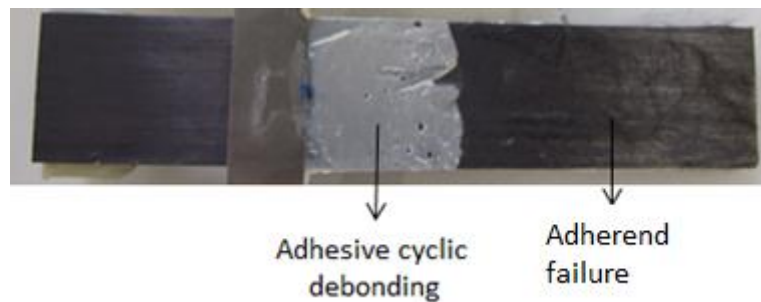


Figure 3.7 – Fatigue failure modes: adhesive debonding and adherend failure.



Figure 3.8 – Fatigue failure by delamination.

Quaresimin and Ricotta [138], [139] have made a long work regarding the effect of the fillet in the life of single lap joints. They found that the fillet extended the life of the joints. They have also

worked on the overlap length, they tested 20 and 40 mm overlaps and found that this is an effective way to improve the fatigue life.

Meneghetti et al. [146], [150] did a continuation of the work started by Quaresimin and Ricotta. They present a final summary of the development in [150]. Several explanations on how damage evolves along the single lap joints' overlap and the parameters that affect them are presented. They defined that: *“among the design parameters taken into account, the most important affecting the fatigue strength of the joints are the corner geometry of the bonded area and the overlap length; the best performance is obtained with a spew fillet edge and 40 mm overlap joints while the worst pertains to square edge and 20 mm overlap joints”*.

Considering temperature, Ashcroft et al. made an extensive research in this area [118], [151]–[155]. They have defined that the adhesive's behavior is sensitive to temperature. In fact, the adhesives changed dramatically their behavior: at lower temperatures they can be brittle while at higher temperatures they can have an extreme ductile behavior, which can promote failure by creep<sup>24</sup> instead of fatigue. Something that has been pointed out, not only by these authors but also by others [156], [157], is that loading frequency can affect the behavior of the adhesive. High frequencies can promote localized creep and this will definitively reduce the fatigue life of a joint. In fact, ASTM recommends for metal SLJ a maximum frequency of 30 Hz [158] and for fatigue delamination of composites [159] they recommend a maximum of 10 Hz to avoid any effects of the temperature in composites (like creep or viscoelastic effects) due to the limitations this material has on thermal conductivity.

### 3.3 Defining Fatigue life

The tests and prediction models are the tools to define the inspection periods and where they should be focused (the critical fatigue zones). For example, blades and aircrafts are obliged to make full scale tests simulating complex conditions and load spectra, to guarantee the life in service. There are different ways to define the fatigue properties. Some analyze the material to find the intrinsic properties influencing fatigue behavior; others make tests with coupons or in scale to obtain limit values for complete life. At this moment, the fatigue life estimation for metals is more mature and has a complete database and established methods, while composite and adhesive joints are still in a less mature phase.

Whatever the material or method, it is important to remember that structural components fail not only by the type of load but also due to the nature of it. This means that the load can come from different sources, e.g., if the structure is subjected to motion, frequently it fails by fatigue.

<sup>24</sup> Shape changes permanently from prolonged stress or exposure to high temperatures [93]

Concerning bonded joints, the behavior is different from the component to be joined and the material (bulk adhesive) which implies that independently of the material used (e.g. composite or metal), the behavior of the designed joint should be studied [160]. This is especially true for composite joints, because the failure can propagate inside the composite or in the adhesive and this affects how the fatigue life evolves.

There are mainly two types of fatigue testing procedures:

- Low cycle fatigue (LCF) occurs when the number of cycles is less than  $10^4$ . The load applied is close to the yield strength and bulk plastic deformation takes place [161]. LCF is normally analyzed as a strain-life approach because it takes into account the plasticity of the material [152]. For example, it can be associated to the pressurization of the cabin which occurs once per flight. In some cases, LCF may operate over a similar period of time as High cycle fatigue but involving lower frequency.
- High cycle fatigue (HCF) is when the load applied is still in the linear domain which leads to macroscopically elastic deformation, even if some small area undergoes plastic deformation [161]. Normally, in structural design the HCF is used and two criteria are generally defined. The first is infinite life design with Stress-Life Methods - this is to define safe-life design behavior. The second is fail-safe and damage tolerant design where crack growth analyses are performed.

Actually, the need for safe-life design, in the US aircraft industry, became evident when six B-47 aircrafts crashed in early 1958 [162], [163]. This aircraft flew first in 1947 and it *“represented a milestone in aviation history and a revolution in aircraft design. Every large jet aircraft today is a descendant of the B-47 (Figure 3.9)”* [164]. The problem was that no fatigue life was specified but it was expected to be in service until 1966 (at least). *“The disasters caused the implementation of an Aircraft Structural Integrity Program. This program saw the fatigue testing of aircraft to establish a safe-life which was the equivalent flight time to failure divided by a safety factor of four”* [162]. The problem arrived when F111 crashed after 107 hours of service in 1969. This failure occurred due a fatigue crack from sharp-edged forging defect in the wing box and the material had low fracture toughness [163]. With this loss, the government mandated *“almost immediately, the Air Force and the Federal Aviation Authority mandated that fracture analysis become part of the aircraft design process”* [165]. This was the beginning of the fail-safe concept. Fail-safe is *“the attribute of the structure that permits it to retain its required residual strength for a period of unrepaired use after the failure or partial failure of a principal structural element”* [166].



Figure 3.9 – B-47 aircraft [164]

Damage tolerance means that the crack will be detected and repaired before reaching the lower strength limit. The Advisory Circular 23-123A [166] defines damage tolerance as being the *“attribute of the structure that permits it to retain its required residual strength for a period of use after the structure has sustained a given level of fatigue, corrosion, accidental or discrete source damage”*.

Damage tolerance is an evolution from fail-safe because it takes not only the damage that occurs by standard conditions but also particular events or unpredicted fatigue conditions. This means that one part of the structure can have a crack but this will not lead to the catastrophic failure of it. In addition, prediction methods shall be used to define maintenance and inspection periods depending on the damage. Multiple load paths, load transfer between members, crack stoppers built at intervals into the structure, and inspection are some of the means used to achieve damage tolerant design. For example United States Air Force (USAF) defined that the critical length of the crack ( $a_c$ ) shall be the one that induces half of the Mode I critical stress intensity factor ( $K_{Ic}$ ). They define the maintenance intervals and repairs based in this limit crack size [163].

In today's industry both concepts are applied (Figure 3.10). The safe-life for an aircraft takes into account a working life of 20 years, while the fail-safe and damage tolerance guarantee the performance during the entire life. Figure 3.10 shows the Federal Aviation Regulations (FAR) (CFR – Code of Federal Regulations), available for fatigue evaluation in metallic and composite aircrafts parts.

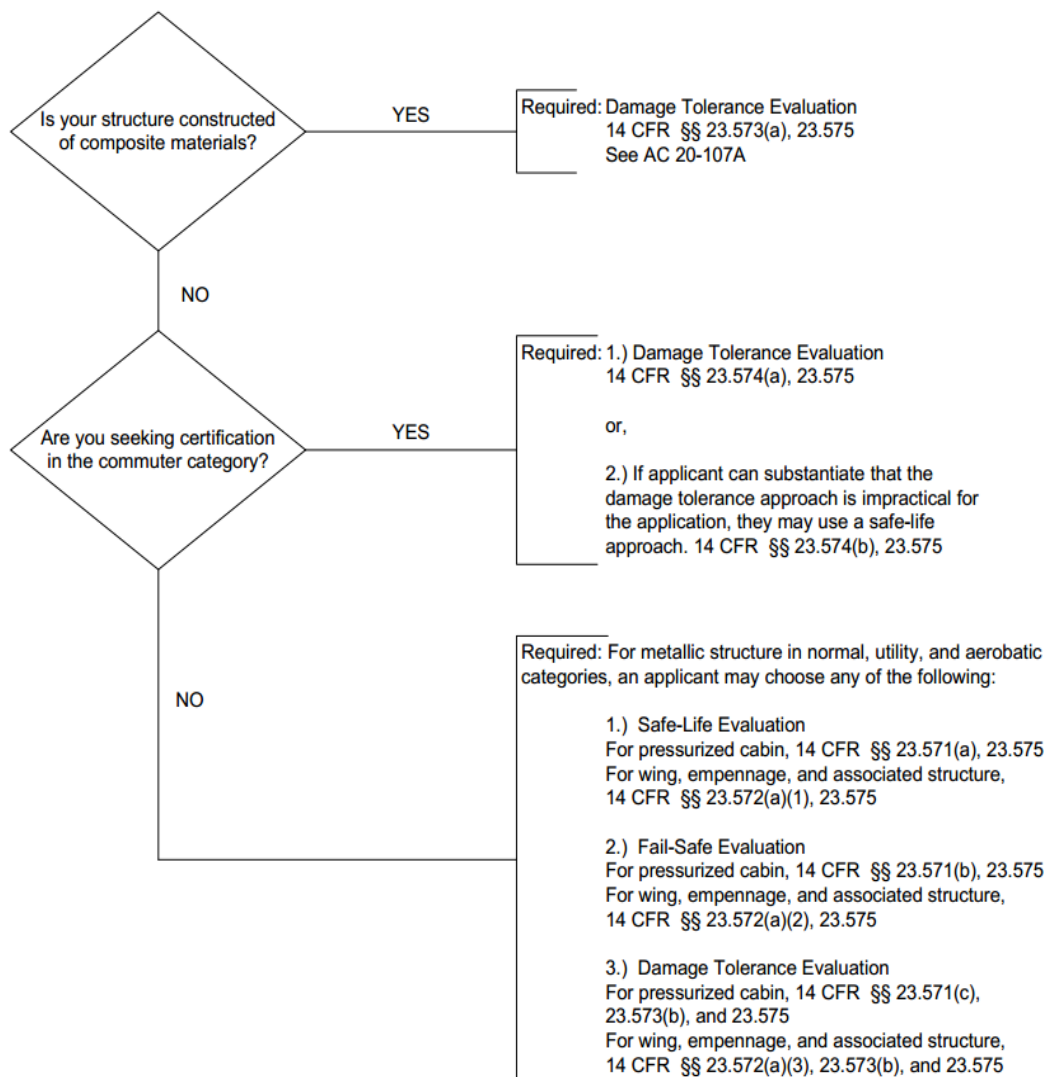


Figure 3.10 – Applicable regulations for the Aircraft Certification taking into account the fatigue requirements [166].

### 3.3.1 Safe-life

These methods are based on S-N curves, also known as Wöhler's curves (Figure 3.11), or Goodman-type diagrams. It consists in a relation between maximum strength and the number of cycles needed to failure in logarithmic scale. One of most common Stress-Life methods requires testing a series of samples at different loads in order to obtain the Wöhler's curve, which consists on the plot of stress (S) versus the number of cycles (N) until failure of each specimen. Normally, the tests are made with 20 or 30 specimens at each load level, thus giving statistical confidence to the S-N curves [167]. The considered stress levels should be markedly different in order to cover all the failure envelop [137]. It is normally done taking into account the stresses used for design.

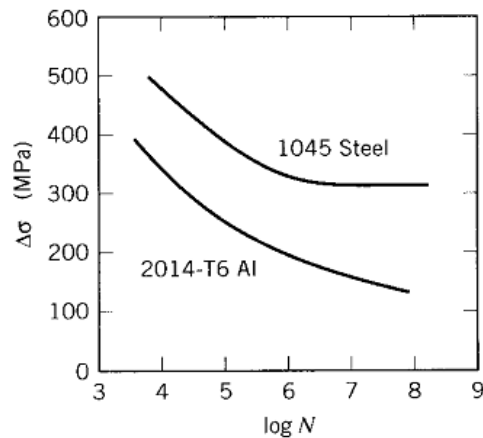


Figure 3.11– S-N curves for aluminium and low carbon steel.

The tests can be done under constant fatigue loading amplitude or displacement and the result may include a fatigue threshold, at which the structure has an infinite life depending on the material [152]. For example some steels have an infinite life at a certain stress level, while aluminum in general does not present this breaking point (Figure 3.11). However, the distribution of stress and the mode of failure are not analyzed in these types of tests.

The aim of the tests (S-N tests) is to define the appropriate working loads to achieve the expected amount of cycles or aim for the spectrum in the infinite life (safe-life). In adhesive joints, the working loads are normally defined as being between 20 and 50% of the static failure loads [69].

### 3.3.2 Damage Tolerant Philosophy

In general, all the predictions and definitions are made to guarantee that all the cracks do not grow beyond the limit. To make it possible, there is a need to analyze how the crack propagates along time. This approach is the Fatigue Crack Growth (FCG). It is a Fracture Mechanics based method [157].

Fracture Mechanics tests have been used to identify the relation between a fracture parameter (stress intensity factor ( $K$ ) or strain energy release rate ( $G$ ) [152]) with the fatigue crack growth rate using experimental data. Indeed, the damaging effects that cyclic loading may have upon adhesively-bonded joints have been quantitatively established [168] [169]. The FCG method is the correlation between the rate of fatigue crack growth per cycle ( $da/dN$ :  $a$  represents the crack length at a certain number of cycles  $N$ ) and the change of one fracture parameter over the crack length. The plotted expression of these two factors in a logarithmic scale has a sigmoidal shape that has been previously observed in studies of FCG for bonded joints and composites [69], [152], [168]–[170], and for a large range it follows a power law. Figure 3.12 shows a typical propagation curve, which characterizes the properties above a certain fatigue threshold value and below the fracture toughness of the adhesive [153], [154], [171]. The plotted relation has three zones that are related to actual fatigue life and

they can be easily identified:

- threshold region: below the fatigue threshold ( $K_{th}$  or  $G_{th}$ ) (Figure 3.12 - threshold region ) the crack growth tends to zero; ASTM standard E647 established empirically this rate for metals as being the value of  $K$  when the crack propagation rate is  $10^{-7}$  mm/cycle [172]; however, this limit does not necessarily apply to composites which means that the threshold behavior has to be assessed independently;
- linear region: where a linear growth is noticed; in this stage the Paris relation or a variation of it (Equation (3.1)) normally fits well the experimental points (Figure 3.12 – linear region). It is normally valid between  $10^{-5}$  and  $10^{-3}$  mm/cycle [118], [139], [160];

$$\frac{da}{dN} = C(\Delta K)^m \quad (3.1)$$

- the third region starts when the crack becomes unstable and is characterized by a rapid crack growth followed by catastrophic failure (Figure 3.12 - fast fracture region).

In most crack propagation tests only the second stage of the plot is studied. Then, Paris power law is applied to the linear part of the plot, and the values of  $C$  and  $m$  are obtained by fitting the law expressed in Equation (3.1) to the experimental curve.

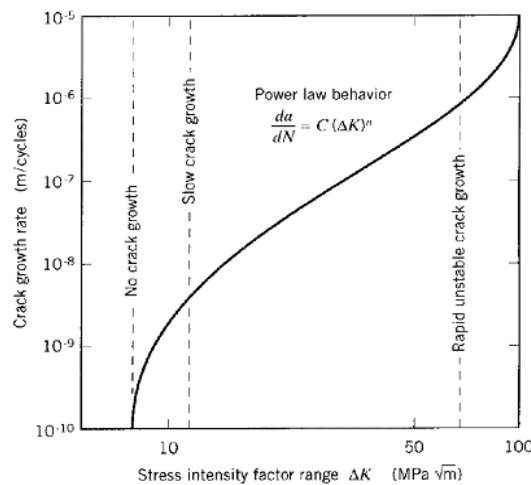


Figure 3.12– Typical  $da/dN$  plot as a function of the stress intensity factor ( $K$ ).

The beginning of the Paris law [165] is associated to aircraft accidents. In fact, two commercial jets Comet (Figure 3.13), failed in 1954 some months apart (January and April) [173]. This “*was the world's first passenger jet airliner, designed and built in Britain*” [173]. One broke up in flight and the other crashed in the Mediterranean Sea. The causes of these failures were stresses in the metal skin caused by the corners of the square windows. However, the Paris law was only taken into account in 1969 with the failure of the US F-111. Paris et al. “*were the first to suggest that the increment of fatigue crack advance per stress cycle,  $da/dN$ , could be related the range of the stress intensity factor*” [174]. The objective of this work was to show that “*the growth of an initial “crack-like”*”



imperfection to a critical size, which causes static failure of a structure, may be described by a single rational theory” [175].

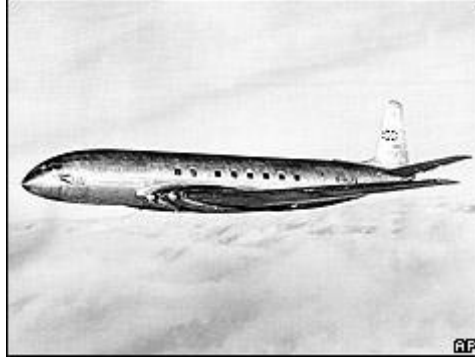


Figure 3.13 – Havilland Comet jets [173].

### 3.4 Fracture Mechanics for Bonded Joints

Fracture mechanics is one of the most common tools to explain the fatigue behaviour. Sancaktar [176] showed that the bond behaviour suffers damage mainly by fracture processes. The duration of this process is known as the duration of fatigue life. In fact, this author considered the two stages: the initiation stage and the propagation stage ( $N_f = N_i + N_p$ )<sup>25</sup>, for his analysis. Most investigations are related to the propagation stage and with fracture mechanics it is possible to describe the growth rate ( $da/dN$ ) of the crack. The equation can be a **modified Paris law** mainly because the  $G_{min}$  in composite bonded joints can be increased by fibre bridging [152]. Equation (3.2) represents this modification:

$$\frac{da}{dN} = C_1 \left( \frac{G_{max}}{G_c} \right)^m \quad (3.2)$$

being  $C_1$  and  $m$  parameters that depend on the material, environment, temperature and stress ratio. Equation (3.2) leads, also, to plots like Figure 3.12 [167]. In this case, the maximum energy release rate ( $G_{max}$ ) is divided by  $G_c$  to obtain a relative value, thus allowing comparison between the different loading modes. It represents the percentage of energy absorbed until it reaches the energy needed to start abrupt failure (Figure 3.12 - this value corresponds to the moment when the third stage of the fatigue starts). In other words, Equation (3.2) represents the FCG rate as function of the relative energy absorbed along the tests during the linear region. These plots can be used to define the parameters  $C_1$  and  $m$ . There are a lot of variations of this power law, and theories that relate the damage parameters to it. For example, Zhang et al. [177] define four major fatigue categories, which are related to different damage metrics for the cumulative damage. These four groups of theories are:

<sup>25</sup>  $N_f$ : number of cycles until catastrophic failure,  $N_i$ : number of cycles until crack's macroscopic formation,  $N_p$ : cycles until the final failure.

- macroscopic failure theories based on modified static criteria to take into account the cyclic damage;
- strength degradation theories that measure the residual strength of a composite after a cyclic program;
- stiffness degradation theories have as a metric the residual stiffness, i.e., they are based on the variation of the stiffness along the fatigue life;
- and damage mechanics theories characterized by the simulation of initiation and growth of the matrix cracks on the fatigue behaviour.

The second and third categories are widely used because they establish phenomenological models with evolutionary laws. These laws describe gradual degradation and damage accumulation through time. The stiffness degradation approach presents some advantages because it can be measured with non-destructive methods and presents less statistical variation than strength data [177]. Also, these theories can be more accurately used for the composite materials [178], since the mechanisms associated are more complex than in metals. In addition, the changes of stiffness, strength or life can be easily measured during the tests [122].

*“Recognizing that debonding can occur slowly over time rather than catastrophically, below the Critical Energy Release Rate ( $G_c$ ), fracture mechanics offers a unique means for designing bonds from a durability perspective. Subcritical cracking or debonding can occur for a variety of loading scenarios, the problem is how to address the stress concentration inside the joint and account for the damage [69]”.*

Mostovoy and Ripling [179] used the Tapered Double Cantilever Beam test (TDCB - Figure 3.14), addressing mode I loading. The specimens were partially coated aluminum adherends. From the results they proposed several patterns but the most important concluding hypothesis are *“that fatigue is more damaging to the interface than static loading”* and *“a high value of  $G_{Ic}$  (material property) allows a slow cracking in fatigue”* [179]. *This basic approach of using the relation between debond growth rate and applied energy release rate can also be extended to other time dependent debonding processes. Knowing the debond characteristics, one can predict the rate debonding due to viscoelastic debonding or sub-critical debonding in the presence of exposure to a variety of environmental conditions including moisture [69].*

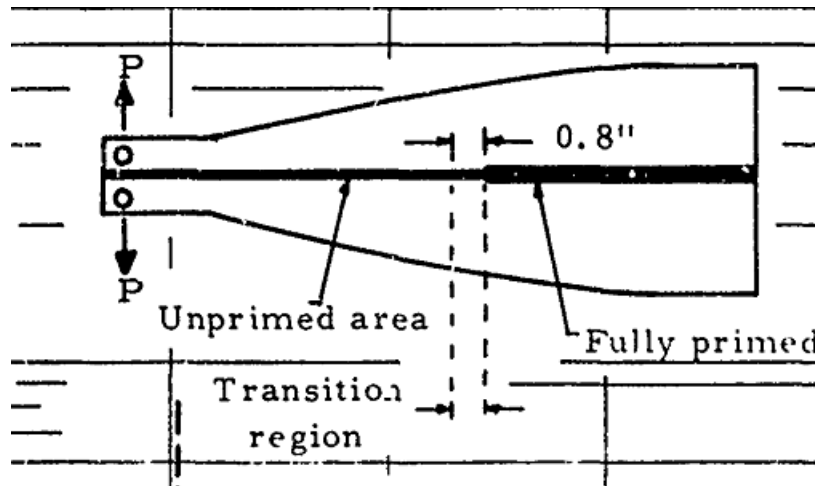


Figure 3.14 – Specimen used in Mostovoy and Ripling work, to assess the behavior of bonded joints under fatigue and Liquid Water Stress Corrosion Cracking [179].

Still for mode I, fatigue work has been done by Abou-Hamda et al. [168], Ashcroft and Shaw [152] and Pirondi and Nicoletto [157]. They have analyzed how different parameters affect the fatigue life in bonded joints. Abou-Hamda et al. [168] addressed the effect of the bondline thickness in DCB aluminum alloy joints with an epoxy adhesive. The applied relation for the Paris law in this work is in Equation (3.3). They have established that the  $m$  value varies from 4.5 to 5.1 for a thickness between 0.3 mm and 1 mm.

$$\frac{da}{dN} = C_1 (\Delta J)^m \quad (3.3)$$

Pirondi and Nicoletto [157] studied the effect of different load ratios ( $R$ ) and frequency. They also used a crack monitoring method based on the compliance of the specimen. They used ASTM D-3433 [180] as a baseline for their work. They found that the effect of frequency is much lower than the effect of  $R$ . The value of  $m$  varies from 3.67 at  $R=0.1$  to 4.21 at  $R=0.4$ . In this work they also validated an analytical model based on a beam elastic foundation.

Finally the work of Ashcroft and Shaw [152], which concerns bonded joints with composite adherends (CFRP), is related with previous studies in static behavior with the effect of temperature variation. In the first part, Ashcroft et al. [118] concluded that “*care needs to be taken when applying beam theory approaches across a wide temperature range*”. In the second part Ashcroft and Shaw [152] defined the calculation based on the secant method in the ASTM E647 where the fit of  $da/dN$  to a polynomial equation is performed using the following equations:

$$a = b_0 + b_1 \left( \frac{N - C_1}{C_2} \right) + b \left( \frac{N - C_1}{C_2} \right)^2 \quad (3.4)$$

$$\frac{da}{dN} = \frac{b_1}{C_2} + 2b_2 \left( \frac{N - C_1}{C_2^2} \right) \quad (3.5)$$

being  $C_1$  and  $C_2$  given by,

$$C_1 = \frac{1}{2} (N_{i-n} + N_{i+n}) \quad (3.6)$$

$$C_2 = \frac{1}{2} (N_{i+n} - N_{i-n}) \quad (3.7)$$

The authors defined that this method is good to reduce the scatter *“but there is a risk of masking the different effects”*. One of the interesting points is the clear description of failure surface and its correlation to the process of the FCG (to the Paris-Law). Finally, they concluded that *“it is felt that the most likely route to improve current predictive methodologies is by developing failure models more closely related to the degradation and failure mechanisms occurring in the joints.”* Still there is much more developed by Ashcroft in the subject of bonded joints. To have a general perspective the work presented in [69] is a good starting point.

For mode II there is not much work developed. One of the reasons could be the difficulties regarding the test procedure and the ability to obtain a stable crack growth [181]–[183]. Mall and Kochhar [184] tested ENF samples to validate this type of tests for under fatigue loading. They used composite laminates with 15 plies with  $0^\circ$  in each adherend. They concluded that [184]:

- *“the end-notched flexure specimen is a viable specimen to study the failure of adhesive bonding for both static and fatigue mode II loading”;*
- *the total Energy Release Rate ( $G_d$ ) is the driving parameter for cyclic debonding;*
- *“the debond growth resistance of the tested bonded system under cyclic loading with full shear reversal (i.e.  $R=-1$ ) is drastically reduced in comparison to the case when subjected to cyclic shear loading with no shear reversal (i.e.  $R=0.1$ )”.*

Considering mixed mode testing there is some work done by Ashcroft also in some of the references presented before [147], [151], [152], [185]. Actually, in [185] the specimens tested are double-lap joints and strap joints. Also Samborsky et al. [186] presented results of CLS specimens tested to validate wind blades' adhesive paste under fatigue. In general, those results prove the suitability of CLS testing procedure to define the fatigue life and behavior of joints. In addition, they are good to understand the impact of the laminate lay-up. The stress distribution and the contribution of the mixed-mode make *“finding”* the  $G_{th}$  and understanding of the different failure modes in a *“real loading scenario”* easier than when studying single lap joints (SLJ).

## 4 Experimental Work

This work is mainly divided into two parts. The first is the validation of an Equivalent Crack Method and an application of an automatic data point gathering system to assess the applicability of a crack growth assessment using fracture mechanics and Paris law. The equivalent Crack Method has been already validated for static tests in previous works [187]–[190]. The second part is related to the impact of the different loading modes in the crack propagation rate as a function of time (Paris Law).

The validation of this work represents an opportunity to facilitate experimental testing. This means to reduce the intensive work regarding fatigue testing and correlating the actual behavior of the joints with the reduction of the stiffness. In addition, it is an opportunity to better understand how the stress concentrations affect the fatigue behavior of a structure.

### 4.1 Materials and Specimens

The experimental work was carried out considering Mode I, Mode II, Mixed-Mode (I + II) loading and was finalized with single lap joints. All specimens were manufactured using the same materials. The CFRP (Carbon Fiber Reinforced Polymer) used was *SEAL™ TexipregHS 160 RM* and the adhesive used was a ductile epoxy adhesive - Araldite 2015 – manufactured by Huntsman. The properties of the bulk adhesive and the adherends were already defined by Campilho et al. [191] and those are the ones presented here. The bulk adhesive elastic properties are  $E$  (Young's modulus) = 1850 MPa, and  $\nu$  (Poisson's ratio) = 0.3 and for the CFRP it is presented in Table 4.1, taking into consideration the different directions (1, 2, 3).

Table 4.1– CFRP elastic orthotropic properties for a unidirectional ply aligned in the 0° direction [192]

<i>Young's Modulus (E)</i>	<i>Poisson's Ratio (<math>\nu</math>)</i>	<i>Shear Modulus (G)</i>
$E_1 = 1.09\text{E}+05\text{Mpa}$	$\nu_{12} = 0.34$	$G_{12} = 4315 \text{ MPa}$
$E_2 = 8819\text{MPa}$	$\nu_{13} = 0.34$	$G_{13} = 4315 \text{ MPa}$
$E_3 = 8819\text{Mpa}$	$\nu_{23} = 0.38$	$G_{23} = 3200 \text{ MPa}$

Figure 4.1 shows schemes of specimens used for fracture characterization of bonded joints. DCB, ENF and SLB were performed for mode I, mode II and mixed-mode I+II respectively. It

should be noted that SLB tests provide mixed-mode fracture characterization for a fixed mode-mixity. Finally SLJ (Figure 4.2) tests were made to compare the actual behavior of this type of joint with the previous tests. A detailed explanation will be presented in the next sections as the different parts are addressed.

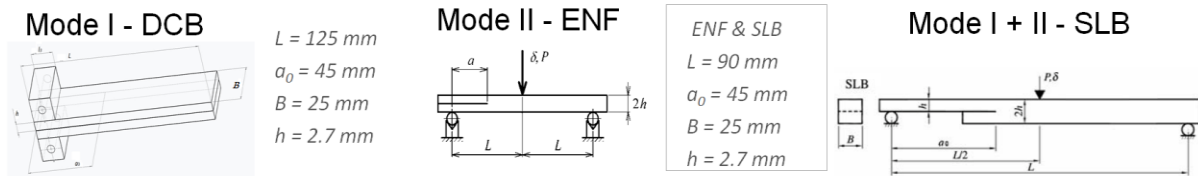


Figure 4.1 – Specimens tested.

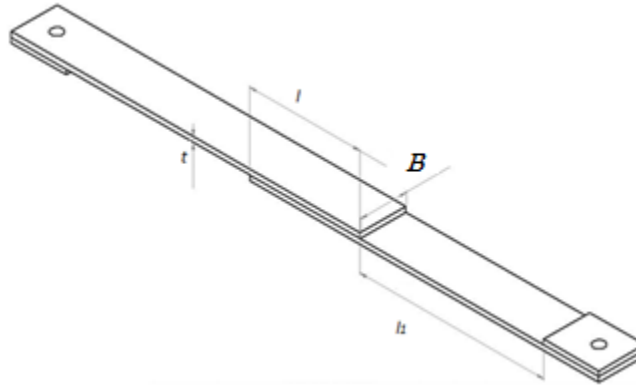


Figure 4.2 – SLJ configuration tested.

## 4.2 Specimen Preparation

The joints tested in this work are secondary bonded joints, i.e., joints manufactured with the two adherends already cured (Section II.1.2 - Composite Bonded joints: Manufacturing Processes & Technologies). All the specimens tested were manufactured as described in the following.

The detailed steps to manufacture the adherend are:

- 1 hour after removing the prepreg from the freezer, it was cut in squares of 300 mm x 300 mm (Figure 4.3).



Figure 4.3 – Cut plies to be laminated.

- The laminate was stacked by hand lay-up, only considering  $0^\circ$  layers. The plies were then piled one at a time, after heating to promote an easier adhesion, followed by the application of pressure on all the surface area with a small scraper (Figure 4.4).



Figure 4.4 – Compaction during the hand lay-up using the scraper [190].

- After the lay-up was completed, it was covered with TEFLON®, on both sides. The laid-up plate has to have the size of the pressure plate to avoid contamination or any contact between the plate and the laminate.
- Adhesive tape was placed on the sides to prevent the fibers from sliding (because this is unidirectional lay-up).
- The laminate, with the TEFLON® was placed, on the pressure plate with spacing bars located along the perimeter to control the pressure applied on the laminate and thickness.

- Afterwards, it was cured by applying the expected curing cycle (pressure and temperature), as shown in Figure 4.5. The plate can only be removed when the temperature is below 60°C.

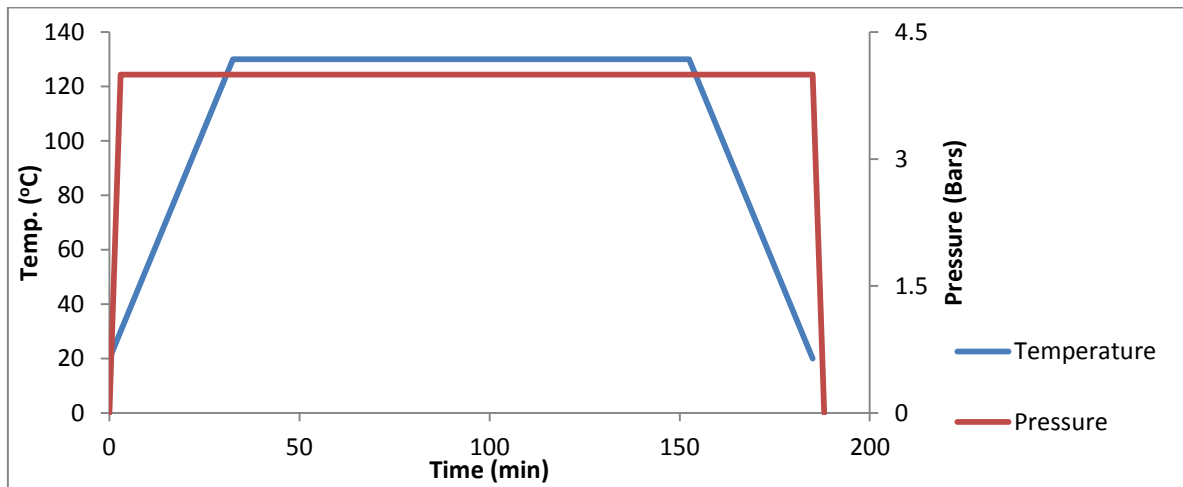


Figure 4.5 – Curing cycle applied to the laminate: pressure and temperature applied.

After removing the plate already cured (Figure 4.6) and prior to bonding the overlap areas were marked and grinded with 180 grit sandpaper until complete removal of the glossy part, avoiding any damage in the fibers.



Figure 4.6 – Cured plate.

For the bonding process, two different procedures were used. For the pure modes the specimens were cut prior to bonding like the method proposed by Campilho [190], while for the SLB and SLJ the plates were bonded prior to cut following the procedure in EN 2243-1 [103]. Pure mode tests (DCB and ENF specimens) were manufactured considering the standard of mode I fatigue delamination (D6115) [159] and the fracture toughness (D-5528) [116] (where the bonding process is not explicitly addressed) while EN2243-1 [103] standard evaluates the properties of structural adhesives of non-metallic materials in single lap shear



tests. This second methodology was used to keep the fidelity between the standard approach in realistic application and the specimens. The main difference lies in how the pressure is applied. The first method does it with the help of grips (Figure 4.7) while in the second the application is done with the pressure plate. Alignment of the specimen in the first case is done with vertical grips (Figure 4.7b)), for the other it is done when the specimens are cut.

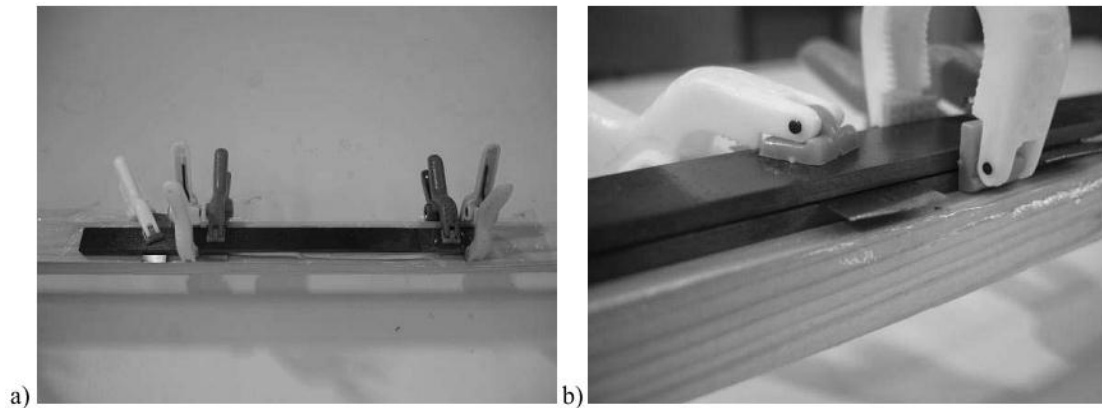


Figure 4.7 – Pressure application with grips a) and detail of the vertical grips (b) [190].

The pre-crack and the bondline thickness were manufactured with 0.2 calibrated steel spacers inserted: one at the end of the specimens, other at the pre-crack region and another at the beginning of the specimen. This last was removed after some hours and the other two spacers remained for 5 days. After the adhesive was cured (5 days), the specimens were finished. In the first case (Figure 4.8), the steel spacers were removed as well as the excess of adhesive by polishing. For the mixed mode specimens (Figure 4.9), the specimens were cut with a precision saw.



Figure 4.8 – ENF Specimen prior finishing.

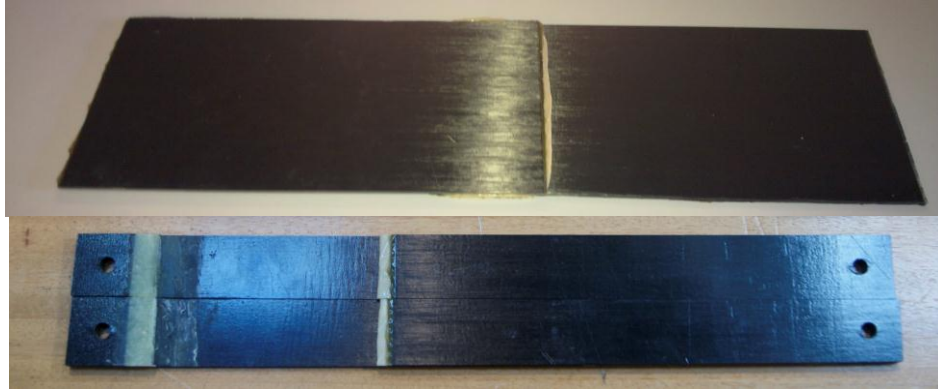


Figure 4.9 – SLJ manufactured following EN2243-1.

## 5 Mode I

These tests were made focusing on the validation of the equivalent crack method. The method is called Compliance Based Beam Method (CBBM) since it is based on the estimation of the equivalent crack from the current compliance. The CBBM was validated using DCB tests because it is easier to measure crack length while the test is running. In fact, the crack length monitoring on Mode II tests (ENF) is very difficult to be performed because of the deflection and the fact that the machine had to be loaded at half of the load when it was in pause which make it even more difficult. Additionally, the crack tends to propagate with the faces in contact which creates difficulties the identification of its tip. Moreover, the measurement of the crack length is a commitment between the pauses needed for this purpose and the influence of them on fatigue. In this case the CBBM is also an excellent option, as the need for stopping the machine is unnecessary and the data acquired through the tests gives enough points to have an appropriate fatigue characterization with the CBBM.

Two different adherend thicknesses ( $h_1 = 5.4$  mm and  $h_2 = 2.7$  mm) were also used to validate the model. The different thicknesses were used to understand the impact on the behavior when changing the adherend thicknesses.

### 5.1 Manufacturing Process

The DCB specimens (Figure 5.1) were made with two beams bonded with a 0.2 mm thick adhesive layer. Each beam was prepared with 36 and 18 plies unidirectional prepreg (CFRP – Carbon Fiber Reinforced Plastic) leading to an arm thickness ( $h$ ) of 5.7 mm ( $h_1$ ) and 2.4 mm ( $h_2$ ) respectively. Two different geometries were defined while the test conditions and manufacturing process remained the same.

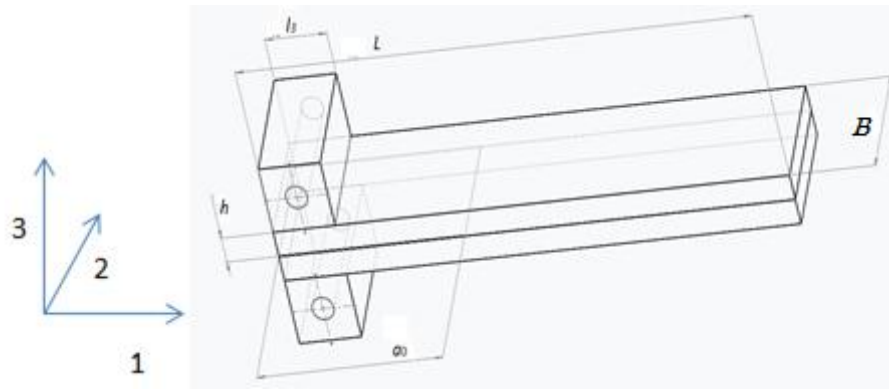


Figure 5.1 — Geometry of a DCB specimen with load blocks [116].

The specimens' dimensions were defined in accordance with ISO 15024 [128] and ASTM D5528 [116] and D6115 [159] standards ( $L = 125\text{mm}$ ,  $a_0 = 45\text{mm}$ ,  $B = 25\text{mm}$ ). The bonded surfaces were ground with sandpaper and cleaned with acetone; being bonded was as described before in the previous Section (III.4 - Experimental Work) The cure of the adhesive was made at room temperature for five days. The final step was fixing the load blocks.

## 5.2 Test Procedure

The cyclic fatigue loading of the DCB specimens was made on a MTS servohydraulic machine, with a frequency of 4Hz, load ratio ( $R$ ) of 0.1 and with constant load amplitude. The maximum load was 50% of the failure load that was defined previously by means of static testing. Two magnification lenses, one at each side of the specimen, were used to monitor the crack length during its propagation. Figure 5.2 shows the used setup.

In addition, a real time data acquisition system (from the MTS machine) was used to automatically save some cycles information (displacement and load) every period of time selected, e.g. to save 10 cycles every 2000 cycles of testing. This procedure was used only for the 2.7 mm specimens while for the others the displacement values were registered by hand. For the automatic registration process, a Matlab program was developed to process the information stored. This program finds the maximum displacement and the maximum load, giving as input the points saved for each period.

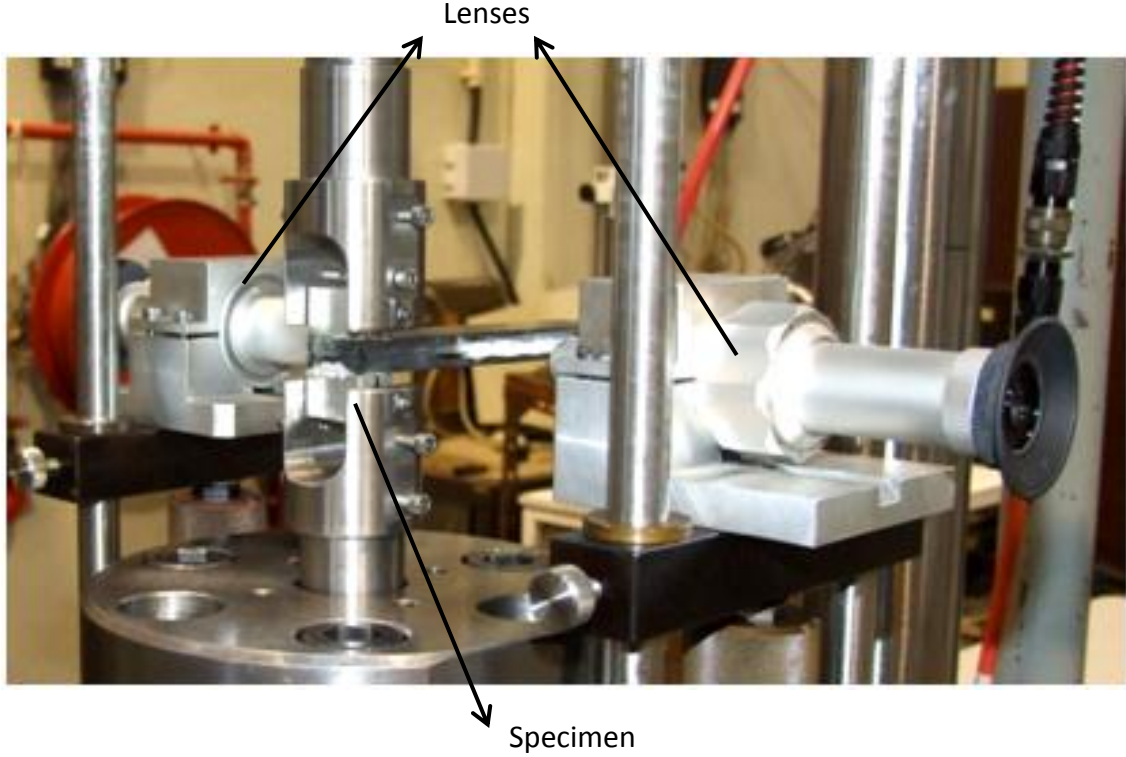


Figure 5.2 - Experimental setup of DCB tests under fatigue cyclic loading.

### 5.3 Model Validation

The value of  $G_I$  was calculated using the classical methods based on the beam theory and compliance calibration. They were used to validate the CBBM, which does not require crack length measurement during propagation. All the methods use the Irwin-Kies equation (Equation (5.1)) [152], [189] to evaluate  $G_I$

$$G_I = \frac{P^2}{2B} \frac{dC}{da} \quad (5.1)$$

where  $B$  is the width of the specimen and  $dC/da$  is the variation of the compliance as a function of the crack length,  $a$ . It should be noted that the compliance was always measured for the peak load in cycles. It is important to remember that the Griffith's theory states that the energy needed for a crack to grow is equal to the change in potential energy stored in the specimen due to crack propagation. In other words, the elastic strain energy released when the crack grows must be the energy required to create new surfaces. The energy dissipation is considered to be located only in a plane and a linear crack front along the specimen width ( $B$ ) is assumed [118], [152].

### 5.3.1 Compliance Calibration Model (CCM)

In this model the compliance is calibrated as a function of crack length by means of a polynomial adjustment of the  $C = f(a)$  relationship, where  $C = \delta/P$ , being  $\delta$  and  $P$  the applied displacement and load, respectively. Equation (5.2) can be used to calculate directly  $G_I$  as a function of  $a$  by defining a third order polynomial curve fit in the plot  $C$  versus  $a$  (Figure 5.3) [152], [118].

$$C = A_1 + A_2a + A_3a^2 + A_4a^3 \quad (5.2)$$

where  $A_1$ ,  $A_2$ ,  $A_3$  and  $A_4$  are the constants of the fitting procedure. The fracture energy can now be obtained by means of the Irwin-Kies relation (Equation (5.1)) and differentiating Equation (5.2).

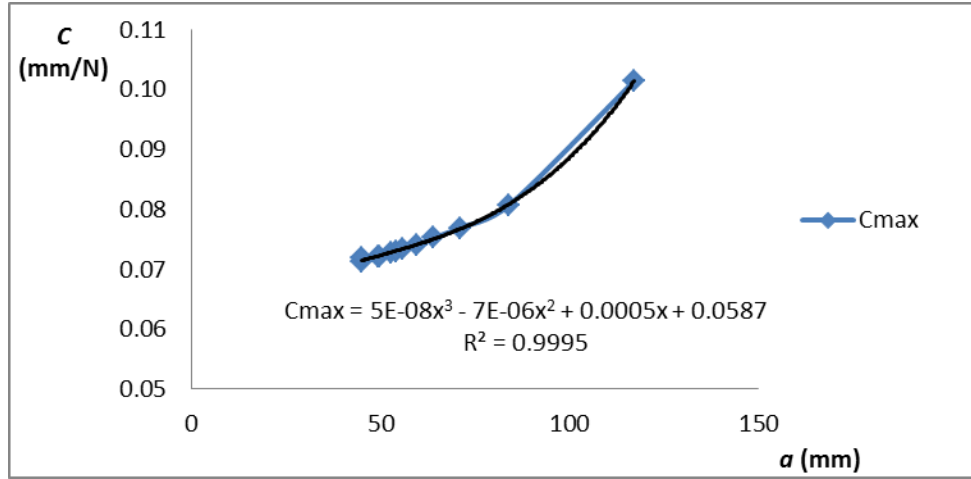


Figure 5.3 - Experimental variation of the compliance ( $C$ ) as a function of the crack length ( $a$ ).

### 5.3.2 Beam on Elastic Foundation Model (BEFM)

Beam theory based methods were presented in previous Section III.2.2 (Fracture Mechanics Approach). Here we refer to a specific beam theory method which accounts for the presence of the adhesive. Pirondi et al. [157] proposed a beam theory based model which accounts for the influence of the adhesive on the joint behavior. The strain energy release rate ( $G_I$ ) is calculated by Equation (5.3), considering the relation between  $C$  and  $a$  developed by Krenk [193], where the joint was modeled as a beam on an elastic foundation

$$G_I = \frac{P^2}{2B} \frac{dC}{da} = \frac{P^2 a^2}{2BEI} (1 + \lambda_\sigma)^2 \quad (5.3)$$

being  $EI$  the bending stiffness ( $EBh^3/12$ ). The second term in the parenthesis represents the effect of the adhesive. The parameter  $\lambda_\sigma$  is given by Equation (5.4) where the value of  $E_\sigma'$  is the modulus of the adhesive considering plane stress conditions (Equation (5.5))

$$\lambda_{\sigma}^4 = \frac{6}{h^3 t} \frac{E_a'}{E} \quad (5.4)$$

$$E_a' = \frac{E_a}{(1-\nu^2)} \quad (5.5)$$

### 5.3.3 Compliance Based-Beam Method

This method is based on the beam theory, specimen compliance and crack equivalent concept. The specimen compliance ( $C$ ) accounting for shear effects can be obtained from [189]

$$C = \frac{8a^3}{E_1 B h^3} + \frac{12a}{5 B h G_{13}} \quad (5.6)$$

being  $E_1$  and  $G_{13}$  the longitudinal and shear modulus of the adherends, respectively. However, it is expected that the compliance of the adhesive and its thickness can influence the global compliance of the specimen and should be accounted for. Consequently, an equivalent flexural modulus  $E_f$  can be estimated from Equation (5.6) considering the initial compliance  $C_0$  and the corrected initial crack length  $(a_0 + |\Delta|)$  instead of  $C$  and  $a$ , respectively

$$E_f = \left( C_0 - \frac{12(a_0 + |\Delta|)}{5 B h G_{13}} \right)^{-1} \frac{8(a_0 + |\Delta|)^3}{B h^3} \quad (5.7)$$

where  $\Delta$  accounts for the root rotation effect at the crack tip and is given by [189]

$$\Delta = h \sqrt{\frac{E_f}{11 G_{13}}} \left[ 3 - 2 \left( \frac{\Gamma}{1 + \Gamma} \right)^2 \right] \quad (5.8)$$

where

$$\Gamma = 1.18 \frac{\sqrt{E_f E_3}}{G_{13}} \quad (5.9)$$

An iterative procedure should be used in Equations (5.7), (5.8) and (5.9) in order to obtain a converged value for  $E_f$ . This procedure also minimizes the influence of any error committed on the initial crack length measurement and the variability of the remaining elastic properties ( $E_3$  – Young's Modulus in direction 3 and  $G_{13}$ ).

During propagation, the energy dissipation at the fracture process zone (FPZ) [121] should not be neglected when ductile adhesives are used. Effectively, in these cases the FPZ extent

justifies its consideration since a non-negligible amount of energy is being dissipated, thus affecting the profile of the load-displacement curve. Additionally, this approach allows overcoming inaccuracies committed during crack length monitoring caused by crack bowing and tilting. This means that an equivalent crack length ( $a_e$  in Figure 5.4) can be calculated as a function of the specimen compliance thus avoiding the experimental crack length monitoring during propagation which can be non-rigorous. The calculation of  $a_e$  can be performed from Equation (5.6), which implies solving a cubic equation using, for example, the Matlab software [189].

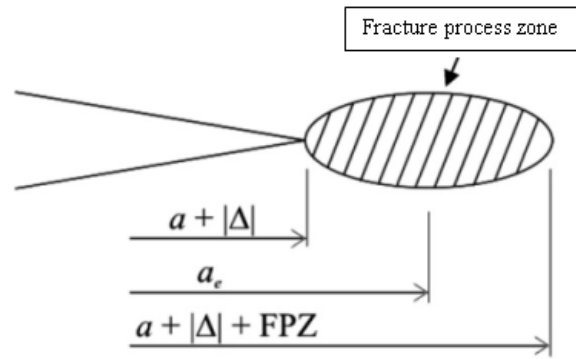


Figure 5.4 - Schematic representation of the crack equivalent concept and FPZ [189].

Finally, the fracture energy in mode I is calculated using Equation (5.10), which is obtained using the Irwin-Kies equation (Equation (2.2)) and Equation (5.6) where  $a$  was replaced by  $a_e$ .

$$G_I = \frac{6P^2}{B^2h} \left( \frac{2a_e^2}{h^2 E_f} + \frac{1}{5G_{I3}} \right) \quad (5.10)$$

#### 5.3.4 Paris Law

In terms of fatigue failure, the relation between the fatigue crack growth (FCG) rate as a function of the number of cycles ( $da/dN$ ) and the energy dissipated can be presented as Equation (5.11), which in fact is Equation (3.2)<sup>26</sup>.

$$\frac{da}{dN} = C_1 \left( \frac{G_{\max}}{G_{Ic}} \right)^m \quad (5.11)$$

In this case the maximum energy release rate ( $G_{\max}$ ) is divided by the critical energy -  $G_{Ic}$  to obtain a relative value thus allowing a posterior comparison between the different loading modes. It represents the percentage of energy absorbed during cyclic loading and assessing

<sup>26</sup>The definition of fatigue life and processes are presented in Section III.3.1 - Fatigue Life

$G_{\text{Imax}}$  leading to failure under fatigue. In other words, Equation (5.11) represents the FCG rate as function of the relative energy absorbed along the tests.

#### 5.4 Fatigue Data Reduction Scheme

The definition presented here is to determine the fatigue crack growth rate ( $da/dN$ ). The  $da/dN$  was calculated with the secant method recommended in ASTM E647 standard [172]. This method consists in evaluating the variation of the crack as a function of the number of cycles considering a discrete number of measurements ( $n$ ) during the fatigue test. The crack growth rate between two consecutive measurements ( $i$  and  $i+1$ ) including at least 1000 cycles is then evaluated with the relation given by

$$\left( \frac{da}{dN} \right)_a = \frac{(a_{i+1} - a_i)}{(N_{i+1} - N_i)} \quad (5.12)$$

$$\bar{a} = \frac{1}{2}(a_{i+1} + a_i) \quad (5.13)$$

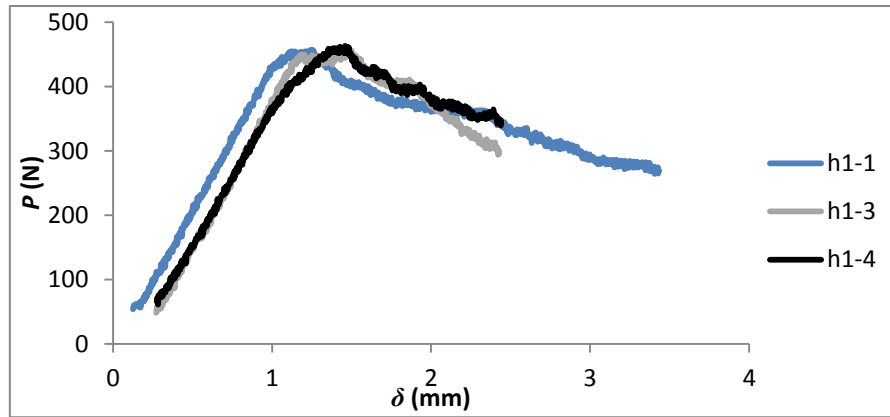
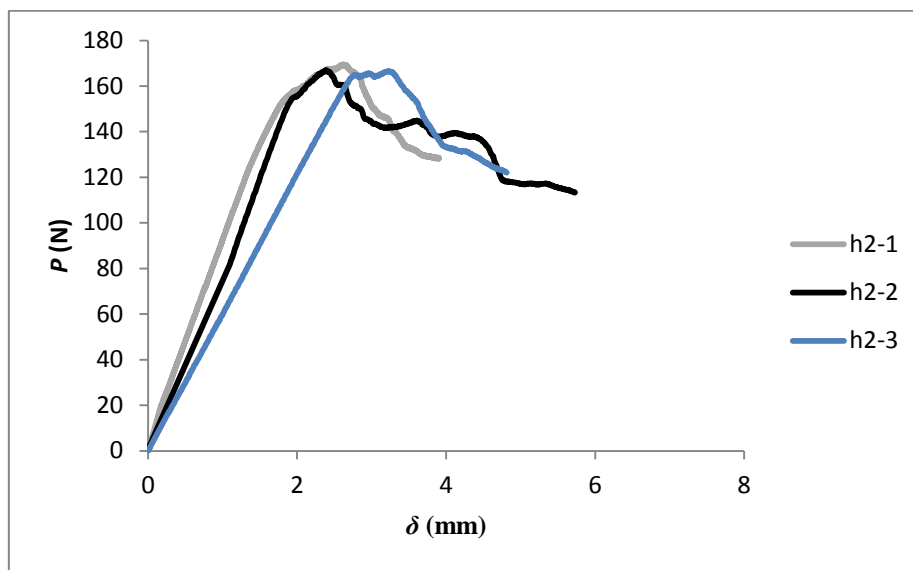
where  $i$  represents the  $i^{\text{th}}$  measurement performed during the test ( $0 \leq i \leq n$ ). This gives an average value of the rate in an increment. The corresponding crack length, for each  $G_i$ , is also the average value of the limits of the increments (Equation (5.13)).

The equivalent crack growth rate was evaluated as a function of the compliance along the fracture test. This variation was registered every 2000 cycles for the tests with  $h_1$  (5.7 mm) adherend thickness

#### 5.5 Static Fracture Characterization

In order to measure the fracture energy ( $G_{\text{IC}}$ ), monotonic quasi-static DCB tests were performed with the same conditions than the ones for fatigue. The specimens tested are designated  $h_1$  ( $h_1 = 5.4$  mm) and  $h_2$  ( $h_2 = 2.7$  mm), according to their thickness. The maximum load was taken from these results to be used as a reference for fatigue testing. Figure 5.5 shows the  $P$ - $\delta$  for specimens  $h_1$ , while Figure 5.6 presents the ones from  $h_2$  specimens. Finally, Table 5.1 presents the summary of these results. In terms of  $P_{\text{max}}$ , all specimens tested were taken into account as a reference.



Figure 5.5 –  $P$ - $\delta$  curve for the  $h_1$  specimens tested statically.Figure 5.6 –  $P$ - $\delta$  curve for the  $h_2$  specimens tested statically.Table 5.1 –  $P_{max}$  for the specimens tested statically.

<u>Specimen</u>	$P_{max} (N)$	
	$h_1$	$h_2$
<u>1</u>	457	170
<u>2</u>	427	167
<u>3</u>	460	167
<u>4</u>	463	--
<b>Av.</b>	<b>452</b>	<b>167</b>
<b>St. Dev.</b>	<b>16.6</b>	<b>1.6</b>

In addition, there results were used to calculate  $G_c$  for these two configurations. Figure 5.7 shows a typical  $R$ -Curve to assess  $G_{Ic}$ , which was considered to be the one corresponding to the plateau value of the  $R$ -curve. Self-similar crack growth occurs when the FPZ is completely developed ahead of the crack tip which reflects on a plateau of the  $R$ -curve. In such

circumstance, the crack propagates self-similarly with a constant FPZ at its tip. The  $G_{Ic}$  values for all tests are presented in Table 5.2. Values obtained for  $h_2$  are slightly higher than the ones for  $h_1$ , which apparently reveals that adherends thickness have some influence on the measured toughness.

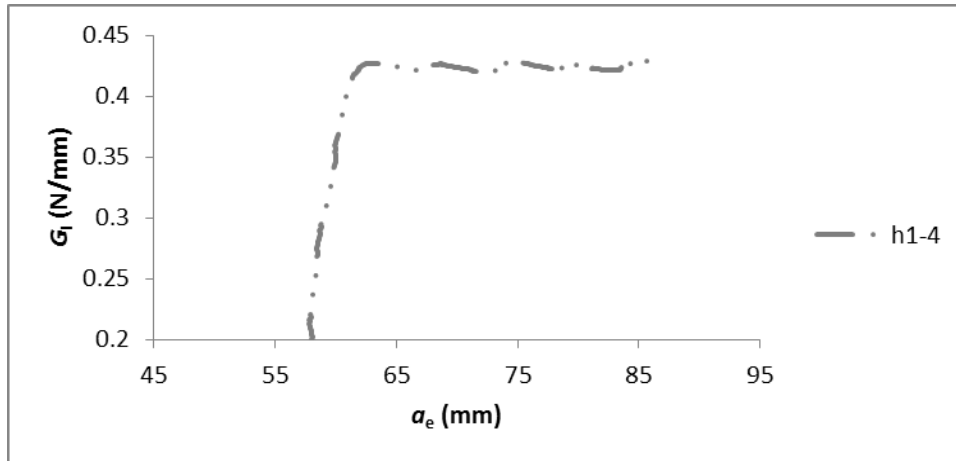


Figure 5.7 – R Curves for  $G_{Ic}$  obtained with DCB specimens.

Table 5.2 -  $G_{Ic}$  obtained for DCB specimens tested statically.

<u>Specimen</u>	$G_{Ic}$ (N/mm)	
	$h_1$	$h_2$
<u>1</u>	---	0.43
<u>2</u>	0.39	0.42
<u>3</u>	0.42	0.47
<u>4</u>	0.42	--
<b>Av.</b>	<b>0.41</b>	<b>0.44</b>
<b>Av. (<math>h_1 + h_2</math>)</b>	<b>0.42</b>	

## 5.6 Fatigue Results

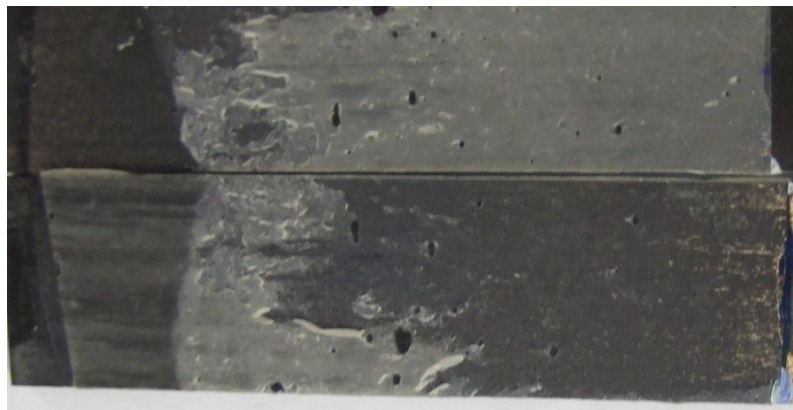
Several fatigue tests were performed for both thicknesses. 12 specimens were tested for  $h_1$ , and 10 for  $h_2$ . Table 5.3 presents the failure mode of the specimens. Only the specimens with cohesive failure (6 of  $h_1$  and 5 of  $h_2$ ) were considered for analysis. In these cases crack propagation occurred within the adhesive, which allows characterizing the fatigue behavior of these bonded joints. Figure 5.8 and Figure 5.9 represent a typical failure surface for both thicknesses respectively. In fact, there are no big differences regarding the failure surfaces. The only visible difference is the tendency of the crack path to go the interface, which for  $h_2$  looks more obvious. This is in agreement with the results presented by Mostovoy and Rippling [179] and Hadavinia et al. [148], [149].

Table 5.3 – Number of specimens failing per type of failure.

<i>Type of failure</i>	$h_1$	$h_2$
Cohesive failure	6	6
Intralaminar failure	2	0
Delamination	4	4



Pre-crack

Figure 5.8 – Fracture surfaces of a bonded joint with cohesive failure for  $h_1$ .

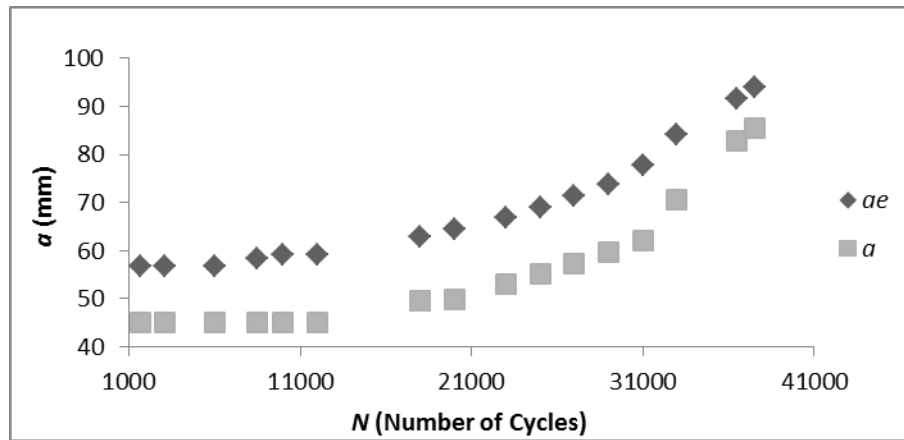
Pre-crack

Figure 5.9 – Fracture surfaces of a bonded joint with cohesive failure for  $h_2$ .

### 5.6.1 Crack length

In order to validate the proposed data reduction scheme (CBBM), the estimated equivalent crack length ( $a_e$ ) was compared with the crack length measured experimentally ( $a$ ). Figure 5.10 and Figure 5.11 show, for a specimen, that both ( $a_e$  and  $a$ ) present similar trends as a function of the number of cycles, being  $a_e$  always larger than  $a$ , as postulated previously. Effectively, taking into account the adhesive ductility, the energy dissipated in the FPZ is not negligible. Considering that  $a_e$  is an equivalent quantity that accounts for all the aspects influencing the specimen compliance, it is logical that  $a_e > a$ . For  $h_1$  the difference is sensibly constant till 31000 cycles, thus reinforcing the statement that during self-similar crack growth the FPZ size is constant ahead of the crack tip. In the last part of the test (after 31000 cycles), the

difference diminishes which reflects that this statement does not apply in the region corresponding to the abrupt final failure. Similar results were obtained for the other specimens.



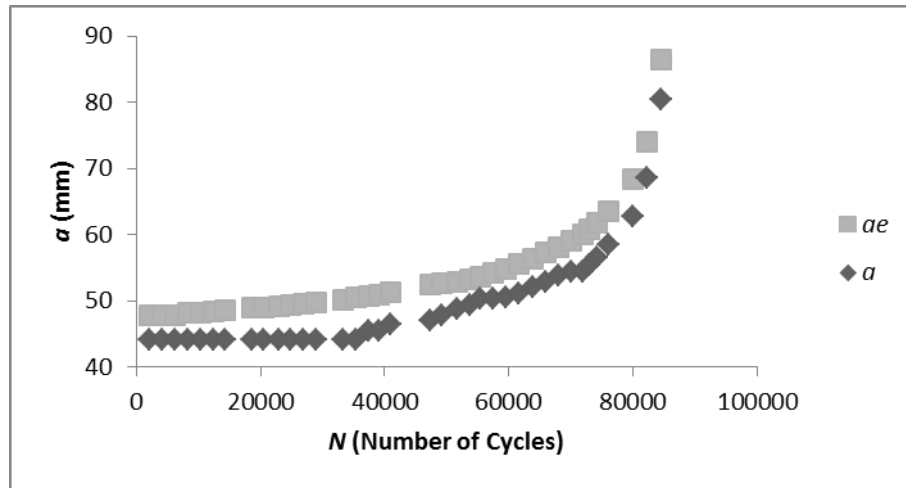


Figure 5.11 – Plot of  $a$  vs.  $N$  to compare the equivalent crack length ( $a_e$ ) and the crack length measured ( $a$ ) for  $h_2$ .

### 5.6.2 Maximum Energy Release Rate

The evolution of  $G_{\text{Imax}}$  as a function of crack length  $a$  provided by the three methods (CCM, BEFM, CBBM – Section III.5.3 - Model Validation) was compared for  $h_1$  specimens (Figure 5.12) with cohesive failure. Although in the CBBM the  $G_{\text{Imax}}$  was calculated from the equivalent crack length, the plot was performed considering the real crack length to provide a better comparison between all methods. It was verified that the BEFM and the CBBM give similar results. However, the CCM method presents remarkable differences relatively to the other methods for lower crack lengths. This can be explained by difficulties of the polynomial adjustment induced by small errors committed during crack length monitoring.

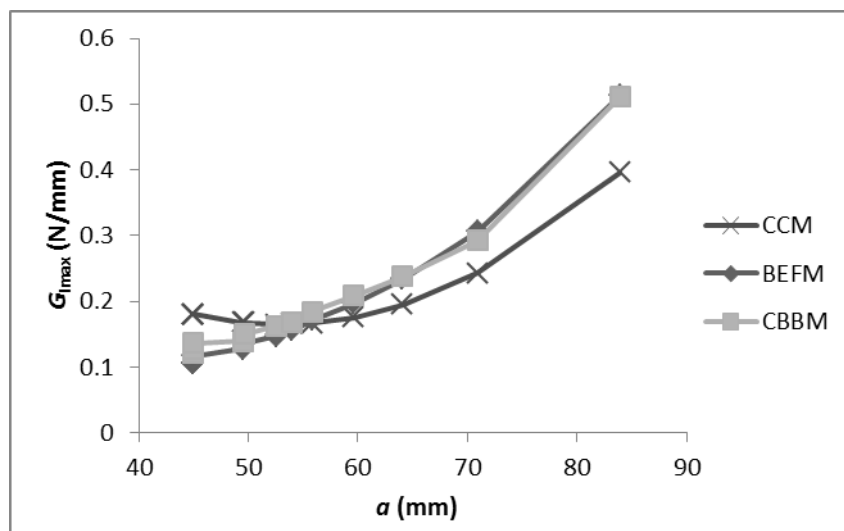


Figure 5.12 – Plot of  $G_{\text{Imax}}$  versus  $a$  considering the three methods for  $h_1$ .

Figure 5.13 presents the evaluation made for the evolution of  $G_{\text{Imax}}$ . The CCM is not presented here due to the limitations when monitoring the crack length and difficulties in the polynomial

adjustment. To guarantee that the CBBM was also valid for  $h_2$  the BEFM is also presented in Figure 5.13. In this plot is also visible how the evolution of the  $G_{\text{Imax}}$  is happening in during the test (along the time with the propagation rate). Comparing, Figure 5.12 and Figure 5.13, there is a similarity between both geometries.

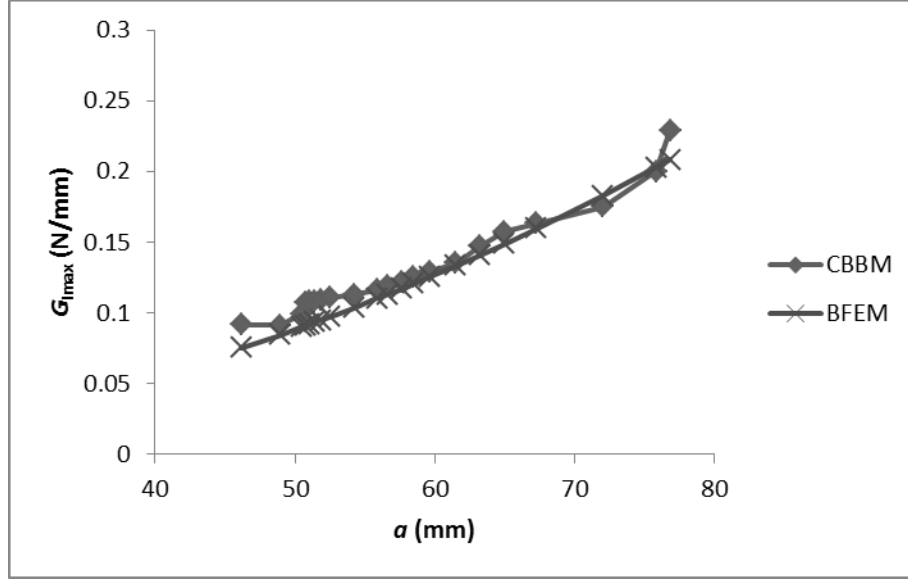


Figure 5.13 – Plot of  $G_{\text{Imax}}$  versus  $a$  considering the two methods ( $h_2$ ).

### 5.6.3 Fatigue Assessment for Specimens $h_1$

#### 5.6.3.1 Fatigue Threshold

The fatigue threshold is an important parameter to define when the initiation stage, defined in the fatigue life (see section III.3.1), is at its end. It corresponds to a change of the slope in the crack propagation rate and also to the beginning of the linear part of the  $da/dN$  versus  $G_{\text{Imax}}/G_{\text{Ic}}$  in a logarithmic scale (Figure 3.12). The corresponding value can normally be defined in the complete fatigue test plot. The energy release rate corresponding to the fatigue crack growth threshold ( $G_{\text{Ith}}$ ) was estimated for all specimens using the three methods. In the CCM and BEFM, the  $G_{\text{Ith}}$  was evaluated as being the energy value from which the crack starts to grow (Table 5.4). Since the CBBM is based on the equivalent crack (not on the real crack length) a different definition of  $G_{\text{Ith}}$  was assumed. In this case,  $G_{\text{Ith}}$  was identified as being the value that leads to increase of  $a_e$ , i.e., when the compliance starts to increase (Figure 5.14). Considering that compliance increase takes place when FPZ develops, the  $G_{\text{Ith}}$  is the value corresponding to damage initiation instead of the one corresponding to real crack starting advance. The CBBM and BEFM present less scatter and provide similar average values (Table 5.4). However, the BEFM is susceptible to reading errors since it is based on rigorous detection of crack starting advance, which is not required in the CBBM, thus constituting an advantage of

this method. The CCM method presented the highest scatter; indeed, for specimens 5 and 6 the energy release rate (CCM) did not provide reliable results. This could be related to the difficulties of the  $C = f(a)$  polynomial adjustment resulting from the sensitivity of the experimental process [152] due to inevitable small errors committed during crack monitoring. These results reinforce the idea that the polynomial adjustment is not an accurate method due to its sensibility to crack monitoring errors.

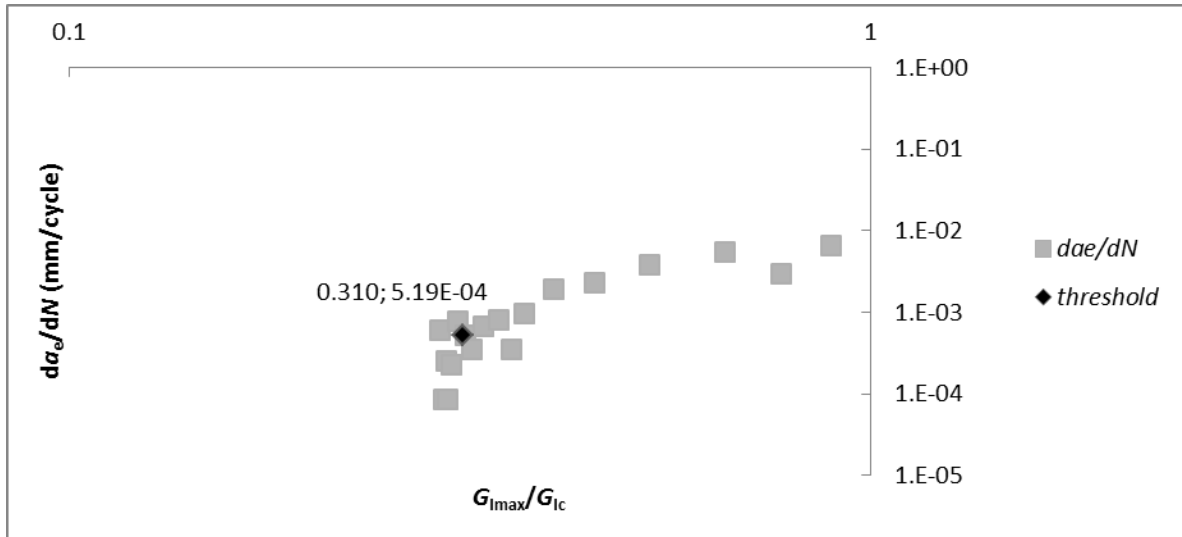


Figure 5.14 – Identification of the  $G_{th}$  in specimen 3 using the CBBM.

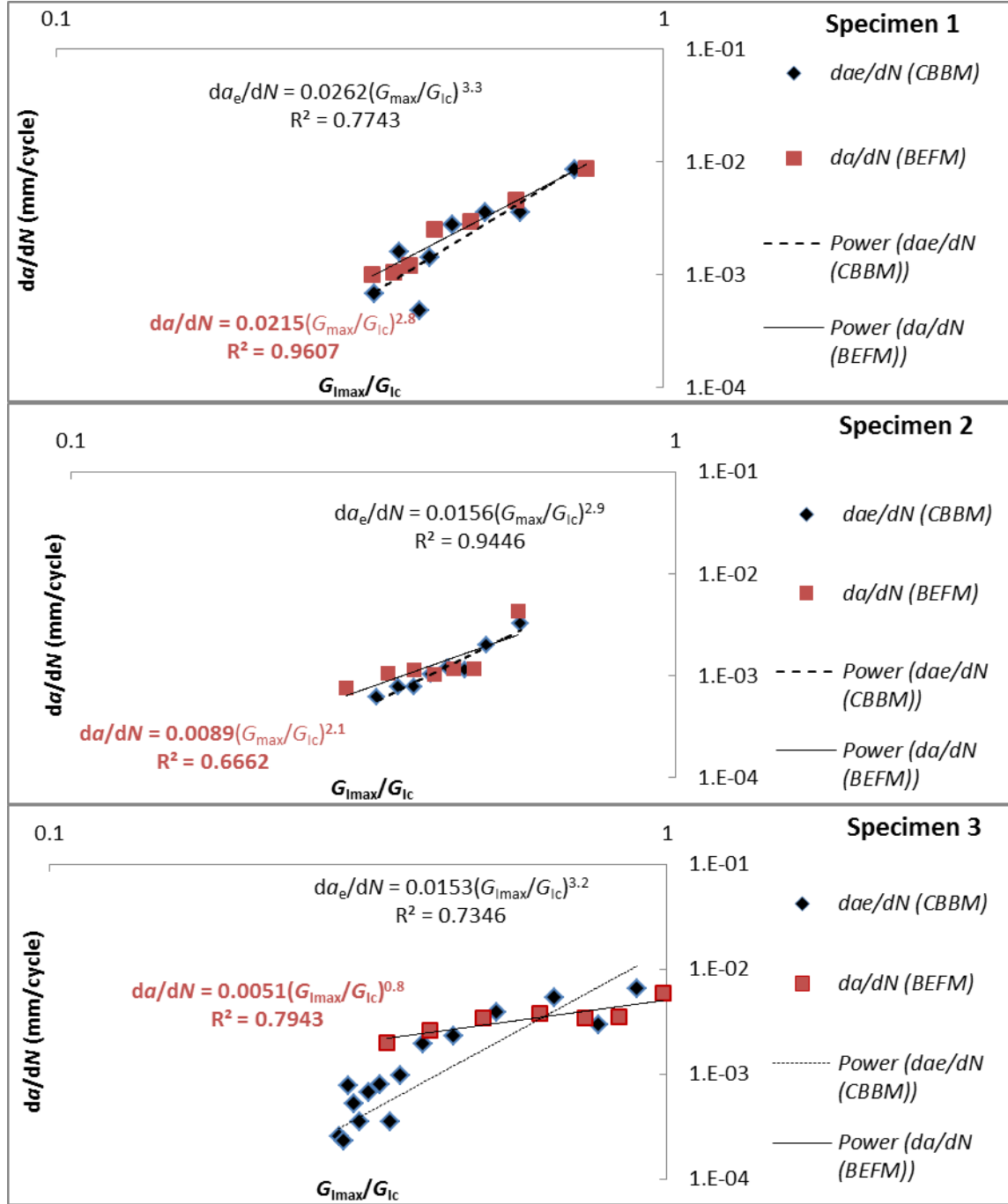
Table 5.4– Energy fatigue threshold of DCB tests ( $h_1$ ).

Specimens	$G_{lth}$ (N/mm)		
	CCM	BEFM	CBBM
1	0.168	0.117	0.127
2	0.190	0.128	0.120
3	0.151	0.116	0.118
4	0.096	0.116	0.116
5	--	0.111	0.138
6	--	0.124	0.140
<b>Average</b>	<b>0.151</b>	<b>0.119</b>	<b>0.127</b>
<b>St. Dev.</b>	<b>0.040</b>	<b>0.006</b>	<b>0.010</b>
<b>CoV (%)</b>	<b>26.5</b>	<b>5.2</b>	<b>8.2</b>

### 5.6.3.2 Fatigue crack growth

Considering the problems inherent to the CCM, the fatigue crack growth ( $da/dN$ ) as a function of energy ratio ( $G_{lmax}/G_c$ ), was determined only considering the CBBM and BEFM (Figure 5.15). Power laws were fitted to establish the relationships given by the two methods. Globally, it can be concluded that both methods provide similar results. The differences are induced by the

inaccuracies committed during crack length monitoring in the BEFM caused by crack bowing and tilting and reading errors. These problems are overcome by the proposed CBBM.





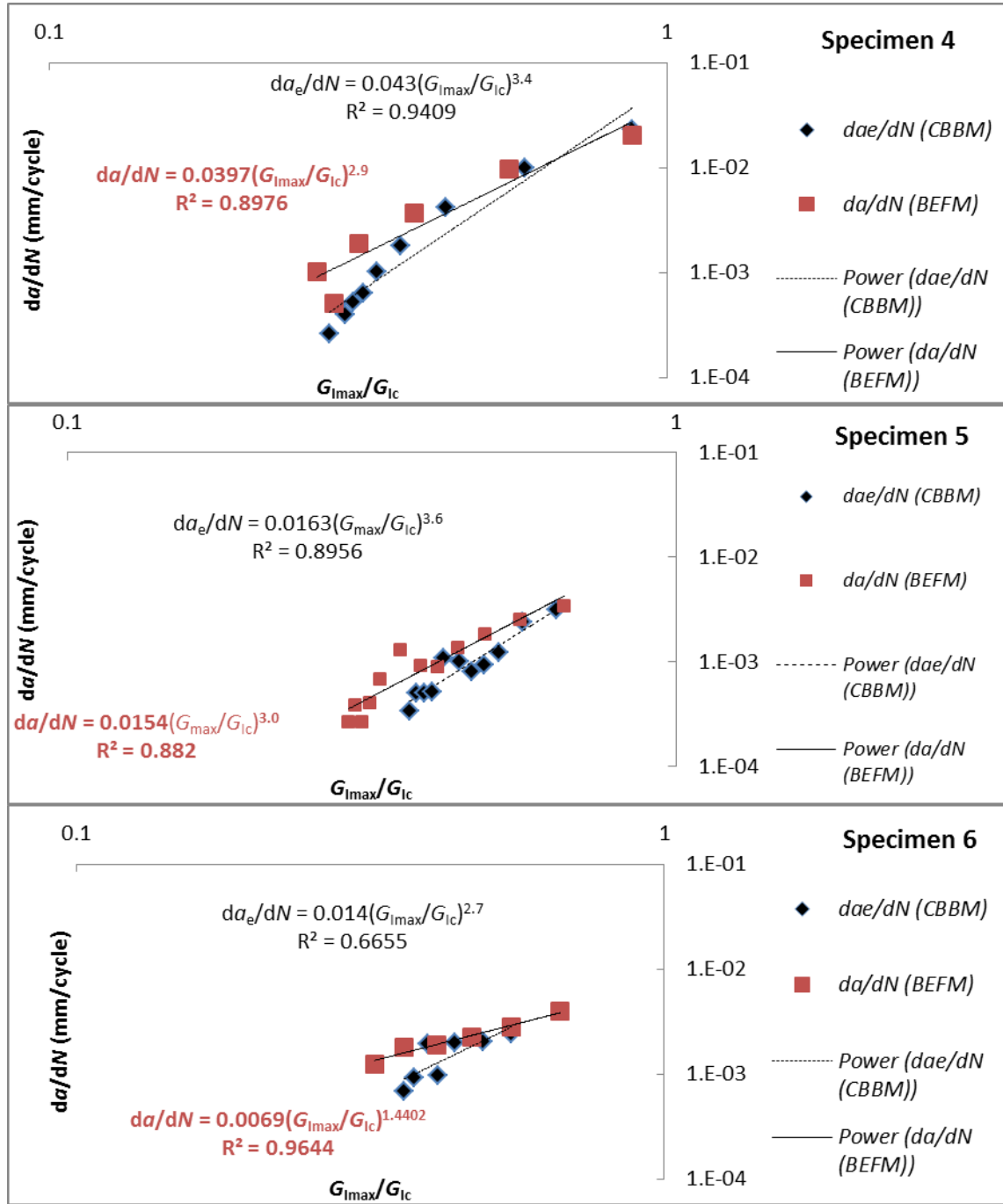


Figure 5.15 – Fatigue crack growth rate as a function of energy ratio  $G_{Imax}/G_{Ic}$  considering the BEFM and the CBBM,  $h_1$  Specimens.

The fitting constants are presented in Table 5.5, where the average for  $C_1$  is 0.02mm/cycle and  $m$  is 3.2. The higher scatter of  $C_1$  (52%) can be explained by the fact that it is also affected by the damage initiation instant, which is influenced by the pre-crack fabrication. This value has lower impact in propagation rate when compared to  $m$ . By consequence, small differences in the cumulative damaging process, prior the crack propagation, can have a large impact in the

scatter of it. To guarantee the good agreement of the results a plot with all the specimens tested was made (Figure 5.16).

Table 5.5 – Paris law constants for  $h_1$  specimens.

<i>Specimen</i>	$C_1$ (mm/cycle)	$m$
<u>1</u>	0.026	3.305
<u>2</u>	0.016	2.916
<u>3</u>	0.015	3.207
<u>4</u>	0.043	3.436
<u>5</u>	0.016	3.624
<u>6</u>	0.014	2.702
<b>Average</b>	0.022	3.192
<b>Std. Dev.</b>	0.011	0.337
<b>CoV</b>	52%	11%

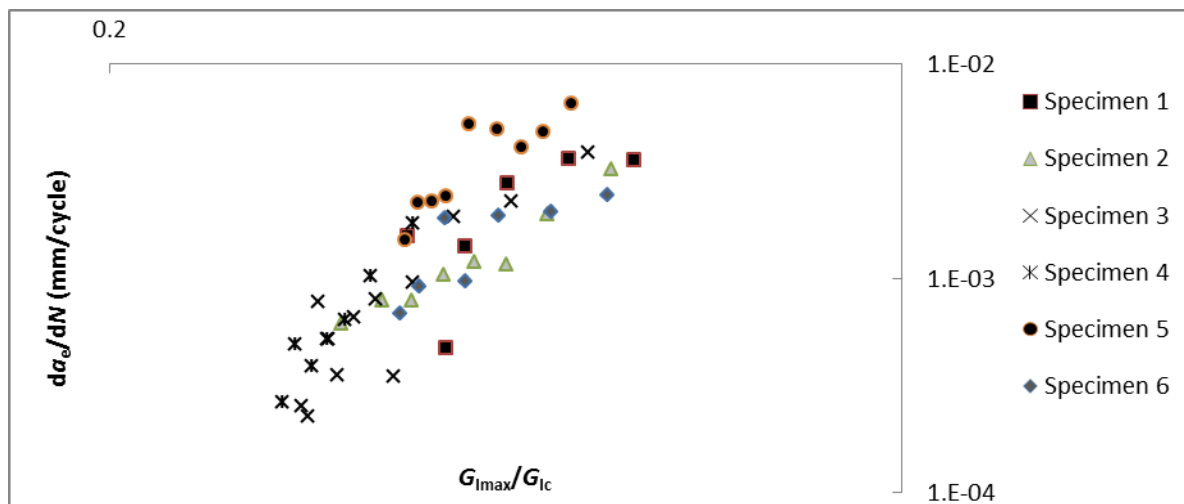


Figure 5.16 – Paris curves for all the specimens tested for  $h_1$ , these points were used to determine the Paris law constants.

## 5.6.4 Fatigue Assessment $h_2$

### 5.6.4.1 Fatigue Threshold

As stated previously, the fatigue threshold was considered as the point where the stiffness starts to vary significantly. Figure 5.17 shows an example of the evaluation for the threshold. The validity of this approach takes into account how fatigue damage is processed in the bonded joint since there is a direct relation between the variation of compliance and damage. This means that the damage assessment is given in terms of compliance. This definition of the threshold is equivalent to the given for  $h_1$  because  $a_e$  is given by the variation of the compliance itself. This approach can also be used to define a threshold without the calculation

the  $G_I$ , only by making the plot  $C$  vs.  $N$  (number of cycles). This methodology was used to see the consistency between the variation of the compliance and the change in the slope of the fatigue curve. In addition, this can be important if real structures are designed allowing a direct association of the behavior of the test with the threshold.

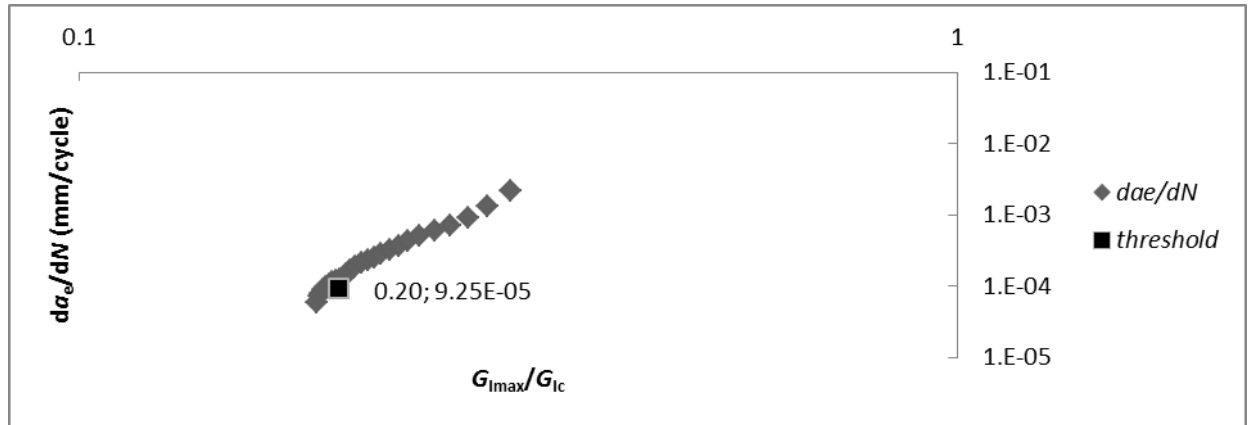


Figure 5.17 - Complete propagation rate for Specimen 5 with the CBBM method to determine  $G_{th}$ .

The  $G_{th}$  was evaluated only using the BEFM and the CBBM (Table 5.6). In this case  $G_{I_{th}}$  is about 20% of  $G_{Ic}$ .

Table 5.6 – Energy fatigue threshold of DCB tests ( $h_2$ ).

Specimens	$G_{I_{th}}$ (N/mm)	
	BEFM	CBBM
<u>1</u>	0.0807	0.076
<u>2</u>	0.0815	--
<u>3</u>	0.0725	0.089
<u>4</u>	0.0736	0.082
<u>5</u>	0.0703	0.078
<b>Average</b>	<b>0.076</b>	<b>0.081</b>
<b>Std. Dev.</b>	<b>0.005</b>	<b>0.006</b>
<b>CoV (%)</b>	<b>6.7%</b>	<b>6.9%</b>

Comparing the values of the threshold and the moment where there is a visible crack initiation ( $a$  in Table 5.7), the difference between  $G_{I_{th}}$  (0.081 N/mm) and  $G_I$  (0.090 N/mm) is 2% of the  $G_{Ic}$ . In other words, the damage initiation defined as “the point where the stiffness starts to vary significantly” is equivalent to the  $G_I$  associated to the actual crack initiation (when the crack starts to be visible). This validates the assumption made before.

In addition, Table 5.7 demonstrates that independently from the initiation moment (visible crack – threshold or end of the initiation phase -  $a$ ) the energy needed to start the propagation is around 0.09 N/mm. In fact, there is a clear variation from 2000 cycles to 58000 cycles which cannot be controlled because the cracks were initiated by fatigue damage. In fact they vary from 0.08 to 0.10 N/mm which represents 5% of  $G_{ic}$ . This means that independently from the initiation moment the energy needed to starts to propagate in a steady state remains constant.

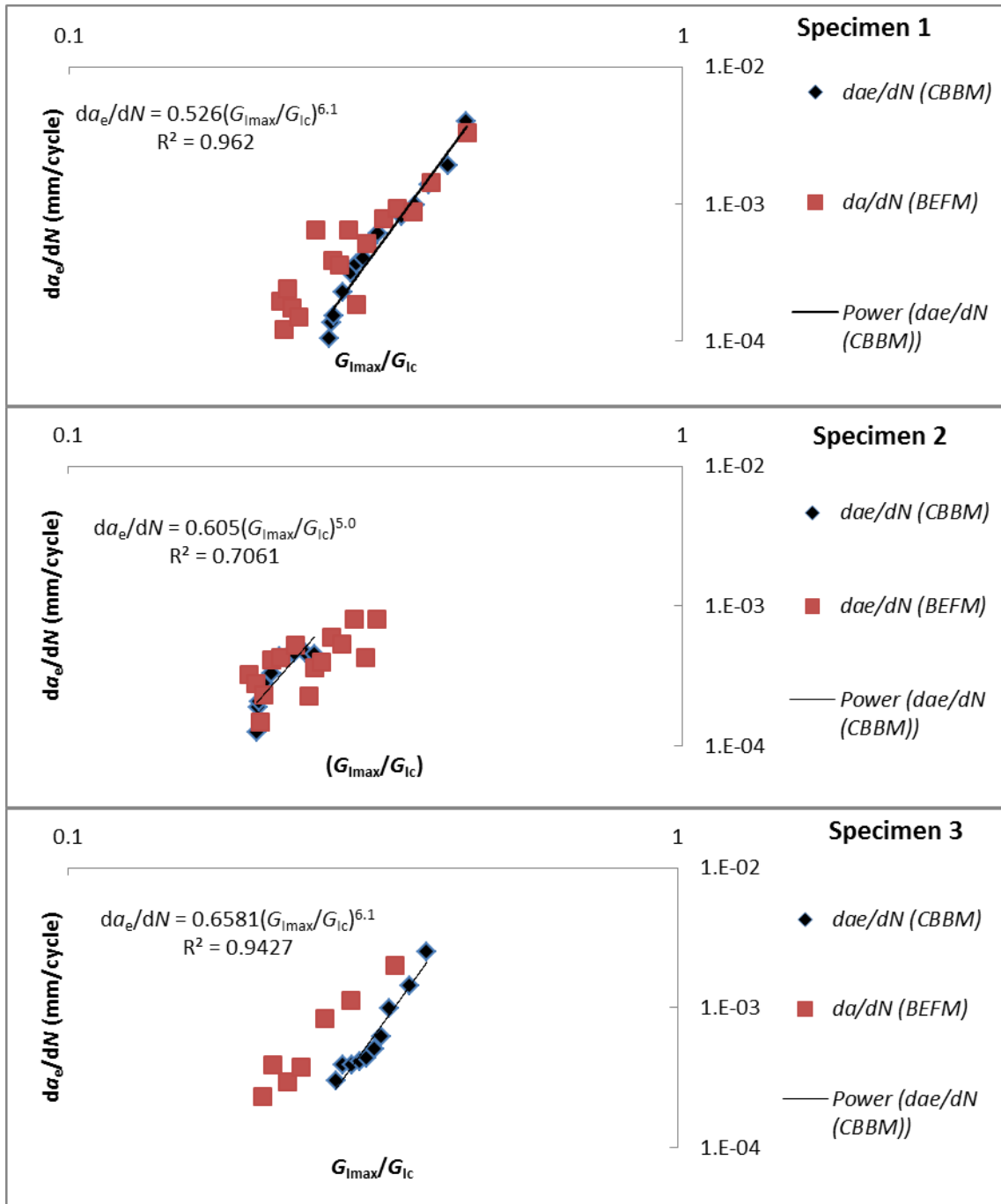
Finally when comparing the threshold definition  $G_{ith}$  (Table 5.6) with the propagation curve (Figure 5.17 - threshold), the initiation energy is consistent with both methods. In fact, independently from the initiation moment, the variation of the compliance and change of the slope in the  $da/dN$  present similar values.

Table 5.7 – Actual initiation for crack growth ( $h_2$ ).

<i>Specimen</i>	<i>N</i>	<i>a</i> (mm)	$\delta$ (mm)	<i>C</i> (mm/N)	<i>a<sub>e</sub></i>	<i>G<sub>i</sub></i> (CBBM) (N/mm)
<u>1</u>	<b>58000</b>	47.40	1.02	1.5E-02	54.45	0.09
<u>2</u>	<b>6000</b>	45.39	0.83	1.2E-02	49.03	0.08
<u>3</u>	<b>2000</b>	45.57	1.00	1.5E-02	50.54	0.10
<u>4</u>	<b>10000</b>	45.33	0.93	1.4E-02	51.54	0.09
<u>5</u>	<b>37400</b>	45.40	0.92	1.4E-02	50.76	0.09
<b>Average</b>		45.82	0.94	1.4E-02	51.26	0.09
<b>Std. Dev.</b>		0.89	0.07	1.1E-03	2.00	0.01
<b>CoV (%)</b>		2%	8%	8%	4%	6%

#### 5.6.4.2 Fatigue crack growth

The first point addressed here is the assessment of the acquired data to see if it fits the expected results. Figure 5.18 show the comparison between the BEFM and the CBBM for five specimens in which the crack was actually measured. As expected from the previous results, there is no big difference between the two methods. The advantage is that more points can be registered when using the CBBM because there is no need to stop the testing equipment. In fact, this can be reflected on the results because for some of the  $h_2$  specimens the linear correlation value ( $R^2$ ) is high in general (close to 1). In specimen 6 it was decided not to stop the test it in order to monitor the crack length. The results presented in Figure 5.19 highlight the excellent correlation which reinforces the advantages of using CBBM. In fact, the high correlation value ( $R^2=1$ ) is an excellent result for fatigue testing.



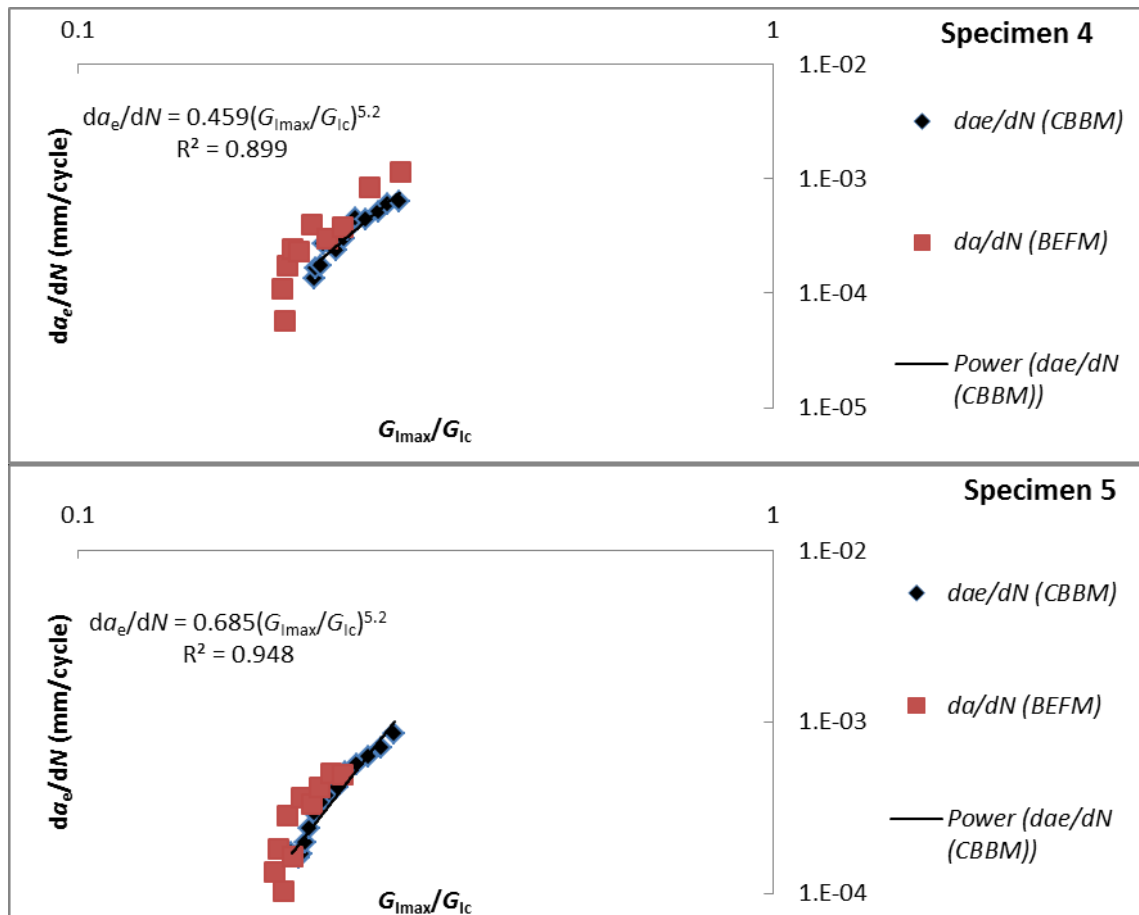


Figure 5.18 - Fatigue crack growth rate as a function of energy ratio  $G_{I\max}/G_c$  considering the BEFM and the CBBM for Specimen- $h_2$ .

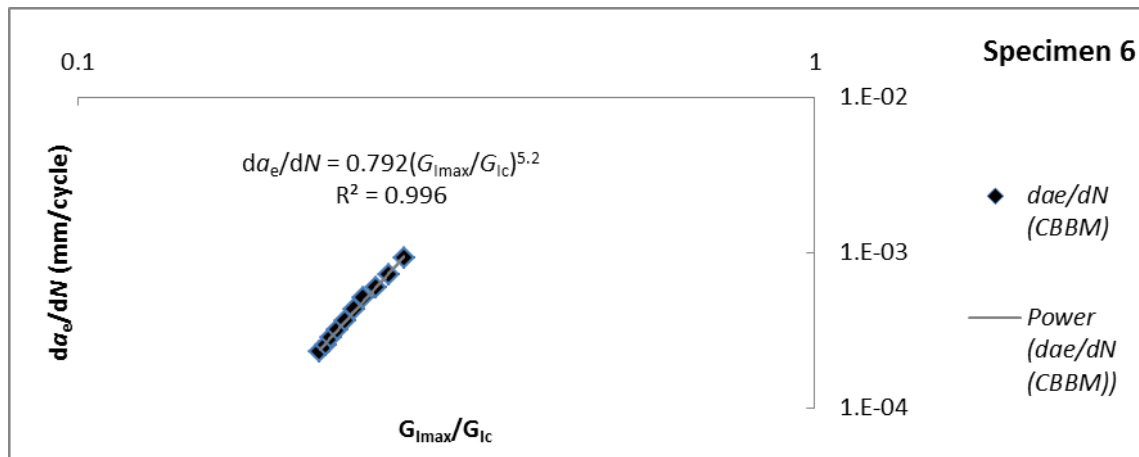


Figure 5.19 - Fatigue crack growth rate as a function of energy ratio  $G_{I\max}/G_c$  considering the BEFM and the CBBM Specimen 6- $h_2$ .

Table 5.8 shows that the values for  $C_1$  and  $m$  are 0.62 mm/cycle and 5.47 respectively, and the CoV (coefficient of variation) is 9% for  $m$  and 19% for  $C_1$ . This means that the procedure used in  $h_2$  specimens is better in registering the moment when the initiation phase ends (threshold).

Table 5.8 - Paris law constants for  $h_1$  specimens.

<i>Specimen</i>	$C_1$ (mm/cycle)	$m$
<u>1</u>	0.526	6.127
<u>2</u>	0.605	5.012
<u>3</u>	0.658	6.065
<u>4</u>	0.459	5.181
<u>5</u>	0.658	5.208
<u>6</u>	0.792	5.248
<b>Average</b>	0.62	5.47
<b>Std. Dev.</b>	0.12	0.49
<b>Scatter</b>	19%	9%

### 5.6.5 Effect of the Adherend Thickness ( $h_1$ and $h_2$ )

From the failure point of view, there is no clear effect of the adherend thickness in the type of failure, which could mean that failure is mostly affected by the manufacturing procedure and not by the thickness itself. Two specimens had intralaminar failure which is probably related to stress concentrations inside induced by a defect in the composite laminate (like a void or misalignment of the fibers).

Considering the threshold, specimens  $h_2$  present lower values than those of  $h_1$ . This shows that the thickness has an effect on how the damage is occurring during the fatigue tests. In fact, the adherend thickness influences the stress distribution [59], leading to a smaller region of the adhesive being loaded which explains the lower threshold values for  $h_2$  relatively to  $h_1$ .

Considering the results, some interesting points have to be pointed out (Figure 5.20):

1. the Paris-law shifts to the left for specimens with lower thickness, implying that the energy needed to propagate the crack is lower. In other words for the same energy level the crack rate is higher (Figure 5.20 - *black arrow*). It is also explained by the fact that FPZ is more confined in the vicinity of the crack tip thus leading to a more critical event;
2. the value of  $m$  is also almost double - for  $h_1$   $m$  is 3.19 while for  $h_2$  it is 5.47. This means that the propagation for  $h_2$  specimens is faster (which is logical from the fact that less energy is needed to propagate).

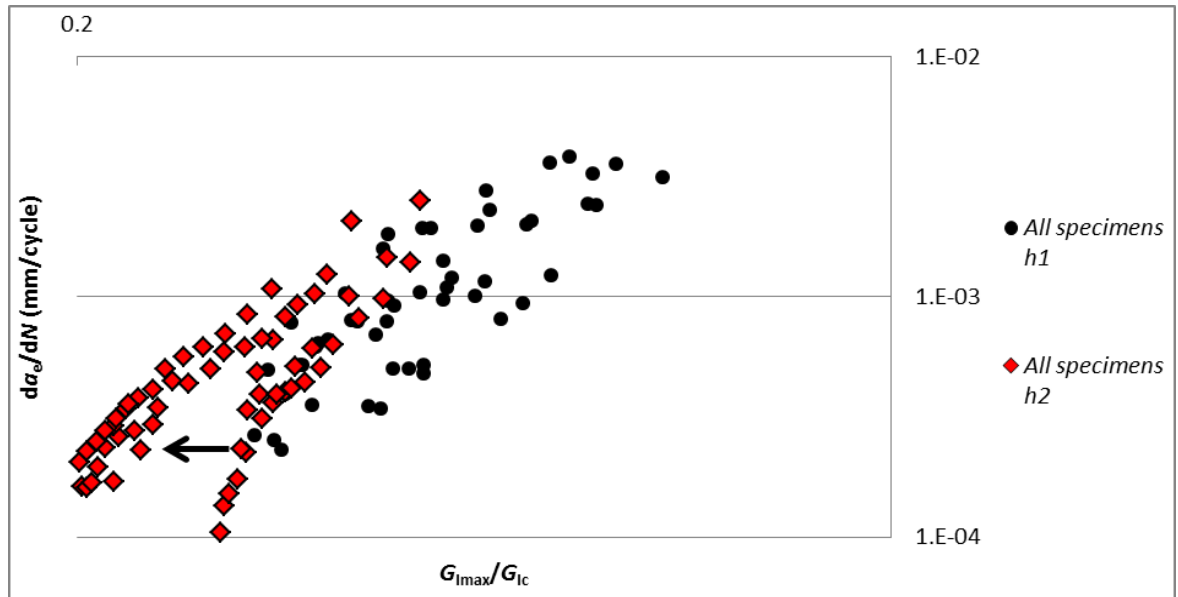


Figure 5.20 – Paris plots for the two thicknesses tested  $h_1$  and  $h_2$  specimens.

These differences could be also related to the tendency of the crack path to go towards the interface. In fact, comparing Figure 5.8 and Figure 5.9,  $h_1$  specimens present a comparable amount of adhesive on both sides (Figure 5.8). On the other hand, for  $h_2$  specimens failure is almost interfacial - one of the sides looks almost like only having the composite. Since the same surface preparation was applied it can be concluded that the more concentrated load in  $h_2$  specimens lead to partial adhesive failure which does not occur in  $h_1$  specimens.

## 5.7 Summary Results

The validation of the CBBM was made by monitoring the crack length and comparing the results with the data acquired (displacement) from the tests. The two thicknesses ( $h_1$  and  $h_2$ ) were used to perform this validation. The methods used for Mode I tests (DCB) allow different ways of calculating the strain energy release rate as a function of crack length, which is a fundamental task to establish a correlation with fatigue crack growth rate. Two classical methods, based on compliance calibration and beam theory, were used to verify the performance of an equivalent crack based method, proposed in this work. It can be concluded that the compliance based beam method gives suitable results and, in case of doubt, the crack can always be measured during the test with more precise and suitable techniques.

A threshold assessment was also made to validate the assumption made before - assessing the threshold as a function of the compliance variation. It was done by comparing the crack initiation moment, with the moment when stiffness start degrading based on one of the cumulative damage theories presented by Zhang et al. [177].



In addition, the Paris-law principle was applied to the linear part of the  $da_e/dN = f(G_{I\max}/G_{Ic})$  plot to validate the procedure. The definition of the material constants ( $C_1$  and  $m$ ), for  $h_1$  and  $h_2$  specimens, was also carried out to understand the influence of the thickness on the threshold and in the propagation rate.

## 6 Mode II

### 6.1 Test Procedure

The specimens made for these tests followed the same manufacturing process of the previous DCB tests. The idea was to present the same conditions and equivalent geometries to assess the different behavior between the two modes. The dimension  $a_0$  was 45 mm,  $L$  was 90 mm,  $h$  was 2.7 mm and the adhesive thickness was 0.2 mm (Figure 6.1). One limitation regarding this configuration is the stable crack propagation. Carlsson et al. [181] have shown that for the End-Notched Flexure test (ENF) the need for a relation  $a_0/L \geq 0.7$  in order to promote stable crack propagation in mode II fracture characterization tests, being  $a_0$  the initial crack length and  $L$  half length of the specimen. In this case, to guarantee enough area to propagate the crack, the relation used here was  $a_0/L = 0.5$ , to try to guarantee that when a crack propagated, it occurred without any spurious influence of the applied load.

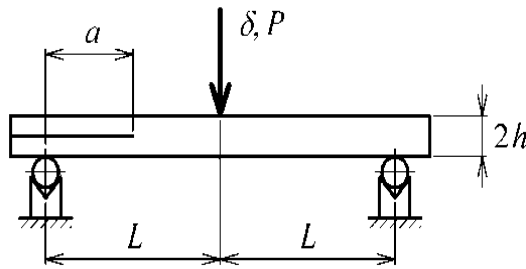


Figure 6.1 - Schematic representation of the ENF test.

The cyclic fatigue loading of the ENF tests (Figure 6.2) was made on a MTS servo-hydraulic machine with a frequency of 4Hz, load ratio ( $R$ ) of 0.1 and with constant load amplitude. The maximum load was 50% of the static failure load, which was defined previously by means of static tests. Considering that monitoring the crack length is labor intensive and inaccurate, a data reduction scheme based on the equivalent crack concept was used and validated.

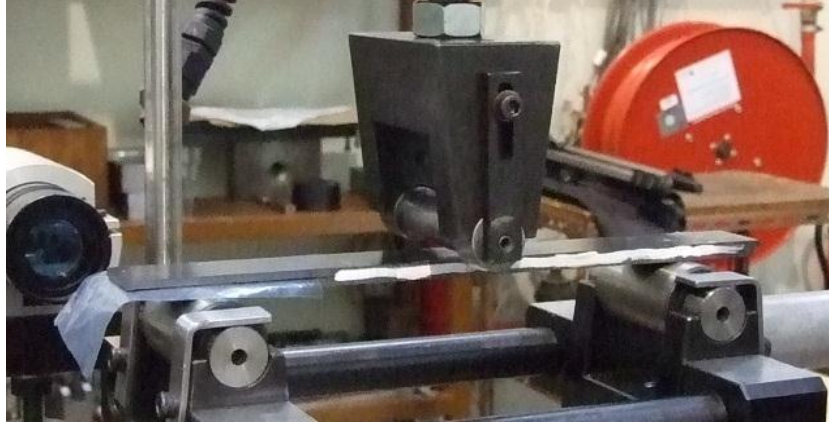


Figure 6.2 - Setup used for the 3-point bending test.

## 6.2 Data Reduction Scheme

The CBBM was also applied in this work considering the ENF test [187]. The main idea was to check the applicability of the principle presented before (for DCB in mode I), to the ENF testing. This means to use the beam theory to obtain the equation that relates the current compliance and the crack length. This equation can be used to estimate the equivalent crack length as a function of the current compliance (equivalent to the one presented for Mode I in Section 5). In addition, the adhesive ductile behavior creates a non-negligible fracture process zone (FPZ) that is responsible for the non-negligible amount of energy dissipation [187], which reflects on the evolution of the damage, i.e., on the specimen compliance. Since the CBBM uses the specimen compliance to estimate the equivalent crack length, it accounts indirectly for the FPZ and avoids the need to monitor the crack length which requires stopping the test.

Following Timoshenko beam theory, the equation of compliance for the ENF becomes

$$C = \frac{3a^3 + 2L^3}{8E_1 B h^3} + \frac{3L}{10G_{13} B h} \quad (6.1)$$

Even in the linear elastic region, this equation does not account for several aspects that influence the load-displacement curve such as the presence of the adhesive and the stress concentration at the crack tip. In order to include these effects indirectly, the known initial crack length ( $a_0$ ) and compliance ( $C_0$ ) can be used to estimate an equivalent modulus

$$E_f = \frac{3a_0^3 + 2L^3}{8Bh^3 C_{0\text{corr}}} \quad (6.2)$$

being

$$C_{0\text{corr}} = C_0 - \frac{3L}{10G_{13}Bh} \quad (6.3)$$

This procedure also takes into account the specificities of each specimen, like variability of the mechanical properties that could be related to the manufacturing process.

During propagation, a damage zone develops ahead of the crack tip, which affects the specimen compliance. To take into account the FPZ, an equivalent crack length must be defined as a function of the current compliance using Equations (6.1) - (6.3).

$$a_e = a + \Delta a_{\text{FPZ}} = \left[ \frac{C_{\text{corr}}}{C_{0\text{corr}}} a_0^3 + \frac{2}{3} \left( \frac{C_{\text{corr}}}{C_{0\text{corr}}} - 1 \right) L^3 \right]^{1/3} \quad (6.4)$$

where

$$C_{\text{corr}} = C - \frac{3L}{10G_{13}Bh} \quad (6.5)$$

Considering the equivalent crack length and equivalent modulus, the strain energy release rate in mode II can now be obtained combining the Irwin-Kies equation

$$G_{\text{II}} = \frac{P^2}{2B} \frac{dC}{da} \quad (6.6)$$

with Equation (6.1),

$$G_{\text{II}} = \frac{9P^2 a_e^2}{16B^2 E_t h^3} \quad (6.7)$$

### 6.3 Static Results

For the evaluation of the failure load, three specimens were tested. The maximum value for the load is around 2000N. Figure 6.3 shows the  $P$ - $\delta$  obtained for the specimens tested statically under mode II.

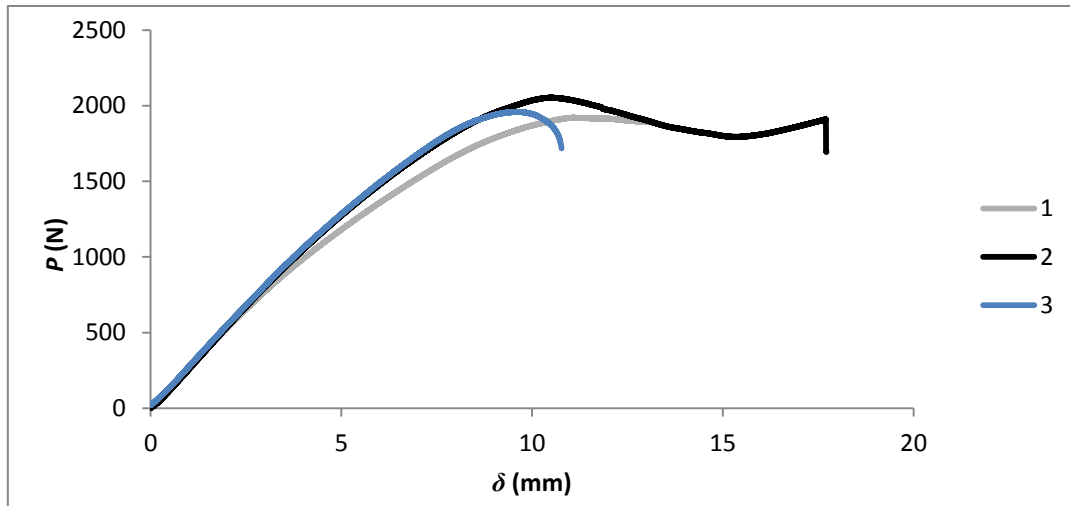


Figure 6.3 -  $P$ - $\delta$  curve for the ENF specimens tested statically.

In this case the values of  $G_{IIC}$  were taken from a previous work where the same adhesive and adherends were used, because the two tests were stopped (specimens 1 and 3) at the initiation, do not allowing any part of the propagation. Figure 6.4 shows the typical R curves obtained by Moura et al. in [120] using the three methods (CCM, CBT and CBBM) described previously. The average value ( $G_{IIC} = 4.67 \text{ N/mm}$ ) was used for this work.

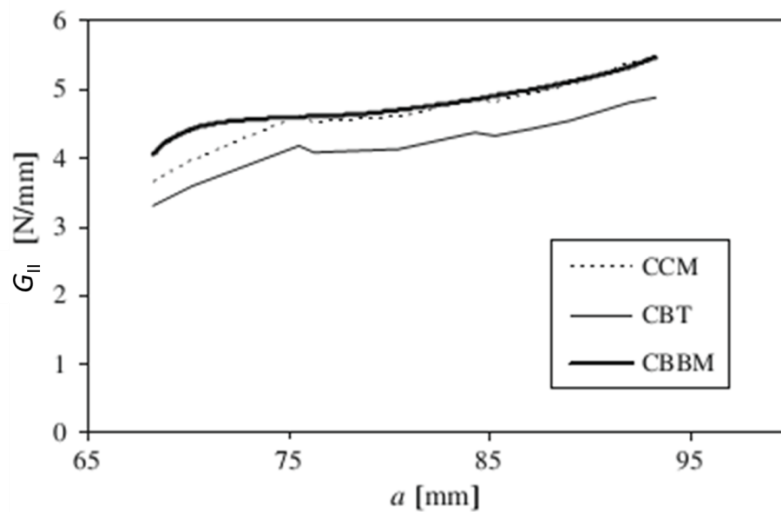


Figure 6.4 – R Curves for  $G_{II}$  obtained with ENF specimens considering the methods described in Section III.5.2 [120]<sup>27</sup>.

## 6.4 Fatigue Results

### 6.4.1 Failure Characterization

Several specimens were tested in fatigue, but only five presented a cohesive failure (Figure 6.5). In these five cases, crack propagation occurred within the adhesive, which allows an

<sup>27</sup> CCM: Compliance Calibrated Method; CBT: Compliance Beam Theory.

adequate characterization of the bonded joint fatigue behavior. The remaining specimens had manufacturing problems like air bubbles or not enough strength of the interface adhesive/adherend as a result of improper surface preparation. The consequence was adhesive or mixed (adhesive and cohesive) failure which obviously affected drastically their fatigue behavior.



Figure 6.5 - Fracture surfaces of a bonded joint with a cohesive failure.

#### 6.4.2 Crack Growth

There is an obvious relation between the compliance and the actual damage of the specimen. From Figure 6.6, it is verified that compliance is constant up to 10000 cycles, after which an increasing trend can be observed. The equivalent crack  $a_e$  versus  $N$  curve shows a similar trend since  $a_e$  is calculated as a function of current compliance, which is influenced by the crack propagation. It should be noted that  $a_e$  is a parameter that evaluates the evolution of damage and not the real crack already opened. In fact, the initial development of the FPZ at the crack tip affects the compliance, which reflects on the increase of  $a_e$ , although a clear crack has not yet propagated from the initial  $a_0$ . In the same figure (Figure 6.6), it is possible to see that the specimen performed around 4000 cycles (approximately between 15000 and 19000 cycles in Figure 6.6) of stable crack propagation, after which the compliance started to remain constant and the crack arrested – third part of the  $a_e = f(N)$  curve which tends to a plateau. This is a spurious effect related to the approximation of the crack to the region influenced by the central loading point. This region is naturally subjected to compressive loads, which hinders a self-similar crack growth. In fact, the FPZ development nearby this region is constrained by the referred compressive effects which reflect on an artificial increase of fracture energy. This

means that the analysis of the results must be stopped at a certain distance of the referred central point in order to avoid spurious overestimations of the bonded joint fatigue behavior.

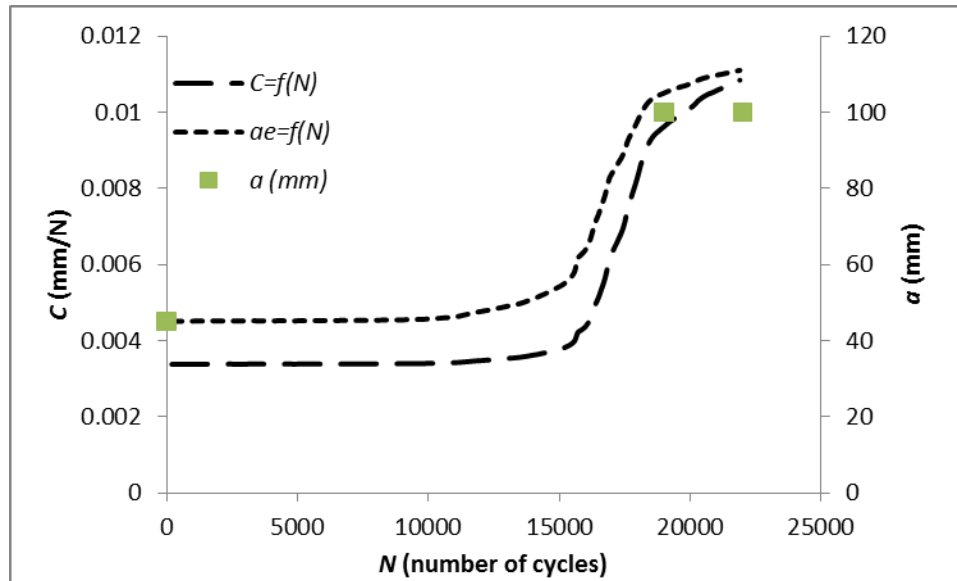


Figure 6.6 - Variation of the compliance ( $C$ ) and the equivalent crack length ( $a_e$ ) as a function of the number of cycles (Specimen 4).

The initial crack length ( $a_0$ ) and the final crack length ( $a_f$  - the moment when the test was stopped) are also marked in Figure 6.6. An intermediate point corresponding to 19,000 cycles is also marked to define a line corresponding to crack arrest. They were measured after testing by opening the specimen to compare the pre-crack and final crack length with the corresponding equivalent values. Table 6.1 presents the results from these measurements for all the tests. On the last specimen the test was stopped some time before the crack arrested, therefore, there is no value associated to the equivalent final crack length ( $a_{ef}$  - crack arrested). Even if the first two specimens presented a length bigger than expected (90 mm) the cause could be that the specimens already suffered compression fatigue, which affects the final crack length.

Table 6.1 – Comparison of the crack length at the beginning and at the end of the test for  $h_1$  specimens.

Specimen	$a_0$ (mm)	$a_e$ (mm)	$a_f$ (mm)	$a_{ef}$ (mm)	
				crack arrested	finished test
<u>1</u>	45	47	100	101	114
<u>2</u>	45	45	100	95	108
<u>3</u>	44	47	89	90	99
<u>4</u>	45	45	95	88	111
<u>5</u>	44.5	45	80		82
<b>Average</b>	<b>44.7</b>	<b>45.8</b>	<b>96</b>	<b>93</b>	<b>108</b>
<b>Std. Dev.</b>	<b>0.45</b>	<b>1.10</b>	<b>8.47</b>	<b>5.48</b>	<b>6.79</b>
<b>CoV</b>	<b>1%</b>	<b>2%</b>	<b>9%</b>	<b>6%</b>	<b>6%</b>

### 6.4.3 Fatigue Threshold

The same methodology used for specimens  $h_1$  was used here.  $G_{th}$  was assumed as being the moment when there is a clear change of slope in the crack propagation curve, Figure 6.7 shows a typical curve, where the threshold represents the point selected in the curve. This correlated the end of the initiation phase and the linear part where crack starts to grow steady with the increase of energy considering a bi-logarithmic representation.

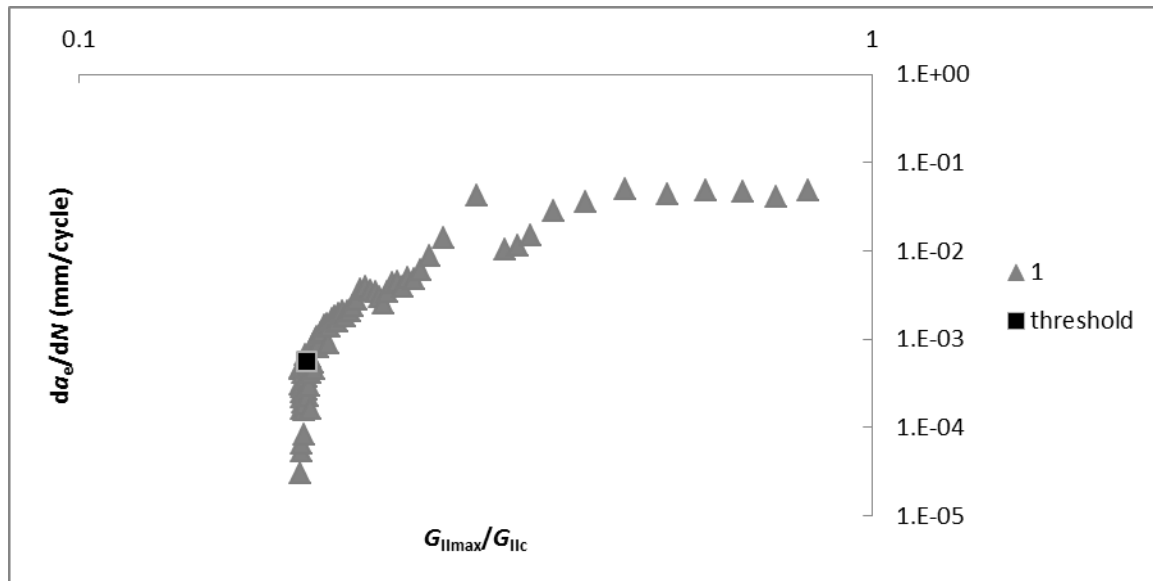
Figure 6.7 – Complete propagation rate curve for specimen 1 with the CBBM to determine  $G_{th}$ .

Table 6.2 presents the  $G_{th}$  and the  $da_e/dN$  for all specimens. The value of  $G_{th}$  has a 5% variation between all the samples. The problem regarding these tests was more related to the rate at which the crack started to grow significantly. In fact,  $da_e/dN$  varies from 5.4E-04 to 8.4E-04 which represents a variation of almost 40%. This can be associated to the instability of the crack propagation, promoting a quicker propagation at the end of the initiation phase. This is related to cumulative damage produced at the initiation and the stress concentrations ahead

of the tip that can make the propagation to occur faster. Finally,  $G_{th}$  is around 18% of  $G_{IIc}$ , which is similar to the values obtained for the mode I samples with the same thickness.

**Table 6.2 – Energy fatigue threshold of ENF specimens.**

<i>Specimen</i>	$G_{thII}$ (N/mm)	$G_{IImax}/G_{IIc}$	$da_e/dN$
<u>1</u>	0.77	16%	5.48E-04
<u>2</u>	0.80	17%	5.26E-04
<u>3</u>	0.79	17%	8.51E-04
<u>4</u>	0.75	16%	6.40E-04
<u>5</u>	0.79	17%	8.08E-04
<b>Average</b>	<b>0.78</b>	<b>18%</b>	<b>6.75E-04</b>
<b>Std. Dev.</b>	<b>0.031</b>	<b>0.007</b>	<b>1.48E-04</b>
<b>CoV</b>	<b>3%</b>	<b>3%</b>	<b>22.0%</b>

#### 6.4.4 Fatigue Crack Growth Rate

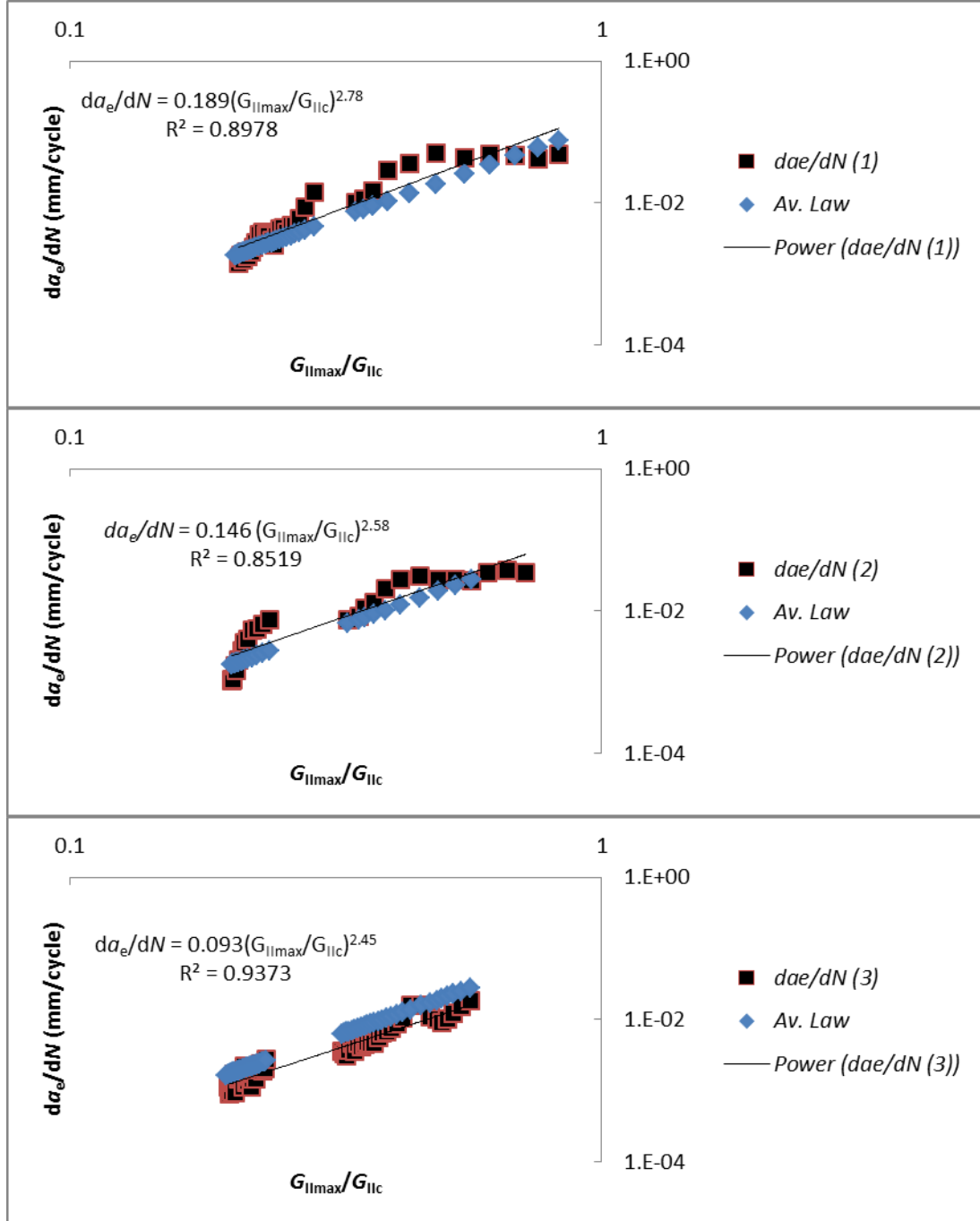
The fatigue crack growth rate ( $da_e/dN$ ) as a function of energy ratio ( $G_{IImax}/G_{IIc}$ ) was determined considering the CBBM described before. Power laws were fitted to establish the corresponding parameters and then a linear representation in a bi-logarithmic scale was used for each specimen. Figure 6.8 shows all the plots obtained. Table 6.3 presents the constants of the Paris law obtained for each specimen that had a cohesive failure and also the resulting average law. From Table 6.3 it can be verified that very consistent results were obtained in which concerns the constant  $m$ . A larger scatter was obtained for parameter  $C_1$  (specimens 3 and 5 have lower  $C_1$  while specimen 5 is around 0.19) which is related to the initiation of the crack, namely its speed at that particular moment. This issue can be explained by the unstable configuration of the ENF test used.

**Table 6.3– Paris law constants of the validated specimens.**

<i>Specimen</i>	$C_1$ (mm/cycle)	$m$
<u>1</u>	0.19	2.78
<u>2</u>	0.15	2.58
<u>3</u>	0.09	2.45
<u>4</u>	0.17	2.86
<u>5</u>	0.06	2.67
<b>Average (Av. Law)</b>	<b>0.13</b>	<b>2.67</b>
<b>Std. Dev.</b>	<b>0.05</b>	<b>0.16</b>
<b>CoV</b>	<b>42%</b>	<b>6%</b>



Finally, an average was determined considering the fatigue parameters, obtained by the plots of all specimens, and applied to the results of each specimen. This was done to verify the accuracy of the procedure (Figure 6.9). It is observed that the average represents, with accuracy, the behavior of the generality of the specimens (Figure 6.8 – Av. Law). It can be concluded that the proposed methodology can successfully define a Paris law representative of the bonded joints behavior under mode II fatigue loading.



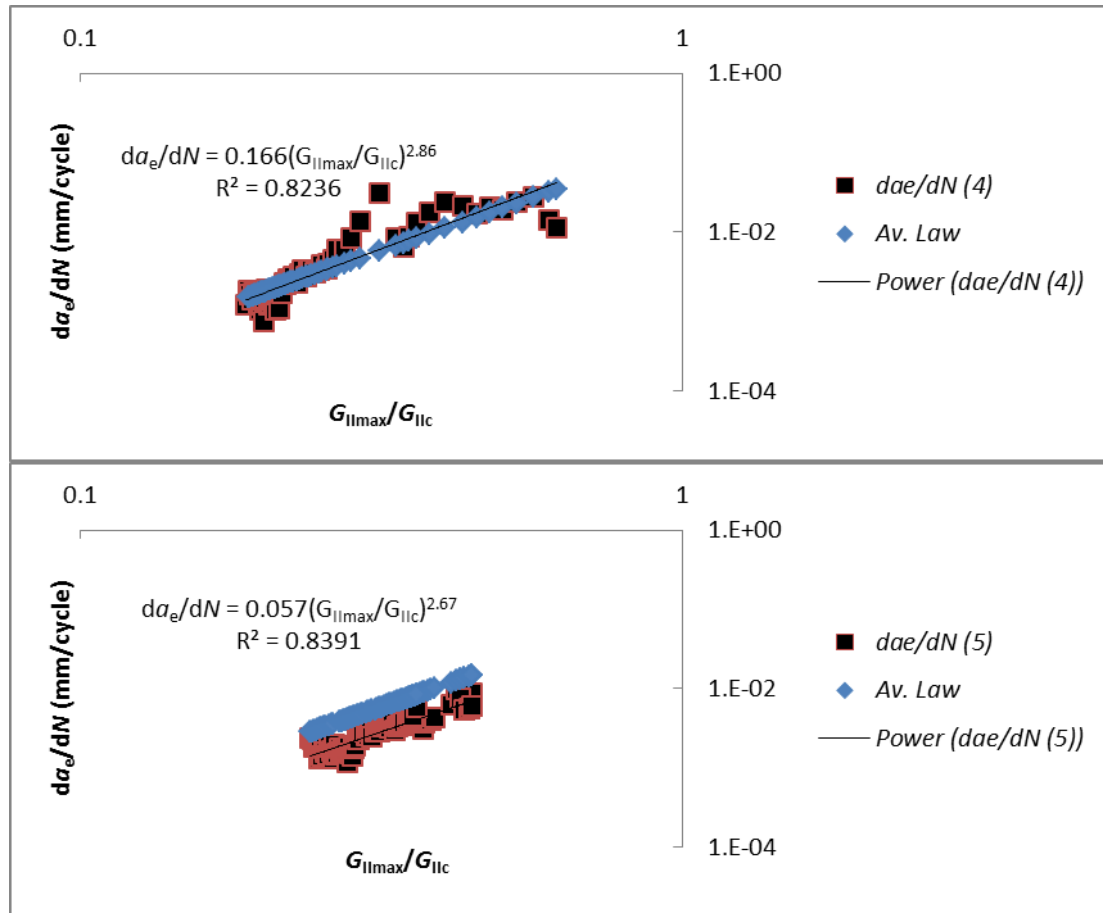


Figure 6.8 – Comparison between the average Paris law with the one obtained for each specimen.

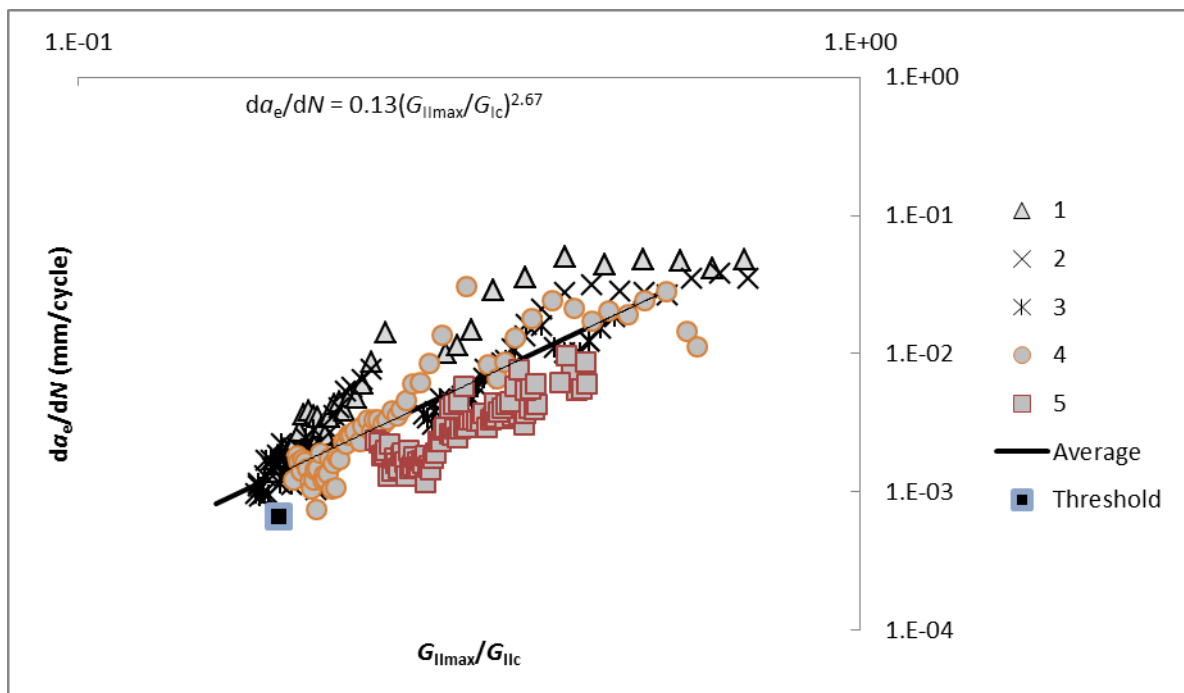


Figure 6.9– Average Paris law adjusted to the results off all specimens.

## 6.5 Summary of the Results

The application of the CBBM allows overcoming some difficulties regarding the crack measurement in these tests. In fact, the comparison between the initial and final crack length ( $a_i$  and  $a_f$ ) with the  $a_e$  was a good suitable solution, guaranteeing the validity of this procedure. It also gave the possibility to address  $G_{th}$ , for Mode II specimens (ENF), accurately. The threshold ( $G_{Ith}$ ) varies less than 5% and it has an average value of 0.78 N/m. The problem is the propagation rate, which varies from  $5 \times 10^{-4}$  to  $8 \times 10^{-4}$  mm/cycle. Looking in detail at the initiation, the instability is also affecting the  $C_1$  constant as it varies almost by 50%. In fact, specimens 3 and 5 have clear different values. For specimen 3, there is a gap between 0.23 and 0.35 while specimen 5 presents a low  $R^2$  value ( $R^2=0.84$ ).

The average obtained from the plot of all valid tests has shown a general good agreement when compared to each tested specimen which reveals the consistency on the results, even with the impact of the unstable crack growth.

## 7 Mixed Mode (I + II)

The SLB presents an excellent compromise between simplicity and equilibrium between the energies dissipated in the two modes. Yoon and Hong [194] showed that for a specimen with equal arm thickness, mode I energy release rate is approximately 57.5% of the total energy, i.e., a mode mixity phase angle  $\psi$  of  $41^\circ$  [194], with  $\psi$  defined by

$$\Psi = \tan^{-1} \left( \frac{G_{II}}{G_I} \right)^{1/2} \quad (7.1)$$

The analysis of fatigue under mixed-mode is important not only because it can be associated to real scenarios, but also because it can promote unstable crack propagation which creates difficulties in the crack rate evaluation [195]. Kenane and Benzeggagh [196] have observed that delamination growth in composite materials under fatigue loading is more stable for low mode ratios which makes possible to correlate the static stability criterion ( $dG/d\alpha < 0$ ) with the linearity of the Paris law results. Szekrényes [182] has analyzed different test configurations for pure and mixed-mode fracture characterization tests on composites. He verified that propagation in monotonic conditions is stable for mode I independently of the geometry. On the other hand, for SLB test, Szekrényes [182] concluded that the relation  $a_0/L > 0.41$  should be satisfied to induce stable crack growth. Since fatigue tests have to take into account the crack stability results from the static tests, the SLB test configuration was defined according to the relationship above. The stability of crack growth and the stable value of mode-mixity during

propagation constitute two remarkable advantages of the SLB test, namely in which concerns the attainment of an appropriate Paris law.

One source of variation is related to failure types. Each type has a different failure working mechanism, which physically reflects on different values of the energy release rate ( $G$ ) as a function of crack length ( $a$ ) and consequently a different behavior of  $da/dN$  [147]. This is analyzed observing failure surfaces after the test is finished.

For this reason, an analysis about the appropriateness and applicability of suitable mixed-mode fatigue/fracture characterization tests is becoming very important.

### 7.1 Test Procedure

The specimen dimensions were defined in accordance with specimens made for mode I and mode II ( $L = 90\text{mm}$ ,  $a_0 = 45\text{mm}$ ,  $B = 25\text{mm}$ ). The bonded surfaces were polished with sandpaper and cleaned with acetone. A 0.2 mm calibrated steel strip was inserted between the two specimen arms to guarantee the adhesive thickness. The next stage was pouring the adhesive, assembling and holding it with pressure. The cure of the adhesive was performed at room temperature for five days. The initial pre-crack was created with a metal strip during the manufacturing of the specimens.

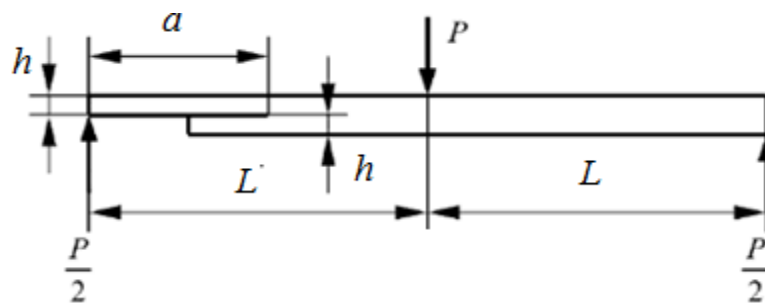


Figure 7.1 – Schematic representation of the SLB test and geometry of the specimens (width B).

The SLB test requires simple experimental equipment [197]. In these tests, the load is applied in the center of the specimen like the End-Notched Flexure tests [198]. Figure 7.1 shows a schematic design of this test. Considering that the purpose of this work was to analyze the applicability of the SLB tests to fatigue/fracture characterization under mixed-mode I+II, two maximum loads were applied. The loads considered were 70% and 50% of the static failure load ( $P_{\max}=360\text{N}$ ), to assess the effect of the maximum load on the crack growth rate. The cyclic fatigue loading of the specimens was carried out on a MTS servohydraulic machine (5 kN load cell), with a frequency of 4Hz, load ratio ( $R$ ) of 0.1 and with constant load amplitude. Figure 7.2 shows the used setup.



Figure 7.2 – Experimental setup of SLB tests under fatigue cyclic loading.

## 7.2 Data Reduction Scheme

The CBBM developed by Oliveira et al. [199] for SLB test was also applied for this case. Using the Timonshenko beam theory, the equation of compliance at the loading point for a crack length  $a$  is [199]

$$C = \frac{7a^3 + 2L^3}{8E_1 Bh^3} + \frac{3(a + 2L)}{20G_{13} Bh} \quad (7.2)$$

The variables are defined in Figure 7.1 and Table 4.1. The initial crack length and the initial compliance can be used in Equation (7.3) to estimate the flexural modulus that will substitute  $E_1$  in Equation (7.2),

$$E_f = \left( C_0 - \frac{3(a_0 + 2L)}{20G_{13} Bh} \right) \frac{7a_0^3 + 2L^3}{8Bh^3} \quad (7.3)$$

This procedure allows accounting indirectly for several specificities that are not included in the beam theory. This is the case of stress concentration in the vicinity of the crack tip, the presence of the adhesive and material variability between different specimens. Equation (7.2) can also be solved in order to get the equivalent crack length during propagation as a function of the current compliance  $C$ , i.e.,  $a_e = f(C)$ . This requires the resolution of a cubic equation which can be easily performed using the Matlab software [199]. By applying the Irwin-Kies equation

$$G_T = \frac{P^2}{2B} \frac{dC}{da} \quad (7.4)$$

the fracture toughness in mixed-mode I+II can be obtained

$$G_T^{SLB} = \frac{21P^2 a_e^2}{16E_f B^2 h^3} + \frac{3P^2}{40G_{13} B^2 h} \quad (7.5)$$

In accordance with Szekrényes [197] the components of strain energy release rate are

$$G_I^{SLB} = \frac{3P^2 a_e^2}{4E_f B^2 h^3} + \frac{3P^2}{40G_{13} B^2 h}; \quad G_{II}^{SLB} = \frac{9P^2 a_e^2}{16E_f B^2 h^3} \quad (7.6)$$

With this procedure the total energy and its components do not depend on crack length measurement during propagation. They depend on the specimen compliance, which is used to estimate an equivalent crack length ( $a_e$ ), hence accounting for the effect of the FPZ, thus constituting an important advantage of this method.

### 7.3 Static Results

For the SLB tests four specimens were tested but only three were taken into account since the fourth presented adhesive failure. In fact these three results were the baseline for the calculation of  $G_T$ , because there was no previous reference available considering this system. In addition the  $P - \delta$  curves (Figure 7.3) were the baseline for the  $P_{max}$  to be used in the fatigue tests.

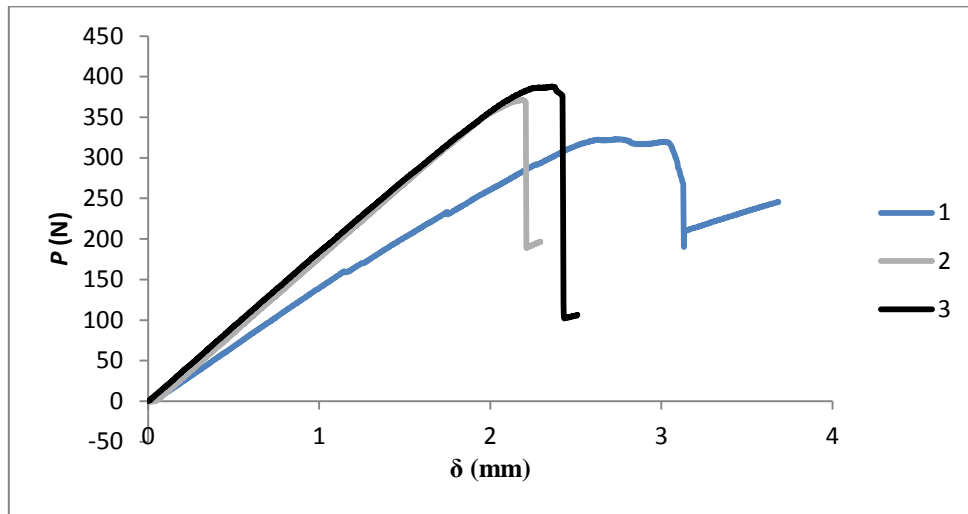


Figure 7.3 -  $P - \delta$  curve for the SLB specimens tested statically.

Figure 7.4 shows the  $R$  curves for the three samples and as a complement, Figure 7.5 shows the relation between the different modes and  $G_T$ . To complete this information, Table 7.1 presents the complete set of values for  $G_{Tc}$  and the corresponding  $G_I$  and  $G_{II}$  values. It also addresses the mixed mode angle ( $\psi$ ) and the % of Mode I.

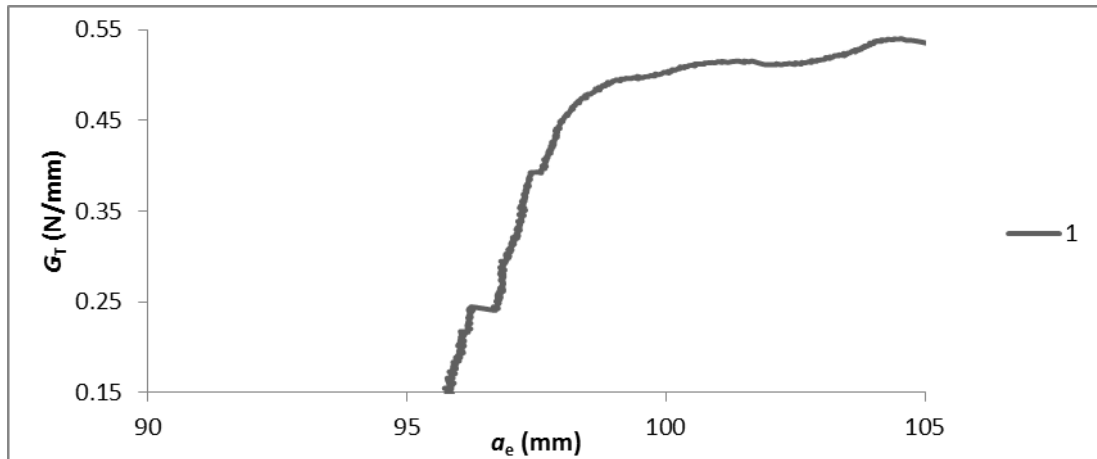
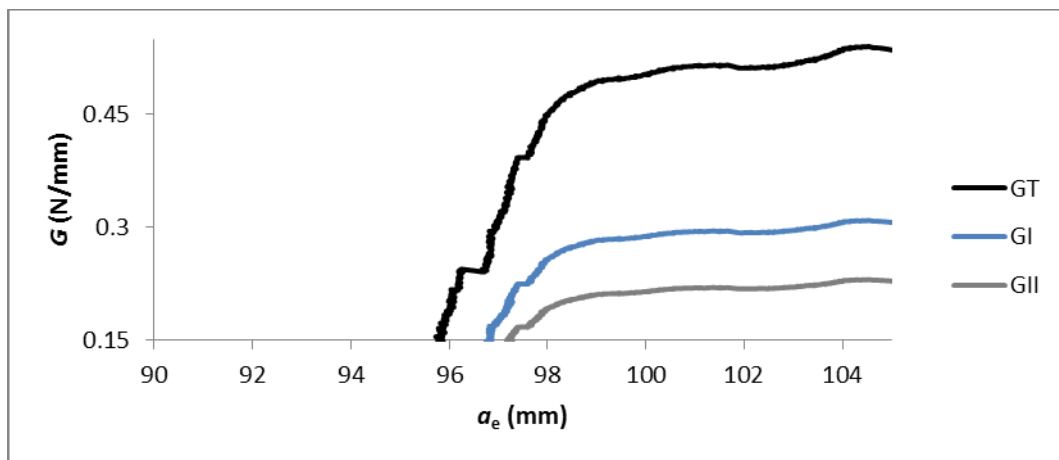
Figure 7.4 - R Curves for  $G_{Tc}$  obtained with SLB specimens.Figure 7.5 - Specimen 1 R Curves for  $G_I$ ,  $G_{II}$  and  $G_T$ .

Table 7.1 – Data obtained from the SLB specimens tested statically.

Specimen	$\delta$ (mm)	$P(N)$	$G_T$ (N/mm)	$G_I$ (N/mm)	$G_{II}$ (N/mm)	$\psi$ (°)	% Mode I
<u>1</u>	3.68	323	0.54	0.31	0.23	45.9	57%
<u>2</u>	2.51	388	0.54	0.31	0.23	45.8	57%
<u>3</u>	2.29	372	0.49	0.28	0.21	45.8	57%
<b>Av.</b>	<b>2.83</b>	<b>360.90</b>	<b>0.52</b>	<b>0.30</b>	<b>0.22</b>	<b>45.9</b>	<b>57%</b>
<b>Std. Dev.</b>	<b>0.75</b>	<b>33.82</b>	<b>0.032</b>	<b>0.017</b>	<b>0.013</b>	<b>0.024</b>	

## 7.4 Fatigue Results

### 7.4.1 Evaluation of the Mixity

The first aspect analyzed was the eventual variation of mode-mixity as the crack grows in the SLB test. Figure 7.6 shows the evolution of the mode mixity phase angle  $\psi$  (Equation (7.1)) as a

function of the equivalent crack length. It was observed that the phase angle is practically constant during the test (a variation between  $40.7^\circ$  and  $40.9^\circ$  was obtained for all the specimens), which confirms the results obtained by other authors in static tests [135], [197]. Also, the evolution of  $G_I$ ,  $G_{II}$  and  $G_T$  is presented in Figure 7.7. The value of  $G_I$  is slightly bigger than  $G_{II}$ , i.e., it corresponds to 57% of  $G_T$ .

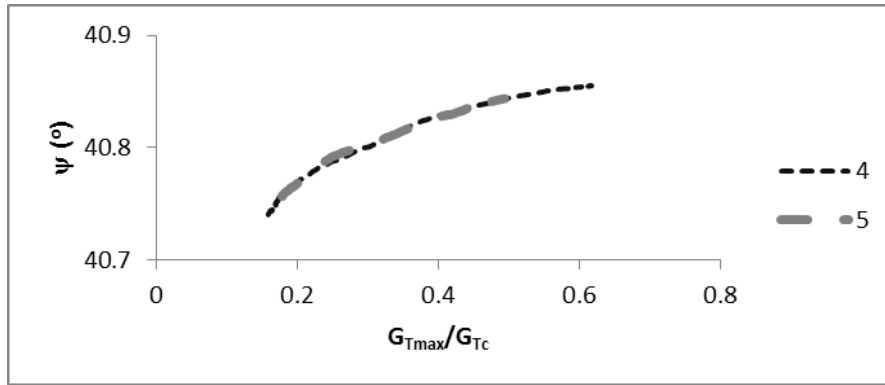


Figure 7.6— Plot of mix ratio as a function of  $G_T/G_{Tc}$  along the test for the specimen 4 and 5 tested with 50% of the static load.

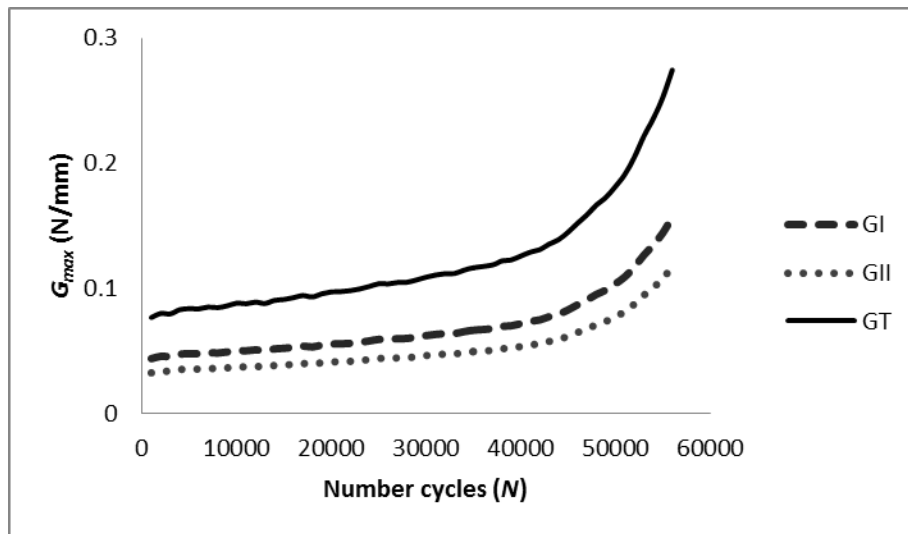


Figure 7.7— Typical evolution of  $G$  along the SLB test for specimen 3.

#### 7.4.2 Failure Characterization and Fracture Surfaces

In all the tested specimens the crack grew towards the interface. The fatigue behavior depends markedly on the maximum load considered. For the 5 specimens tested at 70% of the  $P_{max}$ , only one had cohesive failure. The remaining 4 specimens had delamination problems. This behavior is in agreement with the one observed by Zhang et al. 2010 [200] that observed a deviation of crack path towards the laminate below (small arm). Figure 7.8 a) presents the fracture surface when delamination occurred. The initiation was cohesive inside the adhesive (it was already near the composite surface) but as the crack grew, delamination took place. For



the specimen that had a complete cohesive failure the crack was close to the interface (Figure 7.8 b)). On the other hand, nine specimens were tested at 50% of the  $P_{max}$ : one failed at the interface (adhesive failure), six failed cohesively in the adhesive and two by delamination (similar to the specimens of Figure 7.9). In this case, the cohesive failure was characterized by an initiation zone where the failure looks similar to the fracture zones obtained for Mode II followed by a propagation zone where the surfaces are similar to Mode I fatigue failure (Figure 7.9). This comparison was made with previous works focused on pure modes fatigue/fracture characterization.

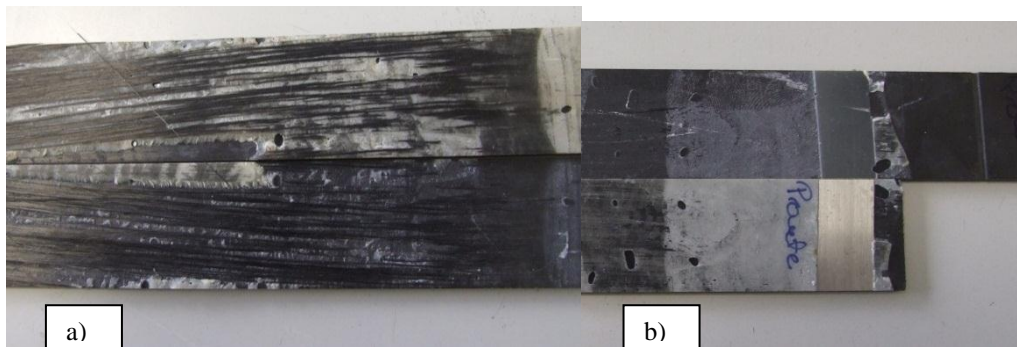


Figure 7.8– Fracture surfaces of the specimens tested with 70% of the load; a) delamination, b) cohesive failure in the adhesive.

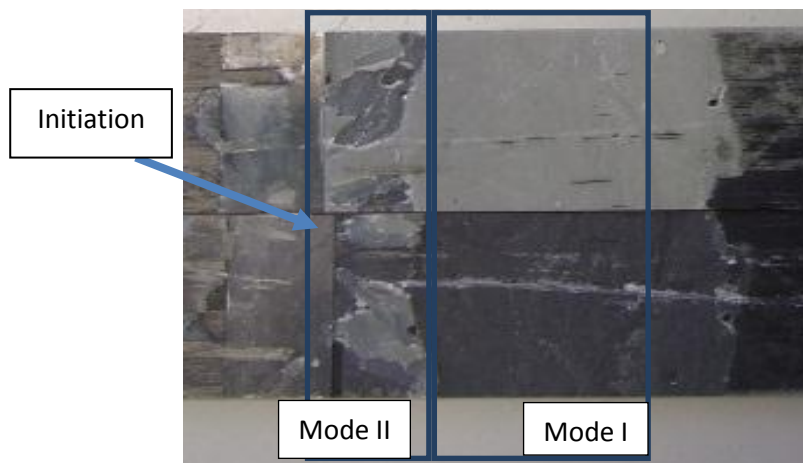


Figure 7.9 – Fracture surfaces of the specimens tested with 50% of  $P_{max}$

#### 7.4.3 Crack Propagation

The tests performed at 70% of the  $P_{max}$  presented an unstable crack growth after initiation. This is clearly visible in the plot of the compliance versus number of cycles ( $C=f(N)$ ) (Figure 7.10). Since the equivalent crack is obtained from the compliance, a similar behavior of  $a_e=f(N)$  can be reported. On the other hand, for the specimens tested at 50% of the  $P_{max}$ , the damage

and crack propagation was stable and a smooth variation of the compliance is visible (Figure 7.11).

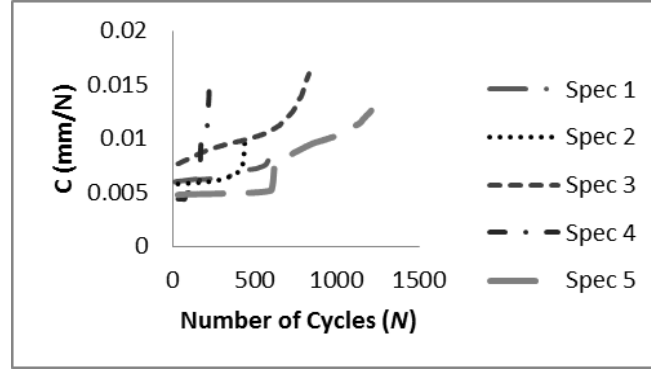


Figure 7.10 – Plot of compliance as a function of the number of cycles (for 70% of  $P_{max}$ ).

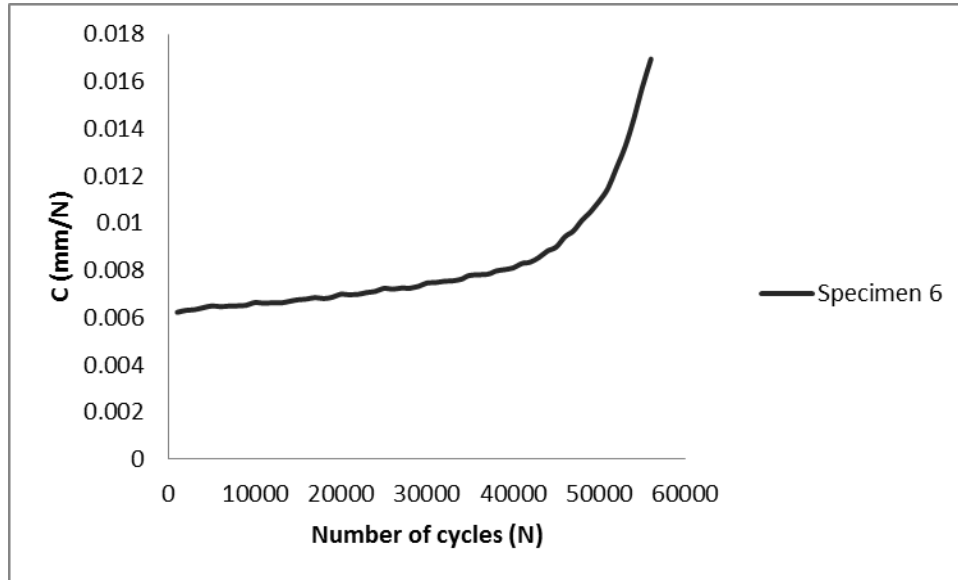


Figure 7.11– Typical compliance (C) versus number of cycles (N) for 50% of  $P_{max}$ .

#### 7.4.4 Fatigue Threshold

The  $G_T$  value (Equation (7.5)) of the threshold ( $G_{T-th}$ ) is the point where propagation rate starts to have a linear growth in a bi-logarithmic representation, i.e., it is the beginning of the second stage (where the Paris law is valid). From the results obtained in this work (Figure 7.12), the  $G_T$  threshold value was obtained for a crack propagation rate of  $10^{-5}$  mm/cycle, because at this value the specimen compliance presented a slight variation corresponding to damage initiation. Table 7.2 presents the values of  $G$  for the threshold. An average value of 0.09 N/mm which is around 17% of  $G_{Tc}$  for this configuration (0.52 N/mm) was found.

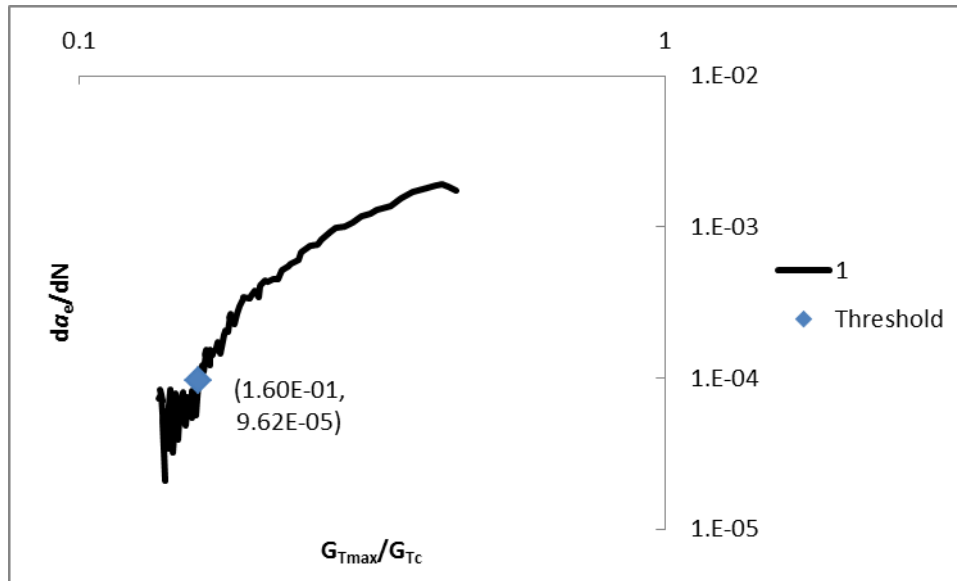


Figure 7.12 – Complete propagation rate for Specimen 1 for 50% of  $P_{max}$ .

Table 7.2– Energy fatigue threshold for SLB Specimens (50% of  $P_{max}$ ).

<i>Specimen</i>	$G_{Tmax} (N/mm)$
<u>1</u>	8.12E-02
<u>2</u>	9.51E-02
<u>3</u>	----
<u>4</u>	8.98E-02
<u>5</u>	----
<u>6</u>	9.09E-02
<b>Av.</b>	8.93E-02
<b>Std. Dev.</b>	5.07E-03
<b>CoV</b>	6%

#### 7.4.5 Paris Law

Owing to the failure mode of the specimens tested at 70% of the failure static load (delamination failure), it can be concluded that this load level does not provide a valuable characterization of bonded joints under mixed-mode loading. Consequently, the Paris law was not obtained for this case.

For specimens tested at 50% of  $P_{max}$ , all of them presented good results (Figure 7.13). The experimental coefficients  $C_1$  and  $m$  are shown in Table 7.3;  $C_1$  varies roughly from 0.029 to 0.044 mm/cycle and  $m$  from 2.9 to 3.1, which leads to a Coefficient of Variation (CoV) of 14% and 2%, respectively. The higher scatter of  $C_1$  can be explained by the fact that this parameter depends also on the damage initiation instant, which is influenced by the pre-crack fabrication.

The correlation coefficient is bigger than 0.9 (Figure 7.14) for the linear region where the Paris law was applied. A general law was defined by using the average values of the specimens (Table 7.3 and Figure 7.13). The correlation between it and the experimental curves shows good agreement (Figure 7.13), i.e., the average law lies in between the specimen's laws. Also, Figure 7.14 show how coincident this law is when compared with the  $da_e/dN$  of each specimen.

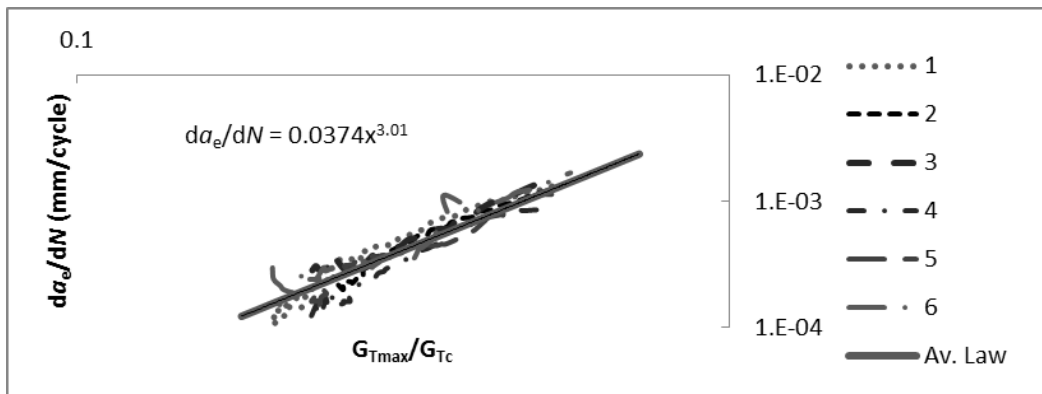
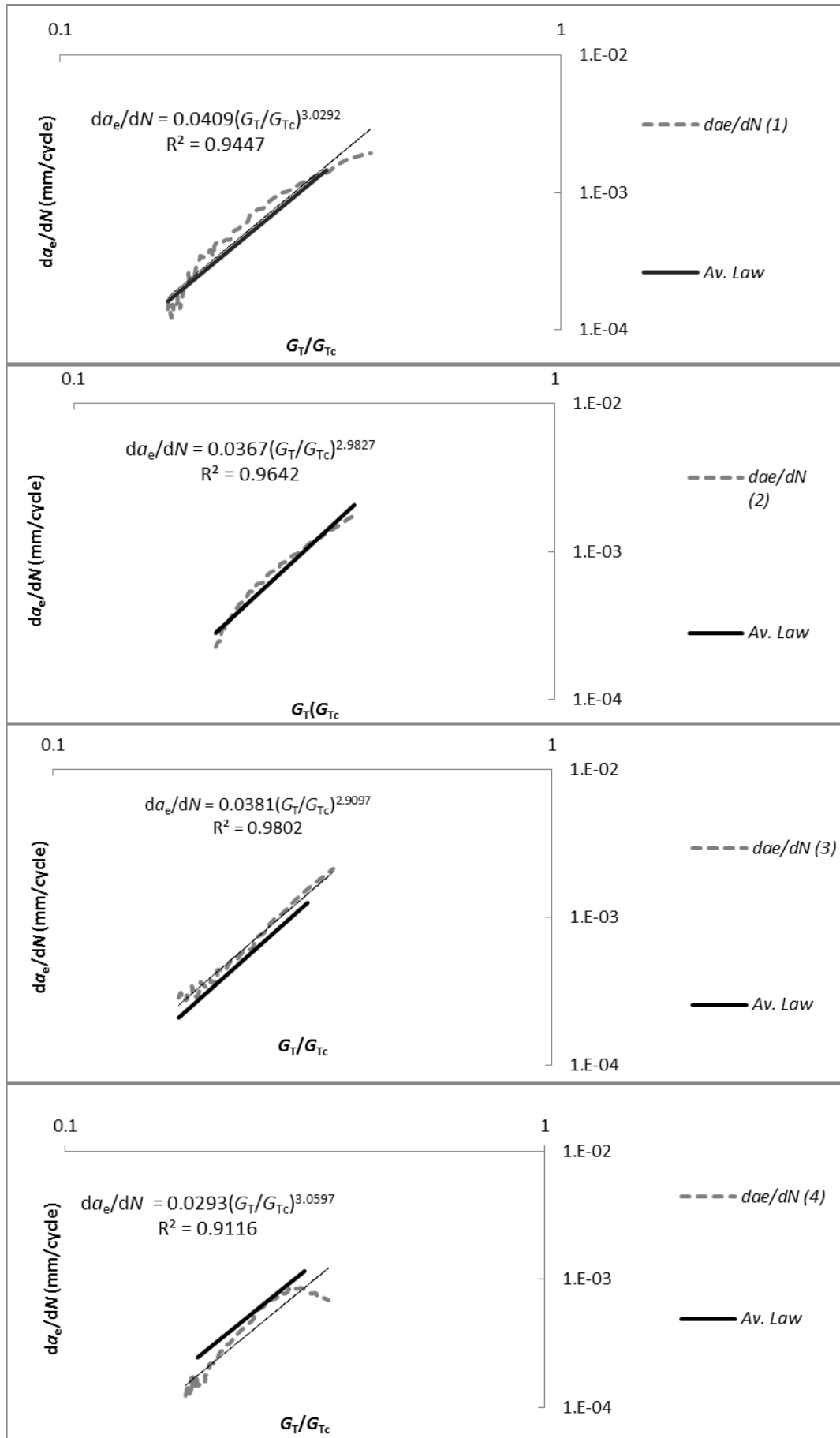


Figure 7.13 – Stable crack growth (linear region) of the six specimens tested at 50% of  $P_{max}$  and the respective average law.

Table 7.3 – Paris law constants of the validated specimens tested at 50% of  $P_{max}$ .

Specimen	$C_1$ (mm/cycle)	$M$
<u>1</u>	0.0409	3.0292
<u>2</u>	0.0367	2.9827
<u>3</u>	0.0381	2.9097
<u>4</u>	0.0293	3.0597
<u>5</u>	0.0354	3.0136
<u>6</u>	0.0441	3.0833
<b>Av.</b>	<b>0.037</b>	<b>3.013</b>
<b>Std. Dev</b>	<b>0.005</b>	<b>0.062</b>
<b>CoV</b>	<b>14%</b>	<b>2%</b>



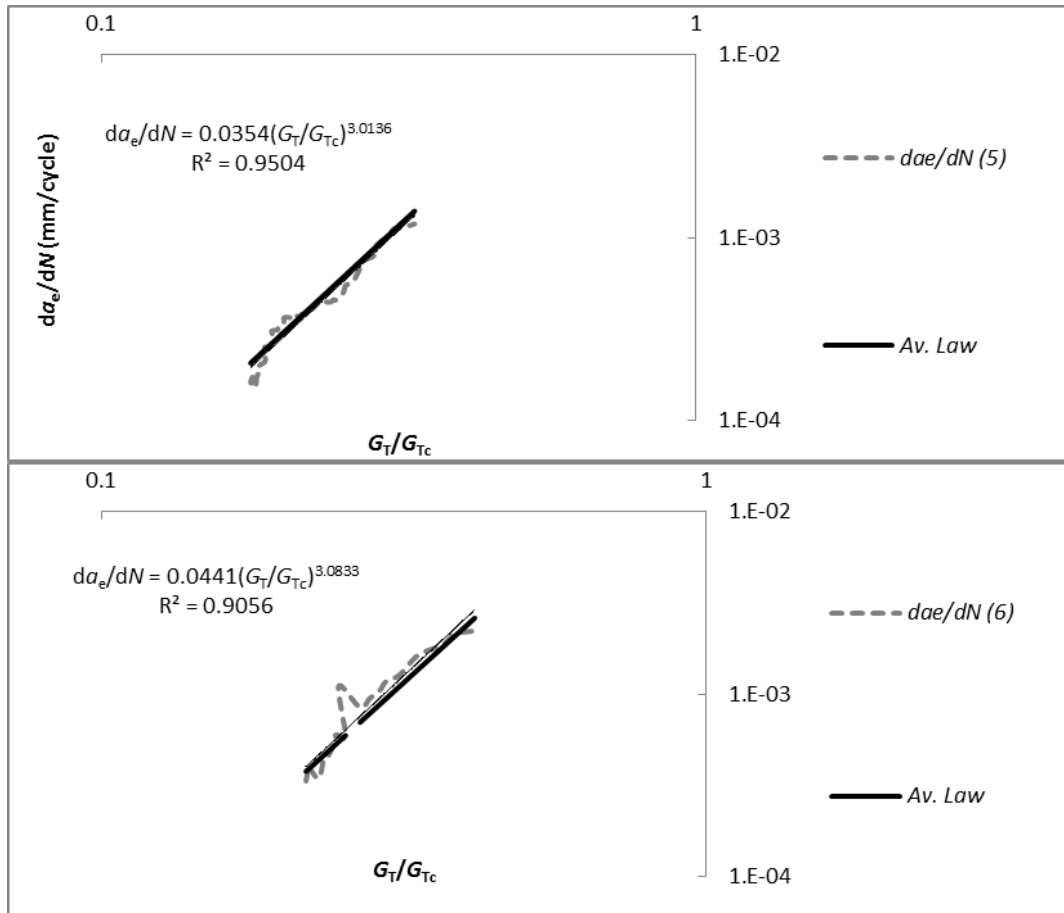


Figure 7.14 – Paris law and verification of the general law for each specimen at 50% of  $P_{max}$ .

#### 7.4.6 Mixed-Mode Correlation for the Paris Law

Finally, an evaluation of the Paris law parameters as a function of the loading mode was performed considering previous results of mode I and mode II. It was found that the propagation rate changes with the type of load (Figure 7.15). The crack propagation rate for mode I specimen is much higher than for mode II and mixed-mode I+II ( $\varphi \approx 41^\circ$ ), which present both similar values. It can be concluded that the presence of mode II loading is beneficial concerning this aspect, since it contributes to delay the final collapse under fatigue loading.

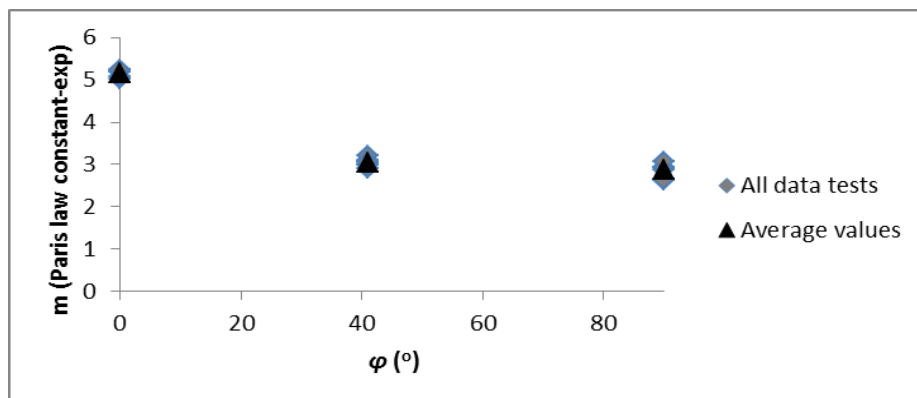


Figure 7.15 – Paris-law  $m$  parameter as a function of the mixity.

Figure 7.16 shows all the points obtained for the three types of tests (Mode I – DCB, Mode II – ENF and Mode I + II – SLB) which clearly show that the threshold ( $G_{th}$ ) and the propagation rate ( $da_e/dN$ ) for the initiation are almost coincident. This means that the relative value for  $G$  is almost similar independently from the mode or the propagation rate. Only one Mode I specimen (specimen 6) had a slight different behavior.

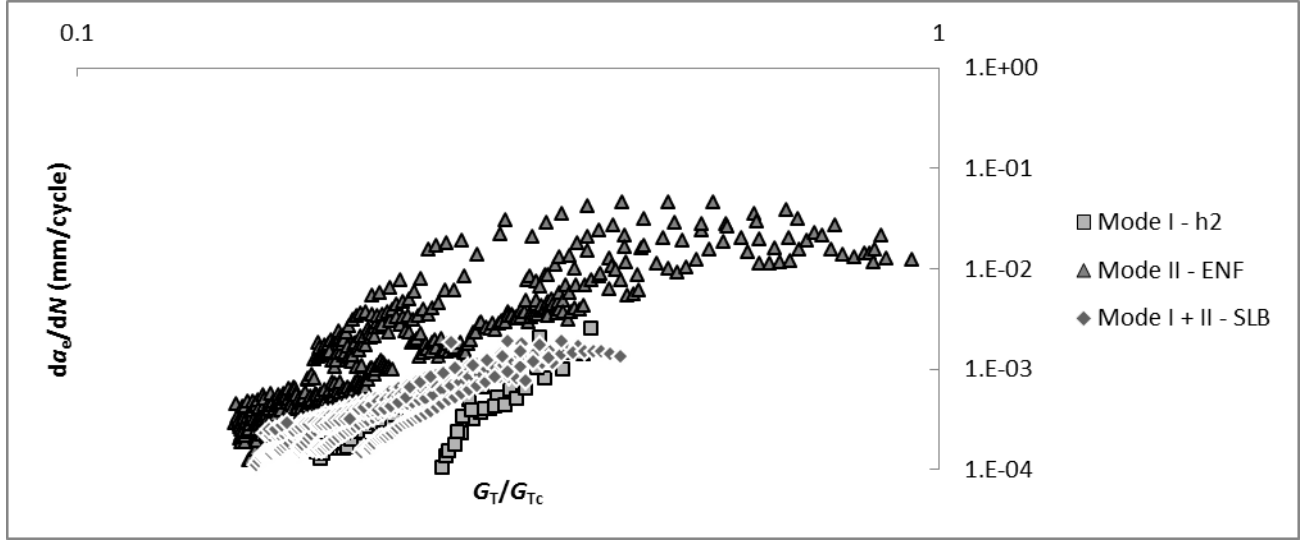


Figure 7.16 – Crack propagation curves for all the samples tested with the equivalent geometry ( $h=2.7$  mm).

### 7.5 Single lap joint Tests

The configuration tested is presented in Figure 7.17 where  $l$  is the overlap length (70 mm),  $B$  is the width (25 mm),  $t$  is the arm thickness (2.7 mm) and  $l_1$  the length outside the overlap (60 mm). Two cameras were placed to control the crack propagation length (Figure 7.18).

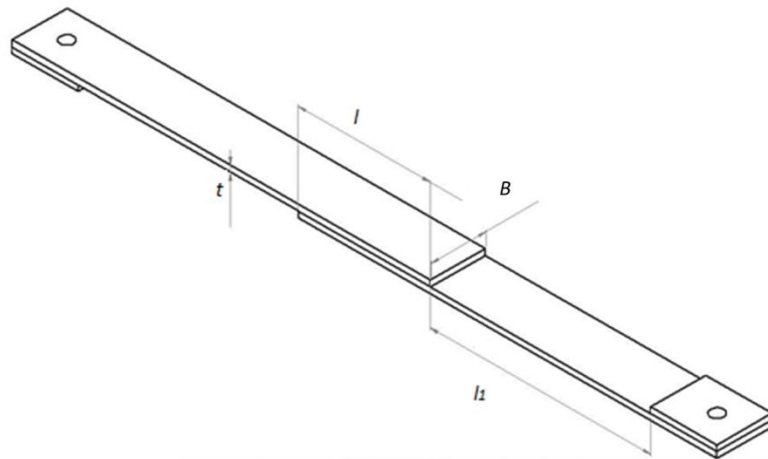


Figure 7.17 – Schematic representation of the SLJ tested.



Figure 7.18 – Setup used SLJ test.

#### 7.5.1 Experimental Results

These tests were performed at 50% of the  $P_{max}$ . In this case only 5 specimens were tested, two in static and three in fatigue loading, also with  $R=0.1$ . It was verified that abrupt failures occurred which impeded the monitoring of crack length in terms of stable crack propagation. Several points were registered, but the abrupt propagation did not allow registering enough points. Figure 7.19 and Figure 7.20 shows how the failure occurred, in Figure 7.19 is visible that at 1000 cycles there was no damage and at 2000 cycles the crack had already propagated around 10 mm in both sides.

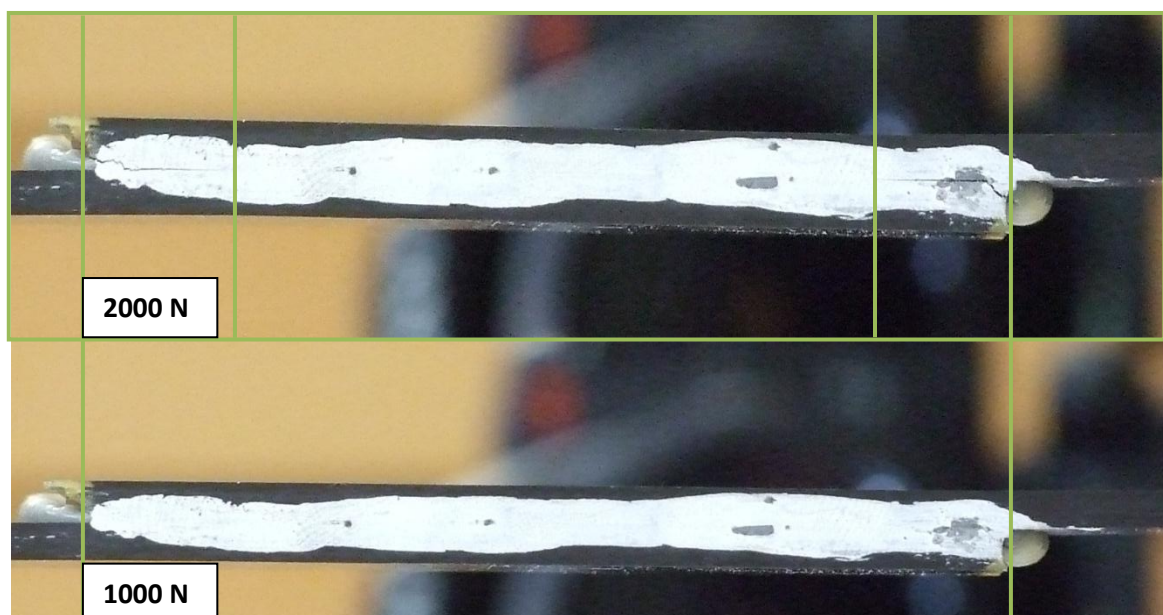


Figure 7.19 – Single lap joint tested (specimen 3): at 1000N and at 2000 N.



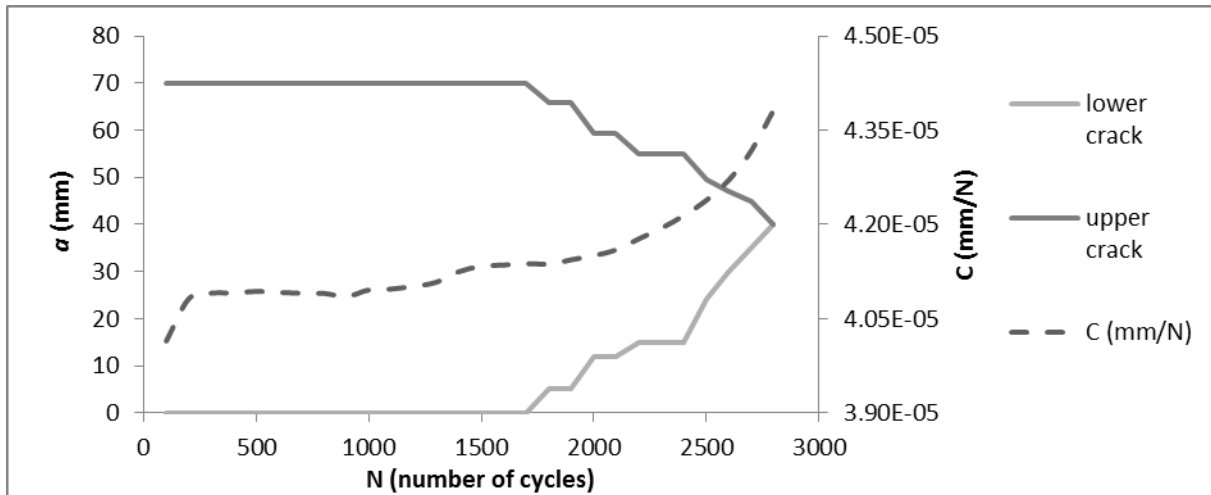


Figure 7.20 – Crack propagation as a number of cycles and the variation of the compliance.

The evolution of the crack presents a clear non-linear development. The crack starts to grow visibly at around 1700 cycles with 5 mm (on each side). At 2000 cycles, it is already 10 mm (on each side) and at 2500 it reaches around 20 mm. Finally the specimen failed at 2800 cycles. In fact, single lap joints are probably not the best method to characterize the crack propagation, since stress concentrations do not allow stable crack propagation. Figure 7.21 presents a typical failure surface for these tests. The tendency of crack monitoring towards the interface is also present here, as the ultimate failure also occurs in the laminate.



Figure 7.21 – Typical failure surface a SLJ tested.

## 7.6 Summary of the Results

In terms of the mixed mode, the SLB test was applied to fatigue/fracture characterization of composite bonded joints under mixed-mode (I+II) loading. It was verified that the test

performed well, i.e., it favors stable crack growth when the maximum load is 50% of the failure static load. For a maximum load of 70% of  $P_{\max}$ , the propagation is unstable making the Paris-law not valid in this region.

For the application of the Paris-law, very consistent results with low scatter have been obtained for SLB tests (mixed-mode). When comparing the loading modes, it was also observed that the  $m$  parameter is clearly affected by the type of loading, which reinforces the importance to design in shear; this is a way to sustain the life of the joint. Thus, it was concluded that the presence of a mode II component has a beneficial effect on bonded joints fatigue life.

Also, the threshold defined here as *“the point where the compliance starts to vary significantly or the energy release rate”* (since both points are directly related in the CBBM) can be considered valid for these results. Even if the actual energy is not the same ( $G_{Ith}=0.081$  N/mm,  $G_{IIth}=0.77$  N/mm and  $G_{(I + II)th}=0.089$  N/mm), the adhesive present the same trend in all conditions. In fact the  $G_{th}/G_c$  is similar in the specimens tested at the same conditions with equivalent geometry. A difference is present only for different thickness (Section 5.6.5 Effect of the Adherend Thickness), varying from 30%, for the thicker specimens, to 20% for the thinner. Still, this point should be taken into account when designing fatigue resistant joints to prevent a premature failure.

It was verified that SLJs do not allow a clear control for the fatigue characterization due to stress concentrations. Configurations like the SLB can present a better option for preliminary testing while final tests can be performed on the designed joints. The application of tests like SLB present the advantage of the specimen simplicity and controlled stress concentrations, leaving the efforts of the designer to define better testing solutions for the final geometry of the joint.

## 8 Perceived Value

Studying the fatigue behavior in detail can give more information regarding how the load is transferred between the adhesive and the adherend under fatigue conditions. In general, the results obtained in terms of crack length and FPZ are just preliminary results that address the importance of this subject.

In this work the most important points addressed are:

- the validation of an equivalent crack method (CBBM) to assess the joints' fatigue behavior;
- the assessment of the FPZ that is taken into account

- in the proposed method;
- the evaluation of a suitable criteria to define the threshold as a function of damage;
- the effect of the adherend thickness in Mode I testing;
- the applicability of the Paris-law for the different modes;
- the effect of the  $P_{max}$  in Mixed-mode testing;
- and the suitability of SLJ tests for fatigue analyses.

The importance of the CBBM is based on the possibility of overcoming some test limitations like:

- the laborious task regarding crack measurements and monitoring while testing;
- the susceptibility to reading errors;
- the limitation associated to test fidelity considering fatigue effect and the fact that the machine has to be on pause to measure the crack length;
- finally, this method accounts for the energy being dissipated in the FPZ, which in the case of ductile adhesives is significant. This is an important issue since it means that this method replicates better the real state of the specimens during the fatigue tests.



## **IV. Concluding Remarks**

The objective of this thesis is to give an overview of how composite bonded joints behave under fatigue loading. Additionally, interrelations between the structure and the technology related with bonded joints fabrication is also analyzed in the present work. In general, the proposed relations drawn here were made to create a reliable basis for future work in any horizontal or vertical project involving bonded technology. The referred relations can also help to define the Product Life Cycle of a structure taking into consideration its joints. The principal outcomes issuing from the two main topics addressed in this work are summarized below.

### **1 Case Study**

The two products addressed here (wind blades and aircrafts) represent two of the most prominent applications for bonded technology regarding composite materials. In fact, blades were chosen because it is a fully bonded structure. In addition, the developments made with the research in this field represent an opportunity to understand and investigate towards having a mature technology.

In general, the case study, with the wind blade manufacturing industry, was an opportunity to learn and understand more about how the joints are manufactured and to work towards a successful process development to guarantee an accurate design with lower costs. These achievements are also important for the aircraft industry because one of its main motivations is to adopt bonding technology to diminish the costs (at least the recurrent costs). In fact, several research programs in the aircraft industry try to achieve the expected results, which are mainly based on a commitment between performance and manufacturing costs.

The experience with the case study has shown that is very important to understand that the bonding process needs to be controlled closely. To have a successful project with implementation in the industry, this part is essential. If something is forgotten or changed, the outcome can be completely different and unexpected. The surface treatment and the choice of the peel-ply shall be tested prior to any tentative of defining mechanical properties. It is very important to avoid any contamination problems and by consequence, avoid any cause that reduces the capability to withstand the load.

Concerning the costs, it was verified in the case study that several parameters have to be taken into account, like the equipment used to apply the adhesive, the adhesive used and its quantity. It has been shown here that these parameters affect the cost of a process by 10%.

One of the major outcomes of the work performed in this thesis was the demonstration that costs can be reduced by focusing on the stabilization of the process. Defining ways of working and good manners are essential to validate an adequate manufacture process.

## 2 Performance

Another main topic of this work was to understand how the joints behave under fatigue loading. In this context, fatigue/fracture characterization of bonded joints under mode I, mode II and mixed-mode I+II loading was performed. The DCB and ENF tests were used for pure mode I and pure mode II loading, respectively and the SLB test was used for mixed mode I + II. A data reduction scheme (CBBM) based on crack equivalent concept, beam theory and specimen compliance was proposed and used with remarkable advantages. In fact, the method allows accounting indirectly for the presence of the adhesive stress concentrations and non-negligible fracture process zones (typical of ductile adhesives) that influence the specimen compliance. Additionally, when applying the CBBM, it is not necessary to monitor the crack length during the course of the test which simplifies the procedure namely in tests like ENF and SLB, where the crack monitoring is complicated. On the other hand, it also improves the quality of the results when applied with an automatic system to acquire the data, making the test steadier and lowering the scatter. Also, it was a baseline to define the threshold and it helps to proof that the variation compliance can be associated to the threshold. This is probably only applicable to composite materials, because there is no plasticization zone, still it can be helpful for hybrid structures.

## 3 Final Conclusions and Future Work

In summary, the multi-subject research was performed to investigate the impact of the manufacturing process and assessing the mechanical behavior under fatigue loading on the designed joint. Some main conclusions were drawn:

- The process needs to be controlled closely to guarantee the proper behavior and the mechanical performance of the joints. The working temperature,  $T_g$  and all other variables shall be considered for this purpose.
- There is a clear relation between the manufacturing process and the mechanical behavior, which is highly dependent of the surface treatment. It affects how the load is transferred to the joint. In this work, three specimens for mode II failed adhesively at the initiation phase which only lasted around 500 cycles, failing abruptly. Actually, these specimens were not accounted at all, because this is not a valid failure mode.

However, it should be noted that adhesive failure has been addressed by several other authors for static samples and it has been proven consistent for fatigue behavior.

- The fatigue behavior is affected by the type of loading and it depends where the crack is propagating. In fact, different failure modes imply different behaviors. The tests carried out here have shown that samples loaded in mode I have higher propagation rates when compared to mode II and mixed-mode I + II for the same geometry. In other words, different load angles give different propagations rates, which are then translated in different time in service (considered as the time a structure is planned to be used). In general, this was addressed as the effect of the loading mode.
- As a consequence of the previous point, it can be concluded that mode I loading should be avoided in the fatigue joints design. The results of this study showed that keeping the mixed mode angle between  $41^\circ$  (SLB) and close to  $90^\circ$  (ENF) may be preferred. On the other hand, the advantage of not having high values of mode II can be addressed in terms of unstable crack propagation, which is a problem for any structure. The major problem is related to the difficulty to define when the maintenance has to be done or when the inspection shall be performed.
- In general, all the characterization of composite bonded joints under fatigue loading was a success considering the advantages presented by the proposed equivalent crack method and the assessment of the threshold. In fact, the DCB, ENF and SLB have been effective in defining the threshold energy ( $G_{th}$ ), under mode I, II and mixed-mode I+II, respectively. Similar comments can be made about the determination of the Paris-law for the different modes. A special remark should be done about the consistent trends which are very difficult to reach for these fatigue characterization tests.
- It is also important to notice that this type of tests define periods in between inspections and these periods have to account for the defects, as they cannot be completely avoided. For that reason, mode I Paris law constants shall be determined and used in fatigue design, since this procedure can give a large margin in assessing the life in service.
- Finally, in terms of adherend thicknesses, the probability of having a defect on the laminate gets higher with the increase of thickness (as shown for the thicker laminate in mode I). In that case special attention has to be paid because the amount of the specimens failing in the laminate can be higher. In addition, as this affects the propagation rate (make it slower), a misleading constant can be obtained if special attention is not paid to the failure mode (with much longer life than expected).

Several points have been studied in detail aiming the improvement of composite bonded joints. The present work represents a contribution to the state of the art on fatigue characterization of composite bonded joints. The work presented here represents an open door for future development and improvement. Future developments can be:

- Research about the impact of the manufacturing process in the fatigue behavior: co-cured, co-bonded and secondary bonded.
- Research the effect of enhanced surfaces (due to special surface treatments, i.e., plasma) in the performance and their applicability in industry.
- How to enhance the interface properties to improve also the behavior, in a way that there is no damage of the laminate when a joint fails.
- Analysis regarding the effect of the adherend thickness in the fatigue behavior:
  - Scanning Electron Microscope (SEM) analysis to see the difference between both thicknesses. This can give the first idea on how the actual failure is happening;
  - Testing different geometries to be able to relate the thickness and the propagation rate; and make Mode II and Mixed mode tests (I + II) to understand the differences as well. This is particularly important because mixed mode is a closer state to the working structures.
- Understand in detail the influence of the adherend compliance:
  - on the stress distribution during fatigue tests to create designs with better fatigue resistance;
  - the impact of the changes in the lay-up as, a source of stiffness variation, but also failure mode.
- Assessment of the Mode II crack stability behavior:
  - by performing other types of tests (like four point bending);
  - study the suitability of the  $dG/da$  criteria for stable crack propagation with fatigue loading. This can be an opportunity to address damage tolerant behavior on the configuration by allowing smooth propagation and inspection intervals.
- Studying several mixed mode angle tests (like Mixed Mode Bending) to get more general design laws, thus providing suitable inspection periods and threshold criteria for the structures.
- Tests on supported SLJ, (Figure 3.1), to assess the fatigue behavior with a configuration used as a standard in the aeronautical industry. In addition, the stress concentration profile of this configuration is more constant, which can make easier to analyze the fatigue phenomena during the tests.



- Creation of prediction tools by defining damage laws and finite element methods (like cohesive elements under fatigue):
  - develop a prediction model taking into account the interaction of the different modes;
  - define a fatigue envelop in terms of loading ratio and maximum load to create a parametric system to predict the mechanical behavior under fatigue loading;
  - apply VCCT fatigue crack growth method to the results to try to predict the fatigue behavior of different specimens or geometries;
  - develop a damage law to be used with cohesive elements.

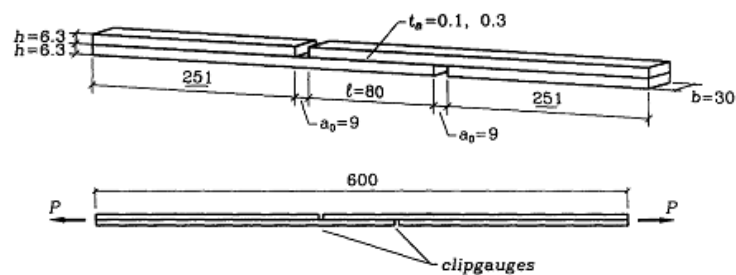


Figure 3.1 – Supported single lap joint configuration (dimensions in mm) [193].



## V. References

- [1] M. Hojo, T. Ando, M. Tanaka, T. Adachi, S. Ochiai, and Y. Endo, "Modes I and II interlaminar fracture toughness and fatigue delamination of CF/epoxy laminates with self-same epoxy interleaf," *International Journal of Fatigue*, vol. 28, no. 10, pp. 1154–1165, 2006.
- [2] G. Gardiner, "A350 XWB Update: Smart Manufacturing: Composites World," *High Performance Composite*, 09-Jan-2011. [Online]. Available: <http://www.compositesworld.com/articles/a350-xwb-update-smart-manufacturing>. [Accessed: 09-Nov-2011].
- [3] "Eurofighter Typhoon," *Eurofighter*, Oct-2012. [Online]. Available: <http://www.eurofighter.com/>.
- [4] "Boeing: Commercial Airplanes - 787 Home." [Online]. Available: <http://www.boeing.com/commercial/787family/>. [Accessed: 30-Aug-2012].
- [5] "Qantas A380 | Enjoy the journey." [Online]. Available: <http://www.qantas.com.au/travel/airlines/a380/global/en>. [Accessed: 30-Aug-2012].
- [6] P. Brondsted, J. W. Holmes, and B. F. Sorensen, "Reliability of Wind Turbine Blades," RISO DTU, 2008.
- [7] D. B. Miracle and S.L. Donaldson, Eds., *Composites*. Materials Park, Ohio: ASM International, 2001.
- [8] "Salvador Caetano e a Airbus Military abrem a porta a novos projectos que podem criar 1.000 empregos- Empresas - Jornal de negócios online." [Online]. Available: [http://www.jornaldenegocios.pt/home.php?template=SHOWNEWS\\_V2&id=571401](http://www.jornaldenegocios.pt/home.php?template=SHOWNEWS_V2&id=571401). [Accessed: 18-Nov-2012].
- [9] J. Porritt, *Capitalism: As if the world matters*, 1st ed. 2005.
- [10] IATA, "Climate Change," <http://www.iata.org/whatwedo/environment/Documents/global-approach-reducing-missions.pdf>, Oct-2012. .
- [11] IATA, "Fact Sheet," [http://www.iata.org/pressroom/facts\\_figures/fact\\_sheets/Pages/technology.aspx](http://www.iata.org/pressroom/facts_figures/fact_sheets/Pages/technology.aspx), Oct-2012. .
- [12] IATA, "Pathway to carbon-neutral growth in 2020." 2009.
- [13] Lufthansa Group, "Balance." Jun-2012.
- [14] GWEC, "The Global Status of Wind Power in 2011," *Global Wind Report - Annual market update*, 2011.
- [15] EWEA, "EU reaches 100GW wind power milestone." [Online]. Available: [http://www.ewea.org/index.php?id=60&no\\_cache=1&tx\\_ttnews%5Btt\\_news%5D=1959&tx\\_ttnews%5BbackPid%5D=1&cHash=b7c78662bbf2d63b09f6d5e714236d69](http://www.ewea.org/index.php?id=60&no_cache=1&tx_ttnews%5Btt_news%5D=1959&tx_ttnews%5BbackPid%5D=1&cHash=b7c78662bbf2d63b09f6d5e714236d69).
- [16] EWEA, "Ten biggest onshore wind farms in Europe." 2012.
- [17] Technology Platform Advisory Council, "Wind Energy: A Vision for Europe in 2030." TPWind Secretariat, EC, Sep-2006.
- [18] EWEA, "Wind Energy Factsheets." 2010.
- [19] K. T. Ulrich and S. D. Eppinger, *Product design and development*, vol. 4th ed. Boston: McGraw-Hill International Editions, 2008.
- [20] "Product Design & Development." [Online]. Available: <http://www.rqriley.com/pro-dev.htm>. [Accessed: 20-Aug-2012].
- [21] Antti Saaksvuori and Anselmi Immonen, *Product Lifecycle Management*, 2nd ed. Springer, 2005.
- [22] G. Thimm, S. G. Lee, and Y.-S. Ma, "Towards unified modelling of product life-cycles," *Computers in Industry*, vol. 57, no. 4, pp. 331–341, May 2006.
- [23] A. Sääksvuori and A. Immonen, *Product lifecycle management*. Berlin: Springer, 2005.
- [24] K. G. McIntosh, "Implementing engineering data management solutions," *World Class Design to Manufacture*, vol. 2, no. 4, pp. 23–30, 1995.

- [25] Task Group SAS-054, "Methods and Models for Lyfe Cycle Costing," NATO, Technical Report TR-SAS-054, Jun. 2007.
- [26] R. B. Chase, N. J. Aquilano, and F. R. Jacobs, *Operations management for competitive advantage with global cases*, vol. 11th ed. Boston: McGraw Hill, 2006.
- [27] H. Takeuchi and I. Nonaka, "The new new product development game.," *Harvard Business Review*, vol. 64, no. 1, pp. 137–146, Jan. 1986.
- [28] M. Taisch, B. P. Cammarino, and J. Cassina, "Life cycle data management: first step towards a new product lifecycle management standard," *International Journal of Computer Integrated Manufacturing*, vol. 24, no. 12, pp. 1117–1135, Oct. 2011.
- [29] K. B. Clark and T. Fujimoto, *Product development performance : strategy, organization, and management in the world auto industry*. Boston, Mass.: Harvard Business School Press, 1991.
- [30] S L Brown and K. M. Eisenhardt, "Product development: Past research, present findings, and future directions," *The Academy of Management review*, p. 343, 1995.
- [31] J. Stark, *Product Lifecycle Management: 21st century Paradigm for Product Realisation*, 1st Edition. Springer, 2004.
- [32] R. García Flores, "Ingeniería concurrente y tecnologías de la información," *Ingenierías*, vol. VIII, no. 22, pp. 39–44, Mar. 2004.
- [33] C. Ribas, "Metodologías de ingeniería concurrente." Universitat Politècnica de Catalunya, España, 2006.
- [34] M. M. Espinosa, "La ingeniería concurrente, una filosofía actual con plenas perspectivas de futuro." .
- [35] J. P. Fielding, *Introduction to aircraft design*. New York: Cambridge University Press, 1999.
- [36] AFS-300, "AC: 121-22C - Maintenance Review Boards, Maintenance Type Boards, and OEM/TCH Recommended and Maintenance Procedures." FAA, Aug-2012.
- [37] A. P. Medeiros, *Aplicação de iniciativas Lean no desenvolvimento de produtos da indústria de móveis*. Porto: [s. n.], 2010.
- [38] K. B. Clark, "Product development in the world auto industry," *Brookings papers on economic activity*, vol. 1987, no. 3, p. 729, 1987.
- [39] A. T. Bahill and B. Gissing, "Re-evaluating Systems Engineering Concepts Using Systems Thinking," *IEEE TRANSACTIONS ON SYSTEMS, MAN, AND CYBERNETICS—PART C: APPLICATIONS AND REVIEWS*, vol. 28, no. 4, pp. 516–527, 1998.
- [40] P. M. Senge, "The Fifth Discipline: The Art & Practice of the Learning Organization," *New York: Currency Doubleday*, 1990.
- [41] "International Council on Systems Engineering Website." [Online]. Available: <http://www.incose.org/>. [Accessed: 05-Aug-2012].
- [42] A. T. Bahill and F. F. Dean, "What Is Systems Engineering? A Consensus of Senior Systems Engineers," 15-Jan-2009. [Online]. Available: [about:home](http://about:home). [Accessed: 11-Jul-2012].
- [43] A. Tetlay and P. John, "Determining the Lines of System Maturity, System Readiness and Capability Readiness in the System Development Lifecycle." Published and used by CSER 2009 with permission, Apr-2009.
- [44] J. C. Mankins, "Technology readiness assessments: A retrospective," *Acta Astronautica*, vol. 65, no. 9–10, pp. 1216–1223, Nov. 2009.
- [45] J. C. Mankins, "Technology readiness and risk assessments: A new approach," *Acta Astronautica*, vol. 65, no. 9–10, pp. 1208–1215, Nov. 2009.
- [46] J. Mankins, "Technology Readiness Levels." NASA, Apr-1995.
- [47] AIR-100, "AC: 20-107B - Composite Aircraft Structure." FAA, Sep-2009.
- [48] J. D. Russell, "Composite Affordability Initiative," *Advanced Materials & Processes*, Jun-2007.
- [49] J. Rouchon, "Certification of Aircraft Composite Structures," *Eurosae*, Apr-2007.
- [50] "Aviation Glossary - Defining the Language of Aviation." [Online]. Available: <http://aviationglossary.com/>. [Accessed: 01-Sep-2012].
- [51] "Airlines for America - A4A." [Online]. Available: <http://www.airlines.org/Pages/Home.aspx>. [Accessed: 01-Sep-2012].

- [52] EASA, "Acceptable Means of Compliance and Guidance Materials." [Online]. Available: <https://www.easa.europa.eu/agency-measures/acceptable-means-of-compliance-and-guidance-material.php>. [Accessed: 01-Sep-2012].
- [53] FAA, "Code of Federal Regulations." [Online]. Available: <http://www.ecfr.gov>. [Accessed: 01-Sep-2012].
- [54] JAA, "JAR Amendment Records." [Online]. Available: <http://www.jaa.nl/publications/section1.html>. [Accessed: 01-Sep-2012].
- [55] L. J. Hart-Smith, "Bolted and bonded joints," in *ASM Handbook Composite*, vol. 21, D. B. Miracle and S. L. Donaldson, Eds. 2001, pp. 449–487.
- [56] L. F. M. Silva, J. P. M. Gonçalves, F. M. F. Oliveira, and P. M. S. T. de Castro, "Multiple-site damage in riveted lap-joints: experimental simulation and finite element prediction," *International Journal of Fatigue*, vol. 22, no. 4, pp. 319–338, Apr. 2000.
- [57] AFGROW, "Handbook for Damage Tolerant Design," 2011. [Online]. Available: <http://www.afgrow.net/applications/DTDDHandbook/>.
- [58] C. Proppe, "Probabilistic analysis of multi-site damage in aircraft fuselages," *Computational Mechanics*, vol. 30, no. 4, pp. 323–329, Mar. 2003.
- [59] W. C. de Goeij, M. J. L. van Tooren, and A. Beukers, "Composite adhesive joints under cyclic loading," *Materials & Design*, vol. 20, no. 5, pp. 213–221, Oct. 1999.
- [60] American Composite Manufacturers Association, "Overview of composite processes," ACMA, 21-Sep-2012. [Online]. Available: <http://www.acmanet.org/bsa/overview-processes.cfm>.
- [61] S. V. Hoa, *Principles of the Manufacturing of Composite Materials*. DEStech Publications, 2009.
- [62] ICarbonBike, "Carbon Fiber," 26-Jul-2012. [Online]. Available: <http://www.icarbonbike.com/blog/>.
- [63] Nelson Kruschandl, "Carbon Fiber," *British Composites Limited*. [Online]. Available: [http://www.speedace.info/composites/carbon\\_fibre.htm](http://www.speedace.info/composites/carbon_fibre.htm).
- [64] "Material Solutions Composite," *Materials Engineering Research Laboratory*. [Online]. Available: <http://www.vircon-composites.com/2sub.asp>. [Accessed: 01-Sep-2012].
- [65] "Definition of Composite Material." [Online]. Available: <http://metals.about.com/library/bldef-Composite-Material.htm>. [Accessed: 30-Apr-2012].
- [66] K.-S. Kim, J.-S. Yoo, Y.-M. Yi, and C.-G. Kim, "Failure mode and strength of uni-directional composite single lap bonded joints with different bonding methods," *Composite Structures*, vol. 72, no. 4, pp. 477–485, Apr. 2006.
- [67] Composite UK, "Adhesive Bonding of Composites." .
- [68] B. Flinn and M. Phariss, "The Effect of Peel-Ply Surface Preparation Variables on Bond Quality," U.S. Department of Transportation FAA, DOT/FAA/AR-06/28, 2006.
- [69] R. D. Adams, Ed., *Adhesive bonding science, technology and applications*. Boca Raton, FL; Cambridge: CRC Press ; Woodhead Pub., 2005.
- [70] IFAM, "European Adhesive Engineer." Fraunhofer, 2011.
- [71] J. C. del Real, Y. Ballesteros, R. Chamochin, J. Abenojar, and L. Molisani, "Influence of Surface Preparation on the Fracture Behavior of Acrylic Adhesive/CFRP Composite Joints," *The Journal of Adhesion*, vol. 87, no. 4, pp. 366–381, 2011.
- [72] J. W. Chin and J. P. Wightman, "Surface characterization and adhesive bonding of toughened bismaleimide composites," *Composites Part A: Applied Science and Manufacturing*, vol. 27, no. 6, pp. 419–428, 1996.
- [73] R. G. Dillingham and B. R. Oakley, "Surface Energy and Adhesion in Composite–Composite Adhesive Bonds," *The Journal of Adhesion*, vol. 82, no. 4, pp. 407–426, 2006.
- [74] R. F. Wegman, *Surface preparation techniques for adhesive bonding*. Park Ridge, N.J., U.S.A.: Noyes Publications, 1989.
- [75] IFAM, "Adhesive bonding in transportation construction." Fraunhofer.
- [76] L. J. Hart-Smith, G. Redmond, and M. J. Davis, "The Curse of the Nylon Peel Ply," *MCDonnell Douglas Paper*, 1996.

- [77] A. V. Pocius and R. P. Wenz, "Mechanical Surface Preparation of Graphite--Epoxy Composite for Adhesive Bonding," *SAMPE J.*, vol. 21, no. 5, pp. 50–58, 1985.
- [78] D. K. Klapprott, "Key Factors Of The Peel Ply Surface Preparation Process." Loclite Aerospace, Mar-2004.
- [79] V. Wright, "What is grit blasting?," *TWI*. [Online]. Available: <http://www.twi.co.uk/technical-knowledge/faqs/process-faqs/faq-what-is-grit-blasting/>. [Accessed: 01-Sep-2012].
- [80] T. Roth, "A Modular Pedestrian Bridge System in FRP." Swissfiber bridge VC02, 2004.
- [81] "Boeing successfully completes 787 wingbox destructive testing," *Composite World*, 17-Nov-2008. [Online]. Available: <http://www.compositesworld.com/news/boeing-successfully-completes-787-wingbox-destructive-testing>. [Accessed: 09-Nov-2011].
- [82] Toshio Abe, "Composite Application Challenge in Primary Aircraft Structures," ICAS Workshop, 2011.
- [83] GAO-11-849, "Status of FAA's Actions to Oversee the Safety of Composite Airplanes." Sep-2011.
- [84] V. P. McConnell, "Past is prologue for composite repair," *Reinforced Plastics*, Mar-2011.
- [85] FAA, "FARs Part 23.573 - Damage Tolerance and Fatigue Evaluation of Structure." Nov-2008.
- [86] "Wind Energy Composite Materials Handbook." [Online]. Available: <http://www.gurit.com/wind-energy-handbook.aspx>.
- [87] B. F. Sørensen, T. K. Jacobsen, B. F. Sørensen, and T. K. Jacobsen, "Joining structural parts of composite materials for large rotorblades (invited paper)." Risø National Laboratory, 2006.
- [88] K. P. Subrahmanian and F. Dubouloz, "Adhesives for bonding wind turbine blades," *Reinforced Plastics*, vol. 53, no. 1, pp. 26–29, Jan. 2009.
- [89] P. Brondsted, J. W. Holmes, and B. F. Sorensen, "Wind Rotor Blade Materials Technology," *European Sustainable Energy Review*, no. 2, 2008.
- [90] A. Extance, "Improving Adhesives for Wind Turbine Blade Production," *SpecialChem*, 03-Sep-2011.
- [91] DOW (R), "AIRSTONE™ Adhesive System: 770E Resin / 771H/772H/778H Hardener," Jun-2011. [Online]. Available: <http://www.dow.com/product-line/airstone/product/airstone-adhesive-system-770e-resin-771h-772h-778h-hardener/>.
- [92] *How to Measure Performance: A Handbook of Techniques and Tools*. U.S. Department of Energy, 1995.
- [93] "Merriam-Webster," 2012. [Online]. Available: <http://www.merriam-webster.com/>.
- [94] "ISO 9001 - Quality Management Systems - Requirements." ISO, 15-Nov-2008.
- [95] J. P. Ciribeli and C. de M. Andrade, "A Aplicação Do PDCA Como Metodologia De Redução Do Índice De Falhas No Processo Produtivo Da Itatiaia Móveis S/A," *Revista Gestão Empresarial*, vol. 1, no. 1, Jul. 2011.
- [96] Gurit, "General Health & Safety advice for Gurit Epoxy Resins & Hardeners." 2002.
- [97] E. . Shehab and H. . Abdalla, "Manufacturing cost modelling for concurrent product development," *Robotics and Computer-Integrated Manufacturing*, vol. 17, no. 4, pp. 341–353, Aug. 2001.
- [98] J. Kennedy, "Cost Analysis for Pollution Prevention." HWTR, Department of Ecology, 2005.
- [99] R. Kirchain and F. Field III, "Process-Based Cost Modeling: Understanding the Economics of Technical Decisions," *Encyclopedia of Materials: Science and Technology*, vol. 2, pp. 1718–1727, 2001.
- [100] F. Field, R. Kirchain, and R. Roth, "Process cost modeling: Strategic engineering and economic evaluation of materials technologies," *JOM Journal of the Minerals, Metals and Materials Society*, vol. 59, no. 10, pp. 21–32, 2007.
- [101] R. Kirchain, "Session 3 - Creating the Model: Initial Steps," Lisbon, 2008.
- [102] Sung H Park and Asian Productivity Organization, *Six Sigma for quality and productivity promotion*. [Tokyo]: Asian Productivity Organization, 2003.
- [103] "EN2243-1 - Aerospace series. Non-metallic materials. Structural adhesives. Test method. Single lap shear." ISO, Jan-2006.

- [104] L. Tong, "Strength of adhesively bonded single-lap and lap-shear joints," *International Journal of Solids and Structures*, vol. 35, no. 20, pp. 2601–2616, Jul. 1998.
- [105] R. D. Adams and W. C. Wake, *Structural adhesive joints in engineering*. London: Elsevier Applied Science, 1984.
- [106] L. J. Hart-Smith, "Adhesive-Bonded Single-Lap Joints," NASA, CR-112236, 1973.
- [107] L. F. M. da Silva, P. J. C. das Neves, R. D. Adams, and J. K. Spelt, "Analytical models of adhesively bonded joints—Part I: Literature survey," *International Journal of Adhesion and Adhesives*, vol. 29, no. 3, pp. 319–330, Apr. 2009.
- [108] F. Mortensen and O. T. Thomsen, "Analysis of adhesive bonded joints: a unified approach," *Composites Science and Technology*, vol. 62, no. 7–8, pp. 1011–1031, Jun. 2002.
- [109] O. Volkersen, "Die Niekraftverteilung in Zugbeanspruchten mit Konstanten Laschenquerschritten," *Luftfahrtforschung*, no. 15, pp. 41–47, 1938.
- [110] D. M. Gleich, "Stress analysis of structural bonded joints," DUP Science, Delft, 2002.
- [111] V. Ratta, "Crystallization, Morphology, Thermal Stability and Adhesive Properties of Novel High Performance Semicrystalline Polyimides," Virginia Tech, Virginia State, 1999.
- [112] L. J. Hart-Smith, "Analysis and Design of Advanced Composite Bonded Joints," NASA, CR-2218, 1974.
- [113] L. F. M. da Silva, P. J. C. das Neves, R. D. Adams, A. Wang, and J. K. Spelt, "Analytical models of adhesively bonded joints—Part II: Comparative study," *International Journal of Adhesion and Adhesives*, vol. 29, no. 3, pp. 331–341, Apr. 2009.
- [114] Flemming Mortensen, "Development of Tools for Engineering Analysis and Design of High-Performance FRP-Composite Structural Elements - Research - Aalborg University," Aalborg University, Aalborg, 1998.
- [115] B. Blackman, J. P. Dear, A. J. Kinloch, and S. Osiyemi, "The calculation of adhesive fracture energies from double-cantilever beam test specimens," *Journal of Materials Science Letters*, vol. 10, no. 5, pp. 253–256, 1991.
- [116] ASTM, "D5528 - Standard Test Method for Mode I Interlaminar Fracture Toughness of Unidirectional Fiber-Reinforced Polymer Matrix Composites." 2007.
- [117] M. F. de S. F. Moura, A. M. B. de. Moraes, and A. G. de Magalhaes, *Materiais compósitos : materiais, fabrico e comportamento mecânico*. Porto: Publindústria, 2005.
- [118] I. A. Ashcroft, D. J. Hughes, and S. J. Shaw, "Mode I fracture of epoxy bonded composite joints: 1. Quasi-static loading," *International Journal of Adhesion and Adhesives*, vol. 21, no. 2, pp. 87–99, 2001.
- [119] B. R. K. Blackman, A. J. Kinloch, and M. Paraschi, "The determination of the mode II adhesive fracture resistance, GIIC, of structural adhesive joints: an effective crack length approach," *Engineering Fracture Mechanics*, vol. 72, no. 6, pp. 877–897, Apr. 2005.
- [120] M. F. S. F. de Moura, R. D. S. G. Campilho, and J. P. M. Gonçalves, "Pure mode II fracture characterization of composite bonded joints," *International Journal of Solids and Structures*, vol. 46, no. 6, pp. 1589–1595, Mar. 2009.
- [121] M. F. S. F. de Moura, R. D. S. G. Campilho, and J. P. M. Gonçalves, "Crack equivalent concept applied to the fracture characterization of bonded joints under pure mode I loading," *Composites Science and Technology*, vol. 68, no. 10–11, pp. 2224–2230, Aug. 2008.
- [122] C. Branco, *Mecânica dos Materiais*. Fundação Calouste Gulbenkian, 1998.
- [123] B. Gross and A. Mendelson, "Plane elastostatic analysis of V-notched plates," *International Journal of Fracture*, vol. 8, no. 3, pp. 267–276, 1972.
- [124] M. F. S. F. de Moura, M. V. C. Fernandez, A. B. de Moraes, and R. D. S. G. Campilho, "Numerical analysis of the Edge Crack Torsion test for mode III interlaminar fracture of composite laminates," *Engineering Fracture Mechanics*, vol. 76, no. 4, pp. 469–478, Mar. 2009.
- [125] M. A. L. Silva, M. F. S. F. de Moura, and J. J. L. Moraes, "Análise Por Elementos Finitos Do Ensaio Ect (Edge Crack Torsion) Para Determinação Das Propriedades De Fractura Da Madeira Pinus Pinaster Ait. Em Puro Modo III," *Mecânica Experimental*, vol. 14, pp. 21–27, 2007.

- [126] T. Strohaecker, "Mecânica da Fractura." Universidade do Rio Grande do Sul, Escola de Engenharia, 2005.
- [127] Simulia, "Abaqus." [Online]. Available: <http://www.3ds.com/products/simulia/portfolio/abaqus/overview/>. [Accessed: 20-Oct-2012].
- [128] "ISO 15024 Fibre-reinforced plastic composites -- Determination of mode I interlaminar fracture toughness, GIC, for unidirectionally reinforced materials." 2001.
- [129] M. A. L. da Silva, *Estudo das propriedades de fractura em Modo II e em Modo III da madeira de Pinus Pinaster Ait.* Porto: [s. n.], 2006.
- [130] X. X. Xu, A. D. Crocombe, and P. A. Smith, "Mixed-Mode fatigue and fracture behaviour of joints bonded with either filled or filled and toughened adhesive," *Int. J. Fatigue*, vol. 17, no. 4, pp. 279–286, 1995.
- [131] B. R. K. Blackman, A. J. Kinloch, F. S. Rodriguez-Sanchez, and W. S. Teo, "The fracture behaviour of adhesively-bonded composite joints: Effects of rate of test and mode of loading," *International Journal of Solids and Structures*, vol. 49, no. 13, pp. 1434–1452, 2012.
- [132] D. A. Dillard, H. K. Singh, D. J. Pohlit, and J. M. Starbuck, "Observations of Decreased Fracture Toughness for Mixed Mode Fracture Testing of Adhesively Bonded Joints," *Journal of Adhesion Science and Technology*, vol. 23, no. 10–11, pp. 1515–1530, 2009.
- [133] G. Fernlund and J. K. Spelt, "Mixed-mode fracture characterization of adhesive joints," *Composites Science and Technology*, vol. 50, no. 4, pp. 441–449, 1994.
- [134] F. J. P. Chaves, M. F. S. F. de Moura, L. F. M. da Silva, and D. A. Dillard, "Numerical analysis of the dual actuator load test applied to fracture characterization of bonded joints," *International Journal of Solids and Structures*, vol. 48, no. 10, pp. 1572–1578, May 2011.
- [135] L. F. M. da Silva, V. H. C. Esteves, and F. J. P. Chaves, "Fracture toughness of a structural adhesive under mixed mode loadings," *Mat.-wiss. u. Werkstofftech.*, vol. 42, no. 5, pp. 460–470, 2011.
- [136] L. F. M. da Silva and A. Öchsner, *Modeling of Adhesively Bonded Joints*. 2008.
- [137] L. F. M. da Silva, A. G. Magalhães, and M. F. de S. F. Moura, *Juntas Adesivas Estruturais*. 2007.
- [138] M. Quaresmin and M. Ricotta, "Life Prediction of Bonded Joints in Composite Materials," *Int J Fatigue*, vol. 28, no. 10, pp. 1166–1176, 2006.
- [139] M. Quaresmin and M. Ricotta, "Fatigue behaviour and damage evolution of single lap bonded joints in composite material," vol. 66, no. 2, pp. 176–187, 2005.
- [140] P. Cheuk, C. Wang, A. Baker, and P. Chalkley, "Fatigue crack growth in adhesively bonded composite-metal double-lap joints," *Compos Struct*, vol. 55, no. 1–4, pp. 109–115, 2002.
- [141] A. Antoniou, F. Sayer, and A. van Wingerde, "Competence Center Rotor Blade," presented at the AB2011, 2011.
- [142] Defense Science and Technology Organization, "Fact Sheet - Structural Fatigue Testing." 2008.
- [143] W. S. Johnson and S. Mall, "Influence of interface ply orientation on fatigue damage of adhesively bonded composite joints," 1985.
- [144] J. M. Whitney, *Composite Materials: Testing and Design (seventh Conference): a Conference : Philadelphia, PA, 2-4 April 1984*. ASTM International, 1986.
- [145] S. Azari, M. Papini, J. A. Schroeder, and J. K. Spelt, "The effect of mode ratio and bond interface on the fatigue behavior of a highly-toughened epoxy," *Engineering Fracture Mechanics*, vol. 77, no. 3, pp. 395–414, Feb. 2010.
- [146] G. Meneghetti, M. Quaresimin, and M. Ricotta, "Influence of the interface ply orientation on the fatigue behaviour of bonded joints in composite materials," *International Journal of Fatigue*, vol. 32, no. 1, pp. 82–93, Jan. 2010.
- [147] I. A. Ashcroft, J. P. Casas-Rodriguez, and V. V. Silberschmidt, "A Model to Predict the Anomalous Fatigue Crack Growth Behaviour Seen in Mixed Mechanism Fracture," *The Journal of Adhesion*, vol. 86, no. 5–6, pp. 522–538, 2010.



- [148] H. Hadavinia, A. J. Kinloch, M. S. G. Little, and A. C. Taylor, "The prediction of crack growth in bonded joints under cyclic-fatigue loading I. Experimental studies," *International Journal of Adhesion and Adhesives*, vol. 23, no. 6, pp. 449–461, 2003.
- [149] H. Hadavinia, A. J. Kinloch, M. S. G. Little, and A. C. Taylor, "The prediction of crack growth in bonded joints under cyclic-fatigue loading II. Analytical and finite element studies," *International Journal of Adhesion and Adhesives*, vol. 23, no. 6, pp. 463–471, 2003.
- [150] G. Meneghetti, M. Quaresimin, and M. Ricotta, "Damage mechanisms in composite bonded joints under fatigue loading," *Composites Part B: Engineering*, vol. 43, no. 2, pp. 210–220, Mar. 2012.
- [151] I. A. Ashcroft, D. J. Hughes, S. Shaw, M. Abdel-Wahab, and A. Crocombe, "Effect Of Temperature On The Quasi-Static Strength And Fatigue Resistance Of Bonded Composite Double Lap Joint," *Int. J. Adhes Adhes*, vol. 75, no. 1, pp. 61–88, 2001.
- [152] I.A. Ashcroft and S.J. Shaw, "Mode I fracture of epoxy bonded composite joints 2. Fatigue loading," *International Journal of Adhesion and Adhesives*, vol. 22, no. 2, pp. 151–167, 2002.
- [153] M.M.Abdel Wahab, I.A Ashcroft, A. J. Crocombe, D. J. Hughes, and S. J. Shaw, "The effect of environment on the fatigue of bonded composite joints. Part 2: fatigue threshold prediction," *Composites Part A: Applied Science and Manufacturing*, vol. 32, no. 1, pp. 59–69, Jan. 2001.
- [154] M. M. A. Wahab, I. A. Ashcroft, A. D. Crocombe, and S. J. Shaw, "Prediction of fatigue thresholds in adhesively bonded joints using damage mechanics and fracture mechanics," *Journal of Adhesion Science and Technology*, vol. 15, no. 7, pp. 763–781, 2001.
- [155] I. J. Ashcroft, M. M. A. Wahab, A. J. Crocombe, D. J. Hughes, and S. J. Shaw, "The effect of environment on the fatigue of bonded composite joints. Part 1: testing and fractography," *Composites Part A: Applied Science and Manufacturing*, vol. 32, no. 1, pp. 45–58, Jan. 2001.
- [156] A. Pirondi and F. Moroni, "An investigation of fatigue failure prediction of adhesively bonded metal/metal joints," *Int. J. Adhes Adhes*, vol. 29, no. 8, pp. 796–805, 2009.
- [157] A. Pirondi and G. Nicoletto, "Fatigue Crack Growth In Bonded DCB Specimens," *Eng. Fract. Mech*, vol. 71, no. 4–6, pp. 859–871, 2004.
- [158] ASTM, "D3166-99 - Standard Test Method for Fatigue Properties of Adhesives in Shear by Tension Loading (Metal/Metal)." 2005.
- [159] ASTM, "D6115 - Standard Test Method for Mode I Fatigue Delamination Growth Onset of Unidirectional Fiber-Reinforced Polymer Matrix Composites." 2004.
- [160] A. Pirondi and A. Moroni, "A Progressive Damage Model For The Prediction Of The Fatigue Crack Growth In Bonded Joints," *J Adhesion*, vol. 5, no. 86, pp. 501–521, 2010.
- [161] A. Manonukul and F. P. E. Dunne, "High- and low-cycle fatigue crack initiation using polycrystal plasticity," *Proceedings of the Royal Society of London. Series A: Mathematical, Physical and Engineering Sciences*, vol. 460, no. 2047, pp. 1881–1903, 2004.
- [162] B. Cotterell, *Fracture and Life*. World Scientific, 2010.
- [163] P. Safarian, "Fatigue and Damage Tolerance," Airbus, 29-Jun-2012.
- [164] Boeing, "B-47 Stratojet," *History*. [Online]. Available: <http://www.boeing.com/history/boeing/b47.html>. [Accessed: 04-Nov-2012].
- [165] D. Lutz, "Paul C. Paris, pioneer of fracture mechanics, honored for his work," *Washington University in St. Louis*, Nov-2010. [Online]. Available: <http://news.wustl.edu/news/Pages/21517.aspx>.
- [166] ACE-100, "AC: 23-123A - Fatigue, Fail-safe and Damage Tolerance Evaluation of Metallic Structure for Part 23 Airplanes - Draft." FAA, 2012.
- [167] D. Roylance, "Fatigue." Department of Material Science and Engineering, MIT, 2001.
- [168] M. Abou-Hamda, M. Megahed, and M. Hammouda, "Fatigue Crack Growth in Double Cantilever Beam Specimen with an Adhesive Layer," *Eng. Fract. Mech.*, vol. 60, no. 5–6, pp. 605–614, 1998.
- [169] A. J. Curley, H. Hadavinia, A. J. Kinloch, and A.C. Taylor, "Predicting The Service-Life Of Adhesively-Bonded Joints," *International Journal of Fracture*, vol. 103, no. 1, pp. 41–69, 2000.

- [170] N. Blanco, E. K. Gamstedt, L. E. Asp, and J. Costa, "Mixed-mode delamination growth in carbon-fibre composite laminates under cyclic loading," *International Journal of Solids and Structures*, vol. 41, no. 15, pp. 4219–4235, 2004.
- [171] S. Azari, M. Papini, J. A. Schroeder, and J. K. Spelt, "Fatigue threshold behavior of adhesive joints," *International Journal of Adhesion and Adhesives*, vol. 30, no. 3, pp. 145–159, Apr. 2010.
- [172] "E 647 Standard Test Method for Measurement of Fatigue Crack Growth Rates." ASTM, 2008.
- [173] "1954: 'Metal fatigue' caused Comet crashes," *BBC*, 19-Oct-1954.
- [174] S. Suresh, *Fatigue of Materials*. Cambridge University Press, 1998.
- [175] P. C. Paris, M. P. Gomez, and W. E. Anderson, "A Rational Analytic Theory of Fatigue," *The Trend in Engineering*, vol. 13, pp. 9–14, Jan. 1961.
- [176] E. Sancaktar, "Fracture aspects of adhesive joints: material, fatigue, interphase, and stress concentration considerations," *J Adhes Sci Technol*, vol. 9, no. 2, pp. 119–147, 1995.
- [177] Y. Zhang, A. P. Vassilopoulos, and T. Keller, "Stiffness degradation and fatigue life prediction of adhesively-bonded joints for fiber-reinforced polymer composites," *Int J Fatigue*, vol. 30, no. 10–11, pp. 1813–1820, 2008.
- [178] A. Whitworth, "A stiffness degradation model for composite laminates under fatigue loading," *Compos Struct*, vol. 40, no. 2, pp. 95–101, 1999.
- [179] S. Mostovoy and E. J. Ripling, "Final Report Fracturing Characteristics Of Adhesive Joints," Materials Research Laboratory, Feb. 1972.
- [180] ASTM, "D3433-99 - Standard Test Method for Fracture Strength in Cleavage of Adhesives in Bonded Metal Joints." 2005.
- [181] L. A. Carlsson, J. W. Gillespie, and Jr. and R. B Pipes, "On the Analysis and Design of the end Notched Flexure (ENF) Specimen for Mode II Testing," *Journal of Composite Materials*, vol. 20, no. 6, pp. 594–604, 1986.
- [182] A. Szekrényes, "Crack Stability of Fracture Specimens used to Test Unidirectional Fiber Reinforced Material," *Experimental Mechanics*, vol. 50, no. 4, pp. 473–482, 2010.
- [183] H. Chai and S. Mall, "Design aspects of the end-notch adhesive joint specimen," *Int J Fract*, vol. 36, no. 1, pp. R3–R8, Jan. 1988.
- [184] S. Mall and N. K. Kochhar, "Characterization of debond growth mechanism in adhesively bonded composites under mode II static and fatigue loadings," *Engineering Fracture Mechanics*, vol. 31, no. 5, pp. 747–758, 1988.
- [185] I. Ashcroft, J. Casas-Rodriguez, and V. Silberschmidt, "Mixed-mode crack growth in bonded composite joints under standard and impact-fatigue loading," *Journal of Materials Science*, vol. 43, no. 20, pp. 6704–6713, 2008.
- [186] D. D. Samborsky, A. T. Sears, J. F. Mandell, and O. Kils, "Static and Fatigue Testing of Thick Adhesive Joints for Wind Turbine Blades."
- [187] M.F.S.F. de Moura, R.D.S.G. Campilho, and J.P.M. Gonçalves, "Pure mode II fracture characterization of composite bonded joints," *Int J of Solid and Struc*, vol. 46, pp. 1589–1595, 2008.
- [188] M. F. S. F. de Moura and A. B. de Morais, "Equivalent crack based analyses of ENF and ELS tests," *Engineering Fracture Mechanics*, vol. 75, no. 9, pp. 2584–2596, Jun. 2008.
- [189] M. F. S. F. de Moura, J. J. L. Morais, and N. Dourado, "A new data reduction scheme for mode I wood fracture characterization using the double cantilever beam test," *Engineering Fracture Mechanics*, vol. 75, no. 13, pp. 3852–3865, Sep. 2008.
- [190] R. D. S. G. Campilho, *Repair of composite and wood structures*. Porto: PhD, FEUP, 2009.
- [191] R. D.S.G. Campilho, Marcelo F.S.F. de Moura, Dimitra A. Ramantani, and João P.M. Gonçalves, "Obtaining the cohesive laws of a trapezoidal mixed-mode damage model using an inverse method," *C.Tecn. Mat.*, vol. 20, no. 1–2, pp. 81–86, 2008.
- [192] R. Campilho, M. Moura, and J. Domingues, "Stress and Failure Analyses of Scarf Repaired CFRP Laminates using a Cohesive Damage Model," *J of Ad Sci and Tech*, vol. 21, no. 9, pp. 855–870, 2007.

- [193] S. Krenk, J. Jönsson, and L. P. Hansen, "Fatigue analysis and testing of adhesive joints," *Engineering Fracture Mechanics*, vol. 53, no. 6, pp. 859–872, Apr. 1996.
- [194] S. H. Yoon and C. S. Hong, "Modified end notched flexure specimen for mixed mode interlaminar fracture in laminated composites," *International Journal of Fracture*, vol. 43, no. 1, pp. R3–R9, 1990.
- [195] J. Hutchinson and Z. Suo, "Mixed Mode Cracking in Layered Materials," *Advances In Applied Mechanics*, vol. 29, 1992.
- [196] M. Kenane and M. L. Benzeggagh, "Mixed-mode delamination fracture toughness of unidirectional glass/epoxy composites under fatigue loading," *Composites Science and Technology*, vol. 57, no. 5, pp. 597–605, 1997.
- [197] A. Szekrenyes and J. Uj, "Beam and finite element analysis of quasi-unidirectional composite SLB and ELS specimens," *Comp. Sci. and Tech*, no. 64, pp. 2393–2406, 2004.
- [198] R. Krueger and T. K. O'Brien, "A shell/3D modeling technique for the analysis of delaminated composite laminates," *Composites Part A: Applied Science and Manufacturing*, vol. 32, no. 1, pp. 25–44, 2001.
- [199] J. M. Q. Oliveira, M. F. S. F. de Moura, and J. J. L. Morais, "Application of the end loaded split and single-leg bending tests to the mixed-mode fracture characterization of wood," *Holzforschung*, vol. 63, no. 5, pp. 597–602, 2009.
- [200] Y. Zhang, A. P. Vassilopoulos, and T. Keller, "Mode I and II Fracture Behavior of Adhesively-Bonded Pultruded Composite Joints," *Engineering Fracture Mechanics*, vol. 77, no. 1, pp. 128–143, 2010.